DRAFT INTERNATIONAL STANDARD
ISO/DIS 19901-4

ISO/TC **67**/SC **7** Secretariat: **BSI**

Voting begins on: **2022-05-19** Voting terminates on: **2022-08-11**

Petroleum and natural gas industries — Specific requirements for offshore structures —

Part 4: **Geotechnical design considerations**

ICS: 75.180.10

This document is circulated as received from the committee secretariat.

ISO/CEN PARALLEL PROCESSING

Reference number
ISO/DIS 19901-4:2022(E)

Contents

Foreword

ISO (the International Organization for Standardization) is a worldwide federation of national standards bodies (ISO member bodies). The work of preparing International Standards is normally carried out through ISO technical committees. Each member body interested in a subject for which a technical committee has been established has the right to be represented on that committee. International organizations, governmental and non-governmental, in liaison with ISO, also take part in the work. ISO collaborates closely with the International Electrotechnical Commission (IEC) on all matters of electrotechnical standardization.

The procedures used to develop this document and those intended for its further maintenance are described in the ISO/IEC Directives, Part 1. In particular, the different approval criteria needed for the different types of ISO documents should be noted. This document was drafted in accordance with the editorial rules of the ISO/IEC Directives, Part 2 (see www.iso.org/directives).

Attention is drawn to the possibility that some of the elements of this document may be the subject of patent rights. ISO shall not be held responsible for identifying any or all such patent rights. Details of any patent rights identified during the development of the document will be in the Introduction and/or on the ISO list of patent declarations received (see www.iso.org/patents).

Any trade name used in this document is information given for the convenience of users and does not constitute an endorsement.

For an explanation of the voluntary nature of standards, the meaning of ISO specific terms and expressions related to conformity assessment, as well as information about ISO's adherence to the World Trade Organization (WTO) principles in the Technical Barriers to Trade (TBT), see www.iso.org/iso/foreword.html.

This document was prepared by Technical Committee ISO/TC 67, *Materials, equipment and offshore structures for the petroleum, petrochemical and natural gas industries*, Subcommittee SC 7, *Offshore structures*.

This third edition cancels and replaces the second edition (ISO 19901-4:2016), which has been technically revised.

The main changes compared to the previous edition are as follows:

- guidance extended on representative and design values for soil parameters (Clause 5);
- guidance added for geotechnical design of intermediate foundations for fixed structures and clause renamed to ‘Design of shallow and intermediate foundations’ (Clause 7);
- requirements added on installation resistance, yield envelope approaches for ultimate limit state, and performance based design for shallow skirted and intermediate foundations (Clause 7);
- new unified CPT method for axial capacity in sands to replace the former main text method, new TZ curve definition in sands, new unified CPT method for clays introduced into the annex, new PY curve methodology for clays to replace the existing method (Clause 8);
- new clause for reassessment of pile capacity for existing structures (Clause 9);
- a new clause for pipelines, conductors and risers, previously only informative (Clause 10);
- references have been reviewed, updated and reduced where possible.

A list of all parts in the ISO 19901 series can be found on the ISO website.

Any feedback or questions on this document should be directed to the user’s national standards body. A complete listing of these bodies can be found at www.iso.org/members.html.

Introduction

The International Standards for offshore structures, ISO 19900 to ISO 19906, constitute a common basis covering those aspects that address design requirements and assessments of all offshore structures used by the petroleum and natural gas industries worldwide. Through their application, the intention is to achieve reliability levels appropriate for attended and unattended offshore structures, whatever the type of structure and the nature of the materials used.

It is important to recognize that structural integrity is an overall concept comprising models for describing actions, structural analyses, design rules, safety elements, quality of work, quality control procedures and national requirements, all of which are mutually dependent. The modification of one aspect of design in isolation can disturb the balance of reliability inherent in the overall concept or structural system. The implications involved in modifications, therefore, need to be considered in relation to the overall reliability of all offshore structural systems.

For geotechnical design, some additional considerations apply. These include the time, frequency and rate at which actions are applied, the method of installation, the properties of the surrounding soil, the overall behaviour of the seabed, effects from adjacent structures and the results of drilling into the seabed. All of these, and any other relevant information, need to be considered in relation to the overall reliability of the structure.

These International Standards are intended to provide wide latitude in the choice of structural configurations, materials and techniques without hindering innovation. Geotechnical design practice for offshore structures has proved to be an innovative and evolving process over the years. This evolution is expected to continue and is encouraged. Therefore, circumstances can arise when the procedures described in this document or in ISO 19900 to ISO 19906 (or elsewhere) are insufficient on their own to ensure that a safe and economical design is achieved.

Seabed soils vary. Experience gained at one location is not necessarily applicable at another. Extra caution is necessary when dealing with unconventional soils or unfamiliar foundation concepts. Sound engineering judgment is therefore necessary in the use of this document.

Some background to and guidance on the use of this document is provided for information in Annex A.

In this document, the following verbal forms are used, in accordance with the latest edition of the ISO/IEC Directives, Part 2:

— ‘shall’ and ‘shall not’ are used to indicate requirements strictly to be followed in order to conform with the document and from which no deviation is permitted;

— ‘should’ and ‘should not’ are used to indicate that among several possibilities one is recommended as particularly suitable, without mentioning or excluding others, or that a certain course of action is preferred but not necessarily required, or that (in the negative form) a certain possibility or course of action is deprecated but not prohibited;

— ‘may’ and ‘may not’ are used to indicate a course of action permissible within the limits of the document;

— ‘can’ and ‘cannot’ are used for statements of possibility and capability, whether material, physical or causal.

Petroleum and natural gas industries — Specific requirements for offshore structures — Part 4: Geotechnical design considerations

1 Scope

This document contains provisions for geotechnical engineering design that are applicable to a broad range of offshore structures, rather than to a particular structure type. This document outlines methods developed for the design of shallow foundations with an embedded length (L) to diameter (D) ratio L/D < 0,5, intermediate foundations, which typically have 0,5 < L/D < 10 (Clause 7), and long and flexible pile foundations with L/D > 10 (Clauses 8 and 9).

This document also provides guidance on soil-structure interaction aspects for flowlines, risers and conductors (Clause 10) and anchors for floating facilities (Clause 11). This document contains brief guidance on site and soil characterization, and identification of hazards (Clause 6).

NOTE ISO 19901-8 and 19901-10 provide requirements and detailed guidance on these topics.

This document does not address aspects of soil mechanics and geotechnical engineering that apply equally to offshore and onshore structures.

Figure 1 set outs a high level typical workflow for design of offshore foundations with reference to other relevant ISO standards.

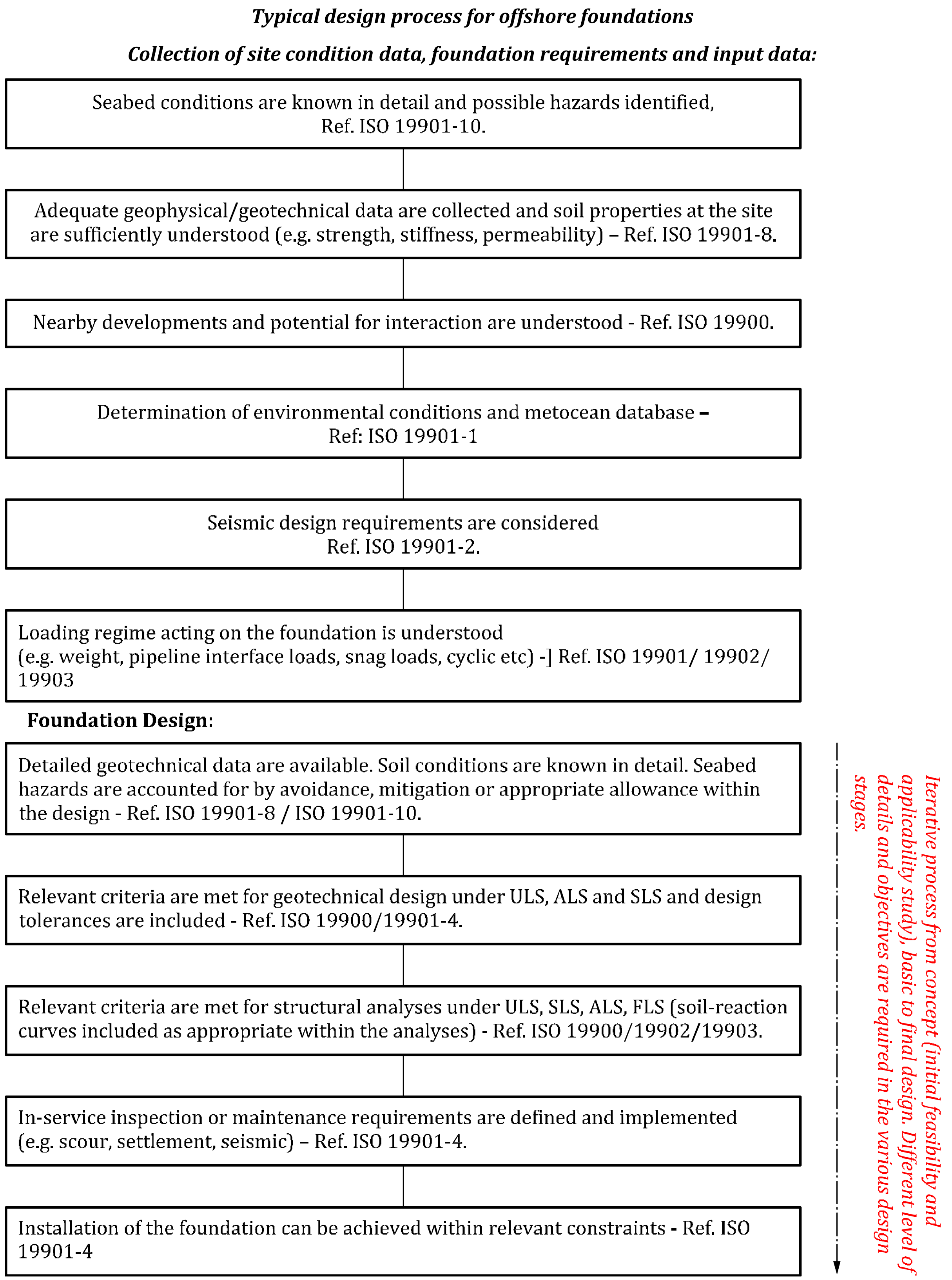

NOTE Specific design and installation constraints can apply for structures in arctic regions (see ISO 19906), for mobile offshore units, especially for jack-ups (see ISO 19905) and for anchors for floating units (see ISO 19901-7).

Figure 1 — Flowchart showing design process for offshore foundations

2 Normative references

The following documents are referred to in the text in such a way that some or all of their content constitutes requirements of this document. For dated references, only the edition cited applies. For undated references, the latest edition of the referenced document (including any amendments) applies.

ISO 19900, *Petroleum and natural gas industries — General requirements for offshore structures*

ISO 19901-1, *Petroleum and natural gas industries — Specific requirements for offshore structures — Part 1: Metocean design and operating considerations*

ISO 19901-2, *Petroleum and natural gas industries — Specific requirements for offshore structures — Part 2: Seismic design procedures and criteria*

ISO 19901-3, *Petroleum and natural gas industries — Specific requirements for offshore structures — Part 3: Topsides structure*

ISO 19901-5, *Petroleum and natural gas industries — Specific requirements for offshore structures — Part 5: Weight control during engineering and construction*

ISO 19901-6, *Petroleum and natural gas industries — Specific requirements for offshore structures — Part 6: Marine operations*

ISO 19901-7:2013, *Petroleum and natural gas industries — Specific requirements for offshore structures — Part 7: Stationkeeping systems for floating offshore structures and mobile offshore units*

ISO 19901-8, *Petroleum and natural gas industries — Specific requirements for offshore structures — Part 8: Marine soil investigations*

ISO 19901-10, *Petroleum and natural gas industries — Specific requirements for offshore structures — Part 10: Marine geophysical investigations*

ISO 19902, *Petroleum and natural gas industries — Fixed steel offshore structures*

ISO 19903, *Petroleum and natural gas industries — Concrete offshore structures*

ISO 19905 (all parts), *Petroleum and natural gas industries — Site-specific assessment of mobile offshore units*

ISO 19906, *Petroleum and natural gas industries — Arctic offshore structures*

3 Terms and definitions

For the purposes of this document, the terms and definitions given in ISO 19900, ISO 19901 (all parts) and the following apply.

ISO and IEC maintain terminological databases for use in standardization at the following addresses:

— ISO Online browsing platform: available at https://www.iso.org/obp

— IEC Electropedia: available at http://www.electropedia.org/

3.1
action
external loading applied to the structure (direct action) or an imposed deformation or acceleration (indirect action)

Note 1 to entry: An imposed deformation can be caused by fabrication tolerances, differential settlement, temperature change or moisture variation. An earthquake typically generates imposed accelerations.

[SOURCE: ISO 19900:2019, 3.3]

3.2
action factor
partial safety factor applied to a design action

3.3
attended
personnel are expected to work and live on the facility 24/7 during its operational life

Note 1 to entry: Usually this entails people working in day and/or night shifts and in an offshore/onshore rota of week(s) on and week(s) off the facility.

Note 2 to entry: In this document only L1 exposure level for attended structures is considered (see ISO 19900 and ISO 19902).

3.4
basic variable
one of a specified set of variables representing physical quantities which characterize actions, environmental influences, geometric quantities, or material properties including soil properties

[SOURCE: ISO 19900:2019, 3.7]

3.5
characteristic value
value assigned to a basic variable with a prescribed probability

Note 1 to entry: In some design/assessment situations, a variable can have two characteristic values, an upper value and a lower value.

[SOURCE: ISO 19900:2019, 3.9]

3.6
derived value of soil parameter
value assigned to a soil parameter for a specific calculation model, reached by reasoning, theory, deduction, inference or empiricism, often considering various sources of data

3.7
design actions
combination of representative actions and partial safety factors representing a design situation for use in checking the acceptability of a design

3.8
design value
value derived from the representative value for use in the design verification procedure

[SOURCE: ISO 19900:2019, 3.14]

3.9
drained condition
condition whereby the applied stresses and stress changes are supported by the soil skeleton and do not cause a change in pore pressure

[SOURCE: ISO 19901–8:2014, 3.11]

3.10
effective foundation area
reduced foundation area having its geometric centre at the point where the resultant action vector intersects the foundation base level

3.11
limit state
state beyond which the structure no longer satisfies the relevant design criteria

[SOURCE: ISO 19900:2019, 3.31]

3.12
material factor
partial safety factor applied to the characteristic strength of the soil, the value of which reflects the uncertainty or variability of the material property

Note 1 to entry: See ISO 19900.

3.13
representative value
value assigned to a basic variable for verification of a limit state in a design/assessment situation

Note 1 to entry: Two types of representative value used in design verification are characteristic value and nominal value.

[SOURCE: ISO 19900:2019, 3.40]

3.14
resistance
ability of a structure, or a structural component, to withstand action effects

[SOURCE: ISO 19900:2019, 3.41]

3.15
resistance factor
partial safety factor applied to the characteristic capacity of a foundation, the value of which reflects the uncertainty or variability of the component resistance including those of material property

3.16
scour
removal of seabed material caused by currents and/or waves

[SOURCE: ISO 19900:2019, 3.45]

3.17
seabed
materials below the seafloor, whether soils such as sand, silt and clay, cemented materials or rock

Note 1 to entry: Offshore foundations are most commonly installed in soils, and the terminology in this document reflects this. However, the requirements equally apply to cemented seabed materials and rock. Thus, the term 'soil' does not exclude any other material at or below the seafloor.

3.18
seafloor
interface between the sea and the seabed

3.19
serviceability
ability of a structure or structural member to perform adequately for a normal use under all expected actions

[SOURCE: ISO 2394:2015, 2.1.32]

3.20
settlement
permanent downward movement of a structure as a result of its own weight and other actions

3.21
strength
mechanical property of a material indicating its ability to resist actions, usually given in units of stress

Note 1 to entry: See ISO 19902.

3.22
unattended/normally unattended
no personnel are expected to work and live on the facility 24/7 during its operational life.

Note 1 to entry: As planned and/or unplanned maintenance will be required, usually reference is made to normally unattended or not normally attended.

Note 2 to entry: Specific requirements can apply to unattended/normally unattended structures or to structures being evacuated in advance of a storm.

3.23
undrained condition
condition whereby the applied stresses and stress changes are supported by both the soil skeleton and the pore fluid and do not cause a change in volume

[SOURCE: ISO 19901–8:2014, 3.42]

4 Symbols and abbreviated terms

4.1 General

Commonly used symbols are listed in 4.2 to 4.5; other symbols are defined in the text following the applicable formula. Symbols can have different meanings between formulae.

4.2 Symbols for shallow and intermediate foundation design

A	actual (cross-sectional plan) foundation area
A'	effective foundation area depending on eccentricity of actions
A_h	vertical projected area of the foundation in the direction of sliding
A_p	projected area of skirt tip
A_s	side surface area of skirt embedded at a particular penetration depth
$A_{idealized}$	idealized rectangular foundation area, for irregular foundation shapes
b_c, b_q, b_γ	bearing capacity correction factors related to foundation base inclination
B	minimum lateral foundation dimension (also foundation width)
B'	minimum effective lateral foundation dimension (also foundation effective width)
C	compression index of soil over loading range considered
d_c, d_q, d_γ	bearing capacity correction factors related to foundation embedment depth
D	foundation diameter (for circular foundations)
D_b	depth below seafloor to foundation base level
e	eccentricity of action
e_0	initial void ratio of the soil
e_1	eccentricity of action in coordinate direction 1
e_2	eccentricity of action in coordinate direction 2
f	unit skin friction resistance along foundation skirts during installation
F	bearing capacity correction factor to account for undrained shear strength heterogeneity
g_c, g_q, g_γ	correction factors related to seafloor inclination
G	elastic shear modulus of soil

h	soil layer thickness
H	horizontal action
H_b	horizontal action on effective area component of the base
H_d	design value of resistance to pure sliding
ΔH_d	horizontal soil resistance due to active and passive earth pressures on foundation skirts
H_{ult}	ultimate horizontal capacity in yield surface design method
i_c, i_q, i_γ	bearing capacity correction factors related to foundation action inclination
K_c, K_q, K_γ	correction factors that account for inclined actions, foundation shape, depth of embedment, inclination of base, and inclination of the seafloor
K_p	coefficient of passive earth pressure
K_{rd}	drained horizontal soil reaction coefficient
K_{ru}	undrained horizontal soil reaction coefficient
L	maximum lateral foundation dimension (also foundation length)
L'	maximum effective lateral foundation dimension (also foundation effective length)
M	overturning moment
M_{ult}	moment capacity in yield surface design method
N_c	undrained bearing capacity factor, equal to 5,14
N_q, N_γ	drained bearing capacity factors, as a function of ϕ'
p'_{in}	*in situ* effective overburden stress at skirt tip level inside the skirts of a skirted foundation
p'_{out}	*in situ* effective overburden stress at skirt tip level outside the skirts of a skirted foundation
q	unit end bearing resistance on foundation skirt tip~~,~~ during penetration
q_d	design value of vertical bearing resistance in the absence of horizontal actions
Q	vertical action
Q_f	skirt friction resistance
Q_p	end bearing resistance from skirt tips
Q_r	soil resistance during skirt penetration
Q_{ult}	vertical capacity in yield surface design method
R	radius of the base of a circular foundation
RP	reference point for action transfer
s_u	undrained shear strength
s_{u0}	undrained shear strength at foundation base level (skirt tip level for skirted foundations)
$s_{u,ave}$	average undrained shear strength from seafloor to foundation base level
$s_{u,2}$	equivalent undrained shear strength below foundation base
s_c, s_q, s_γ	bearing capacity correction factors related to foundation shape
T	torsional moment
u_Q, u_H	vertical and horizontal displacements at foundation base level
β	ground inclination angle in radians, in calculation of inclination factors

δ interface friction angle between soil and foundation

$\Delta\sigma'_{v,z}$ increment of effective vertical stress in a given soil layer at the specified time due to the increment of vertical action applied to foundation

ϕ' effective angle of internal friction angle of the soil for plane strain conditions

γ' submerged unit weight of soil

γ_{D} dead action factor

γ_{L} live action factor

γ_{m} material factor

κ rate of increase of undrained shear strength with depth

σ'_{v0} *in situ* effective overburden stress at foundation base level (skirt tip level when skirts are used)

$\sigma'_{\mathrm{v0,z}}$ effective overburden stress at level of a given soil layer

ν Poisson’s ratio of the soil

υ foundation base inclination angle in radians, in calculation of inclination factors

θ_{M}, θ_{T} displacements at foundation base level under overturning and torsion loading

4.3 Symbols for pile foundation design

A_{pile} gross end area of pile, $A_{\mathrm{pile}} = \dfrac{\pi \cdot D^2}{4}$

A_{r} pile displacement ratio, $A_{\mathrm{r}} = \dfrac{A_{\mathrm{w}}}{A_{\mathrm{pile}}} = 1 - \left(\dfrac{D_i}{D}\right)^2$

A_{w} cross-sectional area of pile annulus, $A_{\mathrm{w}} = \dfrac{\pi}{4} \cdot \left(D^2 - D_i^2\right)$

A_{s} side surface area of pile in soil

C_1, C_2, C_3 dimensionless coefficients determined as function of ϕ', for p–y curves for sand

D pile outside diameter

D_{i} pile inside diameter, $D_{\mathrm{i}} = D - 2\ WT$

D_{50} mean soil particle diameter

D_{CPT} diameter of CPT tool, D_{CPT} = 36 mm for a standard cone penetrometer with a cone area of 1 000 mm^2

D_{r} relative density of sand, for CPT-based methods 1 and 4

E_{S} initial modulus of subgrade reaction

f unit skin friction

$f(z)$ unit skin friction at depth z

$f_{\mathrm{c}}(z)$ unit skin friction in compression at depth z

$f_{\mathrm{p}}(z)$ unit skin friction between sand soil plug and inner pile wall, for CPT-based method 4

$f_{\mathrm{t}}(z)$ unit skin friction in tension at depth z

f_{lim}	limiting unit skin friction value
h	distance above pile tip = $L - z$
J	dimensionless empirical constant, for p–y curves for clay
k	initial modulus of subgrade reaction, for p–y curves for sand
K_0	coefficient of lateral earth pressure at rest
L	embedded length of pile below original seafloor
L_{s}	length of soil plug in sand layers
N_{q}	dimensionless bearing capacity factor
p	mobilised lateral resistance~~,~~ for lateral soil resistance-displacement relationships (p–y curves)
p_{a}	atmospheric pressure (p_{a} = 100 kPa)
$P_{\mathrm{d,e}}$	design value of axial action on the pile, determined from a coupled linear structure and nonlinear foundation model using the design actions for extreme conditions
$P_{\mathrm{d,p}}$	design value of axial action on the pile, determined from a coupled linear structure and nonlinear foundation model using the design actions for permanent and variable actions or the design axial action for operating situations
p_{fa}	mobilised lateral soil resistance-displacement relationships for fatigue analysis after the soil unload-reload secant stiffness and hysteretic damping have stabilized (p_{fa}-y_{fa} curves)
P_{o}	pile outer perimeter = πD
p_{mo}	mobilised lateral soil resistance-displacement relationships under monotonic lateral loading (p_{mo}-y_{mo} curves)
p_{r}	representative value of lateral capacity, for p–y curves, in unit of force per unit length of pile
p_{rd}	representative value of deep lateral capacity, for p–y curves, in unit of force per unit length of pile
p_{rs}	representative value of shallow lateral capacity, for p–y curves, in unit of force per unit length of pile
$p'_{\mathrm{m}}(z)$	*in situ* effective mean stress at depth z
q	unit end bearing at pile tip
$q_{\mathrm{c}}(z)$	CPT cone resistance at depth, z, in stress units
$q_{\mathrm{c,f}}(z)$	reduced CPT cone resistance at depth, z, to account for general scour
$q_{c,av,1,5D}$	average value of $q_{\mathrm{c}}(z)$ between 1,5 D above pile tip and 1,5 D below pile tip
$q_{\mathrm{c,tip}}$	CPT cone resistance at pile tip
Q	mobilised end bearing capacity in Q–z curves
$Q_{\mathrm{f,c}}$	skin friction capacity in compression
$Q_{\mathrm{f,t}}$	skin friction capacity in tension
$Q_{\mathrm{f,i,clay}}$	cumulative skin friction capacity of clay layers within soil plug, for CPT-based method 3
Q_{lim}	limiting unit end bearing value
Q_{p}	end bearing capacity
Q_{r}	representative value of axial pile capacity

$Q_{r,c}$	representative value of axial pile capacity in compression
$Q_{r,t}$	representative value of axial pile capacity in tension
s_u	undrained shear strength
$s_u(z)$	undrained shear strength at depth z
WT	pile wall thickness
t	mobilised skin friction for axial shear transfer t–z curves
t_{max}	maximum skin friction for axial shear transfer t–z curves
t_{res}	residual skin friction for t–z curves
y	lateral pile displacement, for p–y curves
z	depth below original seafloor
z	local pile axial displacement, for axial shear transfer t–z curves
z	axial pile tip displacement, for Q–z curves
z_R	depth below seafloor to bottom of reduced resistance zone, for p–y curves for uniform clays
z'	final depth below seafloor, after general scour
z_{peak}	axial pile displacement at which maximum soil-pile skin friction, t_{max}, is reached, for t–z curves
z_{res}	axial pile displacement at which residual soil-pile skin friction, t_{res}, is reached, for t–z curves
α	dimensionless skin friction factor, for cohesive soils
β	dimensionless skin friction factor, for cohesionless soils
δ_{cv}	constant volume friction angle at sand-pile wall interface
ε_c	strain at one-half maximum deviator stress, for p–y curves for soft clay
ϕ'	effective angle of internal friction of sand, for drained triaxial conditions
γ'	submerged soil unit weight
γ_{pile}	unit weight of pile (steel, concrete, etc.)
γ_{water}	unit weight of water
$\gamma_{R,Pe}$	partial resistance factor for extreme conditions
$\gamma_{R,Pp}$	partial resistance factor for permanent and variable actions for operating situations
Ψ	parameter to determine the dimensionless skin friction factor, for clays = $s_u(z)$ / σ'_{vo} (z) at depth z
$\sigma'_{ho}(z)$	*in situ* effective horizontal stress at depth z
σ'_{vo} (z)	*in situ* effective vertical stress at depth z
$\sigma'_{vo,tip}$	*in situ* effective vertical stress at pile tip
Δz_{GS}	global scour depth
Δz_{LS}	local scour depth
e	base natural logarithms approximately 2,718
ln	natural logarithm (base e)

4.4 Symbols for soil-structure interaction for auxiliary subsea structures, risers and flowlines

D flowline, or pipeline, diameter

f_c dimensionless cyclic factor

f_t dimensionless time factor

f_V dimensionless velocity factor

G_{max} initial elastic (small strain) shear modulus of soil

H lateral (horizontal) soil resistance

K_{max} maximum value of normalized secant stiffness on initial unloading or reloading

I_P plasticity index of soil

k_v secant stiffness of equivalent spring = $\Delta Q / \Delta z$

N integrated normal contact force

N_c dimensionless bearing capacity factor

Q_{smax} maximum suction (uplift) force, per unit length of pipeline

Q_u limiting penetration resistance, per unit length of pipeline

s_u undrained shear strength

s_{uDSS} undrained shear strength in direct simple shear mode

s_{ur} remoulded undrained shear strength

T drained axial resistance per unit length of pipeline

V vertical action on pipeline

z depth to flowline, or pipeline, invert

ΔQ change in vertical force, per unit length of pipeline

Δz change in vertical displacement

Δz_b uplift (break-out) displacement

δ interface friction angle at soil–pipeline interface

μ pipeline–soil friction coefficient

ζ dimensionless enhancement factor

ζ_t dimensionless time factor

ζ_V dimensionless velocity factor

$\theta_{D'}$ half-angle of pipeline–soil contact perimeter

4.5 Symbols for design of anchors for stationkeeping systems

a acceleration of a gravity embedded anchor

A fluke area of a drag anchor

A_{eff} effective area of a plate anchor accounting for shape and projected area

A_{in} plan view inside area of suction anchor pile where underpressure is applied during installation

A_{inside} inside lateral area of suction anchor pile wall

A_p	projected area of a gravity embedded anchor/line
A_{tip}	tip cross-sectional area of an anchor pile
A_{wall}	sum of inside and outside wall areas of an anchor pile
B	fluke width of a drag anchor
C_D	drag coefficient of a gravity-embedded anchor/line
f	coefficient of friction between chain or wire rope and the seafloor
F_b	bearing resistance of a penetrating gravity-embedded anchor/line
F_{drag}	hydrodynamic drag force action on a gravity-embedded anchor/line
F_f	frictional resistance of a penetrating gravity-embedded anchor/line
F_{max}	ultimate holding capacity (UHC) of a plate anchor
FOS_{axial}	factor of safety with respect to axial loading of anchor
$FOS_{combined}$	factor of safety with respect to combined axial and lateral loading of anchor
$FOS_{lateral}$	factor of safety with respect to lateral loading of anchor
H	horizontal action component
H	holding capacity of drag anchor under horizontal action
L	fluke length of a drag anchor
L_{cw}	length of chain or wire rope in contact with the seafloor
m	mass of a gravity-embedded anchor
n	dimensionless holding capacity factor for a drag anchor
N_c	dimensionless bearing capacity factor
P_{cw}	holding capacity of mooring line chain or wire rope
Q_{tot}	total penetration resistance of an anchor pile
Q_{side}	resistance along the sides of an anchor pile
Q_{tip}	resistance at the tip of an anchor tip
S_e	soil strength strain rate factor
S_t	soil sensitivity
s_u	undrained shear strength at the point in question
$s_{u,AVE}$	average undrained shear strength within the failure zone at the design penetration depth, corrected for effects of cyclic loading
$s_{u,tip\ AVE}$	average of triaxial compression, triaxial extension, and DSS undrained shear strength at anchor tip penetration depth
$s_{u,DSS}$	undrained shear strength obtained from direct simple shear tests
t	time
t_r	time of anchor retrieval
v	free-fall velocity of a gravity-embedded anchor
V	vertical action component
W_s	submerged weight of a gravity-embedded anchor

W'	submerged weight of anchor
W'_{cw}	submerged unit weight of chain or wire rope
z	embedment or penetration depth
ΔU_{req}	required underpressure to embed a suction anchor pile
ΔU_{crit}	critical underpressure causing failure of soil plug inside a suction anchor pile
α_{ins}	friction factor during installation of a suction anchor pile or of a gravity-embedded anchor
γ'	submerged unit weight of soil
η	empirical reduction factor accounting for progressive failure of a plate anchor
ρ	fluid density
θ	angle of mooring line at anchor padeye attachment point (measured from horizontal)
θ_{axial}	angle of mooring line at anchor padeye attachment point (measured from horizontal) above which the anchor ultimate capacity is controlled by axial capacity
$\theta_{lateral}$	angle of mooring line at anchor padeye attachment point (measured from horizontal) below which the anchor ultimate capacity is controlled by lateral capacity

4.6 Abbreviated terms

ALS	accidental limit state
BOP	blow-out preventer
CPT	cone penetration test
FEM	finite element method
FLS	fatigue limit state
FOS	factor of safety
PFD	partial factor design
REB	reverse end bearing
SCR	steel catenary riser
SLS	serviceability limit state
SRD	soil resistance to driving
TDP	touch-down point
UHC	ultimate holding capacity
ULS	ultimate limit state
VLA	vertically loaded anchor

5 General requirements

5.1 General

The design methodology inherent to the ISO 19900 set of International Standards is based on the partial factor design (PFD) approach with specified action factors and material factors (see ISO 19900:2019, Clause 9). Requirements regarding partial factors for actions and the combination of actions into design situations are given in the relevant International Standards for offshore structures, i.e. ISO 19900 to ISO 19906.

In some design situations, two representative values can be defined, an upper and a lower value. By using this approach in combination with specified action factors and material factors, geotechnical and foundation designs will result in an offshore structure with a level of reliability in agreement with the requirements of ISO 2394 and ISO 19900.

The material factor for soil can be expressed as the ratio of the representative value of the undrained shear strength to the shear stress mobilised for equilibrium, or as the ratio of the representative value of the tangent of the representative angle of internal friction to the tangent of the angle of internal friction mobilised for equilibrium. The material factor shall not be lower than 1,25. It may be modified by assessing:

a) the consequences of failure;

b) the accuracy of the applied calculation method and the model uncertainty;

c) how the representative strength of the soil material was determined;

d) whether the type of structure is new;

e) whether there is no or little experience with the soil conditions encountered.

The PFD design methodology in this document involves the use of action factors and material factors, which aim to result in comparable overall foundation reliability with that achieved from the use of the working stress design (WSD) methodology in API RP2GEO [22]. For shallow foundations, this comparison is outlined in References [191] and [95], which highlights that broadly comparable foundation size should be obtained to resist a given set of representative values of actions from either method. Although the design recommendations are largely aligned in this document and API RP2GEO [22], the PFD or WSD methods can lead to differences in the design outcome.

The design shall account for static, cyclic, and dynamic actions without causing excessive deformations or vibrations in the structure. The design shall address the possibility of movement of the seabed and any actions resulting from such movements on the structure. The potential for disturbance to foundation soils by conductor installation or shallow well drilling shall be assessed (see 8.7.12).

The guidance herein does not necessarily apply to unconventional soils such as carbonate material (see 6.3), volcanic sands or highly sensitive clays.

5.2 Design cases and safety factors

The design cases that shall be addressed with the corresponding values of partial action factors are given in:

— ISO 19902 for fixed steel offshore structures;

— ISO 19903 for fixed concrete offshore structures;

— ISO 19904 and ISO 19901-7 for floating offshore structures;

— ISO 19905 (all parts) for jack-ups;

— ISO 19906 for arctic offshore structures.

The resistance factors applicable to the design of pile foundations are given in 8.1.1. The material factors applicable to the design of shallow and intermediate foundations designed with the PFD approach are given in 7.3.1 and 7.3.3. In assessing the stability of shallow and intermediate foundations with the PFD approach, the design value of resistance is computed by applying a material factor to the representative soil strength. This differs from the practice for design of piles, where a resistance factor is applied to the representative foundation capacity.

Specific requirements, design procedures and criteria under dynamic actions from earthquakes are given in ISO 19901-2.

5.3 Representative and design values of soil parameters

5.3.1 Generic principles

This subclause provides generic principles and guidelines for selecting representative and design values of soil parameters, in line with the partial factors format or partial factor design (PFD) approach. The term 'soil' is used as per ISO 2394 and ISO 19900. This term is equivalent to 'seabed' defined in 3.17 and in ISO 19901-8 and ISO 19901-10.

Estimation of the representative and design values for soil parameters typically considers the following:

— the extent and quality of soil investigation and possible environmental factors;

— *a priori* knowledge, such as geological information and physically credible values;

— the measurable physical quantities that correspond to the population of soil parameters considered in the calculations;

— the appropriate factors or transformation functions, to convert the parameters obtained from laboratory and/or *in situ* tests or other methods to soil parameters;

— the assumptions in the calculation method(s);

— the uncertainties in the soil parameters.

Additional guidance on the selection of the representative value and uncertainties is given in 5.3.2 and A.5.3.

5.3.2 Determination of representative and design values of soil parameters

For soil parameters, the determination of the representative value and design value shall include all relevant available data for a site, such as:

— geological information;

— study of depositional processes and stratigraphy;

— results of *in situ* tests, including geotechnical and geophysical investigations (refer to ISO 19901-8 and ISO 19901-10);

— results of laboratory tests;

— results of physical model tests;

— reliable correlations (general or regional) for similar soils under similar geological settings and similar stress conditions;

— data from design tables;

— experience and expert opinions.

Figure 2 schematizes the steps for the selection of a representative value and the corresponding design value. The columns in the figure present the sources of data or information, the measurements made, obtaining derived values and obtaining the representative value and the design values. The uncertainties associated with the steps in the determination of the soil parameters are listed, although the list is not exhaustive. A design will usually require more than one basic variable and more than one representative value.

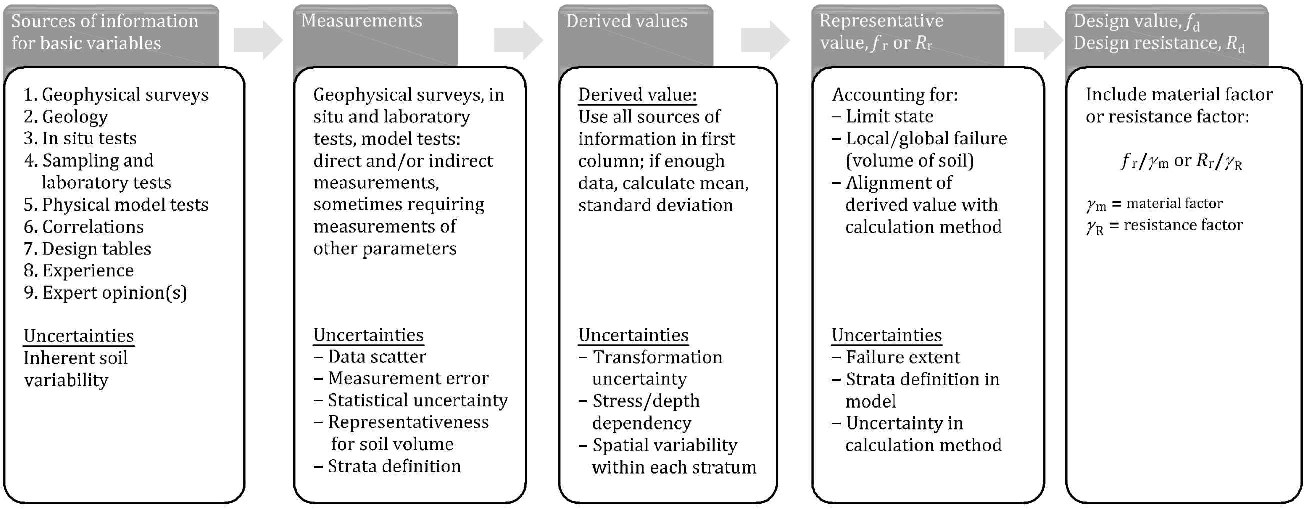

Figure 2 — Steps in selection of a representative value and design value for soil parameters

When there are enough data available, statistical analyses may be used to estimate the mean and standard deviation (uncertainty) of the derived values for key soil parameters for a design or calculation. When combining data from different sources, statistical methods, such as Bayesian updating, can be used to assess the uncertainty in the derived values of the soil parameters.

The representative value to use in the verification of a limit state in a design situation:

— is an estimate of the value(s) affecting the occurrence of the limit state which accounts for uncertainty;

NOTE 1 The uncertainty to be covered by the selection of a representative value is that of the soil parameters governing the limit state, where the uncertainty is due to both lack of knowledge and the natural and spatial variation of a parameter.

— accounts for the extent of the ground volume involved in the limit state, the effects of time, brittleness, soil fabric and structure, and construction processes;

— accounts for transformation of data to the reference scale of the soil parameter required for verification of the limit state, where applicable;

— is not one particular fractile of the results of laboratory tests or *in situ* tests on soil specimens.

NOTE 2 If statistical values in multiple parts of the volume of soil affecting the limit state are available, the representative value can be selected with a 95 % degree of confidence.

— considers both project-specific information and a wider body of geotechnical knowledge and experience;

— encapsulates the designer's expertise and experience.

As an example, when the average value of the soil strength over a large soil volume governs the design of a foundation (e.g. axial capacity of long friction piles), the representative value can be taken close to the mean shear strength value because of the larger scale variations over the volume. When foundation resistance involves a smaller volume of soil (e.g. end bearing of a pile), the representative value is usually defined below the mean value.

The following guidance is presented for selection of a representative value where estimates of the mean and standard deviation of a soil parameter are available for a uniform soil stratum [205][206][224]:

— When the representative value is based on laboratory or few discrete *in situ* data, the representative value can be selected as a value close to the mean ± 0,5 SD, where SD is the standard deviation, for conditions where the limit state depends on the parameter value averaged over a large volume of ground (i.e. a mean value). For a smaller volume of ground involved in the limit state, the representative value can be selected at about the mean ± 1 SD, where SD is the standard deviation.

— When the representative value is based on nearly continuous CPT/CPTU data, and the cone resistance is used directly to compute soil resistance (e.g. for the calculation of pile capacity in sand), the representative value of the cone resistance can be taken close to the mean value, at a value of, for example, mean ± 0,15 SD. When the cone resistance is used through a transformation of the measurement into (e.g. a shear strength), the transformation introduces additional uncertainty that can be accounted for by the selection of a representative value with a larger standard deviation.

Local data, engineering experience and engineering judgment may support selection of values different than those suggested by the above guidance.

The design value is obtained by applying the material factor or the resistance factor for the calculation in question (see Figure 2). The selection of representative value does not require further adjustment of the resistance factors and material factors that are given in 7.3.1, 7.3.3 and 8.1.1.

For soils, the representative value for stability is often different than the representative value for installation (e.g. pile driving). In such cases, the representative value should be selected according to the conditions that are critical for a limit state.

For spring stiffness, lower and higher values can lead to different stresses in a structure. This implies multiple design/assessment situations, each of which require selection of appropriate representative values for soil spring stiffnesses. In many cases, a mean value, and not a cautious value, is the most appropriate as input for the structural analysis. For fatigue limit state, a value lower or higher than the mean is more appropriate.

5.3.3 Geotechnical reliability-based design

The documentation of appropriate levels of performance can be achieved for geotechnical structures and foundation by the limit state verification described in this document. Appropriate levels of performance can be alternatively documented with a reliability-based approach.

The goal of geotechnical reliability-based design (RBD) is to achieve a more uniform level of reliability than that implied in existing limit state verification approaches. Reliability-based design is particularly suitable for the representation of multiple conditions and failure modes and can account for the uncertainties found in geotechnical analysis and design. The process of using an RBD approach can give a better overall understanding of the sensitivity of the outcome to different inputs, assumptions and uncertainties. The reliability approach is well suited for comparing the safety of similar structures and for assessments during the lifetime of an installation. Methods for geotechnical RBD analyses can be found in References [21] and [37].

As a complement to the limit state verification, reliability-based approaches can be used to estimate a reliability level, described with an annual reliability index and annual failure probability, to document a margin of safety.

Reliability-based analyses should include an assessment of all the uncertainties in Figure 2. Additional required inputs for the reliability analysis are the probability distributions of the (1) soil parameter values, (2) loading cases, (3) geometry, and (4) method uncertainty. The identification of the appropriate probability distributions and their mean and standard deviation from limited data also introduces uncertainties that need to be addressed.

Additional guidance on representative values of soil properties is given in A.5.3.

5.4 Testing and instrumentation

Testing and instrumentation can be undertaken to resolve or narrow uncertainty in the behaviour of structures. Stakeholders can conclude that testing and instrumentation are required, if conditions outside industry experience are encountered and safety and economy are of particular concern.

Possible testing and instrumentation methods include the following:

a) Loading tests, model tests and field tests

Loading tests, model tests and large-scale field tests can be performed to address particular uncertainties in the geotechnical capacity and performance, for example where:

— the structure configuration differs significantly from earlier configurations where operational experience exists;

— the soil conditions differ significantly from those where operational experience exists;

— new methods of installation or removal are envisaged;

— a high degree of uncertainty exists as to how the structure or its foundation will behave.

b) Temporary instrumentation

The structure can be fitted with temporary instrumentation where:

— the installation method presupposes the existence of measured data for control of the operation;

— an installation method is to be applied with which little or no experience has been gained.

c) Permanent instrumentation

The structure can be fitted with permanent instrumentation where:

— the safety or behaviour of the structure is dependent on active operation;

— the structure configuration, the soil conditions, or the actions differ substantially from those with which experience has been gained;

— there is a need for monitoring the whole structure with regard to penetration, settlement, tilt, or other behaviour;

— the method of removal presupposes the existence of measured data for control of the operation.

6 Geotechnical data acquisition and identification of hazards

6.1 General

The determination of the values of geotechnical parameters, and the assessment of geological hazards and constraints result from an integrated study of the area using desk study, geophysical and geotechnical surveys and interpretation.

Additional guidance is provided in A.6.1, detailed guidance is provided in ISO 19901-8 and ISO 19901-10.

6.2 Geological modelling and identification of hazards

6.2.1 General

In cases where potentially active geological hazards are identified and future activity can impact proposed facilities, the nature, magnitude and return intervals of these active geological processes shall be evaluated. Site investigation techniques, specialized laboratory testing and analytical modelling can be employed to provide input for quantification of the probability and effects of active geological processes on structures and foundations. Due to uncertainties associated with definition of these processes, a parametric approach to studies can be helpful in the development of design criteria.

6.2.2 Assessment of site geohazards

Most familiar geological hazards with potential design consequences for planned facilities comprise:

— Earthquakes: Areas are considered seismically active on the basis of the historical record of earthquake activity, both in frequency of occurrence and in magnitude, or on the basis of a tectonic review of the region. more details are provided in ISO 19901-2.

— Fault planes: In some offshore areas, fault planes can extend to the seafloor with the potential for vertical and horizontal movement.

— Seafloor instability: Movements of the seafloor can be caused by ocean wave pressures, earthquakes, soil self-weight, hydrates, shallow gas, faults, salt tectonics and other geological processes.

— Scour and sediment mobility: Scour is the removal of seabed soils by currents, waves and ice. Such erosion can be due to a natural geological process or caused by structural components disrupting the natural flow regime above the seafloor. Scour can result in removal of vertical and lateral support for foundations, causing undesirable settlements of shallow foundations and overstressing of attached components. Where scour potential is identified, it shall be accounted for in design or through mitigation [see A.8.1.4.1.2 item c) and A.8.5.6].

— Shallow gas: The presence of either biogenic or petrogenic gas in the pore water of shallow soils can be an important consideration in geotechnical design.

— Seabed subsidence: The nature of the soil conditions and the reservoir and extraction processes should be investigated to establish whether subsidence of the seabed is likely to occur during the field life.

Additional guidance is provided in A.6.2 and in ISO 19901-10.

6.3 Carbonate soils

6.3.1 General

When performing site investigations in frontier areas or areas known or suspected to contain carbonate material, the investigation should include diagnostic methods to determine the existence of carbonate soils. Particularly in sands and silts that contain in excess of 15 % to 20 % carbonate material, foundation or seabed structure behaviour can be adversely affected and a field and laboratory testing programme shall characterise these specific sediments (see A.6.3 and ISO 19901-8). Additional guidance is provided in A.6.3.1.

6.3.2 Characteristic features and properties of carbonate soils

For site characterization, use of local experience is important, particularly in the selection of an appropriate soil investigation and testing programme. In new unexplored waters, where the presence of carbonate soils is suspected, selection of an *in situ* test programme should draw upon any experience with carbonate soils where geographical and environmental conditions are similar. Additional guidance is provided in A.6.3.2.

6.3.3 Foundations in carbonate soils

6.3.3.1 Driven piles and other deep foundation alternatives

Several case histories describe some of the unusual characteristics of foundations on carbonate soils and their often poor performance. Numerous pile loading tests have shown that piles driven into weakly cemented and compressible carbonate sands and silts mobilise only a fraction of the capacity (<15 %) predicted by design and prediction methods for siliceous material.

Piles installed by driving in carbonate soils have experienced free-fall at stab-in, under hammer weight or during the driving process. The possibility of pile free-fall shall be assessed and mitigation measures, such as the use of pile arrestor or other method to reduce the speed of or arrest free-fall, shall be addressed.

Dense, strongly cemented carbonate deposits can provide a very competent foundation material, but difficulty in obtaining high-quality samples and the lack of generalized design methods can make it difficult to predict where problems can occur. Clays where the carbonate content exceeds 50 % and for which no pile test data or local experience exists can be challenging.

Additional guidance is provided in A.6.3.3.1.

6.3.3.2 Shallow foundations

Shallow foundations are suitable for use on carbonate sediments. The important differences between carbonate sediments and silica sands or non-carbonate clays shall be characterized and their effects shall be addressed in design.

Shallow foundations can be attractive for carbonate sediments that exhibit a significant degree of cementation, since they give high bearing capacities, good resistance to cyclic actions and low potential for settlements. However, layered profiles of variably cemented and un-cemented sediments can introduce the risk of a punch-through type of failure.

Additional guidance is provided in A.6.3.3.2.

6.3.3.3 Assessment

To date, general design procedures for foundations in carbonate soils are not available. Acceptable design methods have evolved but remain site-specific and dependent on local experience. Additional guidance is provided in A.6.3.3.3.

7 Design of shallow and intermediate foundations

7.1 General

Shallow foundations in the context of this document include foundations placed directly on the seabed without embedment and embedded foundations with a maximum embedment of half the shortest plan dimension, i.e. an embedment ratio of up to 0,5. Intermediate foundations in the context of this document behave essentially rigidly when laterally loaded such that plastic hinges typically do not form in the steel structure of the foundation; as can be the case for longer more flexible piles that are addressed in Clause 8. Intermediate foundations are typically embedded into the seabed with an embedment between 0,5 and 10,0 times the shortest plan dimension, i.e. embedment ratios between 0,5 and 10,0.

The limits on embedment ratios stated here are indicative and there is some overlap in the foundation behaviour and design methodologies that can be applicable to shallow foundations, intermediate foundations and piles. More important is the actual behaviour of the foundation, which should be assessed by considering aspects such as the foundation dimensions, soil conditions, installation method and applied loading. A shallow foundation is typically designed considering ‘surface’ failure mechanisms, i.e. failure mechanisms that reach the seafloor while an intermediate foundation can be designed against mechanisms that involve both surface and confined (below the seafloor) aspects. Idealized failure mechanisms and action interaction for shallow foundations, intermediate foundations and pile foundations are illustrated in Figure 3. The simplified shallow and intermediate design methodology presented here typically assumes rigid foundation behaviour. Where there is uncertainty over the behaviour of the foundation, and the classification of foundation behaviour in terms of shallow, intermediate or pile, advanced analyses techniques, such as finite element analyses, should be used to ensure that the foundation behaviour is understood.

Guidance in this clause relates to foundations for fixed structures, whether subsea or surface piercing. Examples include shallow and intermediate foundations for surface piercing concrete gravity based structures, steel jacket structures, minimum structures, monotowers; and shallow and intermediate foundations for subsea structures, including manifolds, overtrawl structures, inline structures, pipeline end termination structures and holdback anchors for subsea structures. Foundations are considered in Clause 10 for riser towers and in Clause 11 for floating facilities. A range of structures for which the shallow and intermediate foundations considered in this clause can apply are illustrated in Figure 4. Foundations in this clause can be temporary (e.g. a construction aid during piling) or the main permanent foundation.

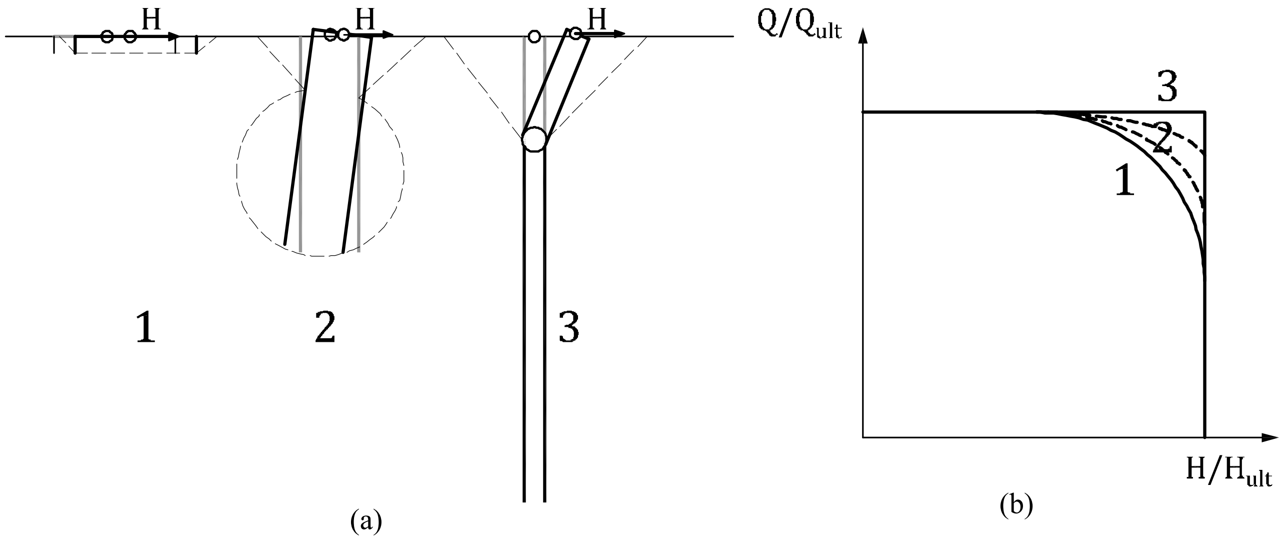

Key

1 Shallow foundation
2 Intermediate foundation
3 Pile foundation, excluding H-Q interaction

Figure 3 — Illustration of (a) failure mechanisms and (b) loading interaction of shallow foundations, intermediate foundations and flexible piles

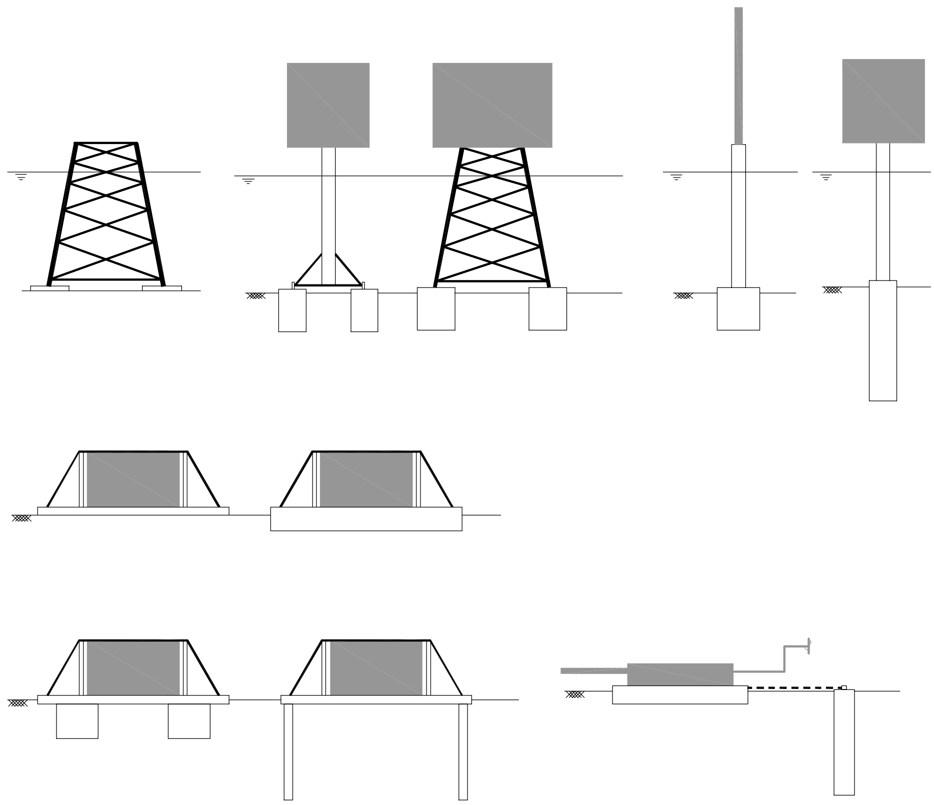

Figure 4 — Illustration of foundation types and applications considered in Clause 7

The formulae presented for evaluating the installation resistance, ultimate limit state (stability) and serviceability limit state (displacement) of shallow and intermediate foundations given are based on solutions for simple soil profiles and idealized soil response, i.e. uniform or linearly increasing strength or stiffness with depth and fully drained or undrained soil response. The formulae shall only be applied to conditions similar to those for which they were derived or for which they can be shown to be applicable.

The methods presented are intended for combinations of dead action, variable live action and environmental action (i.e. wind, wave, current and ice). Where these arise from transient or cyclic actions, they are considered as quasi-static actions. Dynamic actions involve inertial effects (mass-acceleration) and can be monotonic (e.g. ship impact) or cyclic (e.g. seismic). Other cyclic actions involve repetitive loading in which inertial effects are insignificant (e.g. some environmental actions and thermal actions). In some cases, cyclic actions can be considered as pseudo-static and assessed using the calculations outlined in 7.4 (e.g. current loading is often considered as pseudo-static). However, the methods in this clause do not necessarily apply to more complex dynamic loading conditions, such as where the inertia of the structure or foundation soils is important (e.g. seismic loading).

This clause considers verification of limit states governed by soil behaviour and excludes verification of structural integrity of the foundation (steel jacket integrity is covered by ISO 19902). More detailed assessment can be performed for structures sensitive to foundation stiffness.

For large concrete gravity base structures and mobile offshore units, the requirements in this clause shall be supplemented and modified by requirements given in ISO 19903, ISO 19905-1 and ISO/TR 19905-2.

7.2 Principles

7.2.1 General principles

The following general principles shall be adopted in assessing shallow and intermediate foundations:

a) Foundation stability shall be analysed by ensuring equilibrium between design actions and design resistance. Where the possibilities of excessive displacement and deformation of the foundation soil are identified, and where these are critical, more complex analysis approaches than presented in this clause can be appropriate.

b) Calculations using alternative methods of analysis shall be justified.

c) Design actions shall be determined with consideration of the design life of the foundation;.

d) Undrained calculations shall be adopted where no drainage, and hence no dissipation of excess pore pressures, occurs during loading. This can occur as a result of the rate of loading or the impermeable nature of the soil. In contrast, drained calculations shall be adopted where no excess pore pressures arise during loading. Analysis of foundations subject to partial soil drainage during the loading event is not addressed in this clause.

e) design may be based on serviceability (rather than stability) criteria, whereby the deformation of the foundation is assessed against allowable movement criteria. The appropriateness of adopting this approach will depend on the type of structure. The selection of appropriate soil moduli (especially considering strain dependency) is essential in calculation of serviceability limit states.

7.2.2 Foundation embedment

Embedment of shallow and intermediate foundations is typically provided by peripheral vertical ‘skirts’ that penetrate the seabed beneath the foundation top plate. The confined soil within the skirts is typically called the ‘soil plug’. The presence of the skirts will in most cases (i) increase foundation stability, (ii) decrease foundation deformation, and (iii) reduce impact of seabed scour on the foundation. The term ‘skirts’ is used for both shallow and intermediate foundations.

Internal skirts may be provided to increase stiffness of the foundation plate and provide against a soil failure mechanism developing within the soil plug. Stability assessment based on loading at skirt tip level shall verify that an internal failure mechanisms does not form within the skirted compartment, which can lower the overall capacity. Minimum skirt spacing is covered in 7.4.2. Stiffeners may be provided along or around the skirt to increase stiffness of the embedded portion of the foundation and provide additional resistance against buckling.

The level of skirt penetration after installation shall be verified to be equal to the value assumed in design and foundation performance shall be reassessed if it is different.

Design methods presented assume full skirt penetration. The extent of skirt penetration shall be assessed. Installation resistance is covered in 7.87.8 and shall be assessed. Additional geotechnical/structural assessment is required to verify foundation performance in the event full skirt penetration is unachievable and no measure is taken to ensure full penetration.

Examples of embedment configuration for skirted shallow and intermediate foundations are illustrated in Figure 5.

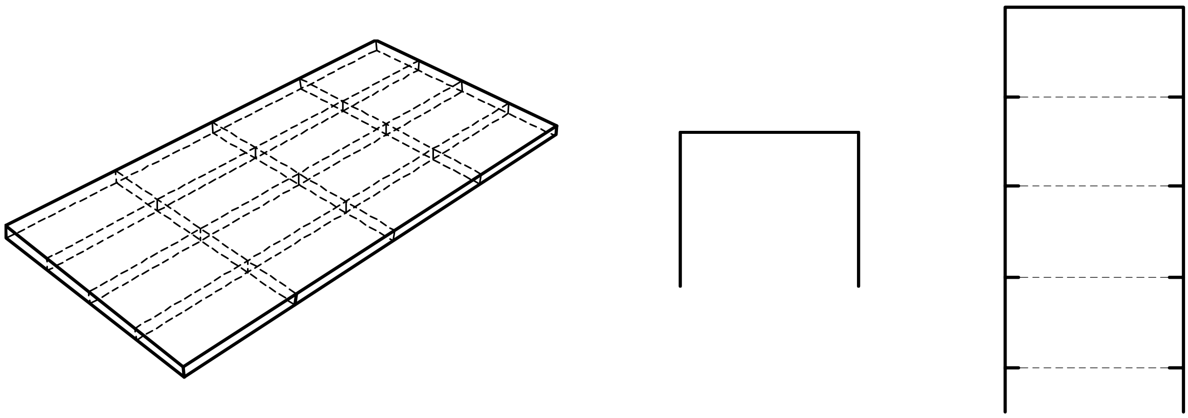

(i) without skirt stiffeners **(ii) with skirt stiffeners**

(a) skirted shallow rectangular mudmat with peripheral and internal skirts **(b) intermediate foundation**

Figure 5 — Example of embedment configuration

Embedment of shallow foundations has historically been idealised by considering a surface foundation at foundation level (i.e. the level of the base of the foundation which is taken as the level of the tip of the skirts) as shown in Figure 6. Soil material properties relevant to foundation level are adopted, overburden stress is considered, and factors are applied to account for additional resistance due to the embedment. This is the case for the formulae presented in 7.5. Seafloor actions shall be transferred to skirt tip level, as described in A.7.2.3.

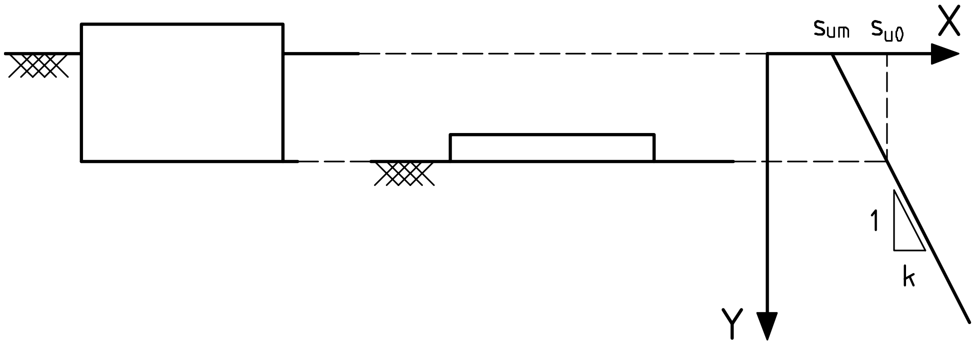

Key

X	undrained soil strength, s_u	s_{u0}	undrained strength at skirt tip
Y	depth below seafloor, z	k	gradient of undrained strength increase with depth
s_{um}	undrained strength at the seafloor		

Figure 6 — Idealization of embedded shallow foundation for conventional design approach

7.2.3 Sign conventions, nomenclature and action reference point

Vertical (Q), horizontal (H), overturning (M) and torsional (T) actions are centric and act at a reference point (RP) taken as the midpoint of the foundation at seafloor level as illustrated in Figure . This is the point of structural action transfer. H and M can be co-planar.

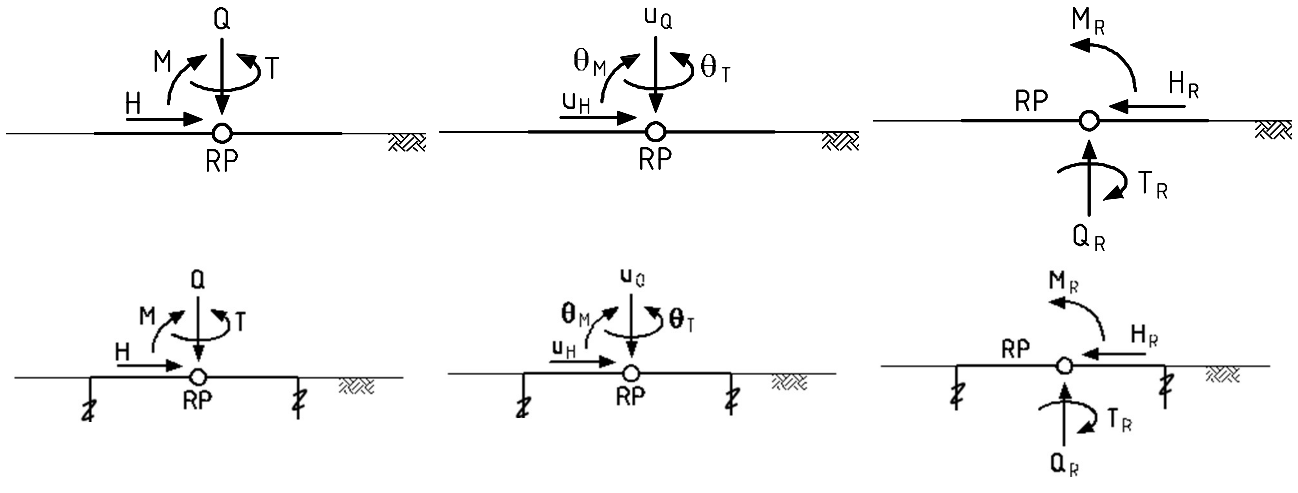

(a) **(b)** **(c)**

Figure 7 — Sign conventions, nomenclature and reference point for analysis of shallow and intermediate foundation (a) actions, (b) displacements and rotations, (c) seabed resistance

7.3 Acceptance criteria

7.3.1 Material and action factors

When assessing accidental limit state, the design soil strength may be determined using a material factor γ_m = 1,0 in accordance with ISO 19900.

When assessing ultimate limit state (stability), the following provisions apply:

a) The design soil strength shall be determined using a minimum material factor γ_m = 1,25 except as indicated in Clause A.7. Increasing the material factor can be warranted where geotechnical data are sparse or site conditions are uncertain, or where uncertainty exists in relation to potential failure mechanisms or methods of analysis.

b) Partial action factors, γ_f, shall be determined based on guidance from the relevant standard of the ISO 19900 series. The weight of the soil, including the soil plug within skirts, should normally be calculated with factors equal to unity (see 7.4.1) if it contributes to the total action. In some situations, an action factor below or above 1,0 may be justified;

c) Action factors for subsea and flowline related structures shall follow the same requirements as those of fixed steel offshore structures, unless specified otherwise. Performance based design approaches may be used to justify specification of lower action factors. Further advice is provided in 7.7.2.

d) Action factors and material factors shall be applied with consistency throughout the design process, respecting the physics of the loading scenario.

When assessing serviceability limit state (displacements), the following provisions apply:

a) All action and material factors may be set to unity when calculating displacements as part of a serviceability assessment. However, where foundation displacement can lead to unacceptable consequences or governs design, factors other than unity may be used.

b) Imposed deformations from external connected objects can impose or induce high actions on the foundation, or vice versa, deformation of the foundation can induce high actions because of the infrastructure it is connected to. It can be acceptable to select reduced partial action factors to characterize the imposed loading, if the incremental deformations are small and have been robustly characterized. Further guidance is provided in 7.7.2.

7.3.2 Use of partial factors in design

A soil resistance envelope, incorporating material factors can be developed with the formulae presented in 7.5 or with numerical methods. Examples of failure envelopes for undrained and drained conditions are presented in Figure 8. Once an envelope is derived, the design actions incorporating partial action factors can be transposed onto this envelope to verify conformance with this document.

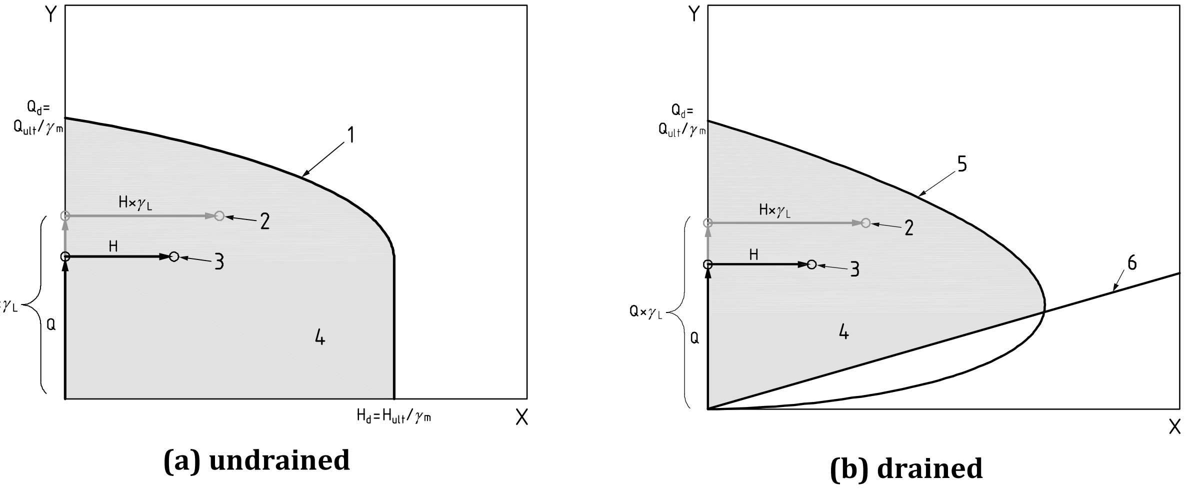

Key

1	envelope of design resistance under undrained bearing/sliding	5	envelope of design resistance under drained bearing
2	design value of action	6	envelope of design resistance under drained sliding
3	applied action	X	horizontal action
4	allowable design actions	Y	vertical action

Figure 8 — Soil resistance envelopes and definition of design actions under (a) undrained and (b) drained conditions

7.3.3 Special cases

For assessment of foundation stability during set-down on the seabed, stability may be assessed based on the applied vertical actions. In this case, the ultimate limit state shall be calculated using a material factor of $\gamma_m = 1,5$. The increased material factor in this case leads to an increased margin of safety against bearing failure during set-down and reduces the settlement and embedment of the foundation into the seabed.

7.4 Design considerations

7.4.1 Adjusting for soil plug weight

The general formulae presented to calculate ultimate limit state (stability) of shallow and intermediate foundations assume there is no difference in the depth of soil inside and outside foundation skirts. In this condition, the soil plug weight is offset by the pressure supplied by the external soil and does not contribute to the total action. However, in some cases the soil height above skirt tip level can be higher inside the skirt than outside the skirt, such as where significant scour has occurred or where significant plug heave has occurred, or lower inside the skirt than outside the skirt, such as where the foundation (base plate and skirts) has penetrated deeper than the depth of the skirts.

In cases where a significant difference exists, the design vertical action may be adjusted by:

$$\frac{\Delta Q}{A} = (p'_{\text{in}} - p'_{\text{out}}) \quad (1)$$

where

ΔQ is the change in design vertical action to account for differences in vertical effective stress at skirt tip level, in which the factor for soil weight is generally equal to unity;

p'_{in} is the *in situ* effective overburden stress at skirt tip level inside the skirts (taken as $\gamma' z_{in}$, where γ' is the submerged unit weight of soil and z_{in} is the depth of soil inside the skirts);

p'_{out} is the *in situ* effective overburden stress at skirt tip level outside the skirts (taken as $\gamma' z_{out}$, where z_{out} is the depth of soil outside the skirts);

A is the actual cross-sectional plan foundation area.

A similar method can be used for embedded shallow foundations without skirts.

7.4.2 Skirt spacing

Skirts can be used on subsea foundations to:

— develop sufficient sliding capacity (especially as seafloor strengths are often low, and difficult to measure);

— protect foundation performance against undermining due to scour.

When skirts are used to develop sufficient sliding capacity, the designer may consider two options:

1) Use of internal and external skirts to the extent that the sliding failure mechanism is that of skirt tip sliding;

2) Acceptance of failure mechanism rising above skirt tip level, if the combination of sliding resistance inside the compartment and flow around the embedded members is sufficient to satisfy overall sliding capacity requirements.

When sliding is at skirt tip level, the number of internal skirts required will depend on the soil condition (e.g. seafloor strength, strength variation with depth, effects of soil consolidation), boundary conditions (e.g. drainage state of foundation underside) and loading condition (e.g. time between foundation installation, and design loading application, time-varying characteristics of the applied operational action).

Guidance on skirt spacing is provided in A.7.4.2.

When stiffeners are adopted, their effect on penetration resistance shall be assessed.

7.4.3 Foundation base perforations

Permanent or temporary perforations, in the foundation base plate are often used to:

— assist in loading out the structure through the splash zone without dynamically overloading of the associated load-out rigging;

— assist the approach of the structure to the seabed without hydraulic/hydrodynamic instability;

— assist in preventing the seabed from being unduly impacted by scour or local bearing failure.

Perforations can also be used to increase the rate of soil consolidation and settlement, and to facilitate removal of the foundation, either to allow repositioning or for end of life decommissioning.

Specific guidance is not provided on the ratio or distribution of top plate perforations. However, effects of perforations on stability shall be addressed in cases where the total area of permanent perforations exceeds 5 % of the base plate area.

References for guidance on foundation base perforations are provided in A.7.4.3.

7.4.4 Skirtless foundations penetrating into soft soils

In soft soils (e.g. normally consolidated clays), shallow skirtless foundations can penetrate into the seabed to the depth at which the soil bearing resistance is in equilibrium with the applied action, which implies no additional margin of safety. Incremental settlements under additional permanent actions, if any, should be addressed. Allowable differential settlement of the structure will depend upon the type of structure and its installation, and should be subject of a risk assessment. Adequate precautions should be taken to minimize differential settlements between foundations. Good practice should ensure that there is an acceptable limit to the penetration.

If the foundation is required to provide permanent support, normal practice is either to use skirts to transfer actions to deeper (more competent) soils to increase foundation area, or to preload the structure to ensure that the foundation stability requirements under the design scenario are met.

7.4.5 Tensile stresses beneath foundations

Reliance on tensile stresses (relative to ambient water pressure) beneath foundations that rest on the seafloor without embedment shall be avoided, because of the potential disturbance to the underlying seabed due to pumping scour, an erosional mechanism whereby rapid movement of water can lead to undermining of the foundation.

Skirted shallow foundations (except those with perforated mudmats) can resist transient tension through generation of negative excess pore pressures between the confined soil plug and underside of the foundation top cover. Cyclic tensile stresses (relative to ambient water pressure) from waves with a few seconds duration may be demonstrated as acceptable in design, while longer duration tensile stresses can be carried by skirted foundations on clays with low permeability. Reliance on tensile stresses beneath a shallow foundation shall be validated with advanced methodologies, which are not explicitly addressed in this subclause.

The design shall address the level of contact between the soil and the underside of the top plate and the value of any post installation measures (e.g. grouting) to establish contact. The design shall address whether or not the foundation top cover will remain sealed for the service life of the foundation, which can influence the mobilization of reverse end bearing.

Uplift capacity may be analysed as a reverse bearing capacity, if the permeability of the soil, drainage paths, duration of action and geometry of the foundation have been demonstrated not to jeopardize the negative excess pore pressures developed during the mobilization of reverse end bearing.

7.4.6 Omni-directional actions

A single loading condition can consist of combined vertical action (Q), lateral action (H), overturning moment (M) and torsion (T), i.e. in all six degrees of freedom, when H and M are co-planar. The design can include many loading combinations.

Under such complex loading conditions, the applicability of effective area approaches, if used, shall be addressed. Yield surface approaches (see 7.7.1) and numerical analyses may be used instead.

7.4.7 Interaction with other structures

Influence of adjacent structures, such as jack-up spudcans or conductors, shall be addressed.

7.4.8 Multiple foundations

For foundations comprising several connected foundations, redistribution of loading between individual foundations generally leads to an improved system performance and may be included. The interaction between foundations can affect foundation capacity, settlement, and rotation and any detrimental effects shall be addressed in the design. Further guidance is provided in A.7.4.8.

7.4.9 Hydraulic stability

7.4.9.1 Scour

Measures to minimize erosion and undercutting of the soil beneath or near the foundation base due to scour shall be addressed where the potential for detrimental impact of scour on the foundation performance has been identified or the effects of erosion are not otherwise accounted for. Possible measures include:

a) using skirts penetrating through erodible layers into scour-resistant soils or to such depths that scour does not reach the foundation base level;

b) placing scour-resistant materials around the edges of the foundation.

Sediment transport studies can be of value in planning and design.

For foundations designed to tolerate erosion of part of or all of the soil above foundation base level, the effect of such erosion on foundation performance and the passive soil resistance along the skirts shall be addressed.

7.4.9.2 Piping

The foundation shall be designed to prevent the creation of excessive hydraulic gradients (piping conditions) in the soil due to environmental actions or operations performed during or subsequent to structure installation.

7.4.10 Unconventional soils or soil profiles

The analysis methods outlined in this document were developed primarily for use in seabed conditions comprising uniform all drained (sand) or all undrained (clay) profiles and shall not be used for unconventional soil conditions, such as:

a) partially drained conditions;

b) cemented material;

c) bedrock;

d) complex soil profiles (e.g. layered and laterally variable);

e) carbonate soils.

The effect of seafloor unevenness shall be addressed.

Surficial crusts of stronger soil overlying weaker soil can be encountered. In such cases, accounting for the surficial crust typically reduces the foundation size. Methods to account for a surficial crust are presented in 7.5.1.5 and A.7.5.1.5.

7.4.11 Selection of soil parameter values for design

7.4.11.1 Shear strength used in stability analysis

Foundation design is strongly dependent on the quality of the site investigation performed and the methods used for determining strength and deformation properties of soils, both *in situ* and in the laboratory. ISO 19901-8 and ISO 19901-10 provide additional information on the requirements and quality of marine soil investigations.

Uncertainty in determining the representative value of shear strength can be significant. These uncertainties are relevant for both drained and undrained shear strengths. The uncertainties shall be addressed in the selection of representative values of parameters (see 5.3, A.5.3 and A.7.5.1.5).

7.4.11.2 Parameters used in serviceability design

Parameter selection for serviceability design should consider the displacement condition being considered. For example, if calculating an upper estimate of settlements, a consistent set of soil parameters should be obtained for the most compressible soil at the site.

If linear elasticity-based calculation methods are used, selection of equivalent linear elastic soil parameters should consider the strain levels that are induced in the seabed as a result of the applied actions.

7.5 Ultimate limit state (stability)

7.5.1 Assessment of bearing capacity of shallow foundations

7.5.1.1 Failure mechanisms

For shallow foundations, bearing failure constitutes any failure mode that can result in excessive combinations of vertical displacement, lateral displacement, or overturning rotation of the foundation; while pure sliding or torsional failure corresponds to a failure mode where the foundation translates or twists only in a horizontal plane.

7.5.1.2 Action transfer

For an embedded shallow foundation action transfer from seafloor to base level (typically skirt tip level for a foundation equipped with skirts) shall be applied in design as described in A.7.2.3.

7.5.1.3 Idealization of foundation area and the effective area concept

The formulae presented in 7.5 for shallow foundations are based on the effective area concept, defined in A.7.5.1.3, which also deals with idealization of the foundation area for use with limit equilibrium methods.

The effective area method is not intended for use with highly compressible or layered soils, or for foundations subject to high overturning moments.

With this method, actions are assumed as acting on the effective foundation area only.

7.5.1.4 Undrained conditions with constant shear strength with depth

In the absence of more definitive criteria, Formula (2) shall be used for determining the design unit bearing capacity for undrained conditions:

$$q_c = N_c \frac{s_u}{\gamma_m} K_c \tag{2}$$

where

q_d is the design vertical bearing resistance, and note that $Q_d = q_d A$;

N_c is the undrained bearing capacity factor, equal to 5,14;

s_u is the representative value of undrained shear strength of the soil;

γ_m is the material factor (see 7.3);

K_c is a correction factor, which accounts for inclined actions, foundation shape, depth of embedment, foundation base inclination and seafloor surface inclination.

Details for calculation of K_c are provided in A.7.

Formula (2) applies to situations with approximately constant undrained shear strength to a depth equal to at least 2/3 of the foundation width.

For a vertical centric action applied to a rough-based foundation at seafloor level where both the foundation base and seafloor are horizontal, Formula (2) is reduced as follows for the following foundation shapes for appropriately factored material shear strength:

a) Infinitely long strip foundation:

$$q_d = 5{,}14 \frac{s_u}{\gamma_m} \tag{3}$$

b) Circular or square foundation:

$$q_d = 6{,}05 \frac{s_u}{\gamma_m} \tag{4}$$

7.5.1.5 Undrained conditions with linearly increasing shear strength with depth

In the absence of more definitive criteria, Formula (5) shall be used for determining design unit bearing capacity for undrained conditions with isotropic undrained shear strength increasing approximately linearly with depth under the foundation.

$$q_d = F\left(N_c s_{u0} + \frac{\kappa B'}{4}\right)\frac{K_c}{\gamma_m} \tag{5}$$

where

- q_d is the design vertical bearing resistance, in which $Q_d = q_d A$;
- F is a correction factor given as function of $\kappa B'/s_{u0}$;
- N_c is the undrained bearing capacity factor, equal to 5,14;
- s_{u0} is the representative value of undrained shear strength of the soil at foundation baseplate level (skirt tip level for skirted foundations);
- K is the rate of increase of the representative value of undrained shear strength with depth;
- B' is the minimum effective lateral foundation dimension (see 7.5.1.3);
- K_c is a correction factor, which accounts for inclined actions, foundation shape, depth of embedment, foundation base inclination and seafloor surface inclination;
- γ_m is the material factor (see 7.3).

Details for calculation of F and K_c are provided in Clause A.7.

7.5.1.6 Undrained conditions with a surface crust overlying linearly increasing shear strength with depth

Bearing capacity of a seabed condition consisting of a surficial crust of undrained shear strength, s_{uc}, over a linearly increasing shear strength, that can be idealized as illustrated on Figure 9, can be estimated as follows.

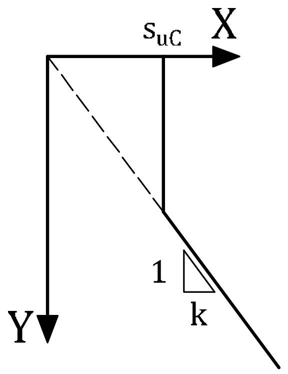

Key

X	Undrained soil strength, s_u	s_{uC}	Undrained strength of crust
Y	Depth below skirt zip, z_{tip}	k	Gradient of undrained strength increase with depth

Figure 9 — Strength profile with surficial crust

The correction factor, F, in Formula (5) is modified by a correction factor to account for a surficial crust, such that:

$$F_m = F_c \times F \tag{6}$$

where

F is the correction factor evaluated for Formula (5)

F_m is the modified correction factor ('F_m' replaces 'F' in Formula (5)), accounting for the surficial crust

F_c is the crust correction factor, detailed in A.7.5.1.6

Under complex loading conditions or more complex crust conditions, the failure envelope parameterisation presented by Reference [134] can be more appropriate.

7.5.1.7 Drained conditions

In the absence of more definitive criteria, Formula (7) shall be used for determining design vertical bearing capacity for drained conditions.

$$q_d = 0{,}5\gamma' B' N_\gamma K_\gamma + \sigma'_{v0}(N_q - 1)K_q \tag{7}$$

where

q_d is the design vertical bearing resistance in the absence of horizontal actions, in which $Q_d = q_d A$;

N_γ, N_q are drained bearing capacity factors, as a function of ϕ';

K_γ, K_q are correction factors that account for inclined actions, foundation shape, depth of embedment, inclination of base, and inclination of the seafloor;

γ' is the representative value of submerged unit weight of soil;

σ'_{v0} is the *in situ* effective overburden stress at foundation baseplate level (skirt tip level when skirts are used, taking care to correct this appropriately as per 7.4.1);

B' is the minimum effective lateral foundation dimension (see 7.5.1.3).

Complete descriptions of the K factors and values of N_q and N_γ as a function of the effective angle of internal friction ϕ', are given in Clause A.7.

Formula (7) has deliberately omitted any component due to an effective cohesion, c', and accompanying bearing capacity factor, N_c. This is mainly because the occasions when it might be appropriate to include a component for bearing capacity due to a presumed effective cohesion are extremely rare. More advice is given in Clause A.7.

For a vertical central action applied to a foundation at seafloor level where both the foundation base and seafloor are horizontal, Formula (7) is reduced as follows for the following foundation shapes:

a) Infinitely long strip foundation:

$$q_d = 0{,}5\gamma' B N_\gamma \tag{8}$$

b) Circular or square foundation:

$$q_d = 0{,}3\gamma' B N_\gamma \tag{9}$$

7.5.2 Assessment of sliding capacity of shallow foundations

7.5.2.1 General

When assessing sliding capacity of foundations, the possible occurrence of discrete layers of low strength soil, which can provide a preferential failure surface, shall be addressed in the site characterization (investigation and interpretation).

When stability has been established using the formulae in 7.6.1, the maximum horizontal capacity shall be limited to that determined for the condition of pure sliding, as defined by Formulae (10) and (11).

If full contact between seabed and foundation is not achieved due to the configuration of the foundation or inadequate skirt penetration or any other reason, the effect on stability shall be assessed.

7.5.2.2 Undrained conditions

In the absence of more definitive criteria, Formula (10) shall be used for determining undrained sliding capacity at the base of a rough foundation (skirt tip level for skirted foundations with appropriate skirt depth to spacing ratio):

$$H_d = \left(\frac{s_{u0}}{\gamma_m}\right) A \tag{10}$$

where

H_d is the design resistance for pure sliding;

s_{u0} is the representative value of undrained shear strength at foundation baseplate level (skirt tip level for skirted foundations);

γ_m is the material factor (see 7.3);

A is the actual cross-sectional plan foundation area.

For undrained cases, where the failure surface occurs between the foundation and soil, a soil friction coefficient, α, ranging from 0 to 1,0 shall be applied to the undrained soil strength at the foundation interface to represent the interface friction. The interface friction can be determined by testing, taking account of the roughness of the underside of the foundation.

The possibility of drained sliding along a sand seam within a competent clay layer should be addressed.

7.5.2.3 Drained conditions

In the absence of more definitive criteria, Formula (11) shall be used for determining drained sliding capacity at the base of the foundation (skirt tip level for skirted foundations with appropriate skirt depth to spacing ratio):

$$H_d = Q\left(\frac{tan\phi'}{\gamma_m}\right) \tag{11}$$

where

H_d is the design resistance of pure sliding;

Q is the factored vertical action during the relevant loading conditions, for which action factors of less than 1 are recommended in cases where increased vertical action has a beneficial effect on the calculated capacity;

ϕ' is the representative value of the effective angle of internal friction;

γ_m is the material factor (see 7.3).

Formula (11) assumes that full soil shear resistance can be mobilized along the interface between the foundation base and the soil (i.e. a fully rough interface is assumed), and that failure does not take place within a shear band (or shear zone) in the soil. If this is not the case, it can be more appropriate to use an interface friction angle (δ) between the foundation soil and the structure rather than the friction angle of the soil (ϕ'). The value of δ accounts for the roughness of the underside of the foundation and can be determined by laboratory testing.

If the failure takes place within the soil (i.e. within a shear band), the sliding capacity becomes also dependent on the soil dilatancy angle. If the dilatancy angle is zero, tan ϕ' should be replaced by sin ϕ'.

7.5.2.4 Horizontal seabed resistance above foundation base level

Skirted or embedded shallow foundations can have increased resistance under pure sliding resulting from soil resistance above skirt tip level. This resistance may be used to offset horizontal actions transferred to the foundation base, such as when calculating inclination factors. All contributions to horizontal resistance from foundation members above foundation base level should be reduced using the material factor given in 7.3.1.

Where installation disturbance or soil conditions can lead to lower resistance from the soil above skirt tip level (e.g. in conditions where soil tension cracking on the active side of the skirt can occur), the reduced resistance shall be accounted for in design.

Where scour potential exists, the effect of scouring shall be addressed in design. The passive resistance offered by the soil in front of the skirt shall be ignored.

Formulae (12) and (13) are for the case where embedded foundations are considered as surface foundations on a reduced seafloor (see Figure 6), and are relevant for a horizontally translating foundation, i.e. without rotation. Rotation of the foundation reduces the mobilizable horizontal resistance.

General formulae for the additional horizontal resistance, ΔH_d, that can be mobilized between seafloor and foundation base level are presented in Formulae (12) and (13). Total horizontal sliding resistance is given by $H_d + \Delta H_d$.

In the absence of more definitive criteria, for undrained conditions, the additional horizontal resistance shall be calculated using Formula (12):

$$\Delta H_d = K_{ru}\left(\frac{s_{u,ave}}{\gamma_m}\right)A_h \tag{12}$$

where

ΔH_d is the horizontal soil resistance due to active and passive earth pressures on foundation skirts;

K_{ru} is the undrained horizontal soil reaction coefficient (see A.7.5.2.4);

$s_{u,ave}$ is the representative value of average undrained shear strength of soil between the seafloor and base level for linearly increasing isotropic undrained shear strength with depth;

γ_m is the material factor (see 7.3.1);

A_h is the vertical projected area of the foundation in the direction of sliding.

In the absence of more definitive criteria, for drained conditions, the additional horizontal resistance shall be calculated using Formula (13):

$$\Delta H_d = K_{rd}(0{,}5\gamma' D_b)A_h \tag{13}$$

where

ΔH_d is the additional horizontal resistance mobilised between the seafloor and foundation base level;

K_{rd} is the drained horizontal soil reaction coefficient, which includes the material factor (see A.7.5.2.4);

γ' is the representative value of the average submerged unit weight of the soil over the depth of embedment;

D_b is the depth to base level;

A_h is the vertical projected area of the foundation in the direction of sliding.

7.5.2.5 Assessment of torsional capacity

Torsional actions decrease the overall bearing and sliding capacity of shallow foundations. Correction factors that account for torsional actions are not available for use with the bearing capacity methods in 7.5.1, or the assessment of pure sliding in 7.6.2. Effects of torsion on foundation stability can be considered through a yield surface approach as described in Clause A.7 and Reference [137], or through analytical approaches as described in Reference [132]. Torsion is also considered in ISO 19906.

Where torsional capacity is critical, the possible occurrence of discrete layers of low strength soil, which can provide a preferential failure surface, shall be addressed in the site characterization (investigation and interpretation). Design for torsion shall address the foundation-seabed contact stress distribution and drainage condition. Internal mechanisms within the confined soil plug (above skirt tip level) that can affect torsion capacity shall also be addressed.

7.5.3 Assessment of capacity of intermediate foundations

Use of shallow foundation methods can be suitable to provide an initial size for an intermediate foundation where loading is simple vertical or simple horizontal and the soil conditions are simple (i.e. no significant layering). For more complex soil conditions or loading, including significant moments or VHMT loading, more appropriate methodologies are available in Reference [199].

Where the soil conditions and loading are complex and the design situation is critical, the sizing shall be validated by use of appropriate methodology, such as finite element analyses or finite element limit analysis.

Methodologies for combined loading of intermediate foundations or piles derived for anchoring applications with a padeye located at an optimal depth below seafloor, are not generally suitable for intermediate foundations for fixed structures where the loading is at topcap level. The p-y method for design of slender (flexible) piles under lateral loading (see 8.5) is not generally applicable to rigid intermediate foundations (e.g. rigid non-slender piles), unless more advanced case-specific soil reaction curves are adopted (see 8.5.5).

The design of intermediate foundations is also addressed by the IEC 61400-3 [180].

7.6 Serviceability limit state (displacements and rotations)

7.6.1 General

The clearance between water level and topsides, the design of connections between subsea structures, and other serviceability limits shall account for the displacements of the foundation over the life of the structure.

7.6.2 Serviceability of shallow foundations under static loading

7.6.2.1 General

Calculation of foundation displacements and rotations can include:

a) immediate displacements and rotations;

b) primary consolidation settlement (displacements and rotations);

c) secondary compression (creep) settlement;

d) differential settlements induced by spatial soil variability, moments, torque and eccentricity.

The formulae for evaluating the static short-term and long-term displacements and rotations of shallow foundations are given in 7.6.2.2 and 7.6.2.3. These formulae are applicable to idealized conditions, and a discussion of the limitations is given in A.7.

7.6.2.2 Immediate displacements and rotations

Displacements of the base of a circular, rigid, foundation that rests on the surface of an isotropic and homogeneous seabed, and where the anticipated displacements are elastic, shall be estimated by Formulae (14) to (17) in the absence of more definitive criteria:

a) Vertical:

$$u_Q = Q\left(\frac{1-v}{4GR}\right) \quad (14)$$

b) Horizontal:

$$u_H = H\left(\frac{7-8v}{32(1-v)GR}\right) \quad (15)$$

c) Overturning:

$$\theta_M = M\left(\frac{3(1-v)}{8GR^3}\right) \quad (16)$$

d) Torsion:

$$\theta_T = T\left(\frac{3}{16GR^3}\right) \quad (17)$$

where

u_Q is the vertical displacement at foundation base level;

u_H is the horizontal displacement at foundation base level;

θ_M is the overturning rotation (in radians) at foundation base level;

θ_T is the torsional rotation (in radians) at foundation base level;

Q is the vertical action;

H is the horizontal action;

M is the overturning moment;

T is the torsional moment;

G is a representative value of the elastic shear modulus of the soil (for the appropriate action and strain level);

ν is the Poisson's ratio of the soil;

R is the radius of the base of a circular foundation.

Design values of actions and moments (V, H, M and T) with an action factor of 1,0 should be used.

Formuale (14) to– (17) can also be used for approximating the response of a square base of equal area.

References for formulae to predict immediate, elastic displacements that account for non-uniform soil profiles (e.g. linearly increasing soil strength), foundation embedment, foundation flexibility and non-uniform base geometries are provided in Clause A.7.

Numerical analysis methods are readily available and shall be evaluated for more complex situations.

The elastic shear modulus of the soil G is not a unique soil parameter and depends on the level of stress and strain applied to each soil element. An appropriate value in design using Formulae (14) to (17) shall be adopted and shall be documented. In the absence of more definitive criteria, Poisson's ratio ν values of 0,5 for undrained soil response and in the range 0,2 to 0,3 for a drained soil response shall be applied.

7.6.2.3 Primary consolidation settlement

Formula () is a widely used simplified estimate of long term or primary consolidation settlement obtained by assuming one-dimensional compression of fine-grained soil layers under an imposed vertical stress. In the absence of more definitive criteria, Formula (18) shall be used to estimate primary consolidation:

$$u_Q = \left(\frac{hC}{1+e_0}\right)\log_{10}\frac{\sigma'_{v0,z}+\Delta\sigma'_{v,z}}{\sigma'_{v0,z}} \quad (18)$$

where

u_Q is the vertical displacement at foundation base level;

h is the layer thickness;

e_0 is the initial void ratio of the soil;

C is the representative value of compression index of the soil over the loading range considered;

$\sigma'_{v0,z}$ is the effective overburden stress at the level of a given soil layer;

$\Delta\sigma'_{v,z}$ is the increment of effective vertical stress in a given soil layer at the specified time.

The compression index, C_c, shall be used in the calculation of consolidation settlements of normally consolidated clays. The swelling index, C_s, shall be used in the calculation of consolidation settlements for over-consolidated clays where the relevant stress range falls on an unload-reload line without reaching the normal compression line. The calculation should be divided into two parts for stress ranges that span the unload-reload and normal compression lines.

For designs sensitive to primary consolidation, compression characteristics of the soil shall be determined based on results from laboratory consolidation tests carried out at appropriate pre-consolidation pressures. However, sampling disturbance can significantly impact test results. Assumptions and corrections adopted in development of selected compression characteristics shall be documented.

A thick homogeneous layer shall be subdivided into multiple thin layers for analysis with each layer prescribed an appropriate value of C and e_0. Where more than one layer is involved, the total settlement estimate is taken as the sum of the settlement of the individual layers.

Formula (18) has application limitations and does not address three-dimensional flow and strain, creep, loading redistributions, differential settlements or different initial conditions such as excess pore pressures.

7.6.2.4 Secondary compression: creep

Depending on the duration of loading and the sensitivity of the design to settlement, additional displacement due to secondary compression (creep) can be significant. In these cases, creep shall be addressed.

7.6.2.5 Differential displacements and rotations

Eccentricity of actions on a foundation can cause a permanent moment to be transferred to the foundation, leading to the potential for differential settlements, both immediately and as a result of consolidation over the life of the structure. Differential displacements can also derive from changing soil conditions across a foundation footprint or across individual foundations on a connected structure. Differential displacements shall be addressed in design, if the foundation or structure are sensitive to such settlements.

7.6.3 Serviceability of intermediate foundations

Where required for structural analyses or serviceability requirements, an initial estimate of foundation stiffness can be made using simplified elastic solutions. Where soil layering or loading is complex or where the situation is critical, the use of a more appropriate methodology shall be employed in detailed design. For monopod foundations, a check for accumulated displacements or rotations can be required.

7.6.4 Serviceability in response to dynamic and cyclic actions

In many cases, cyclic loading leads to generation of excess pore pressures at the end of the event. Dissipation of excess pore pressures leads to additional primary consolidation settlement, beyond that calculated for static loading, and can also increase the amount of creep. Settlement associated with the effects of cyclic actions shall be addressed in design where these actions can result in settlements impactful to the design solution.

7.7 Alternative methods of design

7.7.1 Yield surface approach

Offshore foundations can experience a wide range of loading, encompassing combinations of vertical action (Q), lateral action (H), overturning moment (M) and torsion (T). The conventional design approach for shallow foundations involves transforming the combined action into an equivalent vertical and lateral loading acting on a reduced (effective) foundation area.

While it is generally accepted that the conventional approach to shallow foundation design using the effective area method is conservative where large horizontal action and overturning moment act, using the effective area method can lead to considerable under-prediction of capacity for some loading situations (e.g. References [154], [158] and [343]). Additionally, restrictions apply in the use of the traditional design approach for offshore structures, such as in regards to allowing net tensile stress changes in the soil, which limits its general applicability.

An alternative approach is to derive a fully encompassing yield surface in Q, H, M and T space. This can be used to predict design loading combinations to reach ultimate limit state, as well as an explicit indication of the effect of a change in individual design action components on proximity to an ultimate limit state. The yield surface method can also be extended to define the action–displacement response of a foundation if used in conjunction with a flow rule. In undrained conditions, when normality can be assumed, the flow rule can be directly derived from the yield surface. Additional information on the yield surface approach is provided in A.7.7.

7.7.2 Performance-based design approach

A performance-based design approach shall holistically consider the robustness of the system into which a foundation is connected. System failure modes shall be identified and their likelihood of occurrence minimized with the adopted foundation solution. Further guidance is provided in A.7.7.2,

Deformation induced actions can be imposed on the structure by objects connected to it, or caused by the structure's deformation; and hence deformations that it imposes on connected objects (see 7.3.1).

A design approach that can lead to greater reductions in the deformation induced action is to allow either part of the structure to slide over the foundation, or for the foundation to slide directly over the seafloor.

When the structure is allowed to slide directly over the seafloor, design shall ensure bearing failure of the seafloor is prevented, whereas sliding failure over the seafloor is permissible (and necessary). Serviceability of the system which the foundation is connected within shall be demonstrated. The serviceability assessment shall account for the potential accumulation of foundation displacements and rotations due to repeated loading. Selection of action and material factors and any assumptions adopted in the selection shall be documented.

Further guidance is provided in A.7.7.2.

7.8 Installation

7.8.1 General

Force needs to be applied to penetrate foundation skirts and any other protrusions (e.g. stiffeners) below the seafloor as the soil needs to be displaced to accommodate the skirts and protrusions. The foundation self-weight can provide sufficient force, but when this is not the case, penetration can also be facilitated by providing under-pressure (relative to the ambient hydrostatic pressure) inside the skirt compartments under the foundation, or temporary additional static weight (ballast).

Installation shall be planned so that the foundation can be seated at the intended site without excessive disturbance to the supporting soil. When providing under-pressure, installation procedures shall be planned to avoid unintended disturbance to the soil, including plug uplift, erosion and piping. Installation planning shall address risks related to installation and shall implement measures to mitigate these risks.

The foundation baseplate is not always at seafloor level after installation, as the soil displaced by the skirts can cause internal plug heave within the foundation compartments. Typically it is assumed that:

a) half of the displaced volume of external/perimeter skirts contributes to internal plug heave, if no under-pressure is used;

b) full displaced volume of external/perimeter skirts contributes to internal plug heave, if under-pressure is used;

c) full displaced volume of internal skirts contributes to internal plug heave.

7.8.2 Skirt penetration resistance

Forces acting on a foundation penetrating the seabed are illustrated in Figure 10 sub a). These forces are typically approximated as a bearing component on the skirt/protrusion tip, and friction component on the skirt side.

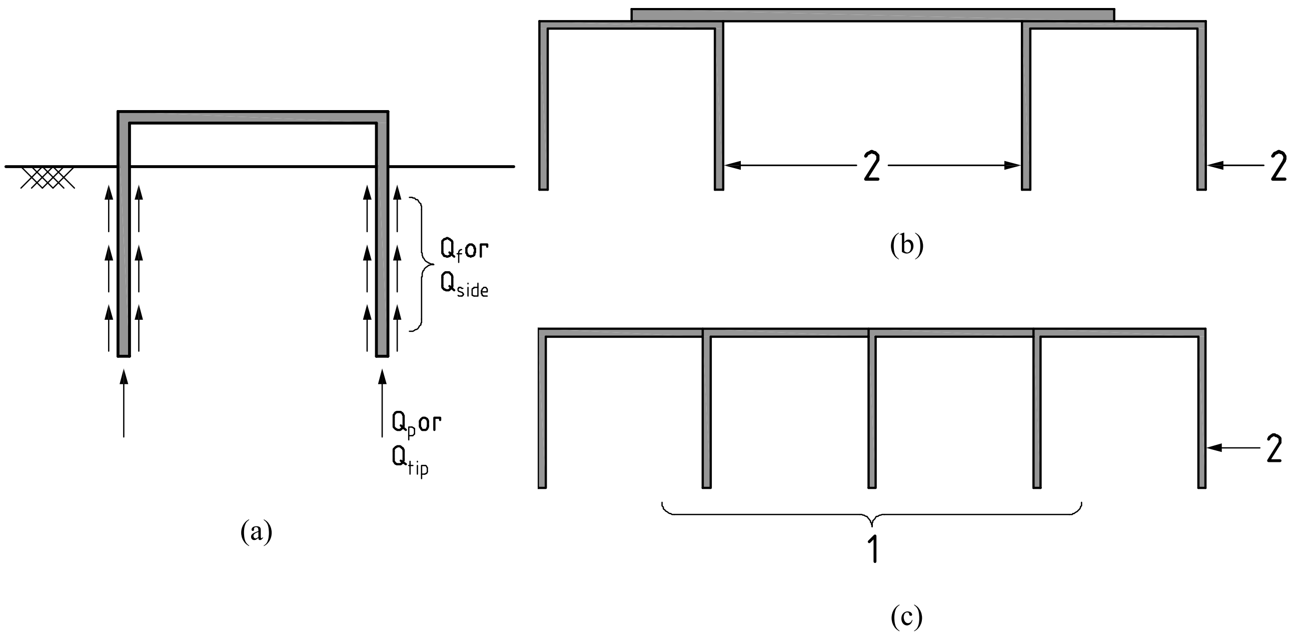

Key

Q_f / Q_{side}	Side/shear resistance acting on skirt side	1	Internal skirt(s)
Q_p / Q_{tip}	Tip resistance acting on skirt tip	k	Gradient of undrained strength increase with depth

Figure 10 — Foundation penetration (a) illustration of tip and side resistance on a single compartment structure (b) foundation consisting of two co-joined compartments (c) multi compartment structure

Methods exist to predict the resistance associated with penetration of foundation skirts. Further guidance is provided in A.7.8.2 and A.11.5.2.2.1. Structural design of the skirts is required. Stiffeners can be required to ensure satisfactory action transfer *in situ*, and during installation (e.g. during load-out).

7.8.3 Required and allowable under-pressure

When under-pressure is used to assist foundation installation, the following two quantities shall be assessed for all penetration depths, in addition to the penetration resistance:

a) the under-pressure necessary to allow embedment,

b) the critical pressure that can cause the soil plug to fail in reverse end bearing (clays) or piping (sands).

The pumping system used during installation shall be capable of generating the necessary under-pressure.

The following aspects shall be addressed:

a) soil variability, layering and presence of any subsurface obstructions, such as cemented layers, or cobbles/ boulders;

b) assurance of minimum self-weight penetration so that a seal is formed prior to under-pressure application;

c) prevention of plug uplift during under-pressure assisted penetration, which can occur due to reverse end bearing (soil flow into the compartment due to excessive under-pressure);

d) avoidance of piping failures through sand materials;

e) avoidance of cavitation, if in shallow water.

Installation design of foundations which consist of multiple compartments or multiple co-joined foundations installed simultaneously (see Figure 10 sub b)) shall include provisions to ensure uniform penetration rate, and vertical penetration.

Further guidance is provided in A.7.8.2 and A.11.5.2.2.1.

7.9 Relocation, retrieval and removal

Foundations occasionally need to be relocated if the required installation tolerances (e.g. verticality) are not achieved. The offset for the new location can be a centre-to-centre spacing of up to three times the foundation diameter/width. A lesser spacing may be acceptable, if the level of seabed disturbance due to the first installation is minimal.

If removal is anticipated, an analysis shall be made of the actions generated during removal so that removal can be accomplished with the available equipment. The analysis shall include increases in soil strength due to consolidation from the time of installation to the time of extraction.

Further guidance for over-pressure assisted removal is provided in A.11.5.2.2.2.

8 Pile foundation design

8.1 Pile capacity for axial compression

8.1.1 General

Design criteria for pile foundations shall be determined in accordance with ISO 19902.

The axial pile capacity shall satisfy the following conditions:

$$P_{d,e} \leq Q_d = Q_r/\gamma_{R,Pe} \tag{19}$$

$$P_{d,p} \leq Q_d = Q_r/\gamma_{R,Pp} \tag{20}$$

where

Q_d is the design axial pile capacity, i.e. the design resistance of the pile;

Q_r is the representative value of the axial pile capacity, as determined in 8.1 and 8.2;

$P_{d,e}$ is the design axial action on the pile [allowed to include the effective pile weight, with ($\gamma_{pile} - \gamma_{water}$) as effective unit weight], and the weight of the soil plug if this can be justified, in case of tensile actions], determined from a coupled linear structure and nonlinear foundation model using the design values of actions for extreme combinations of actions;

$P_{d,p}$ is the design axial action on the pile [including the effective pile weight, with ($\gamma_{pile} - \gamma_{water}$) as effective unit weight, in case of compressive actions], determined from a coupled linear structure and nonlinear foundation model using the design values of actions for operational combinations of actions;

$\gamma_{R,Pe}$ is the pile partial resistance factor for extreme combinations of actions ($\gamma_{R,Pe}$ = 1,25);

$\gamma_{R,Pp}$ is the pile partial resistance factor for operational combinations of actions ($\gamma_{R,Pp}$ = 1,50).

In accordance with ISO 19900, a material factor of 1,0 may be used for evaluation of accidental limit states.

When sizing a pile foundation, the following items shall be addressed:

— design actions;

— diameter;

— penetration

— type of tip;

— wall thickness;

— number of piles;

— spacing;

— location;

— pile head fixity;

— material strength;

— installation method.

The analysis procedure used shall simulate the nonlinear stress–strain behaviour of the soil and ensure force-displacement compatibility between the structure and the pile-soil system. Displacements and rotations of individual piles shall not exceed serviceability limit states.

Pile capacity for axial compression, as discussed in 8.1.2 to 8.1.5, relates to the axial resistance of a pile when the pile head is subjected to compressive actions along the pile axis. Pile capacity for axial tension is addressed in 8.2.

Pile capacities are commonly determined using the simplified calculation model described in 8.1.2; the parameters that are used in this model are determined in accordance with 8.1.3 to 8.1.5. For most fixed offshore structures supported on open-ended pipe piles, experience has shown the adequacy of determining pile penetration based on static capacity evaluations, with design values of static actions and commonly accepted working stress design (WSD) factors of safety that, in part, account for the cyclic effects. The partial action and resistance factors applied for pile design in this document have been based upon these safety factors.

The simplified model for pile capacity described in 8.1.2 to 8.1.5 is based on a (quasi-)static and monotonic application of the axial actions.

In the absence of more definitive criteria, the relationships between mobilized axial shear transfer between pile and soil and the local pile displacement, and between mobilized end bearing resistance and the pile tip displacement, shall be determined in accordance with 8.4.

The design methods presented in 8.1.3 and 8.1.4 only apply to clay soils and sand soils, respectively. The methods shall not be applied to other soil types or unconventional soils without confirming suitability.

The calculated pile capacity takes time to develop after installation. If the design actions are applied to a pile foundation before its calculated capacity has fully developed, the pile capacity shall be adjusted.

8.1.2 Axial pile capacity

In the absence of more definitive criteria, the representative value of the axial capacity of piles in compression, including belled piles, $Q_{r,c}$, shall be determined by:

$$Q_{r,c} = Q_{f,c} + Q_p = f(z)\, A_s + q\, A_{pile} \tag{21}$$

where

$Q_{r,c}$ is the representative value of the axial capacity in compression (in force units);

$Q_{f,c}$ is the representative value of the skin friction capacity in compression (in force units);

Q_p is the representative value of the end bearing capacity (in force units);

$f(z)$ is the unit skin friction (in stress units);

A_s is the side surface area of the pile in soil (m^2);

q is the unit end bearing at the pile tip (in stress units);

A_{pile} is the gross end area of the pile (m^2);

z is the depth below the original seafloor (m).

For open-ended pipe piles in clay, the end bearing capacity, Q_p, shall not exceed the sum of the end bearing capacity of the internal plug and the end bearing on the pile tip wall annulus. Guidance on unplugged end bearing in sands is provided in 8.1.4. In computing the design actions in compression on the pile, the effective weight of the pile shall be included.

In determining the capacity of a pile, consideration shall be given to the relative deformations between the soil and the pile as well as to the compressibility of the soil-pile system. In some circumstances, a more explicit consideration of axial pile performance effects on pile capacity is warranted. Further guidance of these effects is provided in 8.3 and A.8.3.

The foundation configurations should be based on those that experience has shown can be installed consistently and practically under similar conditions with the pile size and installation equipment being used. Possible remedial action in the event that design objectives cannot be obtained during installation should be investigated and defined prior to construction.

In the case of drilled and grouted piles, the end bearing capacity shall be reduced or ignored in the design, depending on pile construction factors, such as the degree of removal of drill cuttings from the base of the hole.

Skin friction on the upper bell surface and, possibly, on the pile for some distance above the bell shall be discounted in computing the skin friction resistance, $Q_{f,c}$. The end bearing area of a pilot hole, if drilled, shall also be discounted in computing the total bearing area of the bell.

8.1.3 Skin friction and end bearing in clay soils

There are a number of methods for calculating the skin friction and end bearing in clay soils. The method described in this section has been developed and applied over many years and is the current industry standard. However, there are many more variables which affect pile capacity than those included in the design Formulae (22) to (24). This matter is discussed in this subclause and in A.8.1.3. An alternative CPT based method for pile capacity in clays is presented in A.8.1.3.2.2. In the absence of more definitive criteria, for driven pipe piles in clay soils the unit skin friction in tension and compression, $f(z)$, in stress units, at depth, z, shall be calculated using Formula (22).

$$f(z) = \alpha\, s_u(z) \tag{22}$$

where

α is the dimensionless skin friction factor, for clays

$s_u(z)$ is the representative value of undrained shear strength at depth z (in stress units).

The factor α shall be computed by:

$$\alpha = 0{,}5\ \Psi^{-0{,}5} \text{ for } \Psi \le 1{,}0 \tag{23a}$$

$$\alpha = 0{,}5\ \Psi^{-0{,}25} \text{ for } \Psi > 1{,}0 \tag{23b}$$

with the constraint that $\alpha \le 1{,}0$

where

$$\psi = \frac{s_u}{\sigma'_{v0}(z)} \text{ at depth } z \tag{24}$$

$\sigma'_{vo}(z)$ is the effective vertical stress at depth z (in stress units).

A discussion of methods for determining the undrained shear strength, s_u, and effective overburden stress, $\sigma'_{vo}(z)$, including the effects of various sampling and testing procedures is included in A.8.1.3. For under-consolidated clays (i.e. clays with excess pore pressures undergoing active consolidation), α can be taken as 1,0.

Due to the shortage of pile loading tests in soils having $s_u(z)/\sigma'_{vo}(z)$ ratios greater than three, the justification for application of Formula (22) shall be documented. Similar justification shall be documented for the application of Formula (22) in low plasticity clays (see A.8.1.3).

For long axial flexible piles some reduction in capacity may be warranted, particularly where the skin friction degrades on continued displacement. This effect is discussed in more detail in A.8.1.3.

In the absence of more definitive criteria, where the pile tip is in clay soils, the unit end bearing stress, q, shall be computed by:

$$q = 9\, s_u \tag{25}$$

The skin friction, $f(z)$, acts on both the inside and the outside of the pile. The total axial resistance for pile compression is the sum of the external skin friction, the end bearing on the pile wall annulus, and the total internal skin friction or the end bearing of the plug, whichever is the lesser. For piles considered to be plugged, the bearing pressure can be assumed to act over the entire cross-section of the pile. For unplugged piles, the bearing pressure acts on the pile wall annulus only. That a pile is considered plugged or unplugged shall be based on static calculations. A pile can be driven in an unplugged condition but behave as plugged under static actions.

Skin friction resistance and end bearing capacity computed on the basis of the requirements above represent long-term capacities. Axial capacity immediately after installation is usually lower, especially in under-consolidated to slightly over-consolidated clays. This is dependent on the development of excess pore pressure in the soil during installation and its subsequent dissipation with time. When the design actions are applied to a pile foundation shortly after installation, the capacity of a pile immediately after installation and the increase in capacity with time shall be addressed in design. Further guidance on the soil-pile set-up behaviour is provided in A.8.1.3.

For piles driven in undersized drilled holes, piles jetted in place (see 10.5.2 for jetted conductors) or piles drilled and grouted in place, the selection of skin friction values shall account for the soil disturbance resulting from installation. In general, $f(z)$ shall not exceed values for driven piles; however, in some cases, for drilled and grouted piles in over-consolidated clay, $f(z)$ can exceed these values. In determining $f(z)$ for drilled and grouted piles, the strength of the soil-grout interface, including potential effects of drilling mud, shall be addressed. A further check shall be made of the allowable bond stress between the pile steel and the grout, as recommended in ISO 19902.

In layered soils, skin friction values, $f(z)$, in the clay layers shall be as given by Formula (22) to (25). End bearing values for piles tipped in clay layers with adjacent weaker layers can be as given in Formula (25) provided that:

a) the pile achieves penetration of two to three pile diameters or more into the clay layer; and

b) the tip is approximately three pile diameters or more above the bottom of the clay layer to preclude punch-through.

Where these distances are not achieved, the design shall account for reduced end bearing.

8.1.4 Skin friction and end bearing in sands

This subclause presents the 'unified CPT method' for assessing pile capacity in sands [218]. Formula (26) to (28) are recommended for the evaluation of static capacity of steel tubular open-ended piles two weeks after driving. The method can be applied to sands with a fines content of less than 12 % (up to 20 % in the case of non-plastic fines). The method shall not be used for sands with unusually weak grains or compressible structure, including those sands containing amounts of mica, volcanic grains or calcium carbonate sufficient to lead to a mechanical response that differs from that of a silica sand, without further validation. Further guidance on other approaches to estimate pile capacity for sands that do not fall within the specified criteria is provided in A.8.1.4.

The unified CPT method shall only be applied to impact driven piles. The unified CPT method shall not be applied to vibro-driven piles, unless the vibrated portion of the pile is restricted to the first 20 % of pile penetration, within which the overall contribution to pile capacity is limited The unified CPT method shall niether be applied to piles installed by jacking.

The reliability of the method has been evaluated and the method was shown, when used with the partial load (action) and resistance factors of ISO 19902, to provide pile foundations that are more reliable than those obtained using the former main text method. The unified CPT method in sand can be used with the unified CPT method in clay, presented in A.8.1.3.2.2, to estimate the static capacity of driven piles in layered stratigraphy with a reliability that is essentially the same as that for cases where piles are installed in one soil type [46]. Further information on the method and Formula (26) to (28) are provided in References [218] and [255].

In the absence of more definitive criteria, the external unit skin friction for capacity two weeks after driving, $f(z)$, in stress units, at depth, z, shall be calculated using Formula (26):

$$f(z) = f_L\,(\sigma'_{rc} + \Delta\sigma'_{rd})tan29^o \tag{26}$$

where

$$\sigma'_{rc} = \left(\frac{q_c}{44}\right) A_{re}^{0.3} \left[Max\left[1,\left(\frac{h}{D}\right)\right]\right]^{-0.4}$$

$$\Delta\sigma'_{rd} = \left(\frac{q_c}{10}\right)\left(\frac{q_c}{\sigma'_v}\right)^{-0.33}\left(\frac{d_{ref}}{D}\right)$$

$$A_{re} = 1 - PLR\left(\frac{D_i}{D}\right)^2$$

where PLR=1,0 for typical offshore piles.

and:

f_L is a loading coefficient taken as 0,75 for tension actions and 1,0 for compression actions;

29° is the angle of interface friction used for calibration of the method, noting that factors, such as paint, coatings or mill-scale varnish, can negatively affect the interface friction that can be mobilized;

σ'_{rc} is the horizontal effective stress acting on a driven pile at a depth, z, about two weeks after driving;

σ'_v is the vertical effective stress at a depth, z;

q_c is the cone resistance at a depth, z;

A_{re} is the effective area ratio, defined above, is a measure of the soil displacement induced by the driven pile and expressed as a fraction of the soil displacement induced by a closed-ended pile (for which A_{re}=1);

D is the pile outer diameter;

D_i is the pile inner diameter;

PLR is the plug length ratio, with a maximum value of 1,0, defined as the ratio of the plug length (L_p) to the pile embedment (L), and for which in the absence of measurements, PLR shall be taken as 1,0 for typical offshore piles;

$\Delta\sigma'_{rd}$ is the change in horizontal stress, acting a depth, z, arising due to interface shear dilation as the pile is loaded;

d_{ref} = 0,035 6 m.

h is the distance above the pile tip at which $f(z)$ acts (= L–z);

In the absence of more definitive criteria, the unit end bearing applied across the full base area of the pile shall be calculated using Formula (27):

$$q = [0{,}12 + 0{,}38A_{re}]q_p \tag{27}$$

where

A_{re} is as defined per Formula (26);

q_p is a representative value of the CPT end resistance within one diameter of the pile tip, taking into account the following:

- To allow for spatial variability, this is taken as the average q_c value within a zone 1,5D above and below the pile tip. However, because end bearing capacity is sensitive to local variations in cone resistance, lower q_p values shall be adopted where spatial variability in the cone resistance indicate potential design sensitivity.
- The end bearing method assumes a plugged base and is applicable for piles with a length to diameter ratio greater than five. For plugs with low permeability within two pile diameters of the pile tip, such as those comprising interbedded clay layers, the end bearing capacity can be reduced and in such cases, it shall be confirmed that unplugged end bearing is not less than plugged end bearing [240], [296]. In the absence of more definitive criteria, a cautious estimate of unplugged end bearing can be taken as follows:

$$Q_p = q_{unplugged}A_{pile} \tag{1}$$

where $q_{unplugged} = A_{re}q_p$.

End bearing capacity is generally more sensitive to local variations in cone resistance than shaft resistance and due allowance should be made for spatial variability in the cone resistance.

The unified CPT method replaces the former main text method and the CPT methods previously defined in the annex. Further information on the latter CPT methods, experience with their application in practice and potential use in cases not covered by the unified CPT method can be found for Fugro [143], ICP [186], [368], NGI [85] and UWA [215]. For existing platforms where there are no CPT data available, the former main text method may still be used and is presented in A.8.1.4.1.3, although it is no longer recommended for calculation of pile capacity in sand.

8.1.5 Skin friction and end bearing in gravels

Characterizing the *in situ* density of gravel materials is difficult, with previous experience suggesting that site investigation results can be unreliable and misleadingly characterize the material as dense while pile driving can indicate a loose material [192]. The CPT based method presented in 8.1.4 and other pile design methods in Clause A.8, including the former main text method in sands in A.8.1.4.1.3, are likely to overpredict driven tubular pile capacity in gravels [167]. As a result, the methods presented in 8.1.4 and Clause A.8 shall-not be used directly for pile design in gravels.

8.1.6 Skin friction and end bearing of grouted piles in rock

The unit skin friction of grouted piles in jetted or drilled holes in rock shall not exceed half the uniaxial compressive strength of the rock or grout, but in general should be much less than this value. The reduction depends on pile construction factors, such as roughness on the side of the hole, and on rock mass factors, such as the presence of discontinuities within the rock mass. The sidewall of the hole can develop a layer of slaked mud or clay, which will never gain the strength of the rock. The bond stress of the steel pile to grout interface shall be checked in accordance with ISO 19902.

The end bearing capacity of the rock shall not exceed the uniaxial compressive strength of the rock or grout multiplied by a bearing capacity factor appropriate for the type of rock. In general, the end bearing capacity is much less or is ignored in the design, depending on pile construction factors, such as the degree of removal of drill cuttings from the base of the hole, and on rock mass factors, such as the presence of discontinuities within the rock mass. The limiting end bearing capacity for this type of pile can be governed by stresses in the grout or in the pile steel.

Design values for (static) unit skin friction and end bearing can be found in various publications (e.g. References [204], [266] and [339]). Most publications on this subject refer to relatively 'stubby' stiff piles as used in onshore practice (bored piles). Owing to the brittle response applicable to unit skin friction, design values given in these publications can be unconservative for long flexible piles as used in offshore practice. In addition, the adverse effects of cyclic actions the axial capacity of such piles shall be addressed. In cemented calcareous or carbonate material the skin friction assessment for grouted piles can be undertaken based on the load transfer (t-z) methodology and cyclic algorithm described in Reference [293]. Site-specific laboratory and field testing shall be undertaken to justify the use of the design method and the assessment of the required design parameters to characterise the cemented material response.

8.1.7 Skin friction and end bearing of driven piles in intermediate soils

In intermediate soils (e.g. silts or low plasticity silty tills), where cone penetration is usually partially drained, the assessment of pile capacity is uncertain. Neither the methods in 8.1.3 for clays nor the methods in 8.1.4 for sands are applicable alone. Interpretations based on CPT resistance and piezocone response generally lead to higher shaft capacities when layers are deemed to be ‘clays’ rather than ‘sands’. For example, the application of clay methods has led to significantly over-predicted axial capacity compared with offshore load tests with transitional soils whose grading curves span the range between the two soil types [64]. In the absence of more definitive criteria, the designer may consider the degree of drainage observed during CPT profiling (ideally assisted with dissipation test data) and may consider the minimum of shaft capacity estimates made by the sand and clay methods, as well as alternative procedures.

8.2 Pile capacity for axial tension

The representative value for pile axial pullout capacity, $Q_{r,t}$, is less than or equal to, but shall not exceed $Q_{f,c}$, the total skin friction capacity in compression. For clay soils, $f(z)$ shall be as stated in 8.1.3. For sands, $f(z)$ shall be computed in accordance with 8.1.4. For rock, $f(z)$ shall be assessed as stated in 8.1.6.

8.3 Axial pile performance

8.3.1 Static axial behaviour of piles

Pile axial deflections shall be within acceptable serviceability limits and these deflections shall be compatible with the internal forces and movements of the structure. Axial pile behaviour is affected by directions, types, rates and sequence of the applied actions, by the installation technique, by soil type, by axial pile stiffness, as well as by other parameters. Some of these effects for clay soils have been observed in both laboratory and field tests.

In some circumstances (e.g. for soils that exhibit strain-softening behaviour), particularly where the piles are axially flexible, the actual capacity that can be mobilised by the pile can be less than that given by Formula (22), which assumes the pile is rigid. If t–z curves that exhibit strain-softening are recommended as per 8.4, maximum axial capacities that explicitly account for the axial flexibility of the pile may be warranted. Other factors, such as increased axial capacity under loading rates associated with storm waves, can counteract these effects. More information is provided in the commentary in ISO 19902 as well as A.8.3.2 and Reference [76].

8.3.2 Cyclic axial behaviour of piles

Cyclic actions, including inertial actions due to environmental conditions such as storm waves and earthquakes, can have two potentially counteractive effects on the static axial capacity. Repetitive actions can cause a temporary or permanent decrease in resistance and an accumulation of deformation. Rapidly applied actions can cause an increase in resistance and stiffness of the pile. Very slowly applied actions can cause a decrease in resistance and stiffness of the pile. The resultant influence of cyclic actions will be a function of the combined effects of the magnitudes, cycles and rates of change of applied actions, the structural characteristics of the pile and the types of soils (see A.8.3.2).

8.4 Soil reaction for piles under axial actions

8.4.1 Axial shear transfer *t*–*z* curves

The relationship between mobilized soil-pile shear transfer and local pile displacement at any depth is described using a *t*–*z* curve. Various empirical and theoretical methods are available for developing curves for axial shear transfer and pile displacement, *t*–*z* curves.

Resistance–displacement relationships for grouted piles are discussed in Reference [299] and [282].

Curves developed from pile loading tests in representative soil profiles or based on laboratory soil tests that model pile installation can also be justified. In the absence of more definitive criteria, the *t*–*z* curves in Figure 11 shall be used for non-carbonate soils.

In clays, a typical value for z_{peak} of 1 % of the pile outer diameter (i.e. z_{peak}/D = 0,01) shall be used for routine design purposes. Values ranging from 0,25 % to 2,0 % may be used in cases where axial pile stiffness is critical for design.

In sands, in the absence of more definitive criteria, Formula (29), which provides a good fit to the unified database employed for derivation of Formula (26), shall be used for routine design of typical offshore piles [214].

$$\frac{z_{peak}}{D} = \frac{{q_c}^{0.5}{\sigma'_v}^{0.25}}{A p_a^{0.75}} \quad A = 1\,250 \text{ (comp)}; A = 625 \text{ (tension)} \tag{29}$$

where

p_a is atmospheric pressure (100 kPa);

q_c is the CPT cone resistance;

σ'_v is the vertical effective stress at the depth of the t-z spring.

The empirical coefficient, *A*, depends on the loading direction and gives z_{peak}/D values in tension that are double those in compression.

The shape of the *t*–*z* curve at displacements greater than that at which t_{max} is reached as shown in Figure 11 should be assessed. Values of the residual friction ratio, t_{res}/t_{max}, and the axial pile displacement, z_{res}, at which it occurs, are a function of soil stress–strain behaviour, stress history, pile installation method, sequence of pile action application and other factors. Typical t_{res}/t_{max} values for clays range from 0,70 to 0,90; laboratory, *in situ* or model pile tests or local experience can provide valuable information for determining values of t_{res}/t_{max} and z_{res} for various soils.

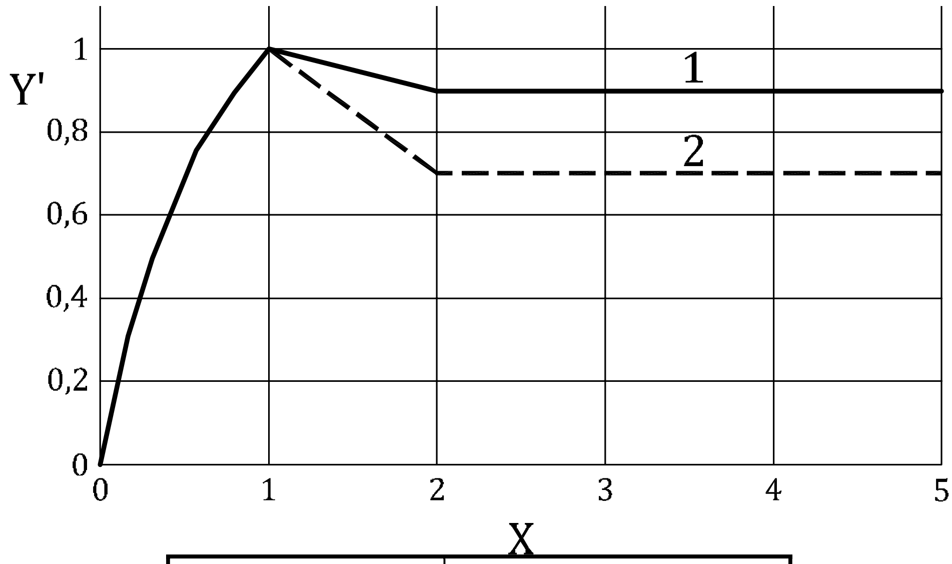

z / z_{peak}	t / t_{max}
	Clays
0,16	0,30
0,31	0,50
0,57	0,75
0,80	0,90
1,0	1,00
2,0	0,70 to 0,90
∞	0,70 to 0,90

Key

X z/z_{peak}

Y' t/t_{max}

1 clay: t_{res} = 0,9 t_{max}

2 clay: t_{res} = 0,7 t_{max}

z local pile axial displacement

z_{peak} displacement to maximum soil-pile unit skin friction

D pile outside diameter

t mobilised soil-pile unit skin friction (in stress units)

t_{max} = $f(z)$ = maximum soil-pile unit skin friction computed in accordance with 8.1 (in stress units)

t_{res} residual soil-pile unit skin friction (in stress units)

z_{res} axial pile displacement at which the residual soil-pile unit skin friction, t_{res}, is reached

Figure 11 — Typical axial pile shear transfer–displacement *t*–*z* curves in clays

8.4.2 End bearing resistance–displacement, *Q*–*z*, curve

Under compression actions, the relationship between mobilized end bearing resistance and axial pile tip displacement is described using a *Q*–*z* curve.

A pile tip displacement of 10 % of the pile diameter can be required for full mobilization of the end bearing resistance described in 8.1 in both sand and clay soils. In the absence of more definitive criteria, the curve shown in Figure 12 shall be applied for both sands and clays.

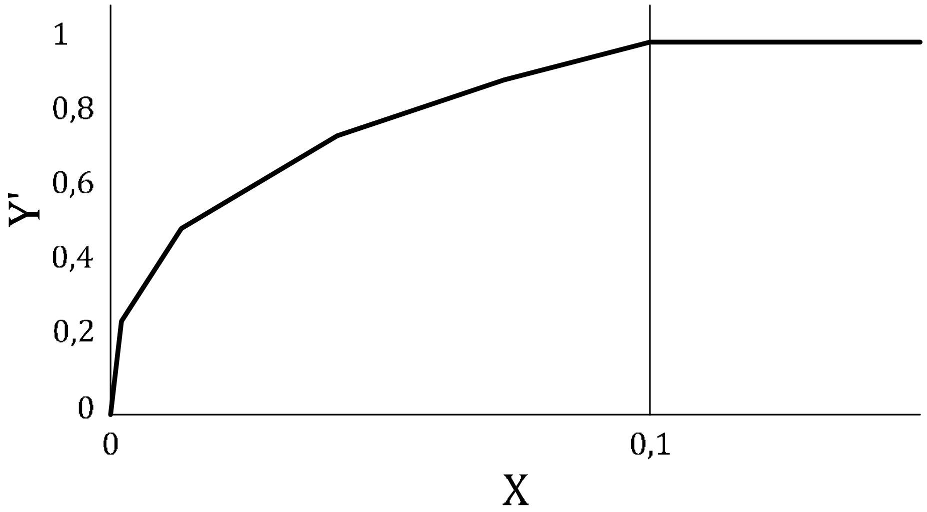

z / *D*	*Q* / Q_p
0	0
0,002	0,25
0,013	0,50
0,042	0,75
0,073	0,90
0,100	1,00
∞	1,00

Key

X z/D

Y' Q/Qp

z axial pile tip displacement

D pile outside diameter

Q mobilised end bearing resistance (in force units)

Q_p representative value of end bearing resistance computed in accordance with 8.1 (in force units)

Figure 12 — Typical pile end bearing resistance–displacement *Q*–*z* curve

8.5 Soil reaction for piles under lateral actions

8.5.1 General

The structural code of reference defines the lateral actions that the pile foundation shall be designed to resist. Such actions can include static, cyclic, fatigue, impact, and earthquake actions.

In the absence of more definitive criteria, the procedures given in 8.5.2 and 8.5.3 shall be used to construct the relationships between lateral soil resistance and lateral displacement, known as *p*–*y* curves.

These relationships are applicable to long slender piles, i.e. piles with length to diameter, L/D, ratios greater than about 10, and are not necessarily applicable to intermediate foundations, (e.g. short stubby piles such as large diameter piles with limited penetration), which can require a different formulation for the *p*–*y* relationships or different methods of analyses, as described in 8.5.4.

The lateral resistance of the soil near the seafloor can be significant to pile design and the possible effects of seafloor scour on this resistance shall be addressed.

In cases of liquified soils near the seafloor, the need to reduce the allowable stress in compression to prevent pile buckling shall be addressed [200].

8.5.2 Lateral soil reaction for clay

8.5.2.1 General

The framework within this clause is intended to provide a best estimate of the soil resistance. The framework was developed from numerical analyses combined with soil stress-strain behaviour, as measured in the laboratory through direct simple shear (DSS) tests performed at a standard shear strain rate of approximately 5 %/hr.

It is applicable to soil consistencies ranging from very soft to very hard and has been validated by hindcast of pile load tests with soil strength values up to 600 kPa (12 531 lb/ft^2). It has not been validated for highly structured clays or carbonate materials.

The monotonic curves are derived as per 8.5.2.2 as a function of I_p and OCR, or from DSS testing.

The cyclic curves are derived as per 8.5.2.3 for three design conditions.

8.5.2.2 P-y curves for monotonic actions

8.5.2.2.1 General

The lateral failure mechanism of long slender piles consists of a wedge mechanism close to the seafloor and a flow-around mechanism at deeper depths.

For monotonic actions, the ultimate unit lateral resistance, p_u, in units of force per unit length of pile, has been found to vary between 9 s_u D and 12 s_u D for the flow-around mechanism. For depths where failure occurs with the wedge mechanism, the lateral capacity is reduced and depends on whether a gap is assumed to form on the back side of the pile.

P-y curves are developed by:

a) calculating p_u according to 8.5.2.2.2;

b) correcting p_u for anisotropy for gapping conditions, as per 8.5.2.2.3;

c) generating normalized *p-y* curves according to 8.5.2.2.4;

d) de-normalizing the *p-y* curves by using the values of p_u and D.

8.5.2.2.2 Ultimate soil resistance for isotropic conditions

In the absence of more definitive criteria, the ultimate soil resistance shall be calculated as:

$$p_u = P_u\, D \tag{30}$$

with

$$P_u = N_p\, s_u$$

$N_p = N_{p0} + \frac{\gamma' z}{s_u} \le N_{pd}$ if gapping is assumed on the back side of the pile;

$N_p = 2N_{p0} \le N_{pd}$ if no gapping is assumed on the back side of the pile;

$$N_{p0} = N_1 - (1 - \alpha_{ave}) - (N_1 - N_2)\left[1 - \left(\frac{z}{dD}\right)^{0.6}\right]^{1.35} \le N_{pd}$$

$$N_1 = 12 \quad N_2 = 3{,}22$$

$$d = 16{,}8 - 2{,}3\, log_{10}(\lambda) \ge 14{,}5$$

$$\lambda = s_{u0} / (s_{u1}\, D)$$

$$N_{pd} = 9 + 3\alpha_{ave}$$

where

d is a model parameter;

D is the pile outside diameter;

P_u is the ultimate soil pressure (in stress units);

p_u is the ultimate soil resistance per unit length (in units of force per unit length);

N_1 is a model parameter;

N_2 is a model parameter;

N_p is the total lateral bearing capacity factor;

N_{po} is the lateral bearing capacity factor due to passive wedge for weightless soil;

N_{pd} is the lateral bearing capacity factor for flow around mechanism;

s_u is the undrained shear strength at the depth in question, as determined from DSS testing;

s_{u0} is the undrained shear strength at seafloor, as determined from DSS testing;

s_{u1} is the rate of increase of shear strength with depth in linearly increasing strength profiles, as determined from DSS testing. For moderately non-linear profiles, s_{u1} varies with depth and can be calculated as:
$s_{u1}(z) = \frac{S_u(z) - S_{u0}}{z}$

z is the depth below original seafloor;

α_{ave} is the average soil-pile skin friction factor, as calculated by Formulae (22) to (24), between the seafloor and a depth of 20 pile diameters, or over the pile length if L/D <20;

γ' is the soil submerged unit weight;

λ is the normalized rate of shear strength increase in linearly increasing shear strength profiles.

NOTE In the absence of DSS shear strength measurements, an equivalent DSS strength profile can be obtained from CPT, T-bar, UU, minivane or other measurements, based on local experience.

If a sand layer is present at the seafloor and overlays clay layers, the total bearing capacity factor N_p may be calculated as $N_p = N_{pd}$ at all depths in the clay layers if the sand layer is thicker than about one pile diameter.

The choice of gapping condition, that is whether a gap is assumed on the back side of the pile or not, rests with the designer. The hindcast of 11 pile load tests suggests that pile behaviour (e.g. deflection, shear force, and bending moment profiles) are best predicted with the following assumptions when calculating N_p:

a) No gapping condition assumed in near-normally consolidated profiles where the shear strength is less than about 15 kPa in the top 10 m, regardless of the magnitude of lateral displacements.

b) Gapping condition assumed at large lateral displacement if the shear strength is less than about 15 kPa at the seafloor and exceeds 15 kPa within the top 10 m. For such strength profiles, no gapping conditions can be assumed at small lateral displacements and gapping condition can be assumed for large lateral displacements.

c) Gapping condition assumed at all values of lateral displacements if the shear strength is greater than 15 kPa at all depths in the top 10 m.

Differences between the above pile load tests and a typical offshore design case can include the presence of mudmats, or other seafloor structures surrounding the piles, which can confine soils and prevent gapping.

8.5.2.2.3 Anisotropy correction of ultimate soil resistance for gapping conditions

The formulae of 8.5.2.2.2 were derived for isotropic conditions. In the wedge failure mechanism, i.e. if N_p < N_{pd}, and for gapping condition only, the strength measured in triaxial extension should be used instead of the DSS strength. In absence of more definitive criteria, where gapping is assumed on the back side of the pile, the bearing capacity factor N_p shall be corrected for anisotropy as follows:

$$N_{p_{cor}} = C_w \, N_{p0} + \frac{\gamma' z}{s_u} \leq N_{pd} \tag{31}$$

with:

$$C_w = 1 + \left(\frac{s_{uTE}}{s_{uDSS}} - 1\right)\left(\frac{N_{pd} - N_p}{N_{pd} - N_p|_{z=0}}\right)$$

where

N_{p_cor} is the total lateral bearing capacity factor corrected for anisotropy;

C_w is the anisotropy correction factor for the wedge failure mechanism for gapping conditions;

$\frac{s_{uTE}}{s_{uDSS}}$ is the average ratio of triaxial extension strength over DSS strength within the depth of the wedge, for which in the absence of site-specific data, a default value of 0,9 is recommended for very soft and soft clays like those of the Gulf of Mexico;

N_p is the total lateral bearing capacity factor for isotropic conditions, as per 8.5.2.2.2.

N_{po} is the lateral bearing capacity factor due to passive wedge for weightless soil for isotropic conditions, as per 8.5.2.2.2.

N_{pd} is the lateral bearing capacity factor for flow around mechanism for isotropic conditions, as per Clause 8.5.2.2.2.

$N_p|_{z=0}$ is the value of N_p for isotropic conditions, as per Clause 8.5.2.2.2, at the original seafloor elevation (i.e. z = 0).

Further guidance on soil anisotropy and soil profiles with seafloor crusts can be found in Clause A.8.5.2.1.2.

8.5.2.2.4 *P–y* curve relationships

Lateral soil resistance–displacement relationships for piles in clays are nonlinear. The *p–y* curves for monotonic actions may be generated by scaling the stress-strain curves measured in the laboratory through DSS testing by either of the two methods presented in A.8.5.2.1.3.

Alternatively, the monotonic *p-y* curves ($p_{mo} - y_{mo}$) shall be generated from the default normalized curves of Table 1, as plotted on Figure 13.

Table 1 — Normalized *p-y* curves for monotonic actions for clay

	$I_p > 30$ %			$I_p \leq 30$ %		
	OCR ≤ 2	OCR = 4	OCR = 10	OCR ≤ 2	OCR = 4	OCR = 10
p_{mo}/p_u	y_{mo}/D	y_{mo}/D	y_{mo}/D	y_{mo}/D	y_{mo}/D	y_{mo}/D
0	0	0	0	0	0	0
0,05	0,000 3	0,000 4	0,000 5	0,000 1	0,000 2	0,000 3
0,2	0,003	0,004	0,005	0,001	0,002	0,003 3
0,3	0,005 3	0,008	0,011	0,001 8	0,004	0,007 3
0,4	0,009	0,015	0,021	0,003	0,0075	0,014
0,5	0,014	0,024	0,034	0,0048	0,012	0,023
0,6	0,022	0,036	0,052	0,007 3	0,018	0,035
0,7	0,032	0,055	0,078	0,011	0,027	0,052

0,8	0,05	0,084	0,12	0,017	0,042	0,08
0,9	0,082	0,14	0,19	0,027	0,07	0,13
0,975	0,15	0,23	0,3	0,05	0,11	0,2
1,0	0,25	0,3	0,4	0,083	0,15	0,27
1,0	∞	∞	∞	∞	∞	∞

Key

p_{mo}/p_u is the normalized lateral soil resistance for monotonic actions.

y_{mo}/D is the normalized lateral displacement for monotonic actions.

OCR is the over-consolidation ratio.

I_p is the plasticity index.

All other variables as defined in 8.5.2.2.2.

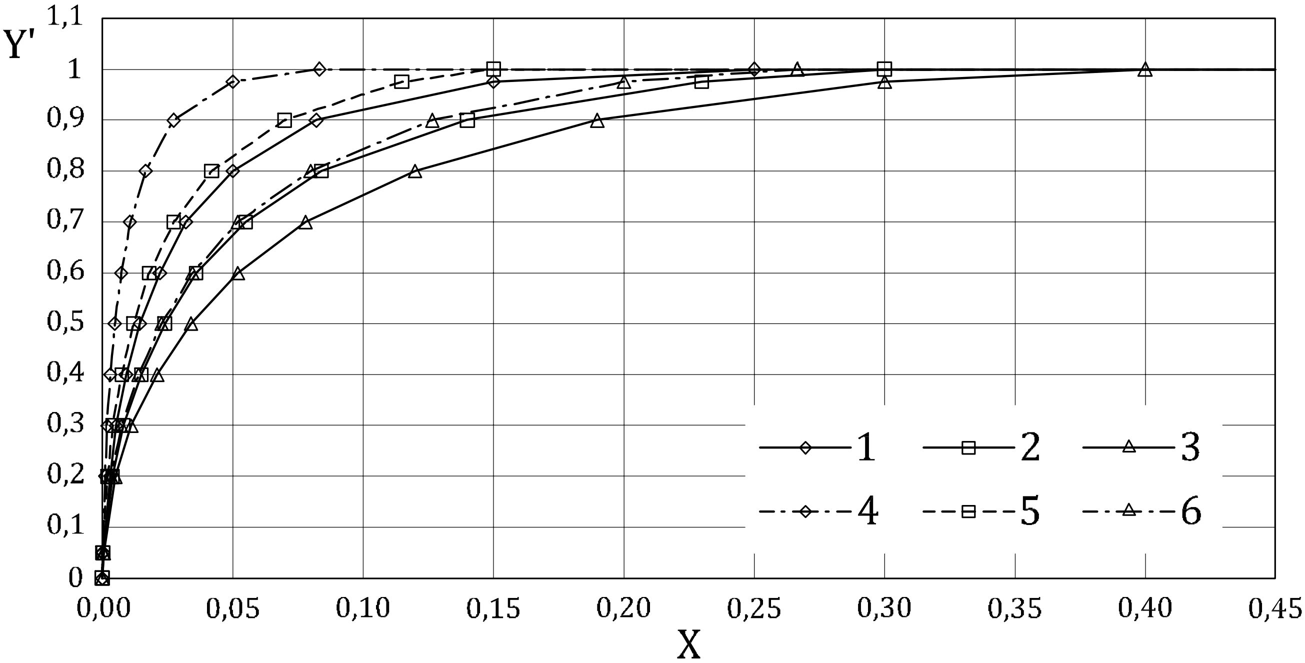

Key

X Normalized lateral displacement, (y/D)

Y' Normalized resistance, (p/p_u)

1 I_p > 30 %; OCR ≤ 2

2 I_p > 30 %; OCR = 4

3 I_p > 30 %; OCR = 10

4 I_p ≤ 30 %; OCR ≤ 2

5 I_p ≤ 30 %; OCR = 4

6 I_p ≤ 30 %; OCR = 10

Figure 13 — Normalized *p-y* curves for monotonic actions for clay

8.5.2.3 *P-y* curves for cyclic actions

The procedure may be applied to three defined design conditions:

a) Gulf of Mexico (GoM) conditions: Piles in clays with OCR less than 2,0, with normalized cyclic shear strength properties like those of the GoM clays and subjected to loading conditions like those experienced by piles on fixed structures in the GoM.

b) North Sea soft clay conditions: Piles in clays with OCR less than 2,0, with normalized cyclic shear strength properties like those of the Drammen clay and subjected to loading conditions like those experienced by piles on fixed structures in the North Sea.

c) North Sea stiff clay conditions: Piles in clays with OCR greater than 4,0, with normalized cyclic shear strength properties like those of the Drammen clay and subjected to loading conditions like those experienced by piles on fixed structures in the North Sea.

In the absence of more definitive criteria, the cyclic *p*-*y* curves ($p_{cy} - y_{cy}$) used to calculate pile behaviour under the maximum storm loading shall be calculated as follows:

$$p_{cy} = p_{mod}\ p_{mo} \tag{32}$$

$$y_{cy} = y_{mod}\ y_{mo} \tag{33}$$

where

p_{cy} is the lateral soil resistance for cyclic actions;

y_{cy} is the lateral displacement for cyclic actions;

p_{mod} is the *p*-modifier model parameter;

y_{mod} is the *y*-modifier model parameter.

The *p*-modifer and *y*-modifer shall be calculated according to the following steps:

1) Determine the depth of rotation of the pile, z_{rot}, under the peak total lateral action.

   The depth of rotation of the pile is defined as the first depth from the seafloor where the lateral displacement is zero.

   If the action, pile diameter, and pile wall thickness schedule are known, the depth of rotation may be determined by a beam column analysis using the *p*-*y* springs calculated for monotonic actions, as per 8.5.2.2.

   Alternatively, the depth of rotation of the pile shall be estimated as $z_{rot} = 15\ D$.

2) Calculate the hybrid factor, h_f, at each depth z and for all points p_{mo}/p_u on the normalized monotonic *p*-*y* curves:

   $$h_f = \frac{p_{mo}}{p_u} - \left(\frac{z}{z_{rot}}\right)^2 \qquad \text{if } z \le z_{rot}$$

   $$h_f = \frac{p_{mo}}{p_u} - 1 \qquad \text{if } z > z_{rot}$$

   where

   h_f is a model parameter and $-1 \le h_f \le +1$.

3) Calculate the number of equivalent cycles, N_{eq}, at each depth z and for all points p_{mo}/p_u on the normalized monotonic *p*-*y* curves:

   $$N_{eq} = \left(\frac{2}{1-h_f}\right)^g \le 25$$

   where

   N_{eq} is a model parameter and $1 \le N_{eq} \le 25$;

   g is a model parameter and:

   g = 1,0 for Gulf of Mexico conditions;

   g = 1,25 for North Sea soft clay conditions;

   g = 2,5 for North Sea stiff clay conditions.

4) Calculate the *p*-modifier and the *y*-modifier at each depth z and for all points p_{mo}/p_u on the normalized monotonic *p*-*y* curves as per Table 2, as plotted on Figure 14.

Table 2 — Cyclic modifiers for *p*-*y* curves in clays

Design condition	Cyclic modifiers	
Gulf of Mexico	$p_{mod} = 1{,}47 - 0{,}14 \ln(N_{eq})$	$y_{mod} = 1{,}2 - 0{,}14 \ln(N_{eq})$
North Sea soft clay	$p_{mod} = 1{,}63 - 0{,}15 \ln(N_{eq})$	$y_{mod} = 1{,}2 - 0{,}17 \ln(N_{eq})$
North Sea stiff clay	$p_{mod} = 1{,}45 - 0{,}17 \ln(N_{eq})$	$y_{mod} = 1{,}2 - 0{,}17 \ln(N_{eq})$

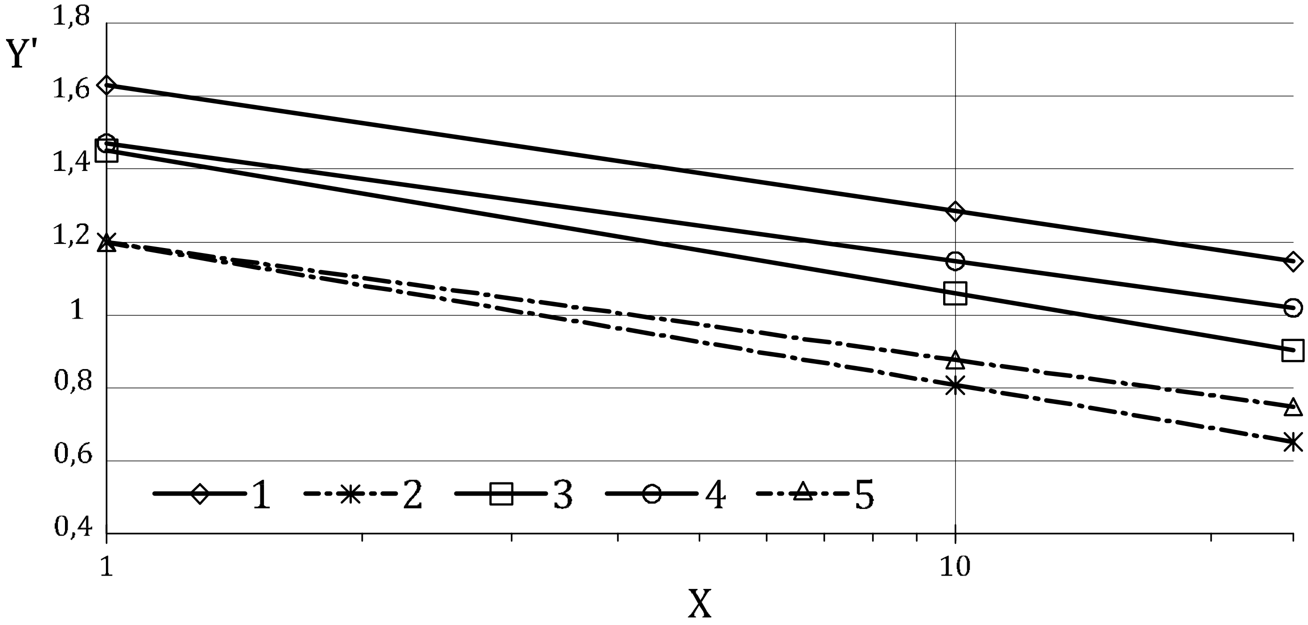

Key

X Number of equivalent cycles, N_{eq} (-)

Y' *P*-modifier, P_{mod}, or *y*-modifier, Y_{mod}

1 P_{mod} - North Sea soft clay

2 Y_{mod} - North Sea soft and stiff clay

3 P_{mod} - North Sea stiff clay

4 P_{mod} - Gulf of Mexico

5 Y_{mod} - Gulf of Mexico

Figure 14 — Normalized *p-y* curves for monotonic actions for clay

8.5.2.4 *P-y* curves for fatigue actions

Fatigue actions typically cause a very large number of cycles of very low pile displacements. The curves for fatigue analyses (p_{fa} - y_{fa}) represent the steady-state conditions after the soil unload-reload secant stiffness and hysteretic damping have stabilized, typically after several hundreds of cycles.

A spring-only model is presented for piles for both static and dynamic, e.g. time-domain, analyses. A spring-dashpot model is presented in A.10.5.5.2.2 for conductors supporting typical subsea wellhead/BOP/LMRP systems, but is not applicable to piles. At very low lateral displacements, the fatigue curves are stiffer than the cyclic curves because the stiffness of the spring-only model includes the effect of hysteretic damping. Further guidance is provided in A.8.5.2.3.

In the absence of more definitive criteria, the (p_{fa} - y_{fa}) curves shall be calculated as:

$$p_{fa} = p_u\, A_s \cdot \left(\frac{y_{fa}}{D}\right)^{-B_s} \tag{34}$$

where

p_{fa} is the lateral soil resistance for fatigue actions;

y_{fa} is the lateral displacement for fatigue actions;

p_u is the ultimate soil resistance calculated as per 8.5.2.2.2, with the no-gapping condition;

A_s is a model parameter; A_s = 0,45 if s_u < 40 kPa and A_s = 0,19 for other conditions;

B_s is a model parameter; B_s = 0,05 for all conditions.

The power-law curve of Formula (34) is discretized as follows:

a) the curve shall pass through the origin $y_{fa} = p_{fa} = 0$;

b) the next point shall be generated for y_{fa}/D=0,001;

c) the following points should be generated at the following y_{fa}/D increments, up to a maximum y_{fa}/D = 0,05:

d) 0,001 for 0,001 < $y_{fa}/D \leq$ 0,010;

e) 0,01 for 0,010 < $y_{fa}/D \leq$ 0,05.

8.5.2.5 *P-y* curves for earthquake actions

The monotonic curves of 8.5.2.2 can be used to analyse piles under seismic actions. They have shown to provide a satisfactory match between measured and calculated bending moments in fixed-structures piles when they are combined with appropriate unload-reload behaviour and parallel dashpots to model radiation damping. Further guidance is provided in A.8.8.2.4.

8.5.2.6 Comparison with previous recommendations

When compared with the *p-y* curve methods in Reference [22], the recommended practice of 8.5.2 will generally give *p-y* curves that are stiffer at low displacements and with greater ultimate resistance.

Comparisons between the curves obtained by previous and current recommendations are provided in A.8.5.2.5.

8.5.3 Lateral capacity for sand

For static lateral actions, the representative unit lateral capacity, p_r, for sand has been found to vary from a value at shallow depths determined by Formula (35) to a value at deep depths determined by Formula (36). In the absence of more definitive criteria, at a given depth, the formula giving the smallest value of p_r shall be used as the representative capacity. These formulae can be un-conservative for layered soil conditions when the sand is overlain by soft clay.

$$p_{rs} = (C_1 z + C_2 D)\gamma' z \tag{35}$$

$$p_{rd} = C_3 D \gamma' \tag{36}$$

where 's' signifies shallow and 'd' signifies deep, and

D is the pile outside diameter;

p_r is the representative lateral capacity (in force per unit length of pile);

γ' is the submerged unit weight of soil (kN/m³);

z is the depth below original seafloor (m);

C_1, C_2, C_3 are dimensionless coefficients as a function of the effective angle of internal friction in sand, ϕ' (see Figure 15):

$$C_1 = \frac{(\tan\beta)^2 \tan\alpha}{\tan(\beta - \phi')} + K_0\left(\frac{\tan\phi' \sin\beta}{\cos\alpha \tan(\beta - \phi')} + \tan\beta(\tan\phi' \sin\beta - \tan\alpha\right) \tag{37}$$

$$C_2 = \frac{\tan\beta}{\tan(\beta - \phi')} - K_a \tag{38}$$

$$C_3 = K_a((\tan\beta)^8 - 1) + K_0 \tan\phi'(\tan\beta)^4 \tag{39}$$

with $\alpha = \frac{\phi'}{2}$; $\beta = 45 + \frac{\phi'}{2}$; $K_0 = 0{,}4$ and $K_a = \frac{1-\sin\phi'}{1+\sin\phi'}$

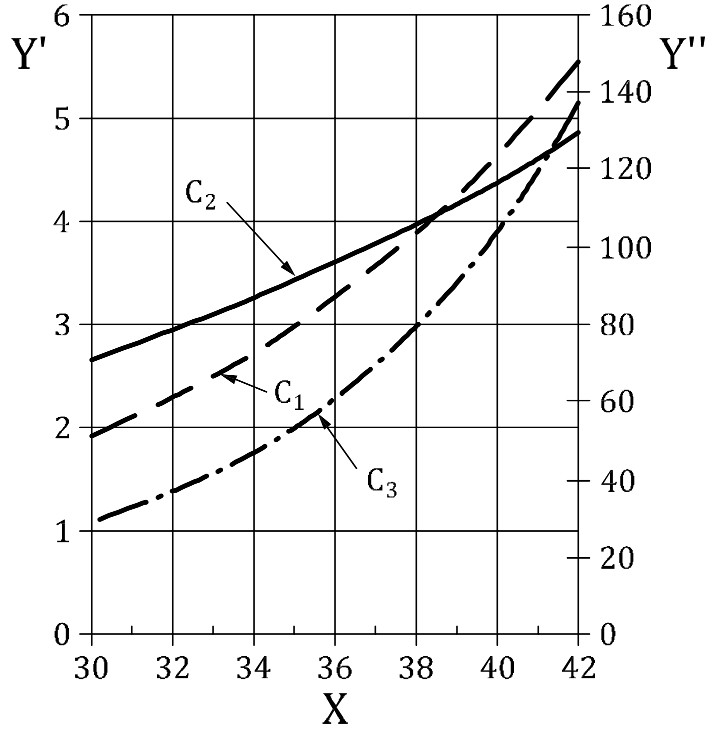

Key

X effective angle of internal friction (ϕ' in degrees)
Y' value of coefficients C_1 and C_2
Y" value of coefficient C_3
1 Coefficient C_1 for lateral capacity
2 Coefficient C_2 for lateral capacity
3 Coefficient C_3 for lateral capacity

Figure 15 — Lateral capacity coefficients for sand

Guidance for scour conditions is given in A.8.5.3.

8.5.4 Lateral soil resistance – displacement *p–y* curves for sand

The lateral soil resistance–displacement *p–y* relationship for a pile in sand is also nonlinear and in the absence of more criteria, at any specific depth, *z*, shall be determined by:

$$p = A.p_r.\tan\phi\left(\frac{k.z}{A.p_r}.y\right) \tag{40}$$

where

A is a factor to account for static or cyclic actions, evaluated by

$A = \left(3{,}0 - \frac{0{,}8.z}{D}\right) > 0{,}9$ for static actions, and

$A = 0{,}9$ for cyclic actions;

p_r is the representative lateral capacity at depth z (force per unit length of pile);

k is the initial modulus of subgrade reaction (force per volume), see Table 3;

z is the depth below original seafloor (m);

y is the lateral displacement at depth z.

The database for the lateral soil-pile behaviour in sands consists of free-head tests on piles in clean sands, with effective angles of internal friction ranging from 34° to 42°, as determined by shear box tests, drained triaxial tests or correlations with *in situ* tests.

Extrapolation of these data to soils outside the limits of experience, particularly to those sands with effective angles of internal friction less than 30°, requires engineering judgement. In particular, laboratory test results on such soils should be reviewed for evidence of anomalous behaviour and for the presence of significant fractions of clay soils, either of which could require a different formulation for the *p–y* relationships.

In the absence of more definitive criteria, the values of the initial modulus of subgrade reaction, *k*, given in Table 3 shall be applied.

Table 3 — Initial modulus of subgrade reaction

ϕ'	k	
	MN/m³	(lb/in³)
25°	5,4	(20)
30°	8,7	(32)
35°	22	(80)
40°	45	(165)

8.5.5 *P–y* curves for fatigue actions

Similar to the recommendations for clays, the curves for fatigue analyses (p_{fa} - y_{fa}) represent the steady-state conditions after the soil unload-reload secant stiffness and hysteretic damping have stabilized, typically after several hundreds of cycles. A spring-only model is presented for piles, to be used for both static and dynamic (e.g. time-domain) analyses.

In the absence of more definitive criteria, the (p_{fa} - y_{fa}) springs shall be calculated as:

$$p_{fa} = 365\, D\, \tau(z) \left(\frac{y_{fa}}{D}\right)^{0.65} \tag{41}$$

where

p_{fa} is the lateral soil resistance for fatigue actions;

y_{fa} is the lateral displacement for fatigue actions;

$\tau(z)$ is the shear resistance. $\tau(z) = \sigma'_{vo}(z) \tan(\phi')$.

The power-law curve of Formula (41) is discretized as per 8.5.2.4.

8.5.6 Refined assessment of lateral pile response

A more advanced one-dimensional (1*D*) pile analysis method, which involves the definition of case-specific soil reaction curves, is set out for applications where the design is either highly sensitive to lateral actions or when the pile *L*/*D* ratio is low [67][71]. The method's development is further described in A.8.5.6.

8.5.7 Lateral soil resistance-displacement curves in calcareous soil, cemented soil and weak rock

The degradation of strength and stiffness of cemented or calcareous soil and weak rock materials under cyclic actions shall be addressed in the design of grouted pile and conductor [212]. The results from site-specific pile test and centrifuge model test data, where available, may also be used to calibrate site-specific *p-y* data.

8.6 Pile group behaviour

8.6.1 General

The effects of closely spaced adjacent piles on the resistance–displacement characteristics of the pile group should be considered. For pile spacing less than 8D, group effects shall be addressed in lateral response design.

The pile group capacity shall conform to the requirements of 8.1.1. Where there is a non-uniform distribution of actions into the piles, the partial resistance factors for individual piles in the group may be less than those specified in 8.1.1, provided it is demonstrated that the displacements and corresponding deformations and stresses of the piles and associated structural members are acceptable.

8.6.2 Axial behaviour

For piles embedded in clays, the group capacity can be less than the single isolated pile capacity multiplied by the number of piles in the group; conversely, for piles embedded in sands, the group capacity can be higher than the sum of the capacities of the isolated piles. The group settlement in either clay or sand is normally larger than that of a single pile subjected to the average action per pile of the pile group.

8.6.3 Lateral behaviour

For piles with the same pile head fixity conditions and which are embedded in either clay or sands, the pile group normally experiences greater lateral displacements than those undergone by a single pile subjected to the average action per pile of the corresponding group. The major factors influencing the group displacements and distribution of actions over the piles are the pile spacing, the ratio of the pile penetration to the pile diameter, the pile flexibility relative to the soil, the dimensions of the group, and the variations in the shear strength and stiffness modulus of the soil with depth.

Of the four group analysis methods examined in Reference [264], the following methods were found to be the most appropriate for use in designing group pile foundations for the given actions:

— for defining initial group stiffness: advanced methods, such as PILGP2R [264];

— for design event actions: the Focht-Koch method [139] as modified by Reese et al. [300] for defining group displacements and average maximum pile moments. Displacements are probably underpredicted at actions giving displacements of 20 % or more of the diameter of the individual piles in the group;

— for evaluating maximum pile action at a given group displacement: largest value obtained from the original or modified Focht-Koch method.

8.7 Pile installation assessment

8.7.1 General

The types of pile foundations used to support offshore structures and considered in this document are:

— Driven piles: Open-ended piles are normally used in foundations for offshore structures (see 8.7.2 to 8.7.7). These piles are usually driven into the seabed with impact hammers, which use steam, diesel fuel or hydraulic power as the source of energy.

— Drilled and grouted piles: Piles that can be used in soils and rocks which will hold an open hole with or without drilling mud (see 8.7.8).

— Belled piles: Bells can be constructed at the tip of piles so as to give increased bearing and uplift capacity through direct bearing on the soil (see 8.7.9). The end bearing capacity of belled piles is to be determined in accordance with the principles given for the design of drilled and grouted piles.

— Vibro-driven piles: The capability of hydraulic vibratory driving hammers to install piles has been demonstrated, in particular for the installation of small diameter piles in sands. Owing to the lack of data with respect to the effect of the installation method on the pile axial capacity, the use of vibratory hammers for installing offshore piles subjected to significant axial actions is not recommended.

The pile wall thickness shall be sufficient to resist axial and lateral actions as well as the stresses during pile installation. The pile stresses and, as a result thereof, the minimum pile wall thickness shall also conform to the requirements from ISO 19902 where the pile strength shall be verified using the steel tubular checking formulae given in ISO 19902 for conditions of combined axial force and bending. Fatigue damage due to pile driving shall be accounted for when calculating the pile fatigue life according to ISO 19902.

All field-made structural connections shall be compatible with the design requirements. Pile sections should be marked to facilitate installing the pile sections in the planned sequence. The closure device on the lower end of the structure's legs and pile sleeves, if required, shall be designed to avoid interference with the installation of the piles.

8.7.2 Drivability studies

Computer analyses (based on the principles of one-dimensional elastic stress-wave theories and commonly known as wave equation analyses) may be used to simulate the hammer-pile-soil system and pile driving behaviour, with the objective of defining the range of blow counts necessary to reach the target design pile penetration and assessing the stresses in the pile resulting from pile driving. The predicted range of blow counts to reach a given penetration is governed by the estimated profile of soil resistance to driving (SRD), by the assumed hammer efficiency, or driving energy transferred to the pile and, to a lesser extent, by the quake and damping parameters in the wave equation model. Selection of these input parameters is based on previous pile driving experience and engineering judgment. For a given rated energy, the energy transferred to the pile is dependent on the type of hammer (i.e. diesel fuel, steam, or hydraulic hammer) and is based on pile driving experience with reliable measurements from pile instrumentation.

The definition of SRD is the main factor that governs the results of the drivability studies and the hammer type required to reach the target pile penetration. Several methods for calculating the SRD in different types of soils have been proposed in the literature (see A.8.7.2).

General procedures cannot be applied at all sites, as piling behaviour is site dependent. Therefore, back-analysis of previous pile driving experience at the site, or at sites with similar soil conditions, should be performed in order to calibrate SRD calculation procedures and improve drivability predictions for other structures at the site. For clays, the SRD calculation should account for the increase in resistance due to pore pressure dissipation (set-up) during driving interruptions (e.g. when delays are necessary for welding pile add-on elements).

To confirm that the hammer performs in accordance with the specifications and with the assumptions made in the drivability predictions, the pile or hammer may be instrumented and monitored during driving. If so, pile instrumentation is preferable, as hammer monitoring provides incomplete information about the driving energy transferred into the pile.

Pile driving instrumentation data, based on measurements from strain and acceleration transducers fixed near the top of the pile, may be used for verifying the actual hammer driving energy and soil stratification, assessing the actual SRD during driving, as well as giving additional information for estimating the pile capacity, particularly if re-strike test data are available. The SRD measured during driving, as back-calculated from pile instrumentation data, should be compared with the predicted range in soil resistance. Such analyses can be used to improve the reliability of subsequent drivability predictions at the site.

Selection of representative parameters or methodology for driveability analyses, or driveability input to fatigue analyses, should account for the experience in the area or in similar soil conditions, with upper estimate parameters being used if experience does not exist or is limited and best-estimate parameters being used otherwise.

8.7.3 Obtaining required pile penetration

The adequacy of the structure's foundation depends upon each pile being driven to or near its design penetration. Where applicable, the driving of each pile should be carried to completion with as little interruption as possible to minimize the increased driving resistance which often develops during delays. Workable back-up hammers with leads should be available, especially when critical pile set-up is anticipated.

The fact that a pile has met premature refusal does not indicate that it can support the design actions. Final blow count alone shall not be considered as assurance of piling adequacy.

In some instances, when continued driving is not successful, the penetration and associated capacity of a pile can be improved by the methods described in 8.7.5.

8.7.4 Driven pile refusal

Pile refusal is defined to:

— establish the point at which pile driving with a particular hammer should be stopped and other methods instituted (see 8.7.5); and

— prevent damage to the pile or hammer.

The definition of refusal should be consistent with the soil characteristics anticipated at the specific location. Refusal should be defined for all hammer sizes to be used and is contingent upon the hammer being operated at the energy and rate recommended by the manufacturer.

The exact definition of pile refusal for a particular installation should be defined in the installation specification. Examples of refusal criteria, for use only if no other requirements are included in the installation specification, are given in A.8.7.4.

If a pile refuses before it reaches design penetration, one or more of the measures given in 8.7.5 may be taken.

8.7.5 Pile refusal remedial measures

8.7.5.1 Review of hammer performance

A review of all aspects of hammer performance, possibly with the aid of hammer and/or pile head instrumentation, can identify problems that can be solved by improved hammer operation and maintenance, or by the use of a more powerful hammer.

8.7.5.2 Re-evaluation of design penetration

Reconsideration of actions, displacements and required capacities of individual piles, of other foundation elements and of the foundation system, can identify available reserve capacity.

An interpretation of driving records in conjunction with instrumentation can allow the design soil parameters or stratification to be revised and the calculated pile capacity to be revised.

8.7.5.3 Modifications to piling procedures

8.7.5.3.1 General

Modifying procedures, can permit the piles to be driven to the required penetration. The modifications described in 8.7.5.3.2 to 8.7.5.3.4 may be used.

8.7.5.3.2 Plug removal

The soil plug inside the pile can be removed by jetting and air lifting, or by drilling, to reduce pile driving resistance. Several soil plug removals and redrives can be required to reach target penetration.

If plug removal results in inadequate pile capacity, the removed soil plug shall be replaced by a grout or concrete plug or a plug made from another suitable material to increase the capacity back to the design level. The minimum axial capacity of the plug shall be equal to the pile end bearing capacity in a plugged condition, if full shear transfer between plug and pile is available. In some circumstances plug removal is not effective in improving driving conditions, particularly in cohesive soils.

8.7.5.3.3 Soil removal below the pile tip

Soil below the pile tip can be removed, either by drilling an undersized hole or by jetting and possibly air lifting. The drilling or jetting equipment is lowered through the pile, which acts as the casing pipe for the operation. Considering the resulting uncertainties with respect to the pile axial capacity, the soil below the pile tip should not be removed to reduce the soil resistance during driving in uncemented soils.

Under special circumstances (e.g. in the case of an intermediate layer of strong cemented material), undersized drilling can be applied to partially remove the hard layer before pile driving can be resumed. The depth of drilling should be restricted to the thickness of the hard cemented layer.

Undersized drilling should be restricted to relatively thin and not too hard layers. In thick and hard rock layers under-reaming of the hole to at least the full pile size should be evaluated to avoid potential risk of pile tip buckling.

Where soil removal below the pile tip has been performed by drilling (undersized or otherwise), the contribution of the relevant zone of soil to the pile capacity should be ignored, unless this zone has been grouted.

Jetting below the pile tip should be avoided because of the unpredictability of the results.

8.7.5.3.4 Two-stage driven piles

A first-stage or outer pile can be driven to a predetermined depth, after which the soil plug is removed and a second-stage or inner pile is driven inside the first-stage pile. The annulus between the two piles is grouted to permit shear transfer between the first- and second-stage piles and to develop composite action.

8.7.6 Selection of pile hammer and stresses during driving

The influence of the hammers to be used shall be evaluated as part of the design process in accordance with ISO 19902 for the definition of pile wall thickness and stresses generated by hammer placement and pile driving. A method of analysis based on wave propagation theory shall be used to determine the dynamic stresses generated by hammer impact.

The type(s) of pile hammer considered for pile driving shall be noted on the installation drawings or specifications. Any change in the hammers to be used for pile driving shall be assessed, to ensure that the consequences of the change are acceptable, including pile drivability, pile capacity, pile and structure strength and fatigue. Detailed guidance is provided in ISO 19902.

Items relevant to pile design and installation assessment are:

— Stresses during driving: The unfactored dynamic stresses should not exceed 90 % of yield, depending on specific circumstances such as the location of the maximum stresses down the length of pile, the number of blows, previous experience with the pile-hammer combination and the confidence level in the analyses.

— Allowance for underdrive or overdrive: With piles having thickened sections at the seafloor, an extra length of heavy wall material in the vicinity of the seafloor may be used so that the pile will not be overstressed at this point if the design penetration is not reached. The amount of underdrive or overdrive allowance provided in the design will depend on the degree of uncertainty regarding the penetration that can be obtained.

— Driving shoe: The purpose of a driving shoe is to assist piles to penetrate through hard layers or to reduce driving resistance, thereby allowing greater penetrations to be achieved than would otherwise be the case. If an internal driving shoe is provided for driving through a hard layer, it shall be checked that the driving shoe does not reduce the end bearing capacity of the soil plug below the value assumed in the design. If an internal driving shoe is used for reducing the internal skin friction during driving in cohesive soils, the effect of the driving shoe shall be taken into account when evaluating the total representative capacity of the pile. External driving shoes are not normally used, as they tend to reduce the skin friction along the length of pile above them. The tip of the driving shoe should be flat or bevelled towards the inside of the pile. Driving shoes with bevels toward the outside of the pile shall not be used when driving through dense and very dense sands as they have been shown to be a contributing factor in observed pile buckling.

8.7.7 Use of hydraulic hammers

Hydraulic hammers are more efficient than steam hammers and the energy transferred to the pile for a given rated energy tends to be greater. They can be used both above and below water for driving battered or vertical piles, through legs or through sleeves and guides, as well as vertical piles alone without lateral restraint. In calculating pile stresses, full account should be taken of wave, current and wind actions, as well as the hammer and section weights both during driving and during hammer stabbing, which can be either above or below water. While for steam hammers the weight of the cage is generally held by a crane, for hydraulic hammers the whole weight of the hammer is borne by the pile.

The energy output is generally varied to maintain a low blow count. Therefore, blow counts do not give a direct guide to soil stratification and resistance. Since the ram is encased, hammer performance cannot be judged visually. The hammer's performance, including ram impact velocity, stroke, pressure of accelerating medium and blow rate, should therefore be measured. Reliable instrumentation of some piles may also be considered to verify the energy transferred to the pile to aid interpretation of soil stratification and to limit pile stresses.

Monitoring of underwater driving requires that easily identified, unambiguous datum points be used, together with robust television cameras or remotely operated vehicles (ROV) capable of maintaining station. Alternatively, for shallow water sites, hammer casing extensions or followers may be used so that blow counts can be monitored above water.

Because no cushion block is used, there is no change in characteristics between ram and anvil as driving progresses and no requirement for cushion changes.

In selecting hydraulic hammers for deep water applications, account should be taken of possible decrease in driving efficiency due to increased friction between the ram and its surrounding air. Sufficient air should be supplied to the hammer so that water ingress is prevented. Water in the pile should be able to escape freely.

8.7.8 Drilled and grouted piles

There are two types of drilled and grouted piles.

1) Single-stage piles: For the single-stage drilled and grouted pile an oversized hole is drilled to the required penetration, a pile is lowered into the hole and the annulus between the pile and the soil is grouted. This type of pile can be installed only in soils which will hold an open hole to the seafloor.

2) Two-stage piles: The two-stage drilled and grouted pile consists of two concentrically placed piles grouted to become a composite section. A pile is driven to a penetration which has been determined to be achievable with the available equipment and below which an open hole can be maintained. This outer pile becomes the casing for the next operation, which is to drill through it to the required penetration for the inner or 'insert' pile. The insert pile is then lowered into the drilled hole, and the annuli between the insert pile and the soil and between the two piles are grouted. The diameter of the drilled hole should be at least 150 mm (6 in) larger than the insert pile diameter.

The hole for drilled and grouted piles can be drilled with or without drilling mud to facilitate maintaining an open hole. Drilling mud can be detrimental to the surface of some soils. If used, mud should be flushed with circulating water upon completion of drilling, provided the hole will remain open. Reverse circulation should normally be used to maintain sufficient flow for removal of cuttings. Drilling operations should maintain proper hole alignment and minimize the possibility of hole collapse.

Centralizers should be attached to the pile to provide a uniform annulus between the insert pile and the hole. A grouting shoe may be installed near the bottom of the pile to permit grouting of the annulus without grouting inside the pile. If a grouting shoe is used, the pile should be tied down to prevent floatation in the grout. The time before grouting the hole should be minimized in soils which can be affected by exposure to sea water. The quality of the grout should be tested at intervals during the grouting of each pile. Means should be provided for determining that the annulus is filled. Holes for closely positioned piles should not be open at the same time, unless there is verification that this will not be detrimental to pile capacity and that grout will not migrate during placement to an adjacent hole.

8.7.9 Belled piles

Drilling of the bell is carried out through the pile by under-reaming with an expander tool. A pilot hole can be drilled below the bell to act as a sump for unrecoverable cuttings. The bell and the pile are filled with concrete to a height sufficient to develop the necessary transfer of forces between the bell and the pile. Bells are connected to the pile to transfer both full uplift and compressive forces using steel reinforcing, such as structural members with adequate shear lugs, deformed reinforcement bars or prestressed tendons.

8.7.10 Grouting pile-to-sleeve connections

The grout-to-steel bond in the connection between pile and sleeve shall be checked in accordance with ISO 19902 addressing grout connections.

8.7.11 Pile installation data

Throughout the driving of piles, comprehensive driving and associated data should be recorded and reviewed for conformance with the installation plan. If significant deviations are observed, corrective measures can be necessary. The recorded data can include:

a) structure and pile identification, water depth and reference elevation of readings of pile markings for pile tip penetration;

b) relevant information on pile stabbing;

c) penetration of the pile under its own weight or under the weight of a new add-on;

d) additional penetration of the pile under the weight of the hammer;

e) data on followers used, where applicable;

f) blow counts throughout driving, with hammer identification and hammer blow rate (blows/minute) after every few metres of penetration;

g) cumulative number of blows at relevant penetrations;

h) driving energy observations and hammer monitoring data, if available;

i) pile instrumentation data, if available;

j) date and time of starts and stops in driving, including set-up time;

k) elapsed time for driving each section, with actual length of pile sections and cut-offs;

l) unusual behaviour of the hammer or the pile during driving;

m) elevations of soil plug and internal water surface after driving;

n) pertinent data of a similar nature covering drilling, grouting or concreting of grouted or belled piles.

8.7.12 Installation of conductors and shallow well drilling

The planning and execution of conductor installation and shallow well drilling should recognize the potential for disturbance to foundation soils and the consequent risk of a reduction in stability of the fixed structure or of adjacent conductors.

During drilling operations, soil disturbance can result from hydraulic fracture, from wash-out or from encountering shallow gas pockets. Hydraulic fracture occurs where drilling fluid pressure is too high and fluid is lost into the formation, possibly softening the surrounding soil. Wash-out (uncontrolled enlargement of the drilled hole) generally occurs in granular soils and can, in part, be induced by high drilling fluid circulation rates. Wash-out leads to stress relief in the surrounding soils. These incidents can be accompanied by loss of circulation of drilling fluids, by return of these fluids to the seafloor other than through the conductor, or by the creation of seafloor craters. In addition, prolonged drilling activities without casing can generate an upwards seepage flow that reduces effective overburden pressure resulting in reduced axial friction capacity of conductors.

If piles are installed within the zone of influence of soil disturbance, reduction in axial or lateral capacity and foundation stiffness can occur. Similarly, the stability of shallow foundations can be reduced and settlements increased. These detrimental effects can occur whether the drilling takes place after installation of the structure or before (e.g. for a pre-installed template or for an exploration well). Conductors installed by drilling or drill-drive techniques can have more detrimental effects than conductors installed by driving alone.

The following recommendations should be evaluated for conductor installation and shallow well drilling:

a) The conductor setting depth should be selected taking due account of hydraulic fracture pressure profiles. The depth should preferably be chosen at a cohesive stratum which is a sufficient distance from the proposed pile tip penetration to minimize the risk of disturbance of foundation soils.

b) In conductor or shallow well drilling operations, fluid pressures should be kept within the calculated hydraulic fracture pressure profile. Flow rates should be controlled to minimize wash-out, particularly in granular soils.

Records of conductor installation and shallow well drilling should be available. The implications for foundation soils of any incidents, of excessive loss of circulation, of return of drilling fluids to the seafloor other than through the conductor, or of creation of seafloor craters shall be assessed. The cuttings from the well drilling operation, if allowed to accumulate on the seafloor, shall be taken into account in the foundation design (including settlement), installation procedure and structure removal.

The skin friction capacity of conductors installed in cohesive soils by jetting is covered in 10.5.2.

9 Reassessment of pile capacity for existing structures

9.1 General

ISO 19901-9 describes the structural integrity management (SIM) activities required to demonstrate the fitness-for-service of existing fixed steel offshore structures throughout the intended design service life.

In the context of the reassessment of the foundation system of an existing structure, this involves an assessment of available geotechnical and foundation data, evaluation of how the original geotechnical design was established and potentially differs from current geotechnical practice, any changes in the use or loading of the system, the effects of drilling and production operations, and the effects of time since the structure installation on the performance of the foundation system.

9.2 Geotechnical and foundation data

9.2.1 Geotechnical data

The original geotechnical site investigation used to establish the foundation response is not always based on current practice. The validity of the existing site and soil investigation data shall be assessed. Older site investigation data may be adjusted to reflect differences between older and modern investigation techniques [150], [280].

More recent soil investigation data or geophysical site investigation data can be available from the project site or from nearby locations in the same geological environment. The distance within which non site-specific data are relevant to the project site depends on the geological environment. Applicability of nearby data where geotechnical stratigraphy and properties are spatially variable shall be assessed based on the understanding of the geological environment.

The feasibility and value of acquiring modern geophysical and geotechnical data close to an existing infrastructure shall be assessed.

9.2.2 Design data

The methods, decisions, geotechnical data and analyses used to demonstrate that the foundations are fit-for-service shall be documented.

Original foundation design data, including the selection of geotechnical parameters, loading criteria and design methods shall be assessed against current practice.

If foundation data or geotechnical data are missing or inaccurate, this additional uncertainty shall be addressed in the choice of representative values and methodologies.

9.2.3 Installation data

As-built foundation installation data including pile driving records and dynamic pile monitoring data shall be used, where available, to back-analyse geotechnical stratigraphy and parameters.

Available installation records shall be used to verify as-built data, such as pile lengths, depths to wall thickness changes, and steel material grades which can differ from those given on design drawings, particularly if the piles were driven to refusal and are short of the original design penetration.

9.2.4 Condition data

Foundation condition data shall include as available:

a) historical condition data relating to changes made to foundations;

b) present condition data relating to the surveyed condition of foundations.

Measurements of scour around existing foundations and measurement-based predictions of future scour may be used in preference to the assumptions made in the original design.

Information on the assessment of foundation capacity based on the historical performance of the pile foundation system is provided in 9.3.

9.2.5 Operational data

Operational data should include, as available, information on:

a) changes in platform actions;

b) exposure to metocean conditions, earthquakes, sediment transport and other environmental events;

c) exposure to accidental events, such as snag actions;

d) envelopes used in operating equipment.

9.3 Evaluation

Quantitative evaluation of existing data shall be undertaken to:

— confirm structural integrity, mitigation strategies, and established risk levels to achieve the required performance level; or

— to identify that mitigation measures are required.

Such quantitative evaluation shall consider:

a) geotechnical and foundation data described in 9.2;

b) foundation capacity and response data based on current practice;

c) criteria data such as updated knowledge of geohazards at the project site (e.g. earthquake or seabed instability) that can result in a degradation of the foundation soil;

d) incident / accident data (e.g. extreme or abnormal seismic event);

e) learnings from similar foundation systems or similar geotechnical conditions.

9.4 Assessment

9.4.1 General

ISO 19901-9:2019, 12.3 describes the different methods that can be used for the assessment of existing structures and the foundation capacity. The geotechnical aspects of a pushover response of an offshore platform supported by pile foundations (ultimate strength method) are described in 9.4.2, with reference to ISO 19901-9:2019, 12.3.4.3.

9.4.2 Pushover response of pile foundation systems

The ultimate overall system (pushover) response and capacity of the pile foundation system is characterized by the failure mechanism. For structures in shallow waters dominated by horizontal actions, the failure mechanism is typically shear, and the system capacity is governed by the lateral response of the piles and well conductors. For structures dominated by overturning moments, the failure mechanism is typically overturning, and the system capacity is primarily governed by the axial response of the piles with some contribution from the moment capacities of the piles and well conductors.

With reference to ISO 19901-9, the pile foundation and conductor system shall be treated as follows in pushover analyses:

a) Model the connection between the pile foundations and the structure in the analyses, with a focus on the rotational stiffness of the system.

b) Include jacket leg stubs that extend below the seafloor in the structural analyses. These leg stubs contribute to the lateral capacity of the piles.

c) Include the well conductors in the structural model of the platform as they can contribute both to the shear resistance and the overturning resistance of the foundation system [150]. Well conductors are modelled in the same way as pile foundations below the seafloor, considering compatibility between forces and displacements between the conductors and the soil and between the conductors and the platform. Conductors shall be modelled to reflect the actual conditions of their guide systems and connections to the jacket.

d) Include the effects of cyclic actions. In Reference [365], it is demonstrated that the use of the cyclic *p*-*y* curves described in 8.5.2.2 in pushover analyses gives a good hindcast of observed platform performance (i.e. structural damage and pile head displacement at the seafloor) during extreme events in the Gulf of Mexico.

e) Check the sensitivity of the foundation system capacity to the lateral and axial capacities of the piles, where the pile foundation system governs the capacity of the platform. If the foundation system capacity is more sensitive to the lateral soil resistance, the failure mode for the pile system is dominated by shear. If the foundation system capacity is more sensitive to the axial soil resistance, the failure mode is dominated by overturning. In such cases, geotechnical factors such as the stratigraphy and the soil properties will govern the response.

f) Check the sensitivity of the pushover capacity for the pile foundation system to the steel yield strength for piles and well conductors. The rated yield strength can underestimate the most likely or expected value [76]. Use unbiased (rather than low) estimates of input values in calibrating historical performance and in predicting future performance.

g) Account for the fact that the axial load-displacement response of the pile foundation system as represented by load-transfer (*t*-*z* and *Q*-*z*) curves can result in an ultimate capacity which is lower than the peak ultimate capacity given in design according to the methods given in 8.1. This is due to the shape of the load-transfer curves and flexibility of the pile. Further guidance is provided in 8.1 and A.8.1.3.2.4 and A.8.4.1.

Survival of a pile foundation system during previous extreme action events shall not be directly used as evidence for increased in situ strength of the soil compared to the original design. Any approach accounting for previous loading events shall address a number of factors of relevance to the entire platform system, as discussed in Reference [150].

9.5 Time-dependent effects on pile foundations

In silica sand, significant increases in axial pile capacity with time have been measured over periods of days up to around one year that are unrelated to pore pressure dissipation (e.g. References [81], [36] and [197]). The mechanisms for this increase in pile capacity, commonly known as "ageing", are still unproven but appear to be related to corrosion and other effects that can raise radial effective stresses and produce a stronger dilation mechanism and higher steel pile-soil interface angles of friction. Loading piles to failure disrupts the ageing process and piles that are loaded to failure show a loss of capacity if re-tested after unloading.

Pile driving in clay normally results in the development of excess pore pressures that produce a low initial axial pile capacity immediately after driving that increases with time as the pore pressures dissipate (see A.8.1.3.2.5). This reconsolidation-related change in axial pile capacity can take months or years, depending on the consolidation characteristics of the clay and the diameter of the pile. However, it has been shown that capacity ageing effects also develop in clay, running in parallel and in addition to the reconsolidation process [197].

Although ageing has been measured on medium to large-scale piles (e.g. the EURIPIDES research piles in very dense silica sands in the Netherlands [202], and the Jamuna Bridge piles in micaceous sands [340]), reliance on ageing effects on large diameter offshore piles experiencing high degrees of long-term cyclic loading without supporting evidence can be inappropriate and should be approached with caution. More conservative assumptions shall be considered when no evidence of ageing effects is available (e.g. for piles driven in carbonate soils). Carefully planned and instrumented re-strike tests can provide evidence of field ageing trends.

10 Soil-structure interaction for subsea structures, risers and flowlines

10.1 General

This clause sets out design criteria and recommendations for subsea production systems that address the interactions of subsea structure foundations, risers or flowlines with marine soils. It provides design criteria and methods for soil–riser and soil–flowline or pipeline interactions that are not addressed in other international standards from the ISO 19900, ISO 13623 or ISO 13628 series. Other methods, based upon local practice and experience, may also provide suitable soil-structure interaction solutions.

The following sections address geotechnical design issues for foundations of pipeline and subsea production structures and for the soil–risers or soil–flowlines interactions and shall be applied to all seabed conditions unless noted by underlying assumptions.

10.2 Geotechnical investigation

The scope of the geotechnical investigation shall anticipate the requirements for design and code conformance. It should include some combination of sampling and/or *in situ* testing techniques to shallow penetrations for flowlines and steel catenary risers and deeper penetrations for riser towers and top tension risers. Example geotechnical investigation techniques include:

— drilled soil borings with downhole soil sampling and *in situ* testing;

— continuous penetration tests (e.g. cone penetration (CPTU), T-bar or ball tests);

— large-diameter piston drop cores or push samples (core barrel length up to 20 m to 30 m);

— gravity drop cores (core barrel length up to 5 m to 10 m) and box cores (for top 0,5 m to 1,0 m of sediments).

Details about equipment and procedures for marine soil investigations are provided in ISO 19901-8.

In addition to index and classification tests (i.e. bulk density, Atterberg limits, moisture content, grain size distribution, specific gravity, and carbonate content), undisturbed and remoulded shear strength shall be measured. An understanding of *in situ* OCR and expected dilatant or contractant behaviour of the soil when sheared can prove useful for the design of flowlines. Depending on the intended application, pH, thermal conductivity and electrical resistivity tests can also be performed to assess the insulating and corrosive properties of the soil.

The site characterization scope should include integration of the geotechnical data, geological study and the shallow high-resolution data, depending on the uniformity of geologic units and soil conditions. The results of the integrated study can be used to assess restraints imposed on flowline and riser design by seafloor features, geohazards, and soil conditions (see ISO 19901-8 and ISO 19901-10).

10.3 Foundations for subsea production structures

Foundation configurations that can be utilized include mudmats without or with skirts, driven piles, pushed pin piles, suction piles, conductors or combinations of these.

The effects of drilling activities on the soil formation and foundation system shall be considered.

The design and installation of shallow and intermediate foundations with or without skirts is addressed in Clause 7 and Clause A.7. More specific design cases for the foundations of manifolds or subsea production structures can comprise:

— actions from the tie-in flowlines, spool-pieces, pipelines and umbilicals, with possible coupling between vertical and horizontal actions;

— effect of heat from produced hydrocarbons, particularly if gas hydrates are present;

— installation tolerances and actions due to re-positioning or levelling, if required.

Contingency methods should be established for situations where the foundation fails to penetrate into the seabed to the target penetration. These methods include ballasting the foundation or grouting the space between the foundation top plate and the seafloor.

10.4 Steel catenary risers

10.4.1 General

The geotechnical properties of the seabed can influence the design conditions for steel catenary risers (SCRs) in two aspects:

1) an ultimate limit state associated with excessive bending and tensile stresses in the riser wall; and

2) a fatigue limit state associated with cumulative damage to the riser from motion-induced changes in bending stress in the region of the touchdown point.

In an SCR, the maximum static curvature occurs within the suspended part of the catenary and the seabed stiffness has a negligible effect on the maximum curvature. Thus, the seabed properties have essentially no influence on the maximum static in-plane bending stresses within the riser. However, the seabed properties have a significant influence on the shear force in the riser, and hence changes in bending moment due to environmentally induced motions of the riser. The seabed properties thus affect fatigue calculations.

In addition, the seabed properties affect local out-of-plane curvature of the riser during extreme environmental events or large transverse or out-of-plane motions, particularly where the riser has become partially embedded within the touchdown zone. Seabed properties can also affect transient bending moments induced in the riser during any position changes of the floating facility from which they are suspended. However, for out-of-plane loading, the maximum stresses occur at different locations around the circumference of the pipe.

10.4.2 Design for ultimate limit state

An ultimate limit state can arise under extreme environmental events that cause out-of-plane motion, particularly when the riser becomes embedded or lies within a trench, thus giving rise to high lateral soil resistance and locally high curvature of the riser. The lateral soil resistance usually exceeds the normal frictional resistance for pipelines lying on the seafloor (e.g. Reference [4]).

An upper estimate of the maximum soil resistance acting on a trenched pipeline may be based on solutions for the limiting action acting on a cylinder moving through fine-grained soil (e.g. Reference [235]), or the horizontal component of resistance for a shallowly embedded pipeline (e.g. Reference [236]).

10.4.3 Design for fatigue state

10.4.3.1 General

The stress ranges used in the fatigue analysis of SCRs are calculated from the changes in riser stress caused by first- and second-order motions. Within the touchdown zone these motions can be simplified to moving the touchdown point (TDP) in-line with the riser and assessing the resulting changes in bending moment. A sketch of the change in maximum pipeline stresses arising from bending moments in the touchdown zone due to example riser motions with both high and low values of soil stiffness is shown in Figure 16.

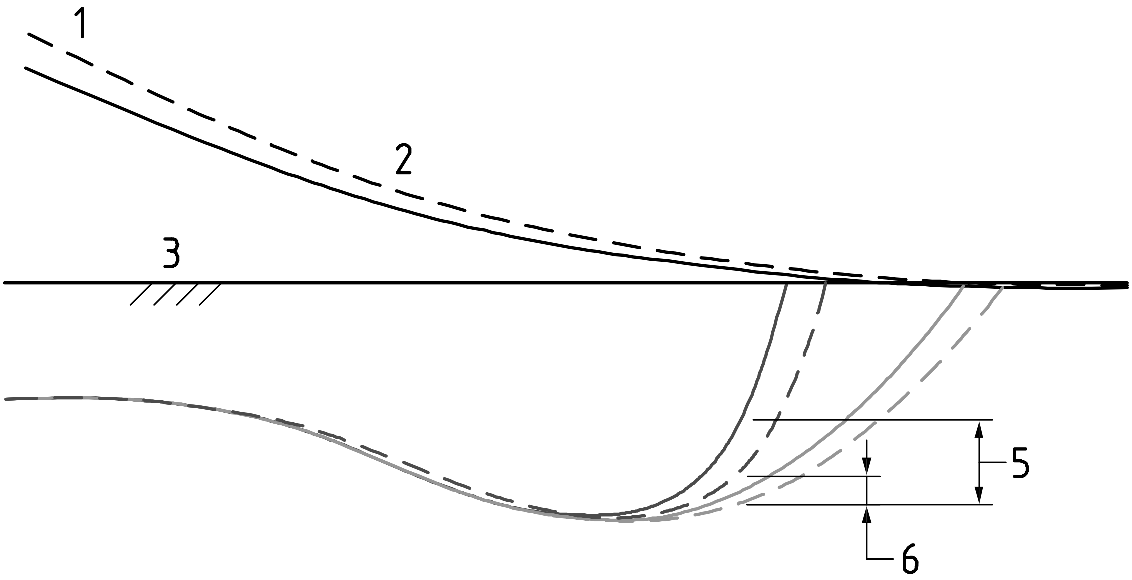

Key

1 Simulated riser motion
2 Riser
3 Seafloor
4 Stress envelopes along riser length near the TDP
5 Stress range, Δσ – stiff soil
6 Stress range, Δσ – soft soil

Figure 16 — Example stress changes for SCR fatigue calculations

The cyclic stress range in the touchdown zone depends on the rate of change of the bending moment with distance along the riser, and thus the shear force. Analysis shows that the maximum shear force varies approximately linearly with the logarithm of the soil stiffness. Fatigue laws follow a power law relationship, with damage proportional to a high power (typically about five) of the cyclic stress amplitude. Therefore, relatively minor differences in the shear force can have a significant effect on the estimated fatigue life, and hence the non-linear response of the soil shall be addressed in design.

Either small or large waves can dominate the fatigue damage in the touchdown zone. The majority of fatigue damage can occur from either large waves (not necessarily the most extreme) with low probability of occurrence or continuous motions from small day-to-day waves. Some of the most damaging waves for fatigue occur with return periods of ½ yr to 2 yrs.

10.4.3.2 Design options

Modelling of the riser-soil interaction for fatigue assessment can include:

1) a uniform elastic soil spring along the entire touchdown region;

2) a non-linear elastic spring based on the soil response in a 'fully degraded' state;

3) a non-linear spring that considers loading, unloading, reloading cycles, penetration into the seafloor and variable shear strengths with depth.

The models increase in complexity with their order. Option 1 is the least complex. However, selection of a single elastic soil spring can be challenging. The actual soil stiffness will vary considerably depending on the range of cyclic displacements, hence the spatial location along the touchdown zone and the magnitude of the riser motions in the water column. Because a single spring cannot capture the spatial and temporal variability, a high (conservative) value of elastic stiffness shall be adopted if this option is followed, as discussed further in A.10.4.

Fatigue damage depends particularly on the soil stiffness within the zone where the riser undergoes periodic lift-off and is therefore likely to entrain water into the underlying soil. The second option is therefore based on the assumption of fully remoulded soil response. Model tests have suggested the use of a simple hyperbolic model of soil response, where the stiffness decreases in inverse proportion to the cyclic displacement range [33]. The results should be normalized for more general application where the stiffness (k) is normalized by the bearing capacity ($N_c s_u D$) and the displacement (z) is normalized by the pipe diameter (D). Normalized curves for the Gulf of Mexico and offshore Angola are included in A.10.4.

The third option, although the most complex, is also the most robust. Alternative non-linear models have been proposed and have been implemented in general purpose software for analysis of vessel and riser dynamics (see References [35] and [294]). The models are relatively sophisticated, requiring a number of parameters. Where no direct calibration of the parameters is undertaken, appropriate conservative values that reduce fatigue life shall be adopted.

10.4.3.3 Trenching effects

Field surveys have shown that in some cases trenches a few metres deep can develop [61]. Analytical work has been performed to assess the impact of the trench on fatigue life [295]. These studies indicate that trenches can affect fatigue life by less than a factor of two [295]. Some studies have suggested a decrease in fatigue life due to trenching for certain combinations of riser geometry and metocean conditions, while the majority of studies suggest an increase. The effect of trenches on riser fatigue life and options for investigating such effect are provided in A.10.4.

10.4.3.4 Cyclic and consolidation effects

Cyclic loading decreases the soil stiffness under undrained loading conditions due to remoulding. However, long term cyclic loading will allow at least partial consolidation, hence partially offsetting the reduction in stiffness. In normally consolidated clays, the long-term stiffness can recover to up to 80% of the initial (pre-remoulding) value, and lower recovery is expected for higher over-consolidation ratios. These considerations should be addressed when selecting appropriate soil-riser stiffness values, or non-linear models. A number of studies have been published regarding the effects of consolidation on riser-soil stiffness (see References [369], [4] and [177]), which are discussed in A.10.4. Stiffness values arising from these studies may be adopted provided soil conditions and riser motions are considered similar to those in the published studies. Alternatively, specific model tests may be undertaken.

10.5 Geotechnical design for top tension risers

10.5.1 General

The geotechnical design of top tension risers is focused on the conductor which is the uppermost section of the well positioned in the seabed. The conductor section provides lateral support under short term ultimate limit state conditions and longer-term fatigue.

10.5.2 Jetted conductors

10.5.2.1 General

In the absence of existing practice and already established installation techniques, the approaches outlined in the following subclause may be used to estimate short-term (<10 days) and long-term (>10 days) axial bearing capacity of jetted conductors installed in normally consolidated to lightly over-consolidated clays. The method outlined herein was initially developed for the Gulf of Mexico clays and, through basin-specific calibration, its use has been extended to other regions.

10.5.2.2 Short-term axial bearing capacity

The guidance provided in Clause 10.5.2 may be applied to basins not covered in this subclause after calibration to basin-specific conditions, but shall not be used in sands.

Conductor configuration and jetting bit, tool joint information and bottom hole assembly information shall be determined for design.

Prior to designing a jetted conductor, a feasibility study shall be performed to assess if site conditions are favourable for installing the conductor using jetting. The following data, as available, shall be reviewed to assess likelihood of premature refusal:

a) geotechnical data, including the presence of sand strata and stiff clays near the seafloor;

b) geophysical data, including the presence of erosional unconformities which can imply stiff to very stiff clays at shallow depths;

c) past installation records, if any.

The immediate axial capacity of the conductor is defined at a time equal to 0,01 day (i.e. 14 mins). In the absence of more definitive criteria, the immediate axial capacity shall be estimated using Formula (42).

$$Q_o = WOB_{last} = R \cdot (W_{cond} + W_{WH} + W_{DC} + W_{CADA}) \quad (42)$$

where

Q_o is the jetted conductor axial capacity immediately after jetting (t=0,01 days);

WOB_{last} is the last weight on bit recorded during installation;

R is the WOB utilization ratio;

W_{cond} is the weight of the surface conductor in water;

W_{WH} is the weight of the wellhead housing in water;

W_{DC} is the weight of the drill collars in water;

W_{CADA} is the weight of the drill-ahead tool in water.

The WOB utilization ratio, *R*, during reciprocation shall be kept less than 1,0 to avoid compression stresses and prevent buckling in the bottom hole assembly (BHA) and running string. An *R* value of 0,8 should be used.

Set-up of jetted conductors shall be estimated using Formula (43).

$$\Delta\alpha_t = \frac{Q_t - Q_o}{\pi \cdot D \cdot L \cdot s_{u_{ave}}} \tag{43}$$

where

$\Delta\alpha_t$ is the change in average friction factor along the conductor, at time = t, due to set-up;

Q_t is the conductor capacity at time = t days < 10 days;

D is the surface conductor diameter;

L is the conductor length below seafloor (i.e. embedded length);

$s_{u_{ave}}$ is the average undrained shear strength over the embedded length of the conductor.

The $\Delta\alpha_t$ relationship with time is developed through regional experience from back-analysis of installed jetted conductors. In the absence of more definitive criteria, Formulae (44) to (46) shall be used provided that:

a) the design WOB profile is constructed based on the criteria outlined in Reference [188];

b) the drill bit stick-out is between 75 mm and 22 8 mm (3 in and 9 in) [376];

c) the conductor reciprocations during installation are performed such that the WOB remains between the minimum and design lines as shown in Figure 17.

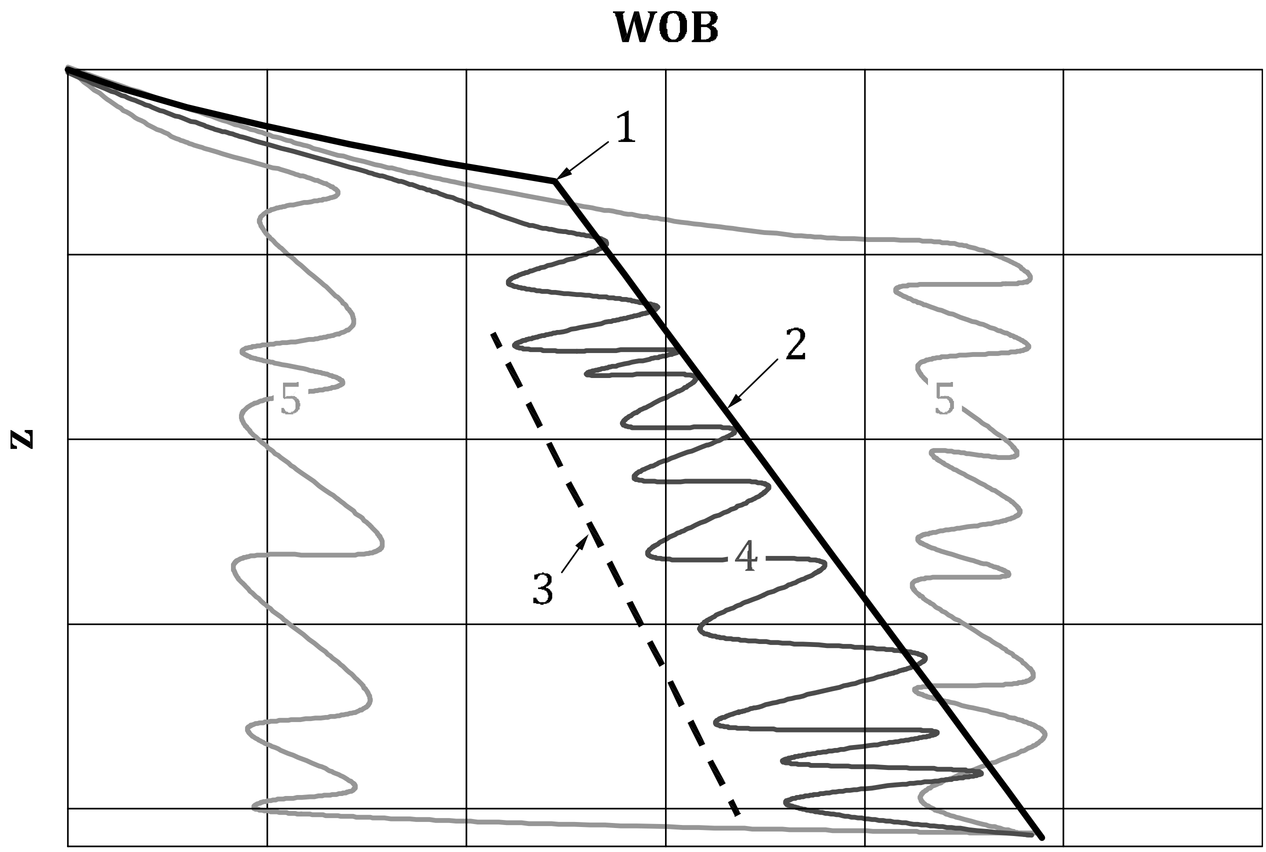

Key

1 End of self-weight penetration

2 Design or recommended maximum WOB profile for jetting

3 Design or recommended maximum WOB profile for jetting (70 % of maximum design profile)

4 Desirable WOB profile

5 Undesirable WOB profile

z Depth below original seafloor

Figure 17— Schematic examples of weight-on-bit (WOB) profiles: design or recommended, desirable and undesirable

$\Delta\alpha_t = 0{,}055 \cdot [2 + log(t)]$ for Gulf of Mexico, (see [188]), offshore Mauritania, Senegal, and Egypt clays (44)

$\Delta\alpha_t = 0{,}035 \cdot [2 + log(t)]$ for Capsian Sea clays (45)

$\Delta\alpha_t = 0{,}038 \cdot [2 + log(t)]$ for offshore Angola clays and conductor length less than 69m (see [129]) (46)

$\Delta\alpha_t = 0{,}029 \cdot [2 + log(t)]$ for offshore Angola clays and conductor length between 69m and 82m (see [129])

The short-term (<10 days) conductor axial bearing capacity at time t shall be estimated using Formula (47).

$$Q_t = WoB_{last} + \Delta\alpha_t \cdot \pi \cdot D \cdot L \cdot s_{u_{ave}} \tag{47}$$

Jetted conductors are considered temporary foundations. To account for uncertainty in action and soil resistance, partial action and resistance factors shall be applied to achieve a minimum overall factor of safety of 1,3.

10.5.2.3 Long-term axial bearing capacity

Jetted piles are piles installed with the jetting technique used for jetting conductors and can be used as permanent foundations for subsea structures. In the normally consolidated to lightly over-consolidated Gulf of Mexico clays and in absence of site-specific data, the long-term (>10 days) axial capacity of jetted piles shall be estimated using Formula (43) with the set-up relationship given in Formula (44) [376]. Partial action and resistance factors equal to those for driven piles shall be used in design, which is often controlled by operating, not extreme, conditions.

10.5.3 Soil-structure interaction for well integrity assessment

The guidance provided in 10.5.4 and 10.5.5 is for developing soil input parameters for integrity assessment of top tensioned riser (TTR) systems. The recommendations provided in 10.5.4 and 10.5.5 for well strength and fatigue assessment are exclusive of any factors of safety or partial factors to loading actions and resistances. Factors of safety may be selected through industry recommended practices (see References [28], [29] and [112]) or chosen by operators based on regional experience or case specific basis.

10.5.4 Geotechnical input to well strength assessment

10.5.4.1 Clays

The lateral capacity of an element of the well conductor in normally consolidated to lightly over-consolidated clays with s_u less than 100 kPa for a well strength analysis shall be assessed using the approach in the main text for the monotonic lateral response of piles in 8.5.2.2.

10.5.4.2 Sands

The lateral capacity of an element of the well conductor in sand for a well strength analysis can be assessed using the approach for the monotonic lateral response of piles in sand in 8.5.3.

10.5.5 Geotechnical input to well fatigue assessment

10.5.5.1 General

The guidance provided in this subclause does not apply to the following unconventional soils and seabed conditions:

— calcareous and carbonate soils;

— structured soils with sensitivity greater than 8,0 or slicken-sided;

— hard glacial till seabed where gravel, cobbles, boulders or hardpan can exist;

— seabed soils with shallow gas or gas hydrate;

— soils disturbed by operating activities;

— soils contaminated by cement and drill cuttings.

Two methods are presented for fatigue assessment of wells in clays: the spring-only method and the spring-dashpot method. The spring-dashpot method is more appropriate where the assessment requires estimation of the dynamic behaviour of the TTR system. The spring-dashpot method accounts for the energy dissipated in the foundation soil during each load-unload loop, termed as hysteretic damping. Experiments and field observations have demonstrated that hysteresis can be important for fatigue assessment of TTR systems installed in clay seabeds. More details are provided in A.10.5.5.

Development of p_{fa}-y_{fa} data shall be based on the best estimate soil strength properties, if site-specific soil properties are available. In the absence of site-specific geotechnical information, engineering judgement may be used to derive the best estimate soil parameters. Sensitivity analysis should be performed with p_{fa}-y_{fa} data derived using upper estimate and lower estimate soil properties, if site-specific soil properties are available. Otherwise, engineering judgement may be used to derive the upper and lower estimates of the soil properties. Laboratory tests may be performed on site-specific samples to directly obtain p_{fa}-y_{fa}. An example of laboratory testing equipment and procedures to obtain p_{fa}-y_{fa} data for well fatigue analysis is presented in Reference [372].

For developing p_{fa}-y_{fa} springs, the following general provisions are given:

— parameters in calculations shall be determined for the p_{fa}-y_{fa} spring depth;

— first soil spring should be at seafloor;

— spacing of p_{fa}-y_{fa} curves along the conductor shall be no greater than:

  — 0,5 m in the top 25 m below seafloor;

  — 1,0 m below 25 m depth below seafloor;

— analyses shall include the following model conditions, unless field observations indicate otherwise:

  — no seafloor scour or erosion;

  — no gapping between the conductor and the seabed;

  — no drill cuttings and cement at seafloor;

— ground model and soil parameters shall extend to at least 45 m below seafloor for the purpose of developing p_{fa}-y_{fa} curves for well fatigue;

— p_{fa}-y_{fa} curve formulations shall only be used for fatigue analysis where rig and riser are in a no-offset position (see A.10.5.4 for discussions on offset conditions).

10.5.5.2 Clays

10.5.5.2.1 Spring-only method

The lateral p_{fa}-y_{fa} response of a soil element for well fatigue assessment in clays shall be assessed using the approach outlined in 8.5.2.4.

10.5.5.2.2 Spring-dashpot method

Soil damping effects can be approximated by introducing equivalent viscous damping with energy dissipation equal to that dissipated by hysteresis. The viscous damping is modelled by a dashpot having a viscous coefficient, c, expressed by:

$$c = \frac{2K_{Sec.ss} \cdot \xi}{\omega} \tag{2}$$

where

$K_{Sec.SS}$ is the soil secant stiffness at the steady-state condition;

ξ is the soil damping ratio;

ω is the motion angular frequency obtained from the modal wave frequency, in riser analysis.

Estimation of the viscous coefficient uses a first approximation of displacements along the well. In the absence of more definitive criteria, the following steps shall be used:

a) perform analysis using spring-only approach as outlined in 8.5.2.4 and obtain displacement amplitude time-histories 4,0 m above seafloor;

b) determine ξ profile for each sea-state motion based on the profiles provided in Figure 18 for maximum one-way displacement amplitudes taken at 4,0 m above seafloor; interpolation can be used where a displacement amplitude falls between the provided profiles;

c) determine $K_{Sec.\_SS}$ for each sea-state motion using Figure 19 with the maximum value not exceeding 700 s_u (with s_u taken at the spring-dashpot depth);

d) calculate c values at each spring location using Formula (48);

e) re-run fatigue analysis with a dashpot viscous coefficient calculated from Formula (2) and p_{fa}-y_{fa} curves calculated from 8.5.2.4 and Formula (34), but with the following A_s and B_s model parameters:

— if $s_u < 40$ kPa, A_s = 0,335 and B_s = -0,03;

— if $s_u \geq 40$ kPa, A_s = 0,27 and B_s = -0,175.

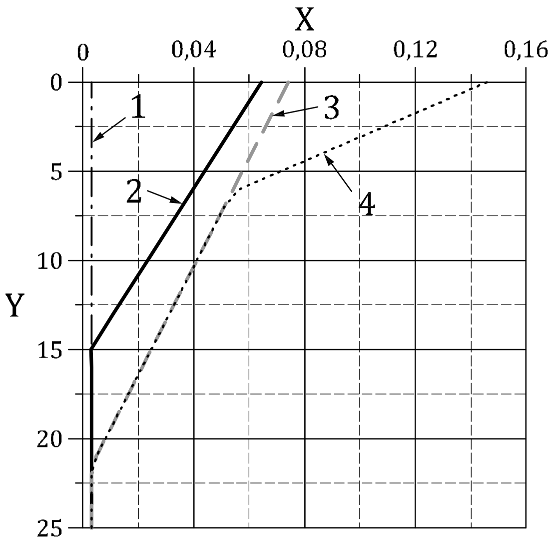

Normally consolidated to lightly over-consolidated clays

Depth BML	***Maximum y amplitude***			
(m)	***<0,025D***	***0,025D***	***0,05D***	***0,1D***
0,0	0,003	0,064	0,074	0,146
7,0	0,003	0,036	0,051	0,051
15,0	0,003	0,003	0,025	0,025
22,0	0,003	0,003	0,003	0,003
25,0	0,003	0,003	0,003	0,003

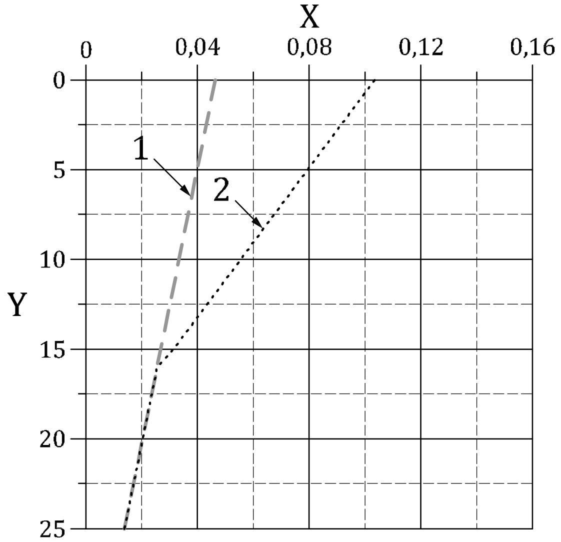

Over-consolidated clays

Depth BML	***Maximum y amplitude***	
(m)	***≤ 0,05D***	***0,1D***
0,0	0,046	0,103
16,0	0,026	0,026
25,0	0,014	0,014

Key

1 Maximum y amplitude < 0,025*D*
2 Maximum y amplitude = 0,025*D*
3 Maximum y amplitude = 0,05*D*
4 Maximum y amplitude ≤ 0,05*D*
5 Maximum y amplitude = 0,1*D*
D Conductor outside diameter
X Soil damping ratio, ξ
Y Depth below original seafloor, z (m)

Figure 18 — Clay soil damping ratio profiles for maximum one-way well displacement amplitudes taken at 4,0 m above seafloor: (top) normally consolidated to lightly over-consolidated and (bottom) over-consolidated [373], [374]

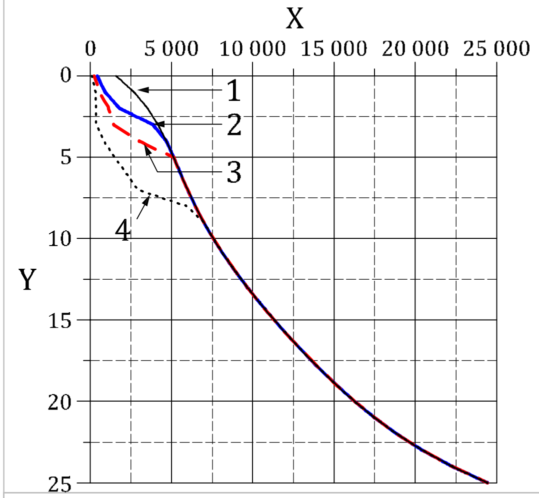

Normally consolidated to lightly over-consolidated clays

$K_{Sec,\_SS}$ value for maximum y amplitudes					
Depth BML (m)	**0,025*D***	**Depth BML (m)**	**0,05*D***	**Depth BML (m)**	**0,1*D***
0,0	421	0,0	224	0,0	95
1,0	905	1,0	561	1,0	326
2,0	1 786	2,0	1 123	2,0	350
3,0	3 844	3,0	1 421	3,0	369
4,0	4 670	4,0	2 943	4,0	823
5,0	5 119	5,0	5 119	5,0	1 480
>5,0	700 s_u	6,0	5 546	6,0	2 216
		>6,0	700 s_u	7,0	2 908
				8,0	5 917
				9,0	6 982
				>9,0	700 s_u

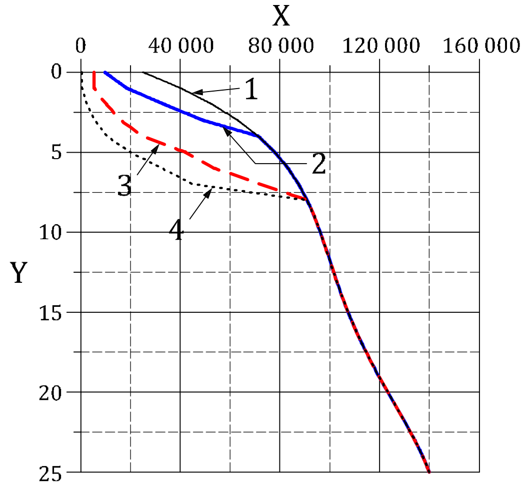

Over-consolidated clays

$K_{Sec,\_SS}$ value for maximum y amplitudes					
Depth BML (m)	**0,025*D***	**Depth BML (m)**	**0,05*D***	**Depth BML (m)**	**0,1*D***
0,0	9 660	0,0	5 457	0,0	673
1,0	18 541	1,0	5 457	1,0	673
2,0	33 553	2,0	10 454	2,0	2 676
3,0	49 060	3,0	16 078	3,0	5 673
4,0	71 305	4,0	24 917	4,0	10 625
> 4,0	700 s_u	5,0	42 117	5,0	19 916
		6,0	53 642	6,0	32 515
		7,0	72 283	7,0	45 115
		8,0	90 925	8,0	90 925
		>8,0	700 s_u	>8,0	700 s_u

Key

1 700 s_u y = 0,0D
2 Maximum y amplitude = 0,025D
3 Maximum y amplitude = 0,05D
4 Maximum y amplitude = 0,1D

D Conductor outside diameter
X Steady-state secant stiffness, $K_{Sec.\_SS}$ (kN/m/m)
Y Depth below original seafloor, z (m)

Figure 19 — Clay $K_{Sec.\_SS}$ profiles for maximum one-way well displacement amplitudes taken at 4,0 m above seafloor: (top) normally consolidated to lightly over-consolidated and (bottom) over-consolidated [373], [374]

10.5.5.3 Sands

The lateral capacity of an element of the well conductor in sand for a well fatigue analysis may be assessed using the approach in the main text for the lateral response of piles in sand (see 8.5.3).

10.5.6 Geotechnical considerations in conductor driving analysis

Geotechnical considerations for conductor driving analyses are similar to the codified methods. Recommendations for the installation of driven foundation piles as outlined in ISO 19902 and in 8.7 . Additional guidance on the following subjects pertaining to conductor pipe driving is provided in A.10.5;

— conductor pipe installation;

— remedial measure when encountering premature refusal during conductor driving;

— stress verification during hammer placement and driving;

— fatigue damage to conductor pipe from driving;

— conductor pipe tip damage and bucking;

— use of inclined shoes to drive conductors.

10.5.7 Geohazards for well installations

Conductors are the foundation for the well. Their main function is to resist the axial and lateral actions imposed at the wellhead. The recommendations in Clause 8 applicable to foundations should be followed. Additional guidance on geohazards specific to well installations is provided in Clause A.10.

10.6 Foundation design for riser towers

10.6.1 General

The riser tower concept consists of a free-standing riser assembly, incorporating several risers in a bundle configuration, tensioned from the top by a buoyancy tank, and anchored to the seabed. The tower is generally connected to the surface vessel or platform by flexible jumpers.

A riser tower supports axial tension generated by buoyancy and by cyclic wave action and a significant part of the tension acts permanently during the life of the structure.

10.6.2 Foundation options

Foundation options include gravity base, suction piles and driven piles, or a combination of these.

The vertical uplift resistance comprises of the following three components:

1) submerged foundation weight;

2) external skin friction;

3) for suction piles, reverse end bearing at the bottom of the pile.

Permanent, i.e. sustained, uplift action can be counter-acted by a ballast weight.

10.6.3 Loading actions and safety factors

10.6.3.1 Loading actions

Design loading actions shall be evaluated for the following conditions:

a) foundation installation and retrieval;

b) operating conditions;

c) extreme conditions.

10.6.3.2 Recommended safety factors

The safety factors recommended by ISO 19901-7 and API RP2T [26] for driven piles and gravity base anchors and by API RP2SK [25] for suction piles should be evaluated for adequacy and may be increased because:

— The API RP2SK safety factors were developed with no consideration of permanent uplift loads on suction caissons. Additional information on permanent uplift loads is provided in A.10.6.

— API RP2T does not address the case of gravity loads explicitly and 10.3.3 of API RP2T, 3rd Edition, July 2010, states that:

For axial pile design where the weight of the foundation system is less than approximately 10 % of the ultimate axial capacity, the underwater weight of the foundation system may be subtracted from the applied loads in determining the safety factor of the foundations. For other weight-dominated systems, the foundation system weight should be added to the resistance side of the formula.

10.6.4 Design challenges

The following general principles shall be addressed in assessing the stability of riser tower foundations:

a) Validated limit equilibrium methods or finite element methods can generally be used to evaluate the capacity of riser tower foundations. The shear strength used in the analysis shall account for effects of creep and potential loss in reverse end bearing from drainage under sustained or long duration loads and cyclic degradation. The potential changes in effective stresses and shear strength due to potential drainage can be studied by finite element analyses.

b) Displacement and deformation during the life of the foundation shall be addressed in design. Where displacement and deformation are critical, finite element analysis methods may be used (see 7.6 and A.11.5). The displacement analysis shall include contributions from undrained shear strains due to application of the sustained actions, undrained creep during the sustained action, and permanent and cyclic components from the wave loading and currents. Displacements due to shear strain, volumetric strains and flow of water through the soil due to potential drainage during the sustained loading period shall also be addressed.

c) The foundations shall be installed within specified tolerances of tilt and mis-orientation. The design analyses shall account for the effect of the tolerance limits.

d) If critical to the design, measures shall be taken to avoid erosion and scour of the soil beneath or near the foundation base.

e) Action combinations shall be assessed to determine the most unfavourable result, for each of the stability mechanisms and deformation analyses performed. For example, sustained loading resulting in reduced soil strength due to creep effect can be followed by a storm dynamic peak action in which case the initial reduced soil strength should be accounted for.

Where removal is anticipated, an analysis shall be made of the forces generated during removal so that that removal can be accomplished with the means available.

10.7 Pipelines and flowlines

10.7.1 Geotechnical pipe-soil interaction (PSI) analysis

10.7.1.1 General requirements

Geotechnical pipe-soil interaction (PSI) analysis shall be performed to estimate the as-laid pipeline embedment, any subsequent changes in embedment during the operating life, and the resulting pipe-soil force–displacement responses in the axial and lateral directions.

Best, lower and upper estimates shall be made of the *in situ* soil parameters as the first step in a PSI analysis. These parameters shall include the strength (intact and remoulded), submerged unit weight and pipe-soil interface strength. They shall be defined from the seafloor to the depth of influence of the pipeline. Parameter selection shall consider the uncertainty in the data and the variability along the route. Further guidance is provided in A.10.7.3.2.

Best, lower and upper estimates of the pipe–soil interaction forces shall be derived, unless it has been identified that one of the extremes will not be detrimental to the pipeline limit states. General advice on the effect of low and high geotechnical parameters on each pipeline design condition is provided in A.10.7.

The low and high estimates of pipe-soil interaction forces shall be assigned a specific probability of exceedance (e.g. P5 and P95 respectively), if they are used in a probabilistic manner in the pipeline design (i.e. in an analysis for which the soil resistance is defined in the form of a probability distribution).

The geotechnical PSI analysis shall estimate the relevant drainage conditions for each action, including the lay process and subsequent pipeline loading events or movements, in order that the relevant soil responses (drained, undrained, intermediate or multiple responses) are used in the PSI analysis (see A.10.7.3.3).

10.7.1.2 Pipeline embedment

The geotechnical PSI analysis shall calculate the as-laid pipeline embedment by:

a) adjusting the submerged pipeline weight for the local force concentration that occurs within the touchdown zone, where the pipeline catenary from the lay vessel reaches the seafloor (see A.10.7.4.3);

b) allowing for additional dynamic effects due to motion of the lay vessel, which can soften or displace the soil at the seafloor (see A.10.7.4.4).

If the seabed is potentially mobile (see 10.7.1.5), the geotechnical PSI analysis shall address through-life changes in pipeline embedment.

10.7.1.3 Axial pipe-soil resistance

The geotechnical PSI analysis shall assess the axial pipe-soil resistance using a method based on estimates of the drained and undrained pipe-soil interface strength, allowing for the roughness of the pipe coating, and supplemented by an adjustment for wedging around the curved pipe surface (see A.10.7.5).

10.7.1.4 Lateral pipe-soil resistance

The geotechnical PSI analysis shall assess the lateral pipe-soil resistance using either:

1) a theoretical yield envelope approach, in which the limiting combinations of vertical pipe-soil loading and lateral resistance are derived for the relevant soil properties; or

2) an empirical expression, in which the lateral resistance is correlated with parameters, such as normalized weight, $W'/s_u D$, normalized embedment, w/D, and strength ratio ,$s_u/\gamma' D$.

Further guidance on these methods is provided in A.10.7.6.

Approach (2) shall only be used if the underlying data used to calibrate the empirical method extends across the design values of flowline parameters (W', D, w/D) and soil properties (s_u, γ', remoulded strength, soil Atterberg limits and mineralogy).

Approach (1) shall be confirmed as appropriate for the site conditions using relevant data from model tests, numerical analysis or field observations. The relevant data shall be based on conditions that are comparable to the site. The data may be in, or referenced by, a publication, database or guideline, or may have been obtained for the specific site.

10.7.1.5 Seabed mobility

Seabed sediments can become mobile when the shear stresses arising from bottom currents and waves at the seafloor exceed the critical shear stress of the sediment. The geotechnical PSI analysis shall address whether seabed mobility – through scour, liquefaction or sediment deposition – can affect the seabed properties and pipeline embedment, by evaluating the potential for sediment transport to occur in the vicinity of the pipe (see A.10.7.7).

10.7.2 Submarine slides and density flows: simulation and pipeline impact analysis

In regions where submarine slides and density flows (both referred to as ‘slides’) can cross pipeline routes, the likelihood and severity of potential future slides and flows, and the consequence of the slide material impact on the pipeline, shall be evaluated.

Assessment for design shall involve analysis of:

a) depositional processes;

b) sub-bottom profiling or other geophysical data;

c) potential slide sources and triggering mechanisms;

d) flow dynamics allowing for interaction with the surrounding water;

e) the strength and speed of the slide or flow at the pipeline;

f) the resulting impact forces and pipeline stresses.

The framework for flow simulation and impact analysis shall involve the following steps:

1) Identify potential sources of slides and flows (e.g. through slope stability analyses and geohazard assessment).
2) Evaluate the seabed strength and flow properties of potential slides for flow simulation and impact analysis. In addition to the conventional soil properties (e.g., moisture content, Atterberg limits, salinity, density, intact and remoulded shear strengths), the rheological flow characteristics are used (see A.10.7.9.3).
3) Conduct flow simulations to obtain the expected ranges of runout distance. Where the flow crosses pipeline routes, extract the flow height, flow velocity, v, and the direction relative to pipeline axis, θ (see A.10.7.9.3).
4) Estimate the impact shear strain rate, $\dot{\gamma}$ (see A.10.7.9.4 and Formula (A.60)).
5) Estimate the corresponding mobilized or apparent shear stress and calculate the non-Newtonian Reynolds number for the impact flow (see Formula A.58 or Formula A.59).
6) Estimate the impact forces on the pipeline (see A.10.7.9.5 and Formulae (A.62) to (A.67)).
7) Assess the structural response of the pipeline.

Examples of submarine slide behaviour and engineering practices for flow-pipeline interaction are presented in References [250], [358], [73], [260] and [230].

11 Design of anchors for floating structures

Geotechnical considerations for the design of anchors for stationkeeping systems for floating structures are given in Clause A.11.

Annex A
(informative)

Additional information and guidance

NOTE The clauses in this annex provide additional information and guidance. The title of each subclause corresponds with the equivalent (sub)clause in the body of this document.

A.1 Scope

There is a large body of technical literature on offshore geoscience studies and offshore geotechnical engineering design (see Bibliography). There are also regular conferences on these topics, including:

- the Proceedings of the International Symposia on Frontiers in Offshore Geotechnics (ISFOG);
- the Proceedings of the Society of Underwater Technology (SUT) conference on Offshore Site Investigation and Geotechnics (OSIG);
- the Proceedings of the Offshore Technology Conference (OTC);
- the Proceedings of the International Symposia on Offshore and Polar Engineering (ISOPE), and on Offshore Mechanics and Arctic Engineering (OMAE).

General guidance on the application of soil mechanics theory to foundation design can be found in various undergraduate and post-graduate text books. Text books covering specific application of soil mechanics to offshore geotechnical design are uncommon though [282], [106].

A.2 Normative references

No additional guidance is offered.

A.3 Terms and definitions

No additional guidance is offered.

A.4 Symbols and abbreviated terms

No additional guidance is offered.

A.5 General requirements

A.5.1 General

No additional guidance is offered.

A.5.2 Design cases and safety factors

No additional guidance is offered.

A.5.3 Representative and design values of soil parameters

A.5.3.1 Generic principles

The representative value for a specific soil property can be a single value, a single value per soil stratum, represented by a formula per soil stratum or by a formula for a point in space and/or time. Usually, some combinations apply. A formula can include functions of geometrical and other material properties included in the calculation method.

Representative values of soil parameters should be estimated for each soil stratum. Soil stratification for a calculation method can differ from the actual stratification of the as-found soil.

Multiple sets of representative values for soil properties can be required for a single calculation, for example because of assumptions made in the calculation method.

A documented calculation method typically includes guidance on selection of the representative values and the corresponding reference scale.

The uncertainties should be assigned for both method uncertainty and uncertainty of soil parameters.

Consideration should be given to a priori knowledge. Examples of a priori knowledge include (i) a thin, continuous failure surface that can be inferred from geological conditions, (ii) a known location of a geological fault, (iii) a lower value of angle of internal friction corresponding to constant volume conditions during shear, and (iv) a likely low value for residual strength under undrained conditions.

When selecting a representative value, one should consider the tendency for a failure surface to follow the path of least resistance which can cause an apparent reduction in the parameter mean.

Particular caution should be exercised in the utilization of a shear strength value that depends on the dilatancy of the foundation soil, i.e. the tendency of a soil volume to increase (drained case) or the tendency of the pore pressure to decrease or become negative (undrained case) with change in shear stress.

The choice for a cautious, mean or high representative value can depend on other soil parameters included in the calculation model, geometry and explicit (or implicit) guidelines for use of the calculation model.

A.5.3.2 Determination of representative and design values of soil parameters

When determining the representative and the design value (or design resistance), one should (see also Figure 2):

a) integrate the reliable data from all available sources of information;

b) include the effect of the uncertainties on the representative value;

c) ensure that the representative value applies to the actual limit state;

d) check that the representative value aligns with the calculation method.

The representative value of a soil parameter for a soil stratum should correspond to the volume of soil influencing the occurrence of the limit state under consideration (e.g. a potential failure volume or failure surface). The domain of influence is also a function of the characteristics of the soil heterogeneity under consideration. The selection of a representative value can be based on sensitivity analysis.

A.5.3.3 Geotechnical reliability-based design

Life of an offshore structure requires decisions of different types and based on different degrees of information, for example for:

— design with respect to ultimate and serviceability limit states;

— testing and quality control during planning, design and operation of the offshore structure;

— planning of inspection and monitoring during installation, operation, repairs or maintenance;

— decisions on life extension and removal/replacement of an offshore structure.

A reliability-based design (or risk-informed decisions) would require that the annual failure probability does not exceed a target annual failure probability and that the annual reliability index exceeds a target annual reliability index. The target reliability level should be selected as a function of the consequence (loss of life, property and environment) and the nature of a potential loss of structural integrity or functional requirements.

ISO 2394:2015 [185] suggests tentative target reliability levels based on life quality index related to one-year reference period and ultimate limit states. In ISO 2394:2015, life quality index does not include considerations for environmental impact.

For reliability-based design of foundations, a target annual reliability index of 4 (or annual failure probability of $3 \cdot 10^{-5}$) can, for example, be used as a target reliability level [206].

A.5.4 Testing and instrumentation

No additional guidance is offered.

A.6 Geotechnical data acquisition and identification of hazards

A.6.1 General

No additional guidance is offered.

A.6.2 Geological modelling and identification of hazards

No additional guidance is offered.

A.6.3 Carbonate soils

A.6.3.1 General

Carbonate soils cover over 35 % of the ocean floor. For the most part, these soils are biogenic. That is, carbonate soils are composed of large accumulations of the skeletal remains of plant and animal life, such as coralline algae, coccoliths, foraminifera, and echinoderms. To a lesser extent, carbonate soils also exist as non-skeletal material in the form of oolites, pellets, grape-stone, etc. These carbonate deposits are abundant in the warm, shallow water of the tropics, particularly between the 30° north and south latitudes. Deep-sea carbonate oozes have been reported at locations considerably outside these mid-latitudes. Since temperature and water conditions (water depth, salinity, etc.) have varied throughout geological history, ancient deposits of carbonate material can be found buried under more recent terrestrial material outside the present zone of probable active deposition. Major carbonate deposits are known to exist in the Gulf of Mexico along the Florida coastline and in the Bay of Campeche, as well as in the Arabo-Persian Gulf and the Red Sea, in the southern Mediterranean Sea, offshore India and in the north-western Australian shelf.

The comments in A.6.3.2 to A.6.3.3 are focused primarily on carbonate silts and sands. Clay soils with varying proportions of carbonate content are common offshore and a low plasticity index is generally specific to such carbonate clays, but there is little guidance as to how conventional design approaches for clay soils should be modified for different carbonate content. Local experience is important in making such assessments.

A.6.3.2 Characteristic features and properties of carbonate soils

Carbonate soils differ in many ways from silica-rich soils. An important distinction is that the major constituent of carbonate soils is calcium carbonate, which has a low hardness value compared to quartz (the predominant constituent of the silica-rich sediments). Susceptibility of carbonate soils to disintegration (crushing) into smaller fractions at relatively low stress levels is partly attributed to this condition. Typically, carbonate soils have large interparticle and intraparticle porosity, resulting in high void ratio and low density and, hence, are more compressible than soils from a terrigenous silica deposit. Furthermore, carbonate soils are prone to post deposition alterations by biological and physiochemical processes under normal pressure and temperature conditions. This results in the formation of irregular and discontinuous layers and lenses of cemented material. These alterations, in turn, profoundly affect mechanical behaviour.

The fabric of carbonate soils is an important characteristic feature. Generally, particles of skeletal material will be angular to subrounded in shape, with rough surfaces, and have intraparticle voids. Particles of non-skeletal material, on the other hand, are solid with smooth surfaces and without intraparticle voids. It is generally understood that uncemented carbonate soils consisting of rounded non-skeletal grains that are resistant to crushing are stronger foundation materials than carbonate soils that show partial cementation but allow a moderate degree of crushing. There is information that indicates the importance of carbonate content as it relates to the behaviour of carbonate sediments. A soil matrix that is predominantly carbonate is more likely to undergo degradation due to crushing and compressibility of the material than soil that has low carbonate fraction in the matrix. Other important characteristic features that influence the behaviour of the material are grain angularity, initial void ratio, compressibility, and grain crushing. These characteristic features are interrelated parameters in the sense that carbonate soils with highly angular particles often have a high *in situ* void ratio due to particle orientation. These soils are more susceptible to grain crushing due to angularity of the particles and thus will be more apt to be compressed.

This subclause gives a general overview of the mechanical behaviour of carbonate soils. For a more detailed understanding of material characteristics, information can be found in the proceedings of the specialized international conferences on engineering of calcareous sediments (see References [20] and [7]).

Globally, it is increasingly evident that there is no unique combination of laboratory and *in situ* testing programme that is likely to provide all the appropriate parameters for design of foundations in carbonate soils. Some laboratory and *in situ* tests have been found useful. As a minimum, a laboratory testing programme for carbonate soils should determine:

a) material composition, particularly carbonate content;

b) material origin to differentiate between skeletal and non-skeletal sediments;

c) grain characteristics, such as particle angularity, porosity, and initial void ratio;

d) compressibility of the material;

e) soil strength parameters and volume change characteristics on shearing, including effects of cyclic actions;

f) formation cementation, at least in a qualitative sense.

No universally recognized classification system is presently available for carbonate materials. Classification charts for carbonate soils and rocks have been tentatively developed [83], [273] based on grain size, carbonate content and unconfined compressive strength of materials. It is recognized today that parameters such as grain crushability or skeleton compressibility play an important role in assessing the engineering properties of carbonate materials. However, in the absence of a more definite classification scheme, the proposed charts can provide useful guidance.

A.6.3.3 Foundations in carbonate soils

A.6.3.3.1 Driven piles and other deep foundation alternatives

The current trend for deep foundations in carbonate sands and silts is a move away from driven piles. However, because of lower installation costs, driven piles still receive consideration for support of lightly loaded structures or where extensive local pile loading test data and experience exists to substantiate the design premise. Furthermore, driven piles can be appropriate in moderately competent carbonate soils. At present, the preferred alternative to the driven pile is the drilled and grouted pile. Drilled and grouted piles mobilise significantly higher unit skin friction. The result is a substantial reduction in the required pile penetration compared with driven piles.

Because of the high construction cost of drilled and grouted piles, an alternative driven and grouted pile system has received some attention in the past [39]. This system has the potential to reduce installation costs while achieving comparable capacity, but quality control of the grout injection between the soil and the pile outer wall is the main uncertainty. For any type of grouted pile, the potential for reduction in friction capacity due to cyclic actions should be considered, especially once slip has been initiated between pile and soil.

A.6.3.3.2 Shallow foundations

Carbonate sands and silts generally have higher friction angles than silica sands and silts, but are more compressible, and these two factors influence bearing capacity in opposite ways. Carbonate sands and silts are also generally less permeable than equivalent silica material, leading to longer drainage times for a given size of foundation. The tendency for volume reduction on shearing, particularly under cyclic actions, combined with longer drainage times, leads to potential for bearing failure induced by soil liquefaction. Undrained cyclic strength of carbonate sands is generally lower than for most silica sands. The high compressibility of most carbonate sediments results in relatively large consolidation settlements, and can give rise to large settlements induced by cyclic actions.

A.6.3.3.3 Assessment

Stemming from some publications describing poor foundation performance in carbonate soils and the financial consequences of the remedial measures, there is a growing tendency to take a conservative approach to design in carbonate soils, even if the carbonate content in the sediment fraction is relatively low. This is not always warranted. As with other designs, the judgment of knowledgeable engineering remains a critical link in economic design of offshore foundations in carbonate soil environments.

A.7 Design of shallow and intermediate foundations

A.7.1 General

The formulae provided in Clause 7 and associated in this clause are limited in nature and are not necessarily appropriate for design in a number of situations.

In circumstances such as these, general guidance cannot be provided and reliance should be placed on experience, published case histories, physical testing and numerical modelling.

A.7.2 Principles

A.7.2.1 General principles

No additional guidance is offered.

A.7.2.2 Foundation embedment

No additional guidance is offered.

A.7.2.3 Sign conventions, nomenclature and action reference point

For an embedded foundation, the actions on the top of the foundation are transferred to the foundation base level (tip of skirt for a skirted foundation). This is done by modifying the factored actions applied to the top of the foundation to account for:

— soil resistance on the sides of the embedded foundation;

— submerged foundation weight;

— submerged soil weight within skirts, if not counteracted by the exterior soil or otherwise applicable.

Partial action factors should be applied to the foundation weight and soil weight. The factor for soil weight is generally equal to unity. Higher or lower factors can be considered in some cases, especially where there is uncertainty and the soil weight leads to improved foundation stability.

The soil resistance on the sides of the embedded foundation consists of:

— horizontal passive and active soil resistance;

— frictional resistance on the skirts.

Frictional resistance on the skirts can reduce the vertical and moment action transmitted to the underlying soil, and can be considered in the design. Specific guidance is not provided here.

A.7.3 Acceptance criteria

A.7.3.1 Material and action factors

Refer to A.7.7.2 for further performance based design guidance.

A.7.3.2 Use of partial factors in design

No additional guidance is offered.

A.7.3.3 Special cases

No additional guidance is offered.

A.7.4 Design considerations

A.7.4.1 Adjusting for soil plug weight

No additional guidance is offered.

A.7.4.2 Skirt spacing

References [231] and [135] provide guidance on skirt spacing for simplified seabed conditions.

A.7.4.3 Foundation base perforations

Reference [333] provides guidance on the impact of perforations on foundation vertical capacity.

A.7.4.4 Skirtless foundations penetrating into soft soils

No additional guidance is offered.

A.7.4.5 Tensile stresses beneath foundations

No additional guidance is offered.

A.7.4.6 Omni-directional loading

Refer to 7.7.1 and A.7.7.1

A.7.4.7 Interaction with other structures

Interaction with spudcans is addressed in ISO 19905. Interaction with conductors is addressed in 10.5.2.

A.7.4.8 Multiple foundations

In many instances, use of multiple shallow foundations can significantly increase overall foundation capacity, as illustrated in References [159] and [195].

A.7.4.9 Hydraulic stability

A.7.4.9.1 Scour

No additional guidance is offered.

A.7.4.9.2 Piping

No additional guidance is offered.

A.7.4.10 Unconventional soils or soil profiles

The methods outlined are strictly applicable to conditions of uniformly varying soil strength, although reasonable assessment of equivalent uniform properties can frequently be made. For example, the potential of a deep bearing failure depends on soil strengths at considerably greater depths than that of a sliding failure. Hence attention should be given to defining the soil parameters throughout the expected zone of influence.

The use of the standard stability formulae presented in this annex are not applicable where:

— foundation conditions are highly heterogeneous or anisotropic;

— loading conditions deviate considerably from the simple conditions assumed in the bearing capacity formulae;

— loading rates are such that the conditions are not clearly drained or undrained; or

— foundation geometries are highly irregular.

In those cases, alternative procedures such as one or combinations of the following should be selected:

a) use of conservative equivalent parameters along with the recommended formulae;

b) use of limit analysis to determine bounds on failure actions and to determine relative sensitivity of failure actions to parameters of interest;

c) use of numerical analysis to solve the governing formulae directly;

d) use of properly scaled model tests to check and verify calculation models and procedures.

References [82] and [385] provide advice on the use and design of subsea gravel and rock fills.

References [388] and [389] provide advice on rock-steel interface properties.

Refer to 7.5.1.5 and A.7.5.1.5 for surficial crusts.

Refer to A.6.3.3.2 for shallow foundations on carbonate soils.

A.7.4.11 Selection of soil parameters for design

A.7.4.11.1 Shear strength used in stability analysis

The following general practices are recommended.

a) For strongly dilatant soils, high undrained shear strengths can be used in design only if the potential loss of dilatancy on shear surfaces has been explicitly addressed.

b) In soft and very soft clays, lab vane, fall cone, unconsolidated undrained triaxial tests and unconfined compression tests are unreliable and should not be used. Consolidated undrained triaxial tests with pore pressure measurement, simple shear tests, *in situ* vane, and penetrometer, ball or T-bar tests (where the correlation between penetration resistance and soil strength is known for a particular soil) are more reliable techniques and should be used for determining undrained shear strength of soft and very soft clays.

c) Soils display undrained shear strength anisotropy, and thus triaxial compression, triaxial extension and simple shear strengths can be significantly different. Care should be taken to adopt an appropriate strength in assessing foundation capacity, and any assumptions made in this regard should be clearly documented.

d) For drained bearing capacity calculations for sands, the effective plane strain angle of friction should be used, which is generally 10 % higher than that measured in a triaxial compression test. This value should be determined at the appropriate stress level.

e) Foundation stability under cyclic loading conditions can be assessed using pseudo-static analysis provided appropriately derived cyclic shear strengths are used. One approach for deriving appropriate cyclic soil strengths for use in pseudo-static stability analysis, taking account of action history and average shear stress. A procedure for how this can be done is presented in Reference [10].

f) In many instances, cyclic performance of non-cohesive soils can be assessed using cyclic undrained soil strengths derived in a manner similar to that used for cohesive soils. A procedure for how this can be done is presented in Reference [10] . In undertaking such analyses, it is important to take due account of the effects of drainage with the potential for dissipation of excess pore pressures to occur over the duration of cyclic loading.

g) The strain rate at which testing is performed can impact the observed result, and rate effects should be considered when assessing foundation response to rapid loading events.

h) Where applicable, the effect of soil consolidation on strength can be considered in design. This will typically increase overall foundation capacity. However, in the case of preloaded foundations, the soil strength enhancement is generally limited to soils directly below the foundation base.

i) In soils that display strain softening behaviour, it can be important to consider the effects of strain compatibility when selecting a value of soil strength. This is likely to be of particular importance for skirted foundations, where contributions to stability come from a combination of base shear (at skirt tip level) and passive resistance, which are typically mobilised at very different strain levels.

j) Where possible, assessment of appropriate soil parameters should involve statistical treatment of the available data.

A.7.4.11.2 Parameters used in serviceability design

No additional guidance is offered.

A.7.5 Ultimate limit state (stability)

The bearing capacity factors used herein are considered those most commonly used, but alternative factors are available and can be applied at the discretion of the designer, subject to appropriate documentation and justification.

A.7.5.1 Assessment of bearing capacity of shallow foundations

The development of the bearing capacity formulae presented is predicated on the assumption that the soil is a rigid, perfectly plastic material that obeys the Mohr-Coulomb yield criterion with associated flow.

The following bearing capacity factors and correction factors primarily come from References [62] and [336]. In general, the formulae and factors outlined in this document should be used with care and their applicability should be checked in each case. Where appropriate, alternative methods of analysis and design approaches should be considered to verify the results obtained.

Rigorous solutions of bearing capacity factors for perfectly plastic materials (with associated flow) can now be determined by select software programs. Notably, the freeware ABC [233] is based on the method of stress characteristics that calculates lower bound solutions for the vertical bearing capacity of surface strip and circular foundations, with a smooth or rough foundation-soil interface, with or without a surface surcharge.

A.7.5.1.1 Failure mechanisms

No additional guidance is offered.

A.7.5.1.2 Action transfer

No additional guidance is offered.

A.7.5.1.3 Idealization of foundation area and the effective area concept

Limiting equilibrium methods are generally based on a two-dimensional model (vertical slice) and three-dimensional effects are included by defining the resistance of the vertical side areas. For irregular foundation shapes, this requires a rectangular idealization of the foundation area. This idealized area can be defined by a rectangle of width B and length L having the same area, A, and the same areal moments of inertia, I_x and I_y, as for the real area:

$$A_{\text{idealized}} = BL = A_{\text{real}} \tag{A.1}$$

$$I_{\text{x,idealized}} = I_{\text{x,real}} \text{ for action effects in the y-direction} \tag{A.2}$$

$$I_{\text{y,idealized}} = I_{\text{y,real}} \text{ for action effects in the x-direction} \tag{A.3}$$

The width, B, and length, L, of the idealized foundation area are determined by solving Formulae (A.1), (A.2) and (A.3).

Action eccentricity decreases the ultimate vertical action that a shallow foundation can withstand. This is accounted for in bearing capacity analysis by reducing the effective area of the foundation.

Figure A.1 illustrates shallow foundations with eccentric actions. The eccentricity, e, is the distance from the centre of a shallow foundation to the point of action of the resultant, measured parallel to the plane of the soil-foundation contact. The point of action of the resultant is the centroid of the reduced area. The distance e is M/Q, where M is the applied overturning moment and Q is the vertical action. Q and M should include appropriate partial action factors, being mindful that increasing the vertical action up to a value of $0{,}5Q_{\text{ult}}$ will increase moment capacity. The partial action factors defined in ISO 19902 for beneficial effects of actions should be used to assess the design vertical action when deriving the eccentricity due to moment loading.

Where a skirted foundation incorporates a sealed base plate and the skirt compartment encapsulates soil of sufficiently low permeability, the vertical action used to calculate the effective area can include a contribution due to soil trapped within the skirted area. The following is noted.

- Drained foundation analysis based on the effective area method should exclude the weight of the soil plug (i.e. the soil trapped within the skirts).
- Where it is considered appropriate to use the weight of the soil plug, the submerged soil weight should be used. It should be ensured that inclusion of the soil plug does not lead to less conservative foundation design. The latter comment relates specifically to soft soil sites, where the design soil strength is insufficient to support the submerged soil weight at the depth of the skirts, sufficient support is an implicit assumption in the use of an effective area approach. In some cases, it can be necessary to adopt an alternative approach to account for moment loading, such as the yield surface method (see A.7.7).
- The submerged unit weight used in the analysis should be based on site investigation and laboratory data, and should incorporate an appropriate level of conservatism to account for any uncertainty. Generally, it is conservative to adopt a lower bound profile of submerged soil weight.

For a rectangular base area Figure A.1 sub b), eccentricity can occur with respect to either axis of the foundation. A simplified means of addressing this is to reduce the dimensions of the foundation in both directions:

$$L' = L - 2e_1 \tag{A.4}$$

$$B' = B - 2e_2$$

With $B' \leq L'$ and where L and B are the foundation length and width, respectively, the prime denotes effective dimensions, and e_1 and e_2 are eccentricities along the length and width.

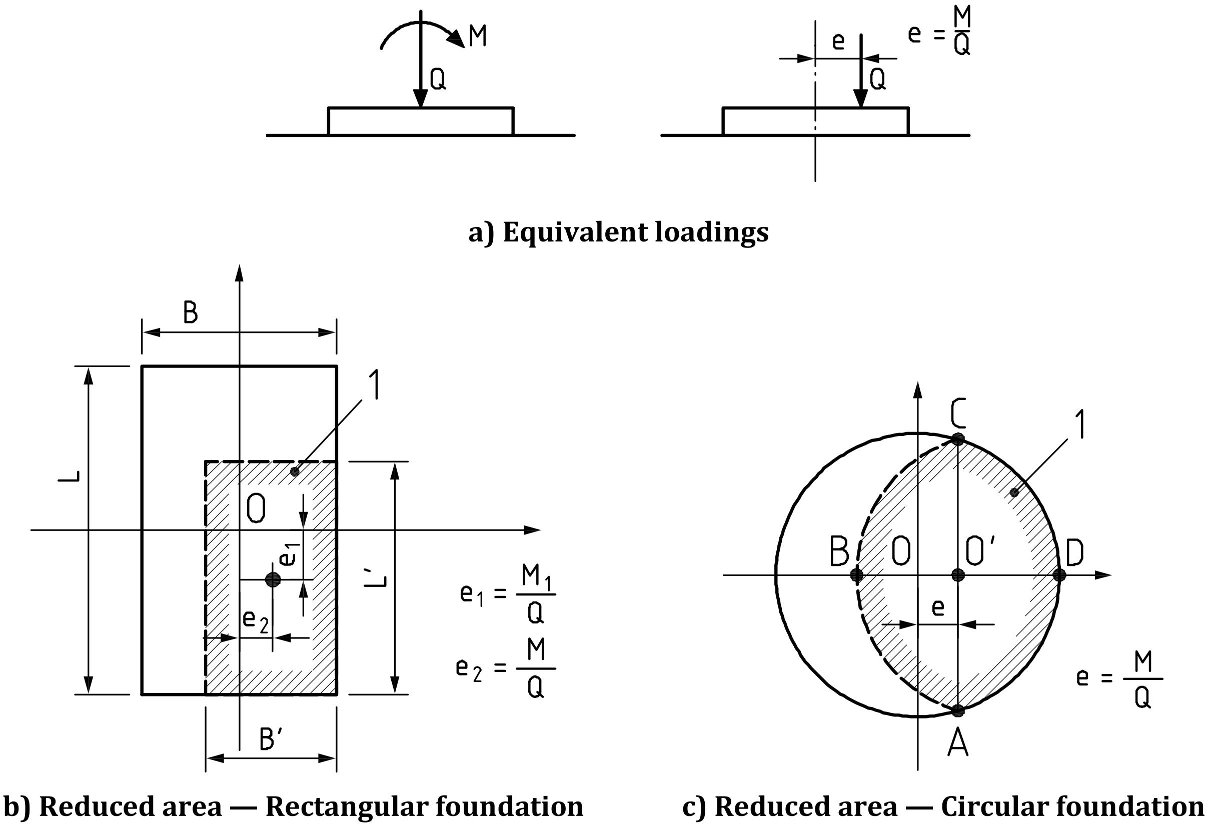

Key

1 reduced area

e1 M1/Q eccentricity due to moment M1, about axis parallel to width, B

e2 M2/Q eccentricity due to moment M2, about axis parallel to length, L

Figure A.1 — Definition of effective area for various foundation geometries

Circular foundations subject to eccentric actions can be idealized as rectangular foundations by solving Formulae (A.1), (A.2) and (A.3). Alternatively, for a circular base with radius, *R*, the effective area can be assumed as shown in Figure A.1 sub c). The centroid of the effective area is displaced a distance, *e*, from the centre of the base. The effective area is then considered to be twice the area of the circular segment ADC.

In addition, the effective area is considered to be rectangular with a length to width ratio equal to the ratio of line lengths AC to BD. The effective dimensions are therefore:

$$A' = 2s = B'L'$$

$$L' = \left(2s\sqrt{\frac{R+e}{R-e}}\right)^{1/2} \tag{A.5}$$

$$B' = L'\sqrt{\frac{R-e}{R+e}}$$

where

$$s = \frac{\pi R^2}{2} - \left(e \times \left(\sqrt{R^2 - e^2}\right) + R^2 \sin^{-1}\left(\frac{e}{R}\right)\right)$$

Examples of effective areas as a function of eccentricity are shown in Figure A.2 in a dimensionless form.

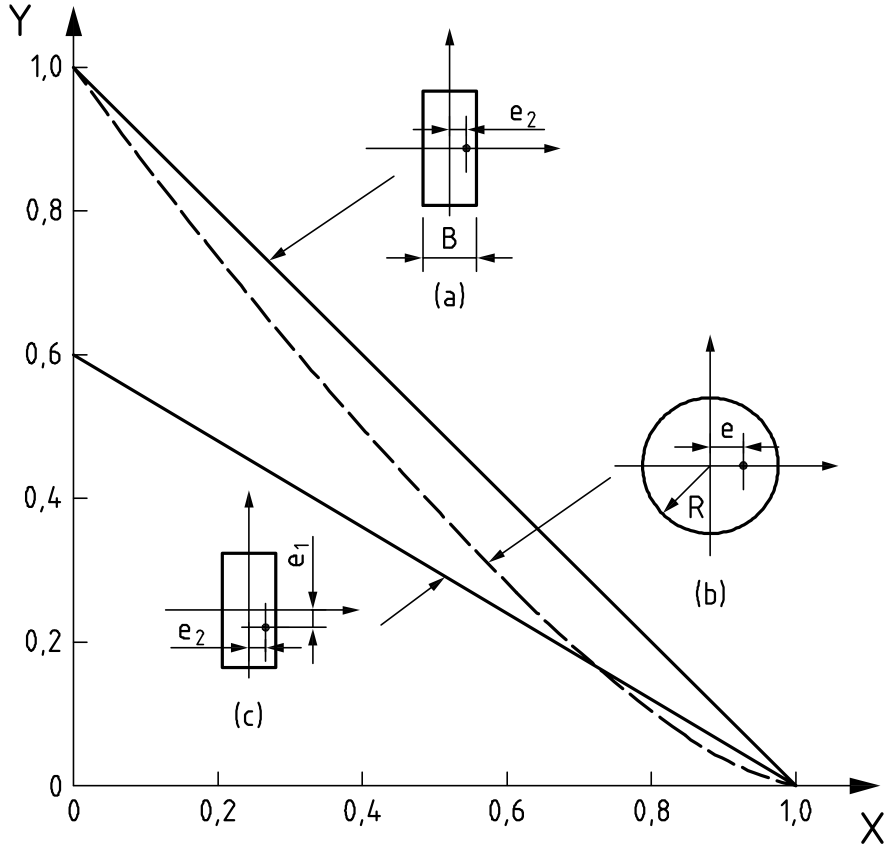

Key

X dimensionless eccentricity $2e_2/B$, e/R

Y dimensionless reduced area A'/A

(a) rectangular – 1 Way loading, e_1/L = 0

(b) circular

(c) rectangular – 2 Way loading, e_1/L = 0,2

Figure A.2 — Area reduction factors for eccentrically loaded shallow foundations

No published data are available on other foundation shapes. If appropriate, intuitive approximations can be made to find an equivalent rectangular or circular foundation when non-standard shapes are encountered. For example, guidance for triangular shaped foundations is given in Reference [169]. Alternatively, an idealized rectangular foundation can be determined by solving Formulae (A.1), (A.2) and (A.3).

Alternative methods exist for assessing the effect of eccentricity in multiple or non-orthogonal directions [170] and these can be more applicable in more complex conditions.

A.7.5.1.4 Undrained conditions with constant shear strength with depth

A.7.5.1.4.1 Bearing capacity factors

The bearing capacity factor, N_c, for a rigid surface strip foundation with horizontal base resting on the surface of a horizontal seafloor, idealized as a perfectly plastic material of uniform strength under uniaxial vertical action in the absence of other actions is given by Reference [278].

$$N_c = 2 + \pi = 5{,}14 \quad \text{(A.6)}$$

Correction factors are applied to extend the basic bearing capacity solution to account for inclined actions, foundation shape, depth of embedment, foundation base inclination and seafloor surface inclination.

A.7.5.1.4.2 Bearing capacity correction factors

For cases of constant isotropic undrained shear strength with depth, the following bearing capacity correction factors are recommended:

$$K_c = 1 + s_c + d_c - i_c - b_c - g_c \tag{A.7}$$

where s_c, d_c, i_c, b_c, and g_c are correction factors related to foundation shape, embedment depth, action inclination, base inclination and seafloor surface inclination, respectively, where:

$$s_c = 0{,}18(1 - 2i_c)\left(\frac{B'}{L'}\right) \tag{A.8}$$

$$d_c = 0{,}3\tan^{-1}\left(\frac{D_b}{B'}\right) \tag{A.9}$$

$$i_c = 0{,}5 - 0{,}5\sqrt{1 - \frac{H_b}{A'\left(\frac{s_{u0}}{\gamma_m}\right)}} \tag{A.10}$$

$$b_c = \frac{2v}{\pi+2} \approx 0{,}4v \tag{A.11}$$

$$g_c = \frac{2\beta}{\pi+2} \approx 0{,}4\beta \tag{A.12}$$

where

— The effective width or effective length is used for action eccentricity parallel to the width or length. The effective width and effective length are used for orthogonal eccentric actions parallel to the width and length. B' and L' are determined from Formulae (A.1), (A.2) and (A.3).

— H_b refers to the factored action applied to the effective area component of the base only. This corresponds to the total lateral action applied to the foundation minus any soil resistance acting on the foundation above skirt tip level, and minus any lateral resistance that can be carried by shearing at skirt tip level outside the effective area. The material factor for pure sliding conditions should be applied to these two resistance components prior to them being subtracted from the total lateral action.

— v and β are base and ground inclination angles in radians. Figure A.3 defines these angles for a general foundation problem.

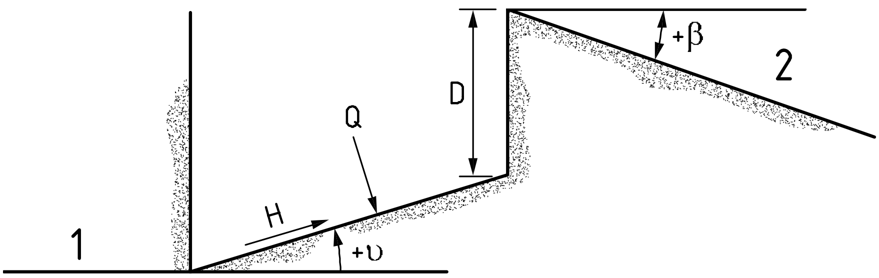

Key

1 horizontal surface

2 ground surface

Figure A.3 — Definitions for inclined base and seafloor surface [62]

The recommended correction factors s_c, i_c, b_c, and g_c are taken directly from Reference [62].

The recommended depth factor d_c is slightly more conservative than specified by Reference [62]. The relevancy of using the above depth factor d_c should be evaluated for individual cases. If the installation procedure or other foundation aspects, such as scour, do not allow for the required mobilization of shear stresses in the soil above foundation base level, it is recommended that $d_c = 0$. In addition, it is recommended that $d_c = 0$, if the horizontal action leads to mobilization of significant passive earth pressure between seafloor and foundation base level.

A.7.5.1.5 Undrained conditions with linearly increasing shear strength with depth

For cases of linearly increasing isotropic undrained shear strength with depth, the following correction factors F and K_c are recommended.

F is an empirical value taken as a function of $\kappa B'/s_{u0}$ and further discussed in Reference [105].

In selection of F, rough conditions can generally be adopted for unpainted skirted foundations. Values of F can be approximated using the relationship:

$$F \approx a + bx - \sqrt{(c + bx)^2 + d^2} \tag{A.13}$$

where

x = $\kappa B'/s_{u0}$ and is valid for $0 \le x \le 25$;

a, b, c, and d are constants that vary with roughness and are outlined in Table A.1.

Table A.1 — Modification factors for soil strength heterogeneity (see Figure A.4)

Constant	Fully rough interface, F_r	Fully smooth interface, F_s
a	2,560	1,372
b	0,457	0,070
c	0,713	−0,128
d	1,380	0,342

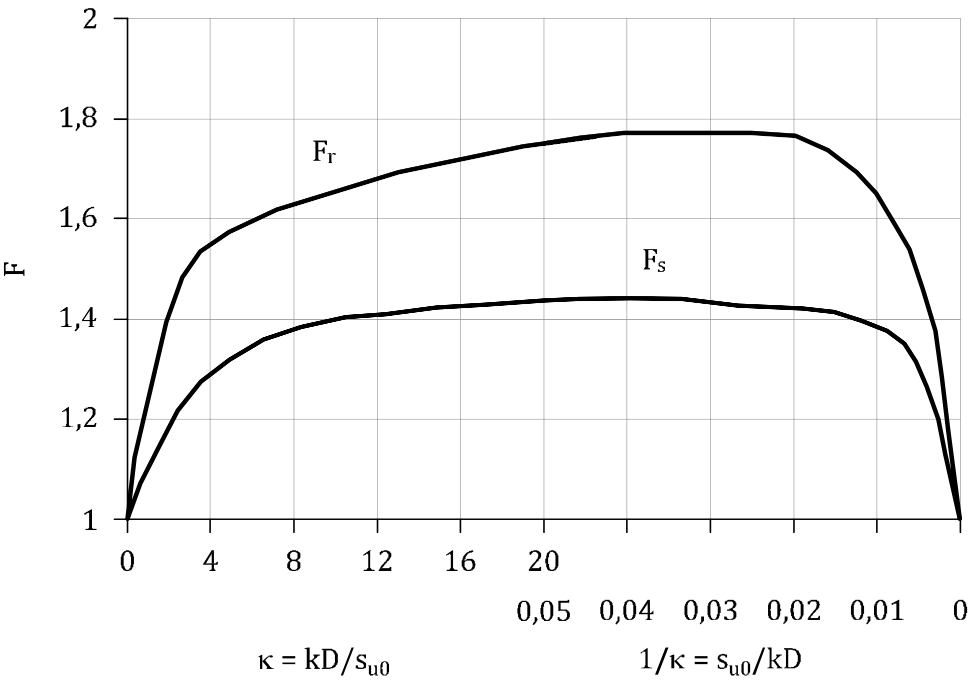

Key

F_s is for no friction at soil–foundation interface (“smooth” foundation)

F_r is for friction equal to the shear strength of soil at the interface (“rough” foundation)

F bearing capacity correction factor

Figure A.4 — Bearing capacity correction factor *F* for linearly increasing isotropic undrained 105hear strength with depth [105]

$$K_c = 1 + s_c + d_c - i_c - g_c - b_c \tag{A.14}$$

where s_c, d_c, i_c, b_c, and g_c are correction factors related to foundation shape, embedment depth, action inclination, base inclination and seafloor surface inclination respectively, as further detailed hereafter:

$$s_c = s_{cv}(1 - 2i_c)\left(\frac{B'}{L'}\right) \tag{A.15}$$

where s_{cv} is taken as function of $\kappa B'/s_{u0}$ and values of s_{cv} can be approximated using the relationship:

$$s_{cv} \approx 0{,}18 - 0{,}155\sqrt{x} + 0{,}021x \tag{A.16}$$

where $x = \kappa B'/s_{u0}$ and is valid for $0 \leq x \leq 10$.

Table A.2 — Shape factor coefficients for circular or square foundations under pure vertical actions

$\kappa B'/s_{u0}$	s_{cv}
0	0,18
2	0,00
4	-0,05
6	-0,07
8	-0,09
10	-0,10

$$d_c = 0{,}3\left(\frac{s_{u,1}}{s_{u,2}}\right) arctan\left(\frac{D_b}{B'}\right) \tag{A.17}$$

where

$s_{u,1}$ is the average shear strength above base level;

$s_{u,2}$ is the equivalent shear strength below base level, given by:

$$s_{u,2} = F\frac{\left(N_c s_{u0} + \frac{\kappa B'}{4}\right)}{N_c} \tag{A.18}$$

$$i_c = 0{,}5 - 0{,}5\sqrt{1 - \frac{H_b}{A'\left(\frac{s_{u0}}{\gamma_m}\right)}} \tag{A.19}$$

$$b_c = \frac{2v}{\pi+2} \approx 0{,}4v \tag{A.20}$$

$$g_c = \frac{2\beta}{\pi + 2} \approx 0{,}4\beta \tag{A.21}$$

The effective width or effective length is used for action eccentricity parallel to the width or length. The effective width and effective length are used for orthogonal eccentric actions parallel to the width and length. B' and L' are determined from Formulae (A.1) to (A.3).

H_b, v and β are as noted under A.7.5.1.4.2.

The recommended d_c is based upon the correction factor for constant isotropic undrained shear strength, but modified to account for linearly increasing undrained shear strength with depth.

The shape factor, s_{cv}, from Reference [309] for axial symmetry and pure vertical action, is assumed to be approximately valid for an equivalent square foundation (B'/L') = 1.

The relevancy of using the depth factor, d_c, should be evaluated in each case. If the installation procedure or other foundation aspects, such as scour, do not allow for the required mobilisation of shear stresses in the soil above foundation base level, it is recommended that d_c = 0. In addition, it is recommended that d_c = 0 if the horizontal action leads to mobilization of significant passive earth pressure between the seafloor and foundation base level.

A.7.5.1.6 Undrained conditions with a surface crust overlying linearly increasing shear strength with depth

The crust correction factor, F_c, may be evaluated from Figure A.5 after Reference [105].

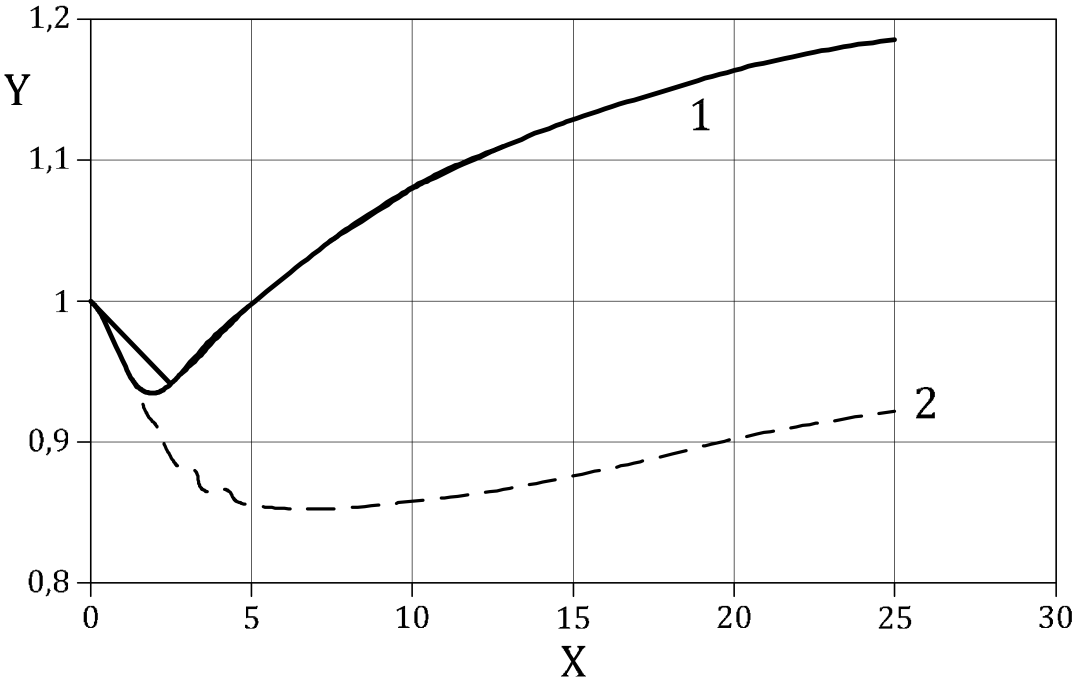

Key

X Normalized undrained strength kB'/s_{uC}

Y Bearing capacity correction factor, F

[1] Fully rough interfaces between foundation and seabed

[2] Fully smooth interfaces between foundation and seabed

Figure A.5 — Bearing capacity correction factor F_c for surficial crust

A.7.5.1.7 Drained conditions

A.7.5.1.7.1 Bearing capacity factors

The bearing capacity factors given in Formulae (A.22) and (A.23) are recommended for pure vertical action on a strip foundation with no embedment, for which Reference [234] provides exact formulations:

$$N_q = \left(\tan\left(\frac{\pi}{4} + 0{,}5\arctan\left(\frac{tan\phi'}{\gamma_m}\right)\right)\right)^2\left(\exp\left(\pi\frac{tan\phi'}{\gamma_m}\right)\right) \quad \text{(A.22)}$$

$$N_\gamma = 1{,}5(N_q - 1)\left(\frac{tan\phi'}{\gamma_m}\right) \quad \text{(A.23)}$$

Effective friction angles, ϕ', between 30° and 42° are considered reasonable limits for general use with Formulae (A.22) and (A.23). Friction angles that fall outside of these limits can indicate non-standard soils or poor quality laboratory testing, especially when falling below 30°.

A.7.5.1.7.2 Bearing capacity correction factors

For drained conditions, the following bearing capacity correction factors are recommended:

$$K_q = s_q d_q i_q b_q g_q \tag{A.24}$$

$$K_\gamma = s_\gamma d_\gamma i_\gamma b_\gamma g_\gamma \tag{A.25}$$

where s, d, i, b and g are correction factors related to foundation shape, embedment depth, action inclination, base inclination and seafloor surface inclination, respectively. The subscripts q and γ identify the bearing capacity factor, N_q or N_γ, with which the correction term is associated.

The factors given in Formulae (A.26) to (A.34) for seafloor surface inclination can be unconservative in cases of loose to very loose sand.

Recommended expressions for the correction factors are:

$$s_q = 1 + i_q \left(\frac{B'}{L'}\right) \sin\left(arctan\left(\frac{\tan\phi'}{\gamma_m}\right)\right) \tag{A.26}$$

$$d_q = 1 + 1{,}2\left(\frac{D_b}{B'}\right)\left(\frac{\tan\phi'}{\gamma_m}\right)\left(1 - \sin\left(arctan\left(\frac{\tan\phi'}{\gamma_m}\right)\right)\right)^2 \tag{A.27}$$

$$b_q = e^{-2v\left(\frac{\tan\phi'}{\gamma_m}\right)} \tag{A.28}$$

$$g_q = g_\gamma = (1 - 0{,}5\tan\beta)^5 \tag{A.29}$$

$$i_q = \left[1 - 0{,}5\left(\frac{H_b}{V_b}\right)\right]^5 \tag{A.30}$$

$$s_\gamma = 1 - 0{,}4 i_\gamma \left(\frac{B'}{L'}\right) \tag{A.31}$$

$$d_\gamma = 1 \tag{A.32}$$

$$i_\gamma = \left[1 - 0{,}7\left(\frac{H_b}{V_b}\right)\right]^5 \tag{A.33}$$

$$b_\gamma = e^{-2{,}7v\left(\tan\frac{\phi'}{\gamma_m}\right)} \tag{A.34}$$

The effective width or effective length is used in the bearing capacity correction factors stated in Formulae (A.26) to (A.34) for action eccentricity parallel to the width or length. The effective width and effective length are used for orthogonal eccentric actions parallel to the width and length.

The relevancy of using the depth factor, d_q, should be evaluated in each case. The effect of foundation embedment is very sensitive to soil disturbance at the soil-structure interface along the sides of the embedded base. If the installation procedure or other foundation aspects, such as scour, do not allow for the required mobilization of shear stresses in the soil above foundation base level, it is recommended that $d_q = 1{,}0$. It is further recommended that $d_q = 1{,}0$ if the horizontal action leads to mobilization of significant passive earth pressure between the seafloor and foundation base level.

H_b, v and β are as noted in A.7.5.1.4.2.

A.7.5.1.7.3 Exclusion of effective cohesion from bearing capacity formulae

The effective strength envelope for a given soil is often quoted in terms of a 'cohesion intercept', c', and effective friction angle, ϕ', with the envelope fitted to results of laboratory tests conducted at different levels of effective confining stress. There has been much debate over whether the deduced c' reflects a true cohesion (or cementation) or is merely an artefact resulting from fitting a tangent to what is, in reality, a curved strength envelope. It has been well established that the friction angle for soils increases as the mean effective stress level decreases, due to increasing dilation. As such, in many cases the effective cementation is an artificial quantity arising from the interpretation of the laboratory tests rather than a true physical quantity. However, there is considerable debate over this among geotechnical specialists as documented in Reference [311].

Examples of where inclusion of an effective cohesion in estimating bearing capacity can be argued as appropriate include:

— Naturally cemented soils (particularly sands)

  In this case, care is needed because of potentially different mobilization rates for the cemented and frictional components of soil strength, and the possibility that progressive failure might occur, with the cementation reducing to zero before the full frictional strength is mobilized.

— Medium to heavily over-consolidated clays

  In this case, ignoring any effective cohesion (or dilation-induced high friction angles at low mean effective stresses) can possibly prove over-conservative. However, inclusion of an effective cohesion in estimating bearing capacity can also prove unduly optimistic, partly because the mean effective stress levels associated with the (drained) bearing capacity can be too high to justify any non-zero effective cohesion, and partly because the level of displacement allowed in design can be too low to fully mobilize the effective cohesion (or dilation-induced high friction angles at low mean effective stresses).

A.7.5.2 Assessment of sliding capacity of shallow foundations

No additional guidance is offered.

A.7.5.2.1 General

No additional guidance is offered.

A.7.5.2.2 Undrained conditions

No additional guidance is offered.

A.7.5.2.3 Drained conditions

No additional guidance is offered.

A.7.5.2.4 Adjusting for horizontal seabed resistance above foundation base level

Contributions to horizontal resistance of an embedded foundation can come from (i) base shear, (ii) soil resistance above skirt tip level due to the difference between active and passive resistance, and (iii) side shear on members located parallel to the direction of lateral loading. The amount of side shear that can be adopted in the design is a function of the shearing on the interface between the embedded member and the soil, and can be influenced by soil disturbance during installation and scour. Specific guidance is not provided in relation to calculating side shear.

In regards to active and passive resistance, the following guidance is provided:

a) Undrained conditions

   The undrained horizontal soil reaction coefficient K_{ru} depends on several factors, such as roughness, foundation shape, side shear, depth of embedment, and possible side gap between foundation and soil due to installation or from scour.

   A value of K_{ru} = 4 is recommended for cases in which both active and passive resistance can be relied upon and significant scour is not expected.

A value of K_{ru} = 2 is recommended for cases in which active soil pressures do not develop, such as due to cracking or installation disturbance, and significant scour is not expected on the passive side of the foundation. In this case, it can be appropriate to also account for the weight of soil within the passive soil wedge. In such cases, the total lateral resistance calculated should not exceed that which will be calculated using K_{ru} = 4.

In some soils it can possibly not be appropriate to include the full soil resistance above skirt tip level in assessing overall sliding stability, due to strain compatibility issues.

b) Drained conditions

The drained horizontal soil reaction factor K_{rd} depends on several factors, such as mobilized soil friction angle, roughness, foundation shape, side shear, depth of embedment, and possible side gap between foundation and soil from installation or from scour. Provided that the installation procedure or other foundation aspects do not require a more accurate assessment of the drained horizontal soil reaction factor, the Formula (A.35) is recommended.

$$K_{rd} = K_p - \left(\frac{1}{K_p}\right) \tag{A.35}$$

where K_p is the passive earth pressure coefficient and is given by:

$$K_p = \left(\tan\left(\frac{\pi}{4} + 0{,}5\,arctan\left(\frac{\tan\phi'}{\gamma_m}\right)\right)\right)^2 \tag{A.36}$$

A.7.5.2.5 Assessment of torsional capacity

Methods that can be used for assessing torsional stability are provided in References [138], [137] and [74].

A.7.5.3 Assessment of capacity of intermediate foundations

No additional guidance is offered.

A.7.6 Serviceability (displacements and rotations)

A.7.6.1 General

Foundation displacements and rotations can be significant at the maximum soil stress levels allowed in this document, such as where foundation loading reaches the soil yield stress.

A.7.6.2 Serviceability of shallow foundations under static loading

A.7.6.2.1 General

Static deformations (displacements and rotations) are generally considered to be of the following two types:

(i) immediate deformation, which is the more or less instantaneous response of a foundation to loading and primarily results from shear deformation (shear straining) of the soil;

(ii) long-term deformation, which occurs over a period of time and is primarily associated with a gradual dissipation of excess pore pressures and associated volume changes of the soil (i.e. primary consolidation).

In addition, secondary displacement due to creep can occur.

A.7.6.2.2 Immediate serviceability (displacements and rotations)

Because soils exhibit nonlinear, path dependent behaviour under loading, the short-term deformation problem is quite complex. For monotonic, low level actions (with respect to failure actions) estimates of deformation can be made assuming the soil to be a homogeneous linearly elastic material.

Solutions for conditions other than those given in 7.5.2.2, including point displacements within the soil mass itself, can be found in Reference [276]. Solutions for rigid, embedded circular foundations are provided in Reference [119].

Considerable care should be exercised in determining the elastic constants of the soil since the elastic moduli of soils depend strongly on the magnitude of effective mean stress and the level of strain. This is particularly significant for highly permeable granular soils where equivalent moduli should be selected from some weighted average mean stress taken over the volume of soil subjected to significant stresses. For relatively impermeable soils, such as clays, a correlation of modulus with strength and over-consolidation ratio can lead to satisfactory results. Further discussion of these points is presented in Reference [176].

Where the foundation base is flexible or the loading is sufficiently severe to create high stresses throughout a significant volume of soil, the formula provided in this document are inappropriate and numerical analyses can be required. Finite element and finite difference techniques have the capability of including complex geometries and loadings and nonlinear, variable soil profiles. The potential effects of softening of the soil (reduction in modulus) under cyclic loading should be considered.

A.7.6.2.3 Long term serviceability (primary consolidation settlement)

Because of the finite extent of the foundation, the vertical stress imposed by the structure should be attenuated with depth. An estimate of such attenuation can be determined from elastic solutions, such as those cited by Reference [276]. This approximate method is particularly appropriate where settlement is governed by thin, near-surface layers.

Rate of settlement is governed by rate of drainage and compressibility. Many soil mechanics textbooks set out methods for one-dimensional consolidation solutions, but in many cases the one-dimensional approximation for flow and strain is unrealistic. Elastic solutions for three-dimensional consolidation settlement around embedded circular foundations are provided in References [156] and [157]. If an accurate prediction of rate of settlement is required, 2D or 3D coupled analysis supported by high quality field data are required.

A.7.6.2.4 Long term serviceability (secondary compression: creep)

No additional guidance is offered.

A.7.6.2.5 Impact of eccentric loading on serviceability (differential displacements and rotations)

No additional guidance is offered.

A.7.6.3 Serviceability of intermediate foundations

No additional guidance is offered.

A.7.6.4 Serviceability in response to dynamic and cyclic actions

In many cases, loading can be considered pseudo-static and the foundation can be treated as an elastic half space subject to the restrictions outlined in 7.5. Consequently, the stiffness of the soil can be calculated in a manner similar to that presented for static conditions.

Half space solutions can be considerably in error where non-uniform soil profiles exist. In addition, for large amplitude environmental loading nonlinear soil behaviour can be significant. In such cases, a numerical analysis can be required or at least a study of a range of soil stiffness properties should be considered.

In some cases, it is not appropriate to treat the foundation as an elastic half space, such as where it becomes necessary to model the energy loss in the soil.

A special case of environmental loading is the response of offshore foundations to cyclic loading arising from waves. The various displacement components and how they can be evaluated are discussed in Reference [10].

A.7.7 Alternative methods of design

A.7.7.1 Yield surface approach

No additional guidance is offered.

A.7.7.2 General

An alternative method of design to assess foundation stability under general loading makes use of yield surfaces, as described in A.7.7.1.2 to A.7.7.1.5.

A.7.7.2.1 Application to design

The general procedure for developing a yield surface for use in design involves the following.

- Defining the 'uniaxial' ultimate limit states Q_{ult} (H = M = 0), H_{ult} (M = 0; and Q = 0 where tensile stresses are allowed beneath the foundation, or Q = Q_{ult}/ 2 if no tensile stresses permitted) and M_{ult} (H = 0; and Q = 0 where tensile stresses are allowed beneath the foundation, or Q = Q_{ult}/ 2 if no tensile stresses permitted) to define the apex points of the yield surface.
- Defining the shape of the interaction diagram through an expression as a function of (Q/Q_{ult}, H/H_{ult}, M/M_{ult}).

The magnitude of the uniaxial capacity and the shape of the yield surface depend on the soil response to loading (undrained or drained), the soil strength profile (uniform or heterogeneous), foundation shape, foundation embedment, structural connection between adjacent foundations, and tension capacity (or not) between the foundation and the soil.

When adopting a yield surface approach, material factor, γ_m, should be applied to the representative value of s_u for undrained conditions and to tanϕ' for drained conditions (not to ϕ').

A.7.7.2.2 Yield surfaces for selected cases

Historically, yield surfaces for undrained conditions have been based on analytical and numerical studies while those for drained conditions have been derived from experimental studies. The latter is due to the relative complexity of an analytical approach for drained soil conditions.

A.7.7.2.3 Undrained conditions

A.7.7.2.3.1 Surface foundations with zero-uplift capacity along the foundation–soil interface

The general 'scallop-shaped' form of the three-dimensional yield surface in vertical, horizontal and moment loading space for undrained failure of a surface foundation with zero-uplift resistance along the foundation–soil interface is shown in Figure A.6 in terms of normalised actions, Q/Q_{ult}, H/H_{ult} and M/M_{ult} (vertical action Q is denoted by V in Figure A.6). The surface is symmetrical in the H–M plane and exhibits diminishing moment capacity as vertical action (Q) falls below 0,5 Q_{ult} as the foundation begins to lift-off from the seafloor.

References [332] and [155] derive yield surfaces for circular and rectangular surface foundations for uniform undrained soil strength with depth and the latter presents approximating expressions for the shape of the yield surface and the uniaxial capacities defining its apex points. Further studies have presented approximating expressions for yield surfaces capturing the effect of linearly increasing undrained strength with depth and loading in six degrees of freedom (VH2M2T), [316], [318].

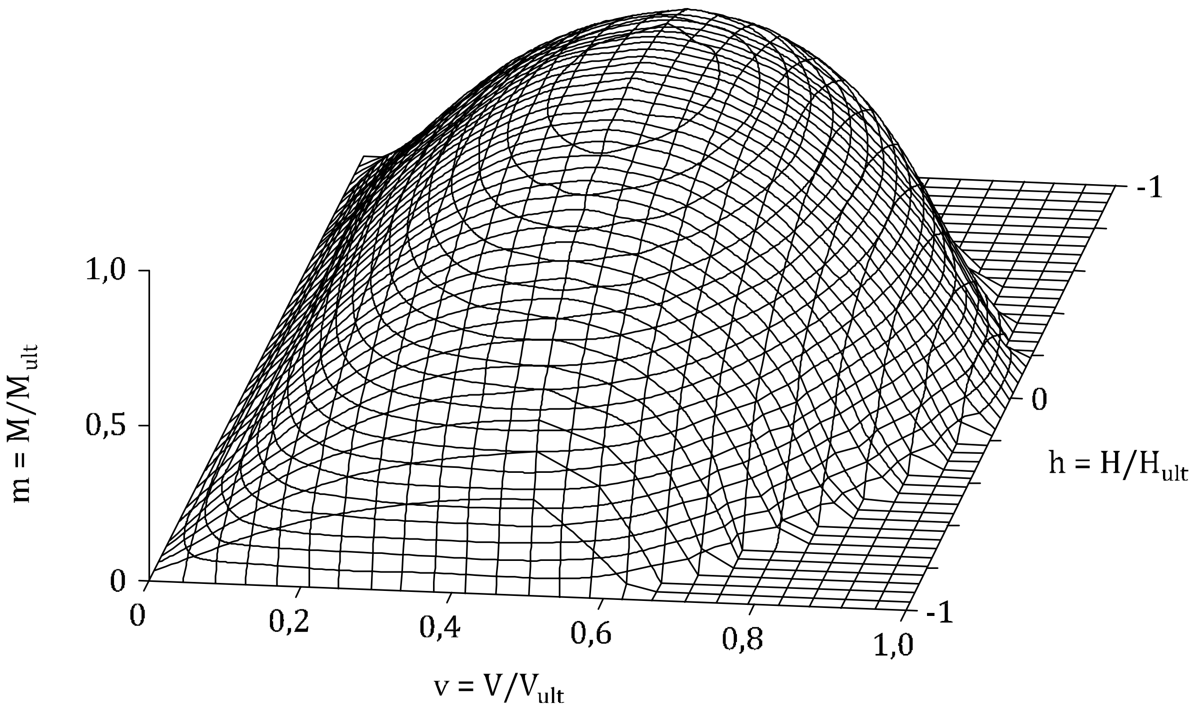

Figure A.6 — Yield surface for undrained conditions for a surface foundation with zero-uplift capacity along the foundation–soil interface [332]

A.7.7.2.3.2 Surface foundations with unlimited-uplift capacity along the foundation–soil interface

In some cases, uplift resistance can be mobilized beneath surface or skirted foundations due to suction and can potentially be relied on for the duration over which undrained conditions prevail.

Uplift resistance provided by foundation skirts can be conceptually represented by modelling a surface foundation with an unlimited tension interface. The general form of the yield surface for undrained failure of a surface foundation with an unlimited tension interface is shown in Figure A.7 (vertical action Q is denoted by V in Figure A.7). The 'walnut-shaped' surface is asymmetric in the H–M plane, with maximum moment capacity mobilized in conjunction with a horizontal action acting in the same direction (i.e. clockwise and left-to-right or vice versa). Moment capacity continues to increase with diminishing vertical action, contrary to the zero-tension interface case, as a foundation with unlimited-uplift capacity will not lift-off from the seafloor.

Yield surfaces and accompanying approximating expressions have been derived for strip, rectangular and circular foundations, both surface and embedded, homogeneous and heterogeneous undrained soil strength profiles, strength profiles with a surficial crust, and consolidated shear strength, although not comprehensively for all combinations (e.g. References [54], [153], [154], [132], [133] and [317]).

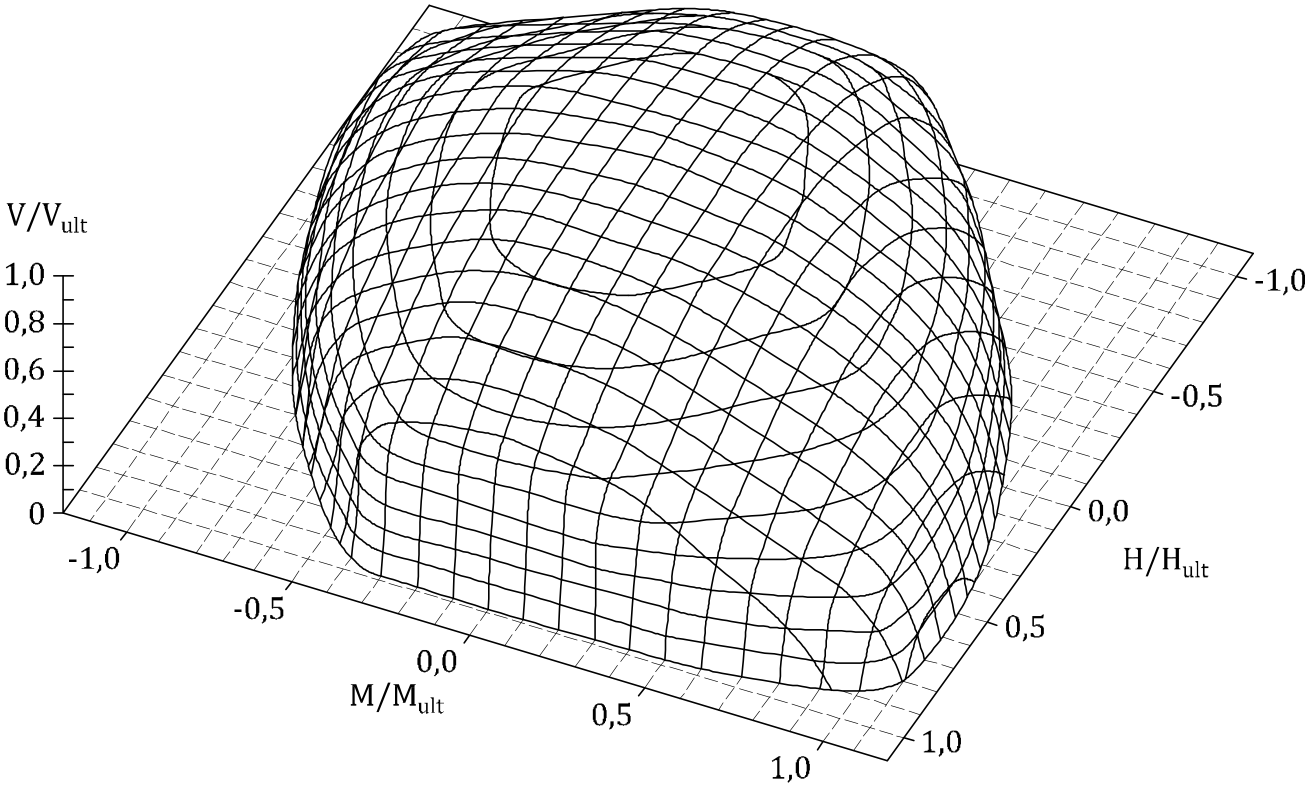

Figure A.7 — Yield surface for undrained conditions for a surface foundation with unlimited-uplift capacity along the foundation-soil interface [55]

The shape of the yield surface for foundations with unlimited-uplift capacity depends on foundation geometry and soil strength profile. In some cases, the normalized size of the yield surface decreases with increasing degree of soil strength heterogeneity; therefore scaling a yield surface derived for homogeneous soil strength by uniaxial ultimate limit states appropriate to a heterogeneous soil strength profile will be un-conservative [158], [155].

A.7.7.2.3.3 Embedded foundations

The coupling of the horizontal and moment degrees of freedom when a foundation is physically embedded leads to an asymmetric and oblique failure surface in the *H*–*M* plane. The asymmetry and obliqueness become more pronounced with increasing embedment ratio. The general form of a yield surface for undrained failure of embedded foundations is shown in Figure A.8 (vertical action, *Q*, is denoted by *V* in Figure A.8).

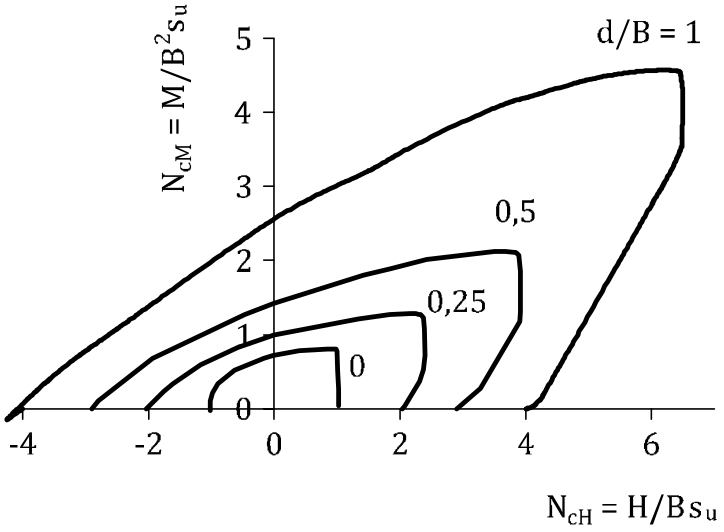

Figure A.8 — Change in shape of yield surface for undrained conditions with foundation embedment d/B [153]

References [153] and [134] present yield surfaces in general loading space for strip and rectangular shallow foundations with embedment ratios in the range zero to one for uniform soil strength and linearly increasing strength with depth.

Existing studies have generally considered embedment in terms of a solid plug, although the capacity of a skirted foundation can be reduced because of the intrusion of the failure mechanism into the soil plug [56]. Modelling a skirted foundation as a solid plug is based on the assumption that sufficient internal skirts are provided to ensure the soil plug displaces as a rigid body. Numerical studies for assessment of critical skirt spacing are presented in References [231] and [131].

A.7.7.2.4 Drained conditions

Yield surfaces for drained conditions incorporate isotropic strain-hardening to accommodate increasing shear strength with increasing stress level. The shape of the yield surface is assumed to be unique and the isotropic expansion and contraction of the surface is defined by a hardening rule (vertical resistance–displacement relationship). Under drained conditions tension cannot be sustained beneath a foundation and therefore the foundation will lift-off from the seabed under moment loading in conjunction with vertical actions, typically for $Q < 0{,}5\ Q_{ult}$ (see References [68] and [249]).

A.7.7.2.4.1 Surface foundations

The general form of the yield surface for drained failure of a surface foundation is shown in Figure A.9. The 'rugby ball-shaped' surface is parabolic in planes of *QH* and *QM* and a rotated ellipse in the *HM* plane (vertical action, *Q*, is denoted by *V* in Figure A.9). Maximum horizontal action and moment capacity are mobilized in conjunction with a vertical action $Q = 0{,}5\ Q_{ult}$ and maximum moment capacity is mobilized in conjunction with horizontal action acting in opposition (i.e. clockwise and right-to-left or vice versa).

Reference [68] proposed the yield surface shown in Figure A.9 along with a closed-form expression to describe its shape. The yield surface was based on results from various experimental studies on rough, rigid, plane strain and rectangular shallow foundations on dense silica sand. A subsequent study considering circular foundations on loose carbonate sand showed a similar form of yield surface and for which a closed-form expression was proposed [69].

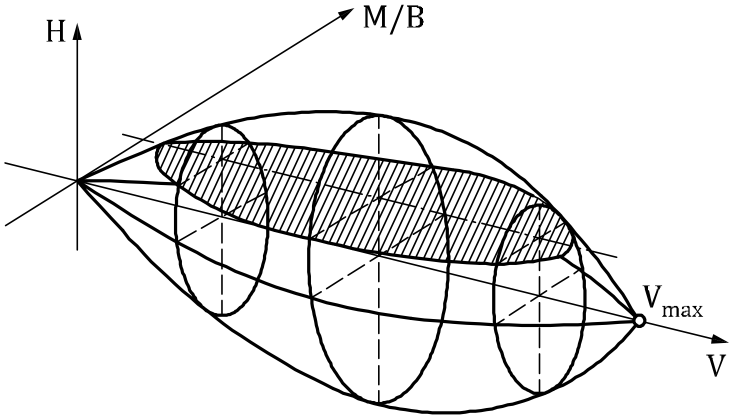

Figure A.9 — Yield surface for drained conditions for a surface foundation [68]

A.7.7.2.4.2 Embedded foundations

The additional capacity available from foundation embedment is accounted for by scaling the envelope for a surface foundation (as shown in Figure A.) by its apex points H_{max}/Q and $Mmax/Q$ [249], [161].

A.7.7.3 Performance based design approach

Typically, foundations for subsea and flowline-related structures follow the same requirements and target probability of failure as that of fixed steel offshore structures. Lower nominal annual target probabilities of failure, compared to L1 exposure levels for fixed steel offshore structures as described in ISO 19902, may be adopted for a subsea and flowline related foundations through system-based design ensuring that the integrity, safety and operability of the system are not compromised.

System failure modes, due to short-term or long-term events, that might need to be evaluated in a performance based design, can include:

a) over-straining/overstressing of pipes, spools/jumpers and connected flowlines;

b) problems with the installation of connections (e.g. pitch rotation beyond the installation tolerance prior to tie-in operations);

c) not fulfilling the specified function or performance standard (e.g. a riser hold-back anchor being pulled-out and no longer supporting the riser; excessive sliding of buckle initiator).

When foundation movements due to the imposed deformations of a system act to reduce the imposed loading, lower partial action factors can be applicable if the imposed deformations have been robustly characterized. This is intended for situations where the foundation movements are 'small' and the response is broadly reversible (i.e. 'elastic').

When the imposed deformation is large (e.g. due to thermal flowline expansion) and the deformation is controlled by allowing the structure (and connected infrastructure) to slide over the foundation or over the seafloor, the following provisions apply:

a) standard partial action factors should be applied for actions transferred between sliding structures;

b) if sliding is permitted over the seafloor, inherently the partial factors are unity, however standard partial factors should be achieved against bearing failure;

c) the characteristic mechanical properties of the sliding interface should be robustly assessed

d) the transfer of actions through the structure to the foundation should be robustly computed.

The design of foundations where foundation movement over the seafloor is permitted is discussed in References [91], [98] and [107].

A.7.8 Installation

A.7.8.1 General

Shallow foundations are often placed on the seafloor from an installation vessel. The vertical heave motions induced by the vessel's motion characteristics and created by the environmental boundary conditions cause the touchdown to be an impact between the seafloor and the structure. This impact is normally controlled by limiting weather criteria and carefully planned and well controlled installation operations. However, it is still the experience that many small structures suffer a foundation failure during installation, mainly in soft soil conditions. Many such incidents can be avoided by observing the following recommendations.

- If the installation is performed under controlled conditions by use of a heave compensator and low rate of descent towards the seafloor (<0,2 m/s), no extra safety margin should be needed.
- If the installation is performed without any control on the rate of descent (no heave compensation), penetration in excess of the failure displacement can occur. The consequences of such additional penetration should be investigated.

The use of relatively small capacity installation vessels can result in foundation failure; vessel heave motions greater than crane pay-out speed can result in the structure having excessive velocity at impact with the seafloor and multiple set-downs. As a result, the foundation can be pulled up after first set-down, thus generating a pull-out failure in the soil (reverse bearing capacity failure). The soil condition under the structure after such an event is close to a remoulded state and normal partial action and material factors can be too small to prevent foundation failure during final set-down.

If there is a risk of significant heave motions or impact on touchdown, higher material factors than outlined in 7.3 should be applied. Shallow foundations, such as those used for temporary support or for subsea structures, are often designed for limited environmental actions. Since the main actions are permanent and due to gravity, the higher material factor in 7.3 should be applied.

A.7.8.2 Skirt penetration resistance

Skirts can provide a significant resistance to penetration. This resistance, Q_r can be estimated as a function of depth in accordance with Formula (A.37):

$$Q_r = Q_f + Q_p = f\,A_s + q\,A_p \tag{A.37}$$

where

- Q_f is the skirt friction resistance;
- Q_p is the total end bearing resistance from skirt tips;
- f is the unit skirt friction;
- A_s is the side surface area of skirt embedded at a particular penetration depth (including both internal and external skirt faces);
- q is the unit end bearing resistance on the skirt tip;
- A_p is the projected area of skirt tip.

The end bearing components can be estimated by bearing capacity formulae or alternatively by the direct use of cone penetrometer resistance q_c corrected for shape difference. It is possible that the latter is not directly applicable for wide concrete skirts. The shaft friction resistance can be determined by laboratory testing or other suitable experience.

In most cases, it is highly desirable to achieve full skirt penetration. This should be considered in selecting high soil strength properties (or CPT q_c values) for use in analysis as low estimates of strength are non-conservative in this case.

Where applicable, previous relevant installation experience should be considered (see Reference [92]) .

In general, water will be trapped within the skirt compartments. The penetration rate should be such that removal of the water can be accomplished without forcing it under the skirts and damaging the foundation. It is often for this reason that foundation base perforations are introduced.

In assessing the penetration of skirts, site conditions should be considered. An uneven seafloor, lateral soil strength variability, existence of boulders, etc. can give rise to uneven penetration or structural damage of skirts. In some cases, site improvements can be required such as levelling the area by dredging or fill emplacement.

A.7.8.3 Required and allowable under-pressure

In some cases, an under-pressure (i.e. negative excess pore pressure or 'suction' relative to ambient pressure) can be used to increase the penetration force. In those cases, analysis should be carried out to ensure that it will not result in damage to the foundation soil.

In general, analysis is more straightforward in lower permeability soils (e.g. clays). In higher permeability soils (e.g. sands) water flow is induced within the soil, which increases the volume of water that should be removed from the can and which alters the effective stress distribution in the soil (typically beneficially). Interlayered low and high permeability soils present further complexities.

Further guidance is provided in A.11.5.2.2.1.

A.7.9 Relocation, retrieval and removal

During removal or retrieval of a skirted shallow foundation, suction forces will tend to develop at the foundation base and the tips of skirts. These forces can be substantial and can usually be overcome by sustained uplift forces (up to the submerged weight of the foundation) and by introducing water into the base compartments to relieve the suction.

Set-up effects can result in higher extraction resistance than installation resistance.

In the case of un-skirted foundations or shallow foundations with short skirts, it is often preferable to lift initially from one corner or side of the foundation, to introduce drainage, and reduce suction effects.

A.8 Pile foundation design

A.8.1 Pile capacity for axial compression

A.8.1.1 General

No additional guidance is offered.

A.8.1.2 Axial pile capacity

In conventional static capacity based design, the pile design actions (factored permanent and variable actions plus factored extreme environmental actions) are compared against the factored pile capacity. The factored actions are defined in ISO 19902. The pile capacity is defined as the integrated friction and tip resistance (see 8.1 and 8.2). This procedure ensures that the pile has an adequate reserve above the design actions in order to accommodate uncertainties in actions and pile resistances.

It is not always correct to add the representative value of the end bearing to the representative value of the skin friction to obtain the representative value of the axial capacity of a pile. This subject is addressed in References [251], [285] and [339]. For the particular case of a belled pile, this matter is discussed in Reference [339].

A.8.1.3 Skin friction and end bearing in clay soils

A.8.1.3.1 General

Estimating pile capacity in clay soils requires considerable judgment in selecting design parameters and in interpreting calculated capacities. Some of the items that should receive design consideration are detailed in A.8.1.3.2.

A.8.1.3.2 Axial pile capacity in clay

A.8.1.3.2.1 Loading test database for piles in clay

Further information on the load test database for piles in clay can be found in References [312] and [217].

A.8.1.3.2.2 Unified CPT method for pile axial capacity in clays

This subclause presents the 'unified CPT method' for assessing driven pile capacity in clays [216]. Formulae (A.38) and (A.39) are recommended for the evaluation of the static capacity of steel piles after consolidation induced by pile driving is completed. Potential long-term ageing effects are not included. The method can be applied to clays in Zones 2, 3 and 4 on the soil behaviour type (SBT) chart as shown in Figure A.10. Assessment of pile capacity for sensitive clays, that fall within SBT chart Zone 1, is more uncertain. Their capacity should be assessed with care and local experience, pile testing and alternative design approaches should be considered where possible. The reliability of the method has been evaluated and the method was shown to provide pile foundations that are more reliable than those obtained using the main text method in 8.1.3. The unified CPT method should only be applied to driven piles and should not be applied to vibro-driven piles unless the vibrated portion of the pile is restricted to the initial 20 % of pile penetration. The method is developed for offshore steel piles. It should be ensured that other factors, such as paint, coatings or mill-scale varnish that are likely to reduce pile roughness below that usually expected (typically around 10 microns centre line average roughness for lightly rusted steel used for offshore piles), do not negatively affect the interface friction that can be mobilized. Further information on the method and Formulae (A.38 and (A.39) is provided in Reference [216].

For the unified CPT method in clays, the (fully consolidated) peak unit skin friction for capacity, $f(z)$, in stress units, at depth, z, can be calculated using Formula (A.38):

$$f(z) = 0{,}07 F_{st} q_t \left[max\left(\frac{h}{D^*}, 1\right)\right]^{-0{,}25} \tag{A.38}$$

where

- F_{st} is 1 for clays with $I_{z1} > 0$, in Zones, 2, 3 and 4 on the SBT chart;
- F_{st} is 0,5 ± 0,2 clays with $I_{z1} < 0$, in Zone 1 on the SBT chart;
- q_t is the corrected CPT cone resistance as defined in ISO 19901-8:2014, 8.3.1;
- h is the distance above the pile tip at which $f(z)$ acts (= $L - z$)
- L is pile embedment length;
- $D^* = \left(D^2 - D_i^2\right)^{0{,}5}$ for an open-ended pile and $D^* = D$ for a closed-ended pile;
- D is the pile outer diameter of a pipe pile;
- D_i is the internal diameter of a pipe pile

I_{z1} can be calculated by:

$$I_{z1} = Q_{tn} - 12exp^{(-1{,}4F_r)}$$

where F_r is the normalized friction given by $F_r = f_s/(q_t - \sigma_{v0})100$ %, ,in which f_s is the CPT sleeve friction and σ_{v0} is the total vertical stress below the seafloor level.

t-z curves can be determined using the friction value combined with the *t-z* curve definition for clays in 8.4.1.

In the absence of more definitive criteria, the total end bearing resistance applied across the full base area of a large diameter pile with a length to diameter ratio greater than five can be calculated using Formula (A.39):

$$q_{b0,1} = q_t \left[0{,}2 + 0., \left(\frac{D^*}{D} \right)^2 \right] \tag{A.39}$$

where q_t is the average corrected CPT end resistance within $20t$ below the pile tip, in which t is the pile wall thickness. The end bearing should be taken as plugged resistance and no additional allowance should be made for internal skin friction.

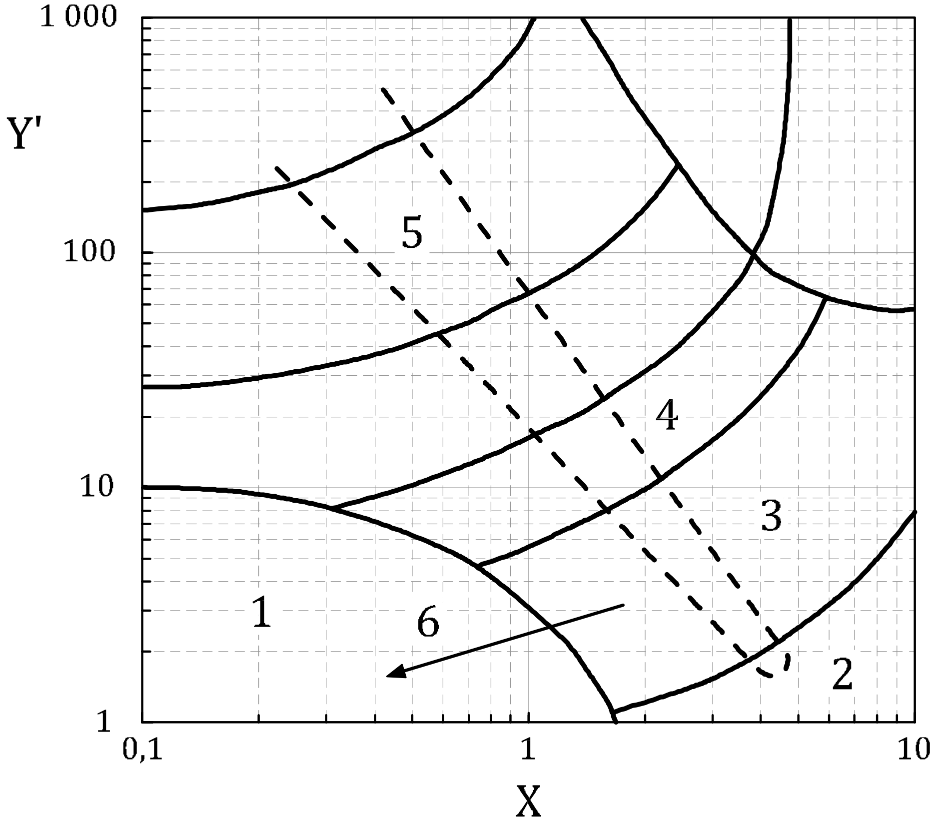

Key

X	Normalized friction ratio, F_r	3	Zone 3 - Clays
Y'	Normalized cone resistance, Q_{tn}	4	Zone 4 – Silt mix
1	Zone 1 – Sensitive clays and silts	5	Normally consolidated
2	Zone 2 – Organic soils	6	Increasing sensitivity

Figure A.10 — Soil behaviour type (SBT) chart [301]

A.8.1.3.2.3 Establishing representative strength and effective overburden stress profiles

The axial pile capacity in clay is directly influenced by the undrained shear strength and effective overburden stress profiles selected for use in analyses. The wide variety of sampling techniques and laboratory and *in situ* testing techniques and the scatter in the shear strength data from the various types of tests complicate appropriate selection of representative shear strength profiles. ISO 19901-8 provides additional information on the sampling and laboratory testing techniques and on the quality of marine soil investigations.

Strength profiles are typically established by combining the results of laboratory tests on undrained unconsolidated samples (e.g. UU triaxial or minivane tests), laboratory tests on consolidated samples (e.g.

direct simple shear tests or consolidated triaxial tests in compression or extension), and *in situ* tests (e.g. cone, ball, or T-bar penetration tests, *in situ* vane tests).

In selecting the representative shear strength value, the sampling and testing techniques used to correlate the shear strength to any available relevant pile loading test data should be considered. The experience with pile performance can also play an important role in assessing the appropriate representative shear strength value.

In situ testing with a vane or penetrometers, such as the cone, piezocone, ball and T-bar, will help in assessing sampling disturbance effects and can provide a continuous shear strength profile. Approaches. such as the SHANSEP (stress history and normalized soil engineering properties) technique as described in References [207] and [208] can help providing a more consistent interpretation of the shear strength profile.

A.8.1.3.2.4 Pile length effect

Long piles driven in clay soils are typically axial flexible and can therefore experience capacity degradation due to:

— progressive failure in the soil due to strength reduction (strain softening) with continued displacement or shearing of a particular soil horizon during pile installation;

— lateral movement of soil away from the pile due to pile 'whip' during driving.

The occurrence of degradation due to these effects depends on many factors related to both installation conditions and soil behaviour. Methods of estimating the possible magnitude of reduction in capacity of long piles can be found in Reference [288].

A.8.1.3.2.5 Changes in axial capacity in clay with time

Existing axial pile capacity calculation procedures for piles in clay are based on experience assisted by the results of axial pile loading tests. In these tests, few of the piles were instrumented and in most cases little or no consideration was given to the effects of time after driving on the development of pile-soil shear resistance. Axial capacity of a driven pipe pile in clay computed in accordance with 8.1.2 and 8.1.3 is intended to represent the long-term static capacity of piles in undrained conditions when subjected to axial actions until failure after dissipation of excess pore water pressure caused by the installation process. Immediately after pile driving, pile capacity in a clay deposit can be significantly lower than the ultimate static capacity. Field measurements have shown that the time required for driven piles to reach ultimate capacity in a clay deposit can be relatively long, as much as two to three years [84], [48], [213]. However, the rate of strength gain is highest immediately after driving, and this rate decreases during the dissipation process. Thus, a significant strength increase can occur in a relatively short time.

During pile driving in normally consolidated to lightly over-consolidated clays, the soil surrounding a pile is significantly disturbed, the stress state is altered, and large excess pore pressures can be generated. After installation, these excess pore pressures begin to dissipate, i.e. the surrounding soil mass begins to consolidate and the pile capacity increases with time. This process is usually referred to as *set-up*. The rate of excess pore pressure dissipation is a function of the coefficient of radial (horizontal) consolidation, pile radius, plug characteristics (plugged versus unplugged pile), and soil layering.

In the case of driven pipe piles supporting a structure where the design actions can be applied to the piles shortly after installation, the time-consolidation characteristics should be considered in pile design. In such cases, the capacity of piles immediately after driving and the expected increase in capacity with time are important design variables that can impact the safety of the foundation system during early stages of the consolidation process.

A number of investigators have proposed analytical models of pore pressure generation and the subsequent dissipation process for piles in normal to lightly over-consolidated clays [247], [291]. Since excess pore pressures are generated by pile driving operations, any dissipation of the excess pore pressures after installation should correspond to an increase in the shear strength of the surrounding soil mass and hence an increase in the capacity of the pile. After dissipation of excess pore pressures, the capacity of a pile approaches long-term capacity, although some strength gain can continue due to secondary processes. In some over-consolidated clays, pile capacity can decrease as pore pressures dissipate, provided the rate of change of radial total stress decreases faster than the rate of change of pore pressure. The analytical models account for the degree of plugging by assuming various degrees of plug formation, ranging from closed- to open-ended pile penetration modes. Input necessary for the analysis includes the soil characteristics (compressibility, stress history, strength, etc.) and the initial site conditions.

In Reference [48], the behaviour of piles subjected to significant axial actions in highly plastic, normally consolidated clays was studied using a large number of model pile tests and some full-scale pile loading tests. From the study of pore pressure dissipation and loading test data at different times after pile driving, empirical correlations were obtained between the degree of consolidation, degree of plugging, and pile shaft shear transfer capacity. The analysis is dependent on the shear strength of the surrounding soil mass. The method is presently limited to use in highly plastic, normally consolidated clays of the type encountered in the Gulf of Mexico, since validation data have been published only for those soils.

In Reference [213], in highly over-consolidated glacial till, capacity was shown to undergo significant short-term reduction associated with pore pressure redistribution and reduction in radial effective stresses during the early stages of the equalization process. The capacity at the end of installation was never fully recovered. Test results for closed-ended steel piles in heavily over-consolidated London clay indicate that there is no significant change in capacity with time [50]. This is contrary to tests on 0,273 m (10,75 in) diameter closed-ended steel piles in over-consolidated Beaumont clay, where considerable and rapid set-up (in four days) was found [267].

Caution should be exercised in using this subclause to evaluate set-up, particularly for soils with different plasticity characteristics and under different states of consolidation (especially over-consolidated clays) and piles with D/WT (pile outer diameter/pile wall thickness) ratios greater than 40.

A.8.1.4 Skin friction and end bearing in sands

A.8.1.4.1 General

This subclause provides guidance for sands that do not fit within the constraints presented in 8.1.4. In particular for coarse sands, normal effective stress levels outside of those considered within the pile database, higher fines content or for unconventional mineralogy, it can be appropriate to consider further laboratory testing including special ring shear interface friction tests [186] and to use an alternative pile design method, such as one of the CPT methods referenced in 8.1.4. The method presented in 8.1.4 was calibrated based upon pile upon tests where the soil generally had a soil behaviour type index, I_c, larger than 2,1, i.e. they were in the category of sand mixtures (silty sand to sandy silt) using the soil behaviour type chart as described in Reference [301].

Recent studies (see Reference [173]) involving ring-shear tests against steel interfaces of appropriate roughness that were designed to replicate driven pile installation suggest that the large shear displacements implicit in pile driving lead to a modest dependency of ultimate (design) δ_{cv} on mean grain size D_{50} among standard pure silica test sands. Reference [223] used the same tools to investigate the influence of non-plastic silt and non-plastic fines contents (up to around 20 %) as well as stress level dependency for natural sand samples taken at both onshore and offshore sites, finding that both variables can affect ultimate critical state (design) interface friction angles, with the latter showing modest increases as normal stress levels rise due to greater interaction of the grains with the steel surface. In cases where such factors merit investigation, site-specific tests that account for pile installation effects can be conducted following the procedures set out in the ICP-05 method [186], provided these apply appropriate normal effective stress levels.

A.8.1.4.2 Parameter value assessment

The soil investigation should provide information that is adequate to capture the spatial variability, horizontally and vertically, of the boundaries and parameter values of all layers.

For any CPT-based method, the computed pile capacity in sand is most sensitive to cone penetration resistance, q_c, followed by tanδ_{cv} and σ'_{v0}. Since an accurate capacity assessment is a function of the accuracy of both the model and the parameters, guidance regarding selecting appropriate parameter values is given in items a) to c).

a) Parameter, $q_c(z)$

The CPT should measure $q_c(z)$ with apparatus and procedures that are in general accordance with ISO 19901-8. In particular, ISO 19901-8 prescribes cones with a base area in the range of 500 mm^2 to 2 000 mm^2 and a penetration rate of 20 mm/s ± 5 mm/s.

The CPT-based design methods were established for cone resistance values, q_c, up to 100 MPa. Caution should be exercised when applying the enclosed methods to sands and sandy tills with higher resistances.

A measured, continuous profile of $q_c(z)$ is preferable to an assumed/interpolated discontinuous profile, but is generally not achievable offshore at large depths below the seafloor with a down-hole CPT apparatus. This is generally due to factors such as limited stroke and/or maximum resistance being achieved. When (near) continuous $q_c(z)$ profiles are needed, overlapping CPT push strokes can be considered.

With discontinuous CPT data, a 'blocked' $q_c(z)$ profile can be used, where the soil profile is divided into layers, in each of which $q_c(z)$ is assumed to vary linearly with depth. 'Blocked' profiles should be assessed, particularly when they contain maximum q_c values at the ends of CPT push strokes. When the push strokes contain no maximum $q_c(z)$ data, a moving window can be used to determine the average profile (and its standard deviation), through which a straight line can be fitted. If present, thin layers of weaker material (e.g. silt or clay) should be modelled conservatively.

For geotechnical investigations where several vertical CPT profiles have been made (e.g. one per platform leg), it is suggested that at least two approaches be employed: pile capacity should first be based on the combined averaged $q_c(z)$ profile and then based on individual $q_c(z)$ profiles. Judgment is required to select the most appropriate $q_c(z)$ profile and to determine the associated final axial capacity.

b) Parameter, $\sigma'_{v0(z)}$

Usually, pore water pressures in sands are hydrostatic and in this case $\sigma'_{v0(z)}$ equals ($\gamma' z$), where γ' is the submerged soil unit weight. Offshore sands are generally very dense and often silty. In general, design γ' values in sands should be based on measured laboratory values (corrected for sampling disturbance effects), which should be compatible with relative density, D_r, estimated from $q_c(z)$ and maximum and minimum dry unit weight values determined in the laboratory.

c) Scour

Scour (seabed erosion due to wave and current action) can occur around offshore piles. Common types of scour are general scour (overall seabed erosion) and local scour (steep-sided scour pits around single piles or pile groups). There is no generally accepted method to account for scour in axial capacity for offshore piles. Reference [360] gives techniques for scour depth assessment. In addition, general scour data can be obtained from national authorities.

In lieu of project specific data, guidance on local scour depth is provided in A.8.5.3.

Scour decreases axial pile capacity in sand. Both friction and end bearing components are usually affected. This is because scour reduces both $q_c(z)$ and σ'_v (vertical effective stress). For excavations (i.e. general scour), Reference [258] recommends that $q_c(z)$ is simply proportional to $\sigma'_{v0}(z)$, i.e.:

$$q_{c,f}(z) = \chi\, q_{c,0}(z) \tag{A.40}$$

where

$q_{c,f}(z)$ is the final reduced CPT cone-tip resistance at depth z, after general scour (in stress units);

$q_{c,0}(z)$ is the original CPT cone-tip resistance at depth z, before general scour (in stress units);

χ is the dimensionless scour reduction factor ($\chi = \sigma'_{vf}/\sigma'_{v0}$);

σ'_{vf} is the final vertical effective stress value, after scour (in stress units);

σ'_{v0} is the original vertical effective stress value, before scour (in stress units).

For large general scour depths and normally consolidated sands, an alternative and conservative approach as described in Reference [140] can be used to determine χ from:

$$\chi = \frac{1}{1+2K_0}\sqrt{\frac{z'+2K_0\sqrt{\Delta z_{GS}\times z'+z'^2}}{\Delta z_{GS}+z'}} \quad \text{(A.41)}$$

where

Δz_G is the general scour depth (m);

z' is the final depth below seafloor, after general scour, ($z' = z - \Delta z_{GS}$)(m);

K_0 is the coefficient of lateral earth pressure at rest, the ratio of the effective horizontal to vertical *in situ* soil stresses, $K_0 = \sigma'_{h0}(z)/\sigma'_{v0}(z)$.

A method to reduce the effective stress, σ'_v, for both general and local scour is provided in A.8.5.

A.8.1.4.3 Former main text method in sands

The former main text method in sands is presented in this subclause due to its historical use for many previous pile designs, although it should no longer be used for pile design or assessment of pile capacity in sand. In exceptional cases, it can be used for assessment of pile capacity for existing piles where there are no CPT data available to use a CPT-based method. In comparison to the method described in this subclause, the unified CPT-based method presented in 8.1.4 is considered to fundamentally better and has shown statistically closer predictions of pile loading test results and is the preferred method.

With the former main text method, for driven pipe piles in sands, the unit skin friction, $f(z)$, in stress units, at depth, z, can be calculated by:

$$f(z) = \beta\, \sigma'_{vo(z)} \quad \text{(A.42)}$$

where

β is the dimensionless skin friction factor, for sands;

$\sigma'_{vo(z)}$ is the effective vertical stress at depth z (in stress units).

In the absence of specific data, β values for open-ended pipe piles that are driven unplugged can be taken from Table A.3. For full displacement piles (i.e. closed-ended or fully plugged open-ended piles), values of β can be assumed to be 25 % higher than those given in Table A.3. For long piles, $f(z)$ does not necessarily increase linearly with the overburden stress as implied by Formula (A.42). In such cases, it is appropriate to limit f to the values given in Table A.3.

For end bearing of piles in sands, the unit end bearing, q, in stress units, can be computed using Formula (A.43):

$$q = N_q\, \sigma'_{vo,tip} \quad \text{(A.43)}$$

where

$\sigma'v_{o,tip}$ is the effective vertical stress at the pile tip (in stress units);

N_q is the dimensionless bearing capacity factor.

Recommended N_q values are presented in Table A.3. For long piles, q does not necessarily increase linearly with the overburden stress as implied by Formula (A.43). In such cases, it is appropriate to limit q to the values given in Table A.3. For plugged piles, the bearing pressure can be assumed to act over the entire cross-section of the pile. For unplugged piles, the bearing pressure acts on the pile annulus only.

In this case, additional resistance is offered by friction between the soil plug and the inner pile wall. Whether a pile is considered to be plugged or unplugged should be based on static calculations using a unit skin friction on the soil plug equal to the outer skin friction. A pile can be driven in an unplugged condition, but can behave as plugged under static actions.

For soils that do not fall within the ranges of relative density and soil description given in Table A.3, or for materials with unusually weak grains or compressible structure, Table A.3 is not necessarily appropriate for selection of design parameters. For example, unconventional soils such as very loose soils or soils containing large amounts of mica or volcanic grains can require special laboratory or field tests for selection of design parameters. Sands containing calcium carbonate, which are found extensively in many areas of the oceans (see A.6.3), are of particular importance.

For piles driven in undersized drilled or jetted holes in sands, the values of $f(z)$ and q should account for the amount of soil disturbance due to installation, but they should not exceed the values for driven piles.

In layered soils, skin friction values, $f(z)$, in sand layers should be computed in accordance with Table A.3. End bearing values for piles tipped in sand layers can also be taken from Table A.3.

Table A.3 — Design parameters for siliceous sand

Relative density[a]	**Soil description**	**Skin friction factor**[b] β	**Limiting unit skin friction values** f_{lim} kPa (kips/ft^2)	**End bearing factor** N_q	**Limiting unit end bearing values** Q_{lim} MPa (kips/ft^2)
Very loose Loose Loose Medium dense Dense	Sand Sand Sand-silt[c] Silt Silt	Not applicable[d]	Not applicable[d]	Not applicable[d]	Not applicable[d]
Medium dense	Sand-silt[c]	0,29	67 (1,4)	12	3 (60)
Medium dense Dense	Sand Sand-silt[c]	0,37	81 (1,7)	20	5 (100)
Dense Very dense	Sand Sand-silt[c]	0,46	96 (2,0)	40	10 (200)
Very dense	Sand	0,56	115 (2,4)	50	12 (250)

NOTE The parameters listed in this table are intended as guidelines only. Where detailed information such as *in situ* CPT records, strength tests on high quality samples, model tests or pile driving performance is available, other values can be justified.

[a] The definitions for the relative density percentage description are as follows:

Soil description	Relative density (%)
Very loose	0–15
Loose	15–35
Medium dense	35–65
Dense	65–85
Very dense	85–100

[b] The skin friction factor β (equivalent to the 'K tanδ' term used in the past) is introduced in this document to avoid confusion with the δ parameter used in the past.

[c] Sand-silt includes soils with significant fractions of both sand and silt. Strength values generally increase with increasing sand fractions and decrease with increasing silt fractions.

[d] Design parameters proposed in the past for these relative density/soil description combinations can be unconservative. Hence, the unified CPT method should be used for these soils (see 8.1.4).

A.8.1.5 Skin friction and end bearing in gravels

No additional guidance is offered.

A.8.1.6 Skin friction and end bearing of grouted piles in rock

No additional guidance is offered.

A.8.1.7 Skin friction and end bearing of driven piles in intermediate soils

No additional guidance is offered.

A.8.2 Pile capacity for axial tension

No additional guidance is offered.

A.8.3 Axial pile performance

A.8.3.1 Static axial behaviour of piles

An analytical method for determining axial pile performance is provided in Reference [140]. This method makes use of t–z curves of local transfer of axial pile shear, t, against local pile displacement, z, to model the axial support provided by the soil along the side of the pile. An additional Q–z curve is used to model the tip end bearing, Q, against tip displacement, z. Methods for constructing t–z and Q–z curves are given in 8.4.

The actual capacity of the pile can be less than the ultimate capacity given by Formula (21) in circumstances, such as for soils that exhibit strain-softening behaviour and/or where the piles are excessively axially flexible. In these cases, these effects on axial capacity should be considered.

A.8.3.2 Cyclic axial behaviour of piles

A.8.3.2.1 Qualification

Modelling cyclic effects explicitly can improve the designer's insight into the relative importance of the cyclic characteristics of the actions. On the other hand, extreme care should be exercised in applying this approach. Historically, cyclic effects have been taken into account implicitly rather than explicitly. Design methods developed and calibrated on an implicit basis generally need extensive modification where explicit algorithms are employed.

A.8.3.2.2 Actions

Axial actions on piles are developed from a wide variety of operating, structural and environmental sources. Permanent and variable actions are generally long duration actions and are often referred to as static actions. Environmental actions are developed by winds, waves and currents, earthquakes and ice floes. These actions can have both low and high frequency cyclic components in which the rates of change of actions and action durations are measured in seconds. Storm and ice can cause several thousand cycles of (relatively speaking) low frequency actions, while earthquakes can induce several tens of cycles of high frequency actions [40].

A.8.3.2.3 Cyclic effects

Cyclic effects should be considered when there are unusual limitations on pile penetrations or when certain soils, conditions related to actions or novel structures (e.g. compliant towers) are involved.

Compared with long-term static actions, cyclic actions can have the following important influence on pile axial capacity and stiffness:

— decrease capacity and stiffness due to repeated actions [58];

— increase capacity and stiffness due to high rates of change of actions [59].

The resultant effect on capacity is primarily influenced by the pile properties (stiffness, length, diameter, material), the soil characteristics (type, stress history, strain rate and cyclic degradation) and the action characteristics (numbers and magnitudes of repeated actions). Cyclic actions can also cause accumulation of pile displacements and either stiffening and strengthening or softening and weakening of the soils around the pile. Hysteretic and radiation damping dissipate the energy provided by the actions in the soil. For earthquakes, the free-field ground motions (independent of the presence of the piles and structure) can develop important cyclic straining effects in the soils. These effects can influence pile capacity and stiffness.

Additional guidance on the effect of cyclic actions on pile axial capacity and stiffness can be found in Reference [187].

A.8.3.2.4 Analytical models

A variety of analytical models have been developed and applied to determine the cyclic axial behaviour of piles. These models can be grouped into two general categories, discrete element models and continuum models.

A.8.3.2.4.1 Discrete element models

The soil around the pile is idealized as a series of uncoupled 'springs' or elements attached between the pile and the far field soil (usually assumed rigid). The material behaviour of these elements can vary from linearly elastic to nonlinear, hysteretic and rate dependent. The soil elements are commonly referred to as t–z (friction resistance–displacement) and Q–z (tip resistance–displacement) elements (see References [239], [275], [41] and [198]). Linear or nonlinear dashpots (velocity dependent resistances) can be placed in parallel and in series with the discrete elements to model radiation damping and rate of change of loading effects [41]. The pile can also be modelled as a series of discrete elements (e.g. rigid masses interconnected by springs), or modelled as a continuous rod, either linear or nonlinear. In these models, material properties (soil and pile) can vary along the pile.

A.8.3.2.4.2 Continuum models

The soil around the pile is idealized as a continuum attached continuously to the pile. The material behaviour can incorporate virtually any reasonable stress-strain rules the analyst can devise. Depending on the degree of nonlinearity and heterogeneity, this model can be quite complicated. Again, the pile is typically modelled as a continuous rod, either linear or nonlinear. In these models, material properties can vary in any direction [261], [302].

There is a wide range of assumptions that can be used regarding boundary conditions, solution characteristics, etc., which lead to an unlimited number of variations for either of the two approaches.

Once the idealized model is established and the relevant formulae are developed, a solution technique should be selected. For simple models, a closed-form analytical approach is sometimes possible. Otherwise, a numerical procedure should be used. In some cases, a combination of numerical and analytical approaches is helpful. The most frequently used numerical solution techniques are the finite difference method and the finite element method. Either approach can be applied to both the discrete element and continuum element models. Discrete element and continuum element models are occasionally combined [40], [275]. Classical finite element models have been used for specialized analyses of piles subjected to monotonic axial actions [261].

For practical reasons, discrete element models, solved numerically, have seen the most use in evaluation of piles subjected to high intensity cyclic action. Results from these models are used to develop information on pile accumulated displacements and on pile capacity following high intensity cyclic actions [275], [198].

Elastic continuum models solved analytically (similar to those used in machine vibration analyses) have proven to be useful for evaluations of piles subjected to low intensity, high frequency cyclic actions at or below design working levels [261], [302]. At higher intensity actions, where material behaviour is likely to be nonlinear, the continuum model solved analytically can still be used by employing equivalent linear properties that approximate the nonlinear, hysteretic effects [229].

A.8.3.2.5 Soil characterization

A key part of developing realistic analytical models to evaluate cyclic effects on piles is the characterization of soil-pile interaction behaviour. High quality *in situ*, laboratory and model-prototype pile loading tests are essential in such characterizations. In developing (soil) characterizations relevant for soil-pile interaction, it is important that pile installation and relevant conditions of the actions on a pile be integrated into the testing programmes [40], [198].

In situ tests (e.g. vane shear, cone penetrometer, ball or T-bar penetrometer, pressure meter) can provide important insights into in-place soil behaviour and stress-strain properties [228], [242]. Both low and high amplitude stress-strain properties can be developed. Long-term (static, creep), short-term (dynamic, impulsive) and cyclic (repeated) actions sometimes can be simulated with *in situ* testing equipment.

Laboratory tests on representative soil samples permit a wide variety of stress-strain conditions to be simulated and evaluated [364]. Soil samples can be modified to simulate pile installation effects (e.g. remoulding and reconsolidating to estimated *in situ* stresses). The samples can be subjected to different boundary conditions (triaxial, simple-shear, interface shear) and to different levels of sustained and cyclic shear time histories to simulate in-place conditions of applied actions.

Tests on model and prototype piles are another important source of data for developing soil characterizations for cyclic analyses. Model piles can be highly instrumented and repeated tests can be performed in soils and for a variety of actions [198], [49]. Geometrical scale, time scale and other modelling effects should be addressed in applying results from model tests to analyses of prototype behaviour.

Data from loading tests on prototype piles are useful for calibrating analytical models [271], [241], [144], [269]. Such tests, even if not highly instrumented, can provide data to guide development of analytical models. These tests can also provide data for verifying results of soil characterizations and analytical models, as shown in References [40], [198], [41], [272] and [42]. Prototype pile loading tests coupled with *in situ* and laboratory soil testing and realistic analytical models can provide an essential framework for making realistic evaluations of the responses of piles to cyclic axial actions.

A.8.3.2.6 Analysis procedure

A.8.3.2.6.1 Actions

The actions on the pile head should be characterized in terms of their magnitudes, durations, sequence and numbers of cycles. This includes both long-term actions and short-term cyclic actions. Typically, the design static and cyclic actions expected during a design event are chosen.

A.8.3.2.6.2 Pile properties

The properties of the pile including its diameter, wall thickness, stiffness, weight and length should be defined. This will require an initial estimate of the pile penetration that is appropriate for the design actions. Empirical, pseudo-static methods based on pile loading tests or soil tests can be used to make such estimates.

A.8.3.2.6.3 Soil properties

Different analytical approaches will require different soil parameters. For the continuum model, the elastic and damping properties of the soil are required. In the discrete element model, soil resistance–displacement relationships along the pile shaft (t–z) and at its tip (Q–z) should be determined. *In situ* and laboratory soil tests and model and prototype pile loading tests can provide a basis for such determinations. These tests should at least implicitly include the effects of pile installation, types of actions and time scales. In addition, the test should be performed so as to provide insight regarding the effects of the characteristics of the actions on the pile. Most importantly, the soil behaviour characteristics should be appropriate for the analytical model(s) used, duly recognizing the empirical bases of these models.

A.8.3.2.6.4 Cyclic analyses

Analyses should be performed to determine the response (resistance and displacement) characteristics of the pile subjected to its design static and cyclic actions. Recognizing the inherent uncertainties in evaluations of pile actions and soil-pile behaviour, parametric analyses should be performed to evaluate the sensitivity of the pile response to these uncertainties. The analytical results should develop realistic predictions of pile resistance and accumulated displacements for design actions. In addition, following the simulation of static and cyclic design actions, the pile should be further analysed so as to estimate its reserve capacity.

A.8.3.2.7 Performance requirements

A primary objective of pile performance analyses is to ensure that the pile and its penetration are adequate to meet the structure's requirements.

The pile performance for explicit cyclic analyses should be evaluated separately. The pile should have a capacity that provides an adequate margin of reserve above the design actions. In addition, the pile should not settle or pull-out, nor accumulate displacements to the extent that can constitute failure of the structure–foundation system.

A.8.4 Soil reaction for piles under axial compression

A.8.4.1 Axial shear transfer t–z curves

Theoretical curves can be constructed in accordance with Reference [203]. Empirical t–z curves based on the results of model- and full-scale pile loading tests can follow the procedures for clay soils described in Reference [100].

The representative pile capacity model in 8.1.2 does not provide any information about axial pile displacements, which are important for serviceability limit states, especially in non-extreme conditions for actions due to permanent, variable and operating environmental actions that are generally well below the design actions. In cases where the representative axial capacity of 8.1.2 is adopted, the axial shear transfer characteristics between pile and soil can be derived as described in 8.4, and analytical models can be employed to investigate axial pile displacements under service limit state conditions. However, using the axial shear transfer data derived using methods as presented in 8.4 (in particular, equating t_{max} with $f(z)$ in clay soils) will not produce the representative axial capacity under ultimate loading conditions.

In some circumstances (e.g. for soils that exhibit strain-softening behaviour or where long piles can be axially flexible), the axial capacity of the pile should be derived explicitly accounting for the post-peak degradation of the unit skin friction at large strain.

A.8.4.2 End bearing resistance–displacement Q–z curves

No additional guidance is offered.

A.8.5 Soil reaction for piles under lateral actions

A.8.5.1 General

Lateral soil resistance–displacement *p*–*y* curves should be constructed using stress–strain data from laboratory soil samples. The ordinate for these curves is soil resistance, *p*, and the abscissa is the pile wall displacement, *y*. By iterative procedures, a compatible set of lateral resistance-displacement values for the pile-soil system can be developed.

More detailed study of the construction of *p*–*y* curves can be found in the following sources:

— Reference [238] for monotonic curves in clays;

— References [298] and [383] for cyclic curves in clays;

— Reference [45] for fatigue curves for clays and sands;

— Reference [268] for monotonic and cyclic curves in sand

— Reference [149] for layered soils.

A.8.5.2 Lateral soil reaction for clay

Reference [238] describes the numerical analyses and the extensive database of 537 DSS tests that were used to develop the p-y curve framework. It also details the hindcast of eleven pile load tests which demonstrated the wide range of applicability of the method.

A.8.5.2.1 *p*–*y* curves for monotonic actions

A.8.5.2.1.1 Ultimate soil resistance for isotropic conditions

The recommended values of p_u will generally be higher than those of API RP 2GEO 1st edition as shown in Figure A.11. Extensive comparisons between various recommendations can be found in Reference [238].

Example	s_{uo} (kPa)	s_{u1} (kPa/m)	D (m)	γ (kN/m³)	α (-)	$\frac{s_{uTE}}{s_{uDSS}}$	Gap	J (1st Ed. Only)
1	2	1,2	0,914	7	1	0,9	No	0,5
2	150	0	2,134	8	0,5	0,7	Yes	0,5

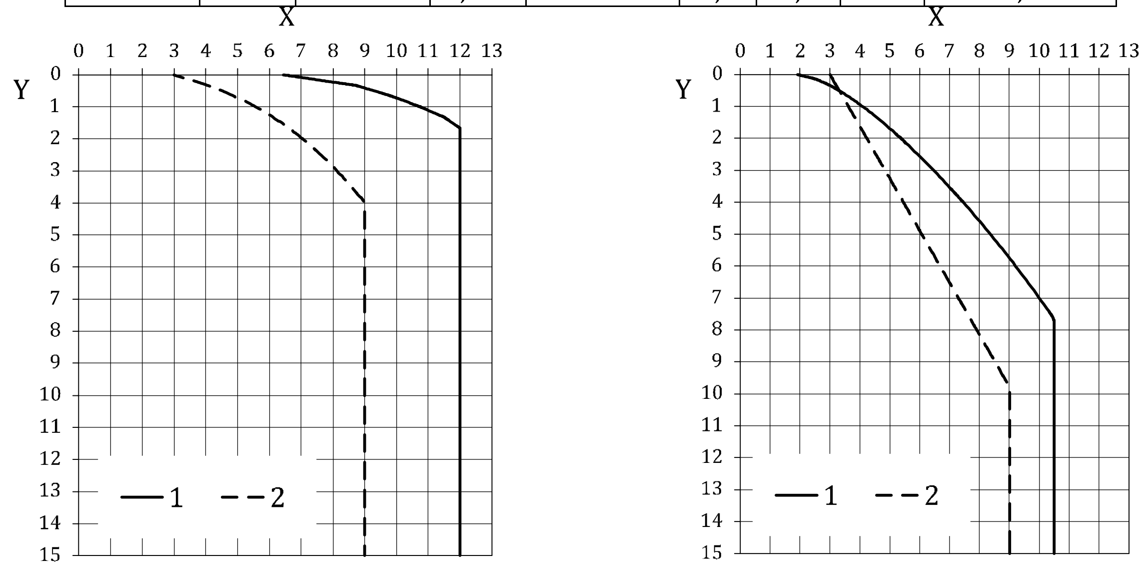

Key

X Lateral bearing capacity factor, N_p (-)

Y Normalised depth, z/D (-)

1 ISO 19901-4 3rd Ed – this document

2 ISO 19901-4 2nd Ed

Figure A.11 — Comparison of total lateral bearing capacity factor N_p according to API RP 2GEO 1st edition and 2nd edition for example 1 (left) and example 2 (right)

A.8.5.2.1.2 Anisotropy correction of ultimate soil resistance for gapping conditions

Two types of anisotropy are considered in the p-y curve:

1) Difference in strength between the triaxial extension and DSS failure modes:

   — Detailed discussion on anisotropic clay properties can be found in References [238] and [219] for GoM clays, and Reference [19] for Drammen clay.

   — Anisotropy considerations are usually not warranted for very soft clays close to the seafloor because:

     - a laterally loaded pile in such clays will typically behave in a non-gapping condition;

     - the DSS shear strength is typically a reasonable estimate of the average of the triaxial compression shear strength and the triaxial extension shear strength (as is the case for GoM clays).

   — In the flow-around mechanism (i.e. when $N_p = N_{pd}$), the value of p_u is solely based on the DSS strength and needs no correction for anisotropy between the triaxial and DSS failure modes.

2) Difference in DSS strength on a vertical plane and a horizontal plane in the flow-around mechanism:

   — In principle, the DSS tests should be performed on vertically trimmed samples to measure the strength on the *in- situ* vertical plane and better simulate the flow around conditions. However, industry practice is to perform DSS tests on horizontally trimmed samples and measure the strength on the *in situ* horizontal plane.

   — Data suggest that the ratio of the strength on the *in situ* horizontal plane over the strength on the *in situ* vertical plane is close to unity for clays with I_p greater than 30 % and therefore no correction is needed when measuring s_u on a horizontally trimmed sample. The influence of this inherent anisotropy should be evaluated for I_p < 30 %. More guidance can be found in Reference [238].

For highly non-linear profiles (e.g. profiles with a crust near the seafloor or a large step-increase in shear strength), guidance on how to calculate the bearing capacity factor N_p can be found in References [163] and [162].

A.8.5.2.1.3 *P-y* curve relationships

Guidance on how to scale laboratory DSS stress-strain curves to obtain *p-y* curves can be found in Reference [238]. Normalized *p-y* curves, (p/p_u) vs (y/D), are obtained from normalized DSS curves, (τ/s_u) vs γ.

The default normalized curves of Table 2 for I_p greater than 30 % were obtained by substituting the following values in Equation 1 of Figure A.12 to obtain a set of three normalized DSS curves:

— For OCR ≤ 2: γ_f = 0,15; a = 2,38;

— For OCR =4: γ_f = 0,15; a = 1,5;

— For OCR = 10: γ_f = 0,15; a = 1,0;

Each of these normalized DSS curves was then scaled twice as per method 2 of Figure A.12 and as per the full procedure as described in Reference [382] to obtain two *p-y* curves. Each of the default normalized curves of Table 2 is a best fit through these two obtained *p-y* curves.

The default normalized curves of Table 2 for I_p less than 30 % were obtained, based on experience with Drammen clay, by multiplying the (y/D) abscissa on the normalized curves for I_p greater than 30 % for the same OCR as follows:

— For OCR ≤ 2: (y/D) abscissa multiplied by 0,33;

— For OCR =4: (y/D) abscissa multiplied by 0,5;

— For OCR = 10: (y/D) abscissa multiplied by 0,66;

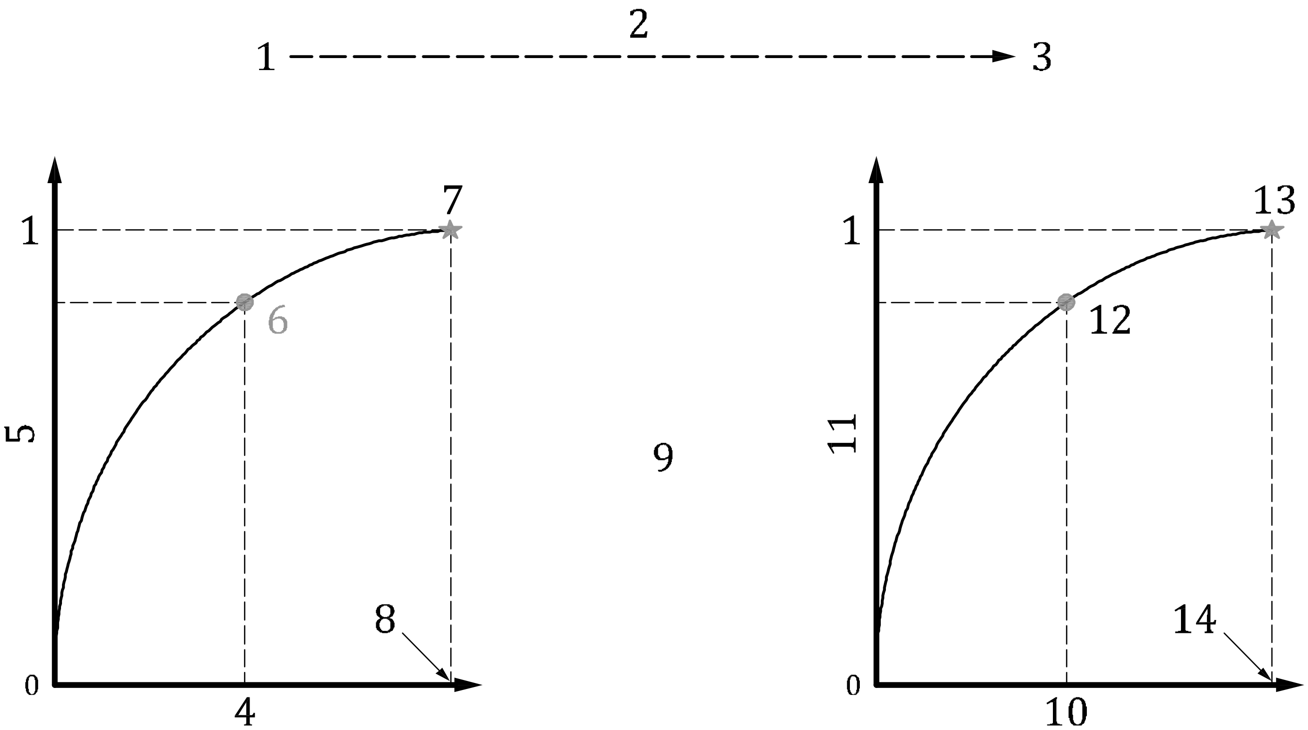

Key

1 Normalized DSS curve, up to peak shear stress
2 Scaling
3 Normalized *p-y* curve
4 Shear strain, γ
5 Normalized shear stress, τ/s_u
6 (γ , τ/s_u)
7 Failure
8 γ_f
9 Method 1:
$p/p_u = \tau/s_u$
$y/D = (1{,}35 + 0{,}25\ a)\ \gamma$
Method 2:
1- Determine strain at failure, γ_f
2- Curve fit normalized DSS curve with Eq. 1 below and obtain parameter “a”, which typically ranges from 1,0 to 3,5.

$$\frac{\tau}{s_u} = \frac{\tanh\left[a\cdot\left(\frac{\gamma}{\gamma_f}\right)^{0,5}\right]}{\tanh(a)} \qquad \text{Equation 1}$$

3- Obtain normalized p-y curve as

$$\frac{p}{p_u} = \frac{\tanh\left[A\cdot\left(\frac{y/D}{y/D_f}\right)^{0,5}\right]}{\tanh(A)} h$$

With $A = 1{,}33 + 0{,}45\ a$ and $(y/D)_f = \gamma_f\,(2{,}5 - 1{,}2\ \ln(a))$

10 Normalized pile displacement, y/D
11 Normalized soil resistance, p/p_u
12 (y/D , p/p_u)
13 $(y/D)_f$

Figure A.12 — Methods to obtain *p-y* curves from DSS curves

A.8.5.2.2 *P-y* curves for cyclic actions

The full method to develop cyclic *p-y* curves for GoM and North Sea conditions can be found in References [384] and [383]. Validation of the method and comparison with cyclic pile load test results can be found in Reference [383].

The p-y curve method includes an iterative process and requires knowledge of the design action and the detailed pile characteristics. The method in the main text is a simplified approach and is intended to moderately overestimate cyclic effects.

Contrary to previous recommendations in API RP 2GEO 1st edition, the cyclic curves are stiffer and have higher ultimate resistance than the monotonic curves. This arises in part because the previous recommendations were developed from a single series of tests performed with 200 cycles to 400 cycles at each lateral loading increment and were intended to provide a lower bound of soil resistance.

In contrast, the new recommendations provide best-estimate soil resistance for loadings acting on jacket structures. The number of equivalent cycles varies with depth and with lateral displacement, but is less than 25 for such structures. For these low number of cycles, the soil cyclic strength is greater than the reference monotonic strength, and the *p*-modifier is greater than 1,0.

The normalized cyclic curves vary along the depth of the pile. An example calculation as per 8.5.2.2 is presented in Figure A.13 for an illustrative clay soil profile with I_p > 30 %, OCR < 2, and for GoM cyclic loading conditions.

s_{uo} (kPa)	s_{u1} (kPa/m)	D (m)	γ (kN/m³)	α (-)	$\frac{s_{uTE}}{s_{uDSS}}$	Gap	Estimated pile rotation depth (m)
2	1,2	2,134	7	1	0,9	No	32

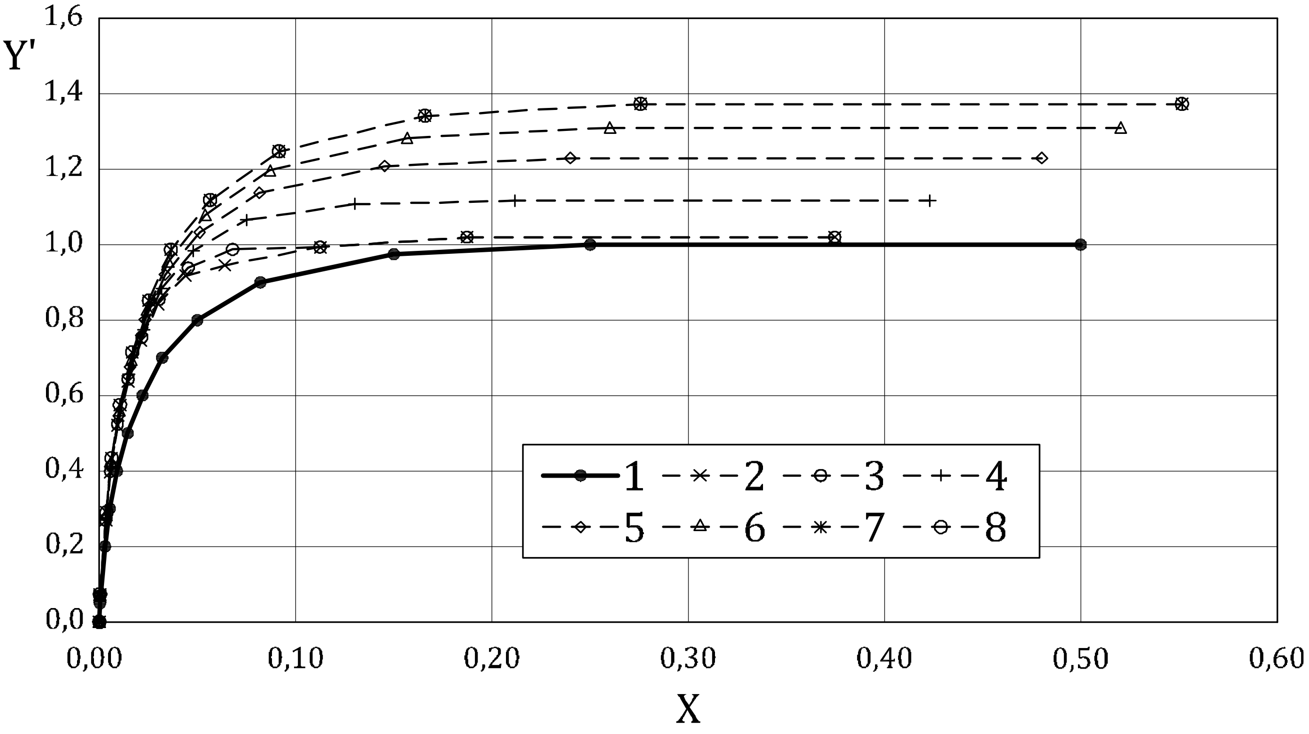

Key

X Normalized lateral displacement, (y/D)
Y' Normalized soil resistance, (p/p_u)
1 Monotonic curve - I_p > 30 %; OCR < 2
2 Cyclic curve ; Z/Z_{rot} = 0
3 Cyclic curve ; Z/Z_{rot} = 0,2
4 Cyclic curve ; Z/Z_{rot} = 0,4
5 Cyclic curve ; Z/Z_{rot} = 0,6
6 Cyclic curve ; Z/Z_{rot} = 0,8
7 Cyclic curve ; Z/Z_{rot} = 1,0
8 Cyclic curve ; Z/Z_{rot} = 1,1

Figure A.13 — Cyclic normalized curves for illustrative clay soil profile with I_p > 30 %, OCR < 2, and for GoM cyclic loading conditions

A.8.5.2.3 *P-y* curves for fatigue actions

Development and validation of the p-y curves for fatigue actions can be found in Reference [378] where hindcast of conductor/wellhead/BOP/LMRP motions are compared with those predicted using the recommended *p-y* curves.

A.8.5.2.4 *P-y* curves for earthquake actions

Reference [221] details the results of centrifuge tests which showed that, for a jacket in soft clay, the structural natural period and bending moment profile along the piles were accurately predicted with:

— the *p-y* curves derived as per Reference [189];

NOTE The recommendations of 8.5.2.1 are an update from Reference [189] and give similar results for OCR < 2, I_p > 30 %, non-gapping clays with a skin friction factor, α, equal to 1,0.

— hysteretic unload-reload behaviour;

— lateral and axial radiation damping;

— depth-varying ground motion input.

A.8.5.2.5 Comparison with previous recommendations

The monotonic, cyclic and fatigue curves in Clause A.8.5.2 are compared with the monotonic and cyclic curves recommended by API RP 2GEO 1st edition in Figure A.14 for an illustrative soil profile and GoM conditions. The input parameters for the comparison are given in Table A.4.

Table A.4 — Input parameters for comparison of *p-y* curves

s_{uo} (kPa)	s_{u1} (kPa/m)	D (m)	γ (kN/m³)	α (-)	$\frac{s_{uTE}}{s_{uDSS}}$	**Gap**	**Estimated rotation depth** (m)	**ε_c for API RP 2GEO 1st edition method for soft clays**
2	1,2	2,134	7	1	0,9	No	32	0,02

The vertical axis on Figure is labelled "p/s_uD" and is unitless with the definition of "p" as a force per unit length. The unit of "p" is now consistent with the units for the *p-y* curves in sands. In the 1st edition of API RP 2GEO, "p" had a unit of pressure and "P" had a unit of force per unit length. Therefore, the values calculated with the 1st edition of API RP 2GEO as shown in Figure A.14 are actually "P/s_uD" when using the definitions in that document.

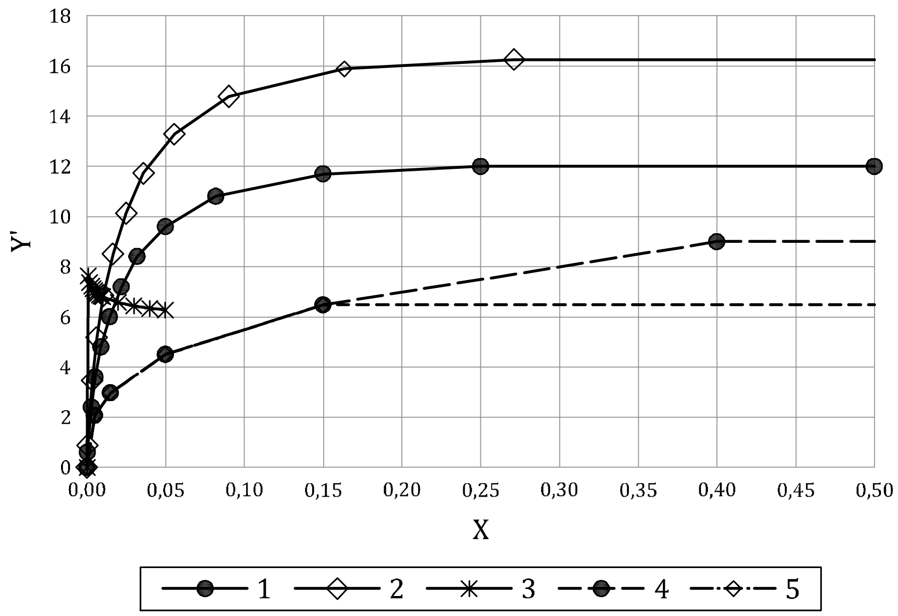

Figure A.14 a)

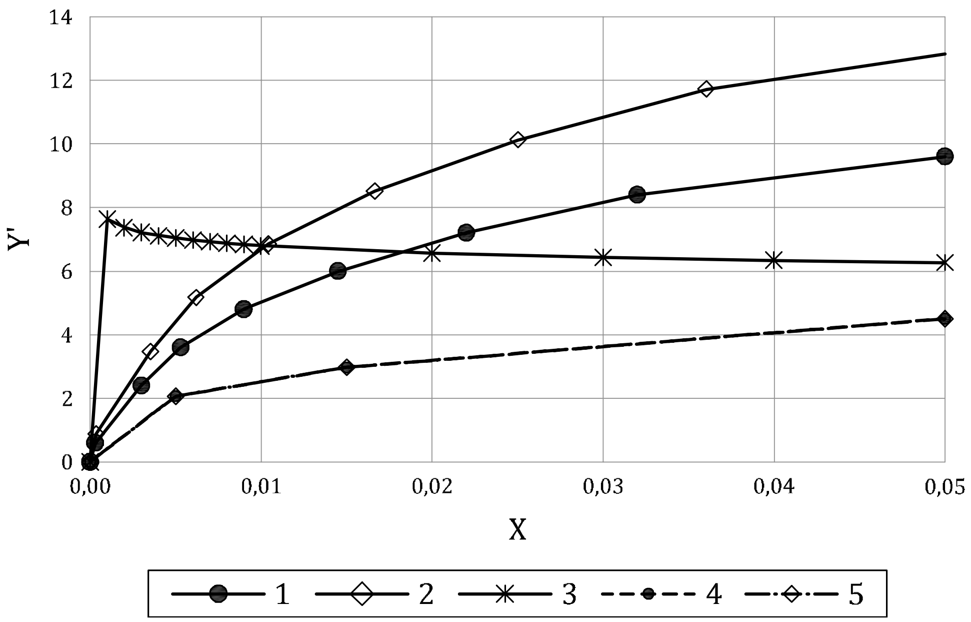

Figure A.14 b)

Key

X Normalized lateral displacement (y/D)

Y Normalized soil resistance (p/p_u)

1 Monotonic curve – API RP 2GEO 2nd Ed., 8.5.2.1 - I_p > 30 %; OCR < 2

2 Cyclic curve – API RP 2GEO 2nd Ed., 8.5.2.2 - GoM condition

3 curve – API RP 2GEO 2nd Ed., 8.5.2.3

4 Monotonic curve – API RP 2GEO 1st Ed.

5 Cyclic curve – API RP 2GEO 1st Ed.

Figure A.14 — Comparison of *p-y* curve recommendations between RP 2GEO 1st and 2nd Editions at a depth z = 30 m for illustrative clay soil profile for GoM conditions: a) full scale and b) low y/D displacements

A.8.5.3 Lateral capacity for sand

Scour (i.e. seabed sediment erosion due to wave and current action) can reduce lateral soil support around offshore piles, leading to an increase in pile maximum bending stress. Scour is generally not a concern for clay soils, but should be considered for sands.

In the absence of project specific data, for an isolated pile a local scour depth equal to 1,5 D and an overburden reduction depth equal to 6 D may be adopted, D being the pile outside diameter; see Figure A.15.

Reduction in lateral soil support is due to two effects:

— a lower ultimate lateral pressure caused by decreased vertical effective stress, $\sigma'_{vo}(z)$;

— a decreased initial modulus of subgrade reaction, E_S.

There is no generally accepted method to allow for scour in the p–y curves for offshore piles. Figure A.1 suggests one of the methods for evaluating $\sigma'_{vo}(z)$ and E_S as a function of scour depths. In this method, general scour reduces the $\sigma'_{vo}(z)$ profile uniformly with depth, whereas local scour reduces $\sigma'_{vo}(z)$ linearly with depth to a certain depth below the base of the scour pit. Subgrade modulus reaction values, E_S, can be computed assuming the general scour condition only.

Other methods, based upon local practice, model testing [189] and/or experience, can be used instead.

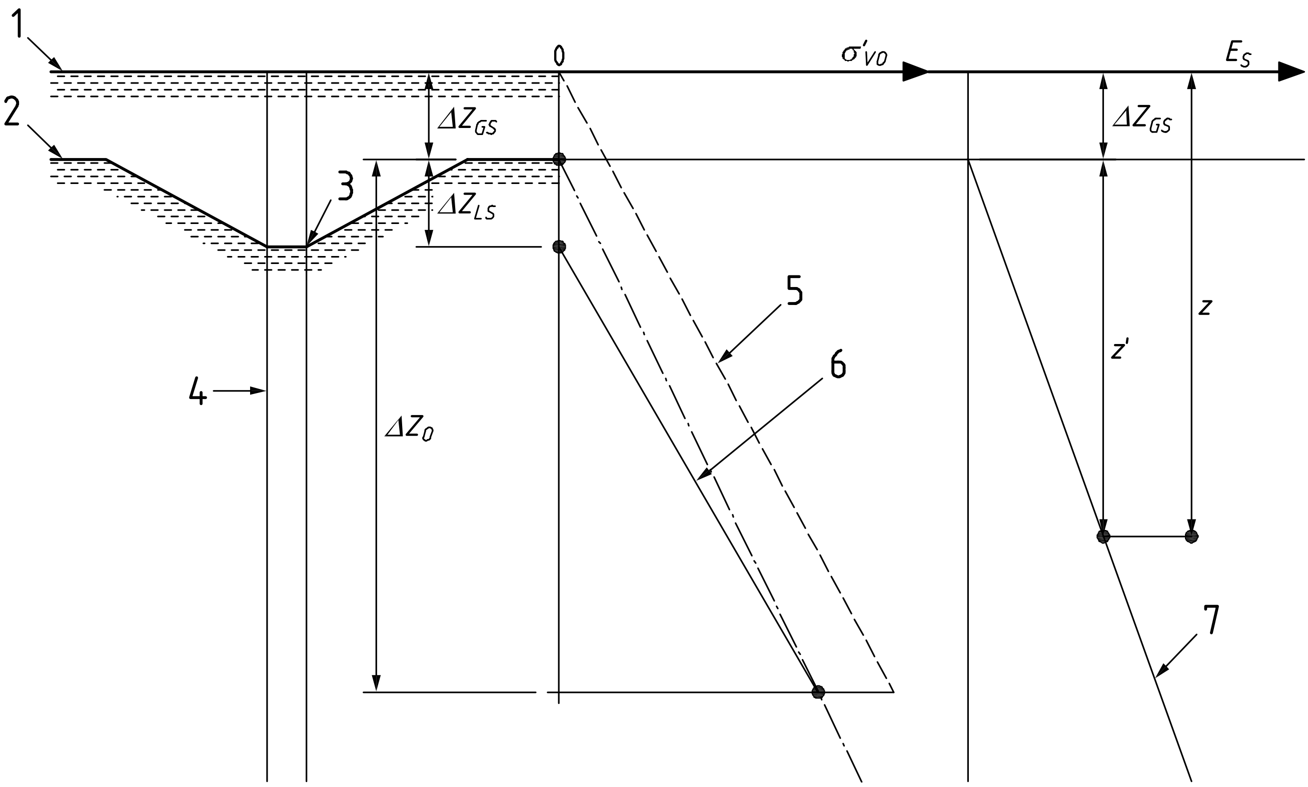

Key

1	original seafloor level	Δz_{GS}	global scour depth
2	level after general scour	Δz_{LS}	local scour depth (1,5 D typical)
3	level of local scour	Δz_0	overburden reduction depth (6 D typical)
4	pile	σ'_{vo}	vertical effective stress
5	no scour case	E_S	initial modulus of subgrade reaction
6	local scour case	z	depth below original seafloor
7	$E_s = k\,z'$ (see Table 3 for k)	z'	final depth below seafloor, after general scour

Figure A.1 — *p*-*y* lateral support — scour model

A.8.5.4 Lateral soil resistance-displacement *p-y* curves for sand

No additional guidance is offered.

A.8.5.5 *P–y* curves for fatigue actions

No additional guidance is offered.

A.8.5.6 Refined analysis for cases that are sensitive to lateral loading response

For intermediate foundations where the pile or caisson L/D ratio is low (i.e. less than about 10), or when the design is highly sensitive to lateral actions, more advanced analysis methods which involve the definition of case-specific soil reaction curves defined through, for example, finite element analyses are available.

References [72] and [70] describe the 'PISA' 1D modelling procedure which recognizes that further soil reactions develop in addition to the lateral soil reactions considered in *p-y* calculations. As illustrated in Figure A.16, four separate soil reaction components are considered at the soil-pile interface: (i) distributed lateral actions, (ii) vertical shear tractions combining to form a moment, (iii) a horizontal force at the pile base, and (iv) a moment at the pile base.

Each of the soil reaction components is related in the model to the local lateral displacement or rotation (i.e. adopting a 'Winkler' approach) by a calibrated parametric function referred to as a 'soil reaction curve'. In the computational implementation (the 1D model illustrated in Figure A.17 (b)), the pile is represented as an embedded beam, which is best represented by Timoshenko beam theory. A distributed lateral action p and a distributed moment m are assumed to act along its length. The distributed moment represents the moments associated with the vertical shear tractions induced at the soil-pile interface. Additionally, a horizontal force H_B and a moment M_B act on the pile base. Figure A.17 sets out two alternative processes that can be followed to define the sets of soil reaction curves:

a) Rule-based method: This approach employs pre-defined curves that are either in the wider literature or can be derived through analytical methods. Examples of such curves include existing published formulations for the *p-y* method (see Reference [238]) or new bespoke sets of all four soil reaction curves for glacial clay till (see Reference [71]) and marine dense sand (see Reference [67]) that are linked to soil parameters acquired through appropriate soil investigations. Application to layered soil profiles is addressed in References [70] and [66].

b) Numerical-based method: This approach adopts finite element calculations to generate and calibrate site-specific or regional soil type reaction curves that can be used in the 1D model calculations. This requires the following steps:

   1) A characterization of the site ground model and the properties of the soils present that is sufficiently thorough to inform accurate non-linear modelling of their non-linear stiffness and failure behaviour. This will usually require detailed knowledge of undrained strength in clays, relative density and CPT cone resistance in sands and reliable information on soil stiffness (see Reference [380]).

   2) Specification of the soil investigation and laboratory testing program to provide the data required for step 1).

   3) Appropriate calibration of the soil constitutive model used for the finite element calibration analysis, based on the information obtained in step 2) (see, for example, References [372] and [331]).

   4) A specification of the design parameter space for the finite element analyses, within which the soil reaction curves will be calibrated (e.g. pile geometry, loading conditions), and over which the calibrated 1D model is valid.

   5) A choice of the functional form of the non-linear curves used as the basis function for the soil reaction curves, calibrated via data abstracted from the finite element analyses.

6) A procedure for abstracting the soil reaction curve data from the finite element analyses, and providing an optimization of fit of the soil reaction curve basis function against the abstracted data from the finite element analyses.

7) Development of a scaling procedure that allows the soil properties from step 1) to be input to steps 5) and 6) so that the derived soil reaction curves can be more widely applied in the simplified 1D design model across the proposed design space.

Option a) may be adopted for design where site investigation data are limited, or at an early stage of the design process. Option b) may be incorporated as part of the detailed design procedure. Implementation of option b) at different sites will increase, over time, the spread of cases for which calibrated soil reaction curves are available to apply option a). Further details of the method can be found in References [72], [70], [71], [67] and [66].

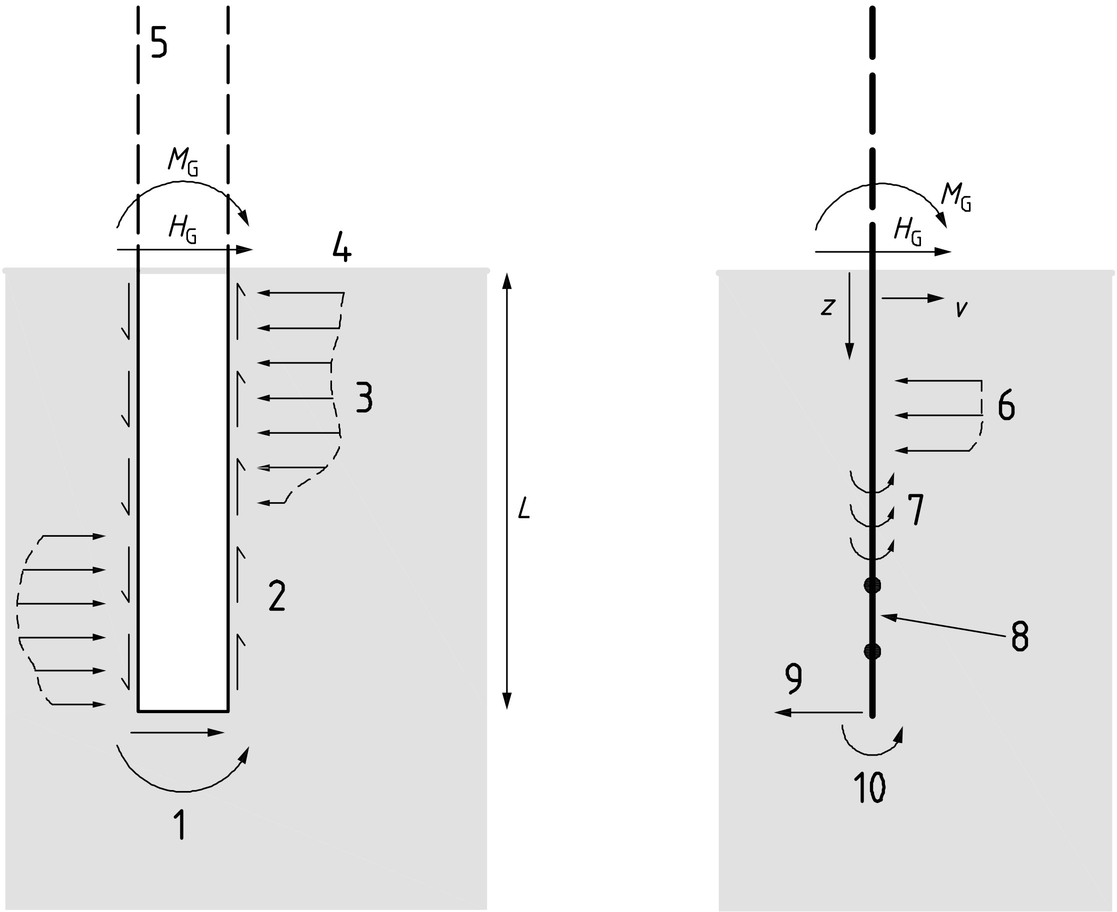

(a) (b)

Key

1	Horizontal force and moment applied at the pile base	6	Distributed lateral load $p(z,v)$
2	Vertical shear force tractions at soil-pile interface	7	Distributed moment m(z,⍰⍰)
3	Distributed lateral load	8	Timoshenko beam elements
4	Ground level	9	Base horizontal force $H_B(V_B)$
5	Tower	10	Base moment M_B(⍰⍰⍰)

NOTE The reactions are depicted in Figure (a) as acting in the expected direction. In Figure (b) the reactions are shown in directions that are consistent with the coordinate directions shown.

Figure A.16 — (a) Idealization of the soil reaction components acting on a monopile (b) 1D finite element implementation of the model

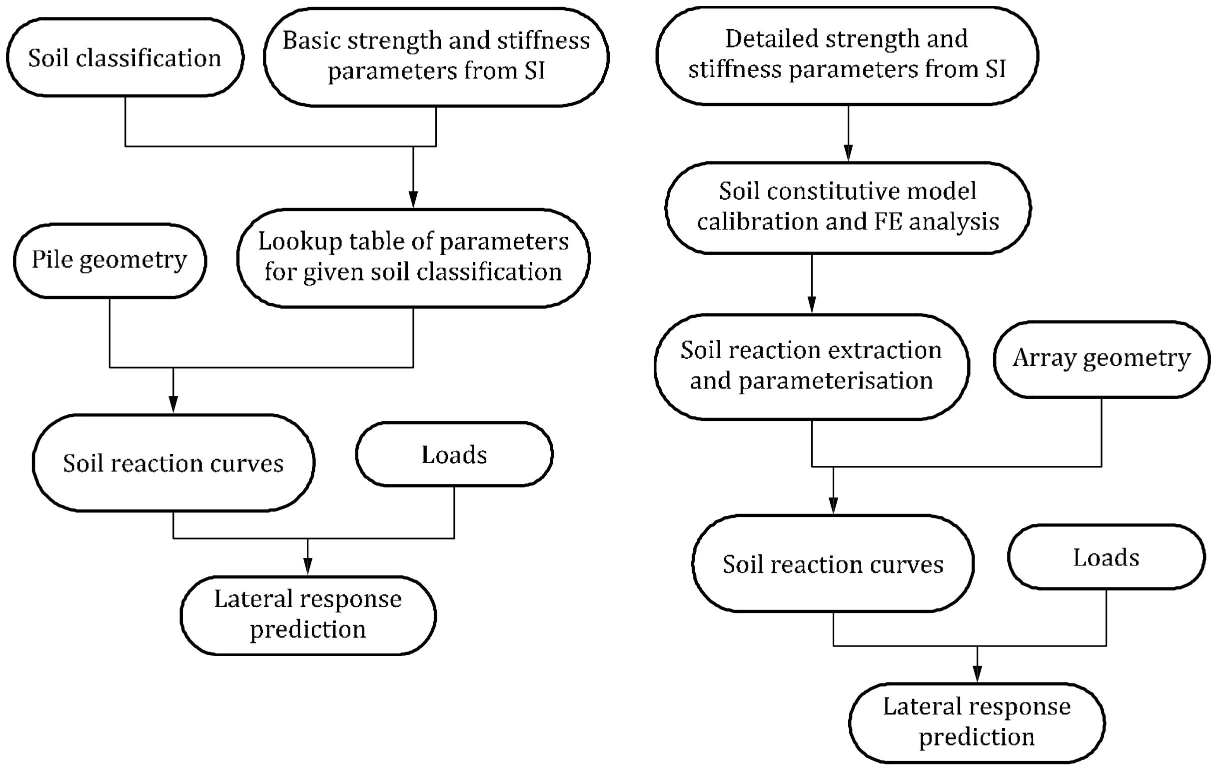

a) rule-based method   b) numerical-based method

Figure A.17 — Application modes for the design method

A.8.6 Pile group behaviour

A.8.6.1 General

Routine numerical analysis of pile groups can be divided into two main categories.

The first category, which is computationally the simplest, uses algebraic expressions to define the elastic single pile resistance to general (axial, lateral and torsional) actions [277]. The group resistance is determined by modifying the single pile expressions to account for elastic pile-soil-pile interaction.

The second category, which is normally performed for offshore pile groups, is more rigorous. Methods are usually hybrid, employing a mixture of discrete p–y curves (Winkler approach) and continuum soil behaviour, first described in Reference [139] for lateral analysis. Since then, numerous programs have been developed worldwide for general types of action. Typically, the nonlinear single pile resistances to general actions are computed using axial t–z and lateral p–y curves and combined with elastic interaction expressions similar to the first category. The resulting formula are solved for various pile head fixity conditions and/or pile cap restraint to determine the nonlinear group resistance and individual pile forces and moments, plus the so-called 'z- and y-modifiers'.

References [277] and [263] provide more detailed discussions.

A.8.6.2 Axial behaviour

In general, group effects depend considerably on pile group geometry and penetrations and thickness of any bearing stratum underneath the pile tips [277], [263].

A.8.6.3 Lateral behaviour

Experience confirms that the available tools for analysis of pile groups subjected to lateral actions provide approximate answers that sometimes deviate significantly from observed behaviour, particularly with regard to displacement calculations. Also, limitations in soil investigation procedures and in the ability to predict soil-pile interaction behaviour for a single pile produce uncertainty regarding proper soil input to group analyses. Therefore, multiple analyses should be performed for pile groups using two or more methods of analysis and upper-bound and lower-bound values of soil properties in the analyses. By performing such analyses, the designer will obtain an appreciation for the uncertainty involved in his predictions of foundation performance and can make more informed decisions regarding the structural design of the foundation and structure elements.

A.8.7 Pile installation assessment

A.8.7.1 General

Drivability studies are carried out in accordance with the principles given in 8.7.2 and A.8.7.2 in order to define the type of hammer necessary to reach the target design pile penetration. The design penetration of driven piles should not be determined upon any correlation of pile capacity with the number of blows required to drive the pile a certain distance into the seabed.

Vibratory hammers can be considered for installing well conductors, or piles which are predominantly subjected to horizontal actions, such as reaction piles for start-up of pipelines or anchor piles. They can also be used where extraction and repositioning can be required. Vibratory hammers can further be considered as complementary tools to impact hammers, i.e. for initial driving [194].

In order to minimize delays in installation, a pile acceptance procedure should be established. The procedure should outline the measures to be taken on location for adjusting planned pile driving scenarios, in case of, for example, premature pile driving refusal or a significantly lower blow count than anticipated at design target pile penetration.

A.8.7.2 Drivability studies

Drivability studies are required to cover a wide range of soil types and driving conditions and should take into account local experience. The principles of drivability are presented in References [319] and [341], with friction fatigue effect discussed in Reference [168] and damping parameters presented in Reference [303]. Soil resistance to drive for a variety of different soil types and driving conditions are defined in References [328] and [6]. For Gulf of Mexico clays, guidance is given in Reference [379] and more specifically in Reference [121] for tension leg platform piles and in Reference [126] for deep water cases. For North Sea cases, guidance is given in Reference [284] and in References [6] and [130] for hard clays. For West Africa soils, guidance is given in Reference [97] and in Reference [279] for soft carbonate rocks.

A.8.7.3 Obtaining required pile penetration

No additional guidance is offered.

A.8.7.4 Driven pile refusal

The following are two examples of driven refusal criteria.

a) In soft soils, pile driving refusal for a properly operating hammer is defined as the point where pile driving resistance exceeds either 1 000 blows/m (330 blows/ft) for a consecutive 1,5 m (5 ft) of penetration, or 800 blows for 300 mm (1 ft) of penetration. This definition applies when the weight of the pile does not exceed four times the weight of the hammer ram. If the pile weight exceeds this, the above blow counts are increased proportionally, but in no case should they exceed 800 blows for 150 mm (6 in) of penetration.

b) In hard clays and dense sands, pile driving refusal can be defined as the point where driving resistance exceeds one of the following criteria:

- in continuous driving, a minimum of 125 blows/250 mm (165 blows/ft) over 6 consecutive intervals of 250 mm, or a minimum of 200 blows/250 mm over 2 consecutive intervals of 250 mm;

- in the last interval of 250 mm at the end of driving, 325 blows/250 mm (400 blows/ft);

— at restart of driving after a stoppage for 1 h or longer, 325 blows/250 mm over 2 consecutive intervals of 250 mm.

In soils where hard driving conditions are anticipated, such as in the presence of boulders or of strong cemented layers, the definition of pile refusal criteria cannot be based solely on a blow count value, and the potentially high local driving stresses induced in the pile should also be taken into account. The stress level in the pile steel can be calculated from wave formula analyses, and can be estimated from the stress measurements from pile instrumentation. An example of refusal criteria for pile driving in strongly cemented carbonate soils is given in References [327] and [363].

The potential consequences of hard driving conditions in strong cemented layers (i.e. damage of the pile, hammer or structure) are highly dependent on the hammer type and size, on the pile wall thickness (D/WT ratio, presence of a driving shoe), and on possible defects and irregularities in the pile shape, as well as on the soil conditions (in particular, strength and thickness of the rock layer, and soil type below the rock formation). Moreover, the reflected stress level (ratio of the maximum reflected stress to the initial peak stress), as measured from pile instrumentation at the pile head, only gives an estimate of the average stress in the pile wall; more severe stresses can be experienced locally at the pile tip during driving. Therefore, the definition of driven pile refusal criteria in cemented soils should preferably be based on local piling experience at the site. Correlation charts, similar to the one proposed in Reference [279], can be developed as an aid in deciding whether pile driving through a cemented layer can be attempted, or if drilling of the rock below the pile tip is necessary.

A.8.7.5 Driven pile refusal measures

No additional guidance is offered.

A.8.7.6 Selection of pile hammer and stresses during driving

The designer should be aware that pile buckling and pile refusal incidents in very dense sands have been associated with the use of external chamfers at the pile tip. Although factors other than the shape of the pile tip contribute to buckling, the use of an external chamfer can increase the potential for buckling and/or refusal.

A.8.7.7 Use of hydraulic hammers

No additional guidance is offered.

A.8.7.8 Drilled and grouted piles

No additional guidance is offered.

A.8.7.9 Belled piles

In general, drilling of bells for belled piles should employ only reverse circulation methods. Drilling mud should be used where necessary to prevent caving and sloughing. The expander or under-reaming tool used should have a positive indicating device to verify that the tool has opened to the full width required. The shape of the bottom surface of the bell should be concave upward (sides higher than the centre) to facilitate later filling of the bell with tremie concrete.

To aid in concrete placement, longitudinal bars and spiral steel reinforcements should be well spaced. Reinforcing steel can be bundled or grouped to provide larger openings for the flow of concrete. Undue congestion at the throat between the pile and the bell should be prevented, where such congestion can trap laitance. Reinforcing steel cages or structural members should extend far enough into the pile for an adequate transfer of forces to be developed.

Concrete should be placed as for tremie concrete, with the concrete being ejected from the lower end of a pipe at the bottom of the bell, always discharging into fresh concrete. Concrete with aggregates of 10 mm (3/8 in) and less in size can be placed by direct pumping. Because of the long drop down along the pile and the possibility of a vacuum forming with subsequent clogging, an air vent should be provided in the pipe near the top of the pile. To start placement of concrete, the pipe should have a steel plate closure with soft rubber gaskets in order to exclude water from the pipe. Unbalanced fluid heads and a sudden discharge of concrete should be prevented. The pile should be filled to a height above the design concrete level equal to 5 % of the total volume of concrete, placed so as to displace all laitance above the design level. Suitable means should be provided to indicate the level of the concrete in the pile. Concrete placement in the bell and adjoining section of the pile should be as continuous as possible.

A.8.7.10 Grouting pile-to-sleeve connections

The equipment should have sufficient capacity to achieve the grout filling in a single continuous operation. Grouting should not commence unless there are sufficient materials available, including a contingency, to complete the task. Grout slurry stored in a holding tank should be continuously stirred and should not be held for more than 30 min prior to pumping. In case of rapid hardening mixes, the storage duration in a holding tank should be reduced to less than 30 min. Further details concerning quality control as well as requirements for conducting grout trials that addresses cement grout for connections and repairs can be found in ISO 19902.

Prior to grouting and after activating any sealing devices, dyed water should be flushed through the complete grouting system to both remove any deleterious matter and to prove its functionality. A pressure test can be appropriate for closed systems. The annulus should then be carefully filled by maintaining a continuous grout flow through the lowest practical point.

Grout returns to allow surface sampling are preferable. If these are provided, grout samples for strength conformance testing can be taken from the returns in addition to the slurry specific gravity measurements. If surface returns are not provided, visual inspection to confirm that grout has completely filled the annulus should be performed immediately after cessation of grout pumping and again after initial grout set, typically 12 hours.

A.8.7.11 Pile installation data

No additional guidance is offered.

A.8.7.12 Installation of conductors and shallow well drilling

Additional guidance about the installation of conductors by driving is provided in A.10.5.6.

A.9 Reassessment of pile capacity for existing structures

A.9.1 General

In accordance with ISO 19901-9:2019, Clause 9 is limited to the capacity reassessment for driven piles and conductors making the foundation system of fixed steel offshore structures.

A.9.2 Geotechnical and foundation data

No additional guidance is offered.

A.9.3 Evaluation

No additional guidance is offered.

A.9.4 Assessment

A.9.4.1 General

No additional guidance is offered.

A.9.4.2 Pushover response of pile foundation systems

The following guidance is offered for how the pile foundation and conductor system should be treated in pushover analyses:

- Effects of cyclic actions: The cyclic stress-strain behaviour of the soil can be assessed from a series of laboratory tests or centrifuge tests, which can then be used in an analysis together with the cyclic load history to evaluate the performance of the whole foundation system. Cyclic pile loading tests can also be used as reference to understand the likely response during a pushover analysis. Additional guidance about the cyclic behaviour of piles is provided in A.8.3.2;
- Conductors: Care should be exercised in how the platform and conductor guide framing that constrains and engages the conductors is modelled so that the lateral displacements of the conductors at the seafloor are consistent with the behaviour of the overall structure under a given loading condition, and that the conductor guide framing will fail at the appropriate loading levels.

Other risk implications than for a pile foundation should be considered, if the conductors fail before the platform system. These are not considered in this document; specific advice from well specialists should be sought in these cases.

Caution should be exercised if increasing the shear strength of the soil to account for unexpected survivals of pile foundation systems in extreme loading events. The limited available information to date suggests that the performance of platform foundation systems in hurricanes is consistent with predictions based on design capacities [150]. When increasing the strength of the soil in an attempt to explain a pile foundation system survival in an extreme loading event, the following factors should be considered:

a) If the axial capacity of the pile is mostly due to sands acting in skin friction or end bearing, then increasing the undrained shear strength of clay layers alone (a common practice due to its simplicity) will have very little impact on the axial capacity.

b) If sands are present, use of CPT-based methods of predicting skin friction and end bearing will provide more reliable estimates of pile capacity (see 8.1.4).

c) If the pile system is failing in shear, the capacity of the system is much more sensitive to the bending moment capacity of the piles and conductors than to the shear strength of the soil. A relatively small increase in bending moment capacity, such as with an average versus a nominal steel yield stress, can have a greater effect on the capacity of the pile system.

d) The shear strength of the soil is being used as a convenient surrogate for lateral and axial soil resistance, since the soil shear strength can be changed easily as input to a pushover analysis. However, the relationship between lateral or axial soil resistance and shear strength is not directly proportional. Increasing the undrained shear strength of clay layers causes them to be treated as more heavily over-consolidated in the design recipe for axial side shear. In this case, the greater the undrained shear strength, the less sensitive the axial capacity will be to an increase in the undrained shear strength.

When a CPT-based method is used for predicting the pile capacity in a pushover analysis, consistent axial response of the pile foundation system as represented by shear and end bearing transfer t-z and Q-z curves should be defined, i.e.:

- the shape of the t-z and Q-z curves can be defined in accordance with 8.4.1 and 8.4.2, but with the maximum soil-pile unit skin friction, t_{max}, at any depth along the pile length, and the representative end bearing resistance, Q_p, determined with the CPT-based method;
- an appropriately brittle t-z curve should be adopted.

A.9.5 Time-dependent effects on pile foundations

Ageing over a period of about one year leads to significant gains in the shaft friction of driven piles in sands in first-time loading. Smaller gains have been observed for driven piles that are re-tested and, by inference, working piles that experience high levels of cycling. Until such time as the mechanisms of ageing are better understood, and if field measurements confirming ageing effects on piles or conductors in similar conditions do not exist, adopting the lower bound ageing characteristics presented in Reference [147] can be considered.

Sensitivity analyses should be performed where increases in pile shaft capacity due to ageing can result in structural issues.

A.10 Soil-structure interaction for auxiliary subsea structures, risers and flowlines

A.10.1 General

No additional guidance is offered.

A.10.2 Geotechnical investigation

No additional guidance is offered.

A.10.3 Foundations for manifolds and subsea production structures

No additional guidance is offered.

A.10.4 Steel catenary risers

A.10.4.1 General – seabed response in vertical plane

Riser interaction with the seabed involves complex non-linear processes including plastic penetration during initial touchdown, softening during cycles of upward and downward motion and potential suction-induced tensile resistance prior to breakaway. In most cases, design is undertaken using simplified models where the riser–soil interaction is idealized by a series of linear springs with zero tension capacity distributed along the riser throughout the touchdown zone. Ideally, the choice of spring stiffness should consider the amplitude of vertical displacement and other effects such as the cyclic motion of the riser. While the soil response will also be affected by out-of-plane motion of the riser, the discussion in this subclause is restricted to vertical stiffness of the seabed.

The conceptual description of the seabed resistance as shown in Figure A.18 for a robust action cycle involving soil–riser separation is complex. Following initial riser penetration into the seabed, unloading occurs as the pipe is uplifted. The soil response in the early stages of uplift is much stiffer than that under conditions of virgin penetration as shown in the ‘unloading’ curve in Figure A.18. With continued uplift, the net resistance force goes into tension (‘pipe-soil suction’ in Figure A.18) until maximum uplift resistance of the soil is reached and the pipe begins to detach from the soil. Uplift resistance decreases until the pipe completely detaches from the soil. Upon re-penetration, the pipe comes back into contact with the soil, with the re-loading stiffness typically being less than the unloading stiffness. Upon completion of a full action cycle, the action path does not return to the initial point of departure from the backbone curve; rather the pipe penetrates a small additional depth into the soil. The effects from cyclic loading will reduce the stiffness upon subsequent cycles although long term consolidation can result in an increase in soil stiffness.

The information provided in this subclause for motions in the vertical plane has been largely developed based on model test for typical deep-water clay deposits with an overlying crust about 1 m in thickness overlying normally consolidated clays. The results and conclusions derived from these tests should not be considered appropriate for other soil conditions.

NOTE The uplift resistance is referred to here as ‘suction’ although, strictly speaking, under submerged conditions pore pressures normally remain positive. For consistency with much of the published literature, the term ‘suction’ is retained, understanding that it refers to a net upward force acting on the seabed, accompanied by a decrease in pore pressure relative to ambient conditions.

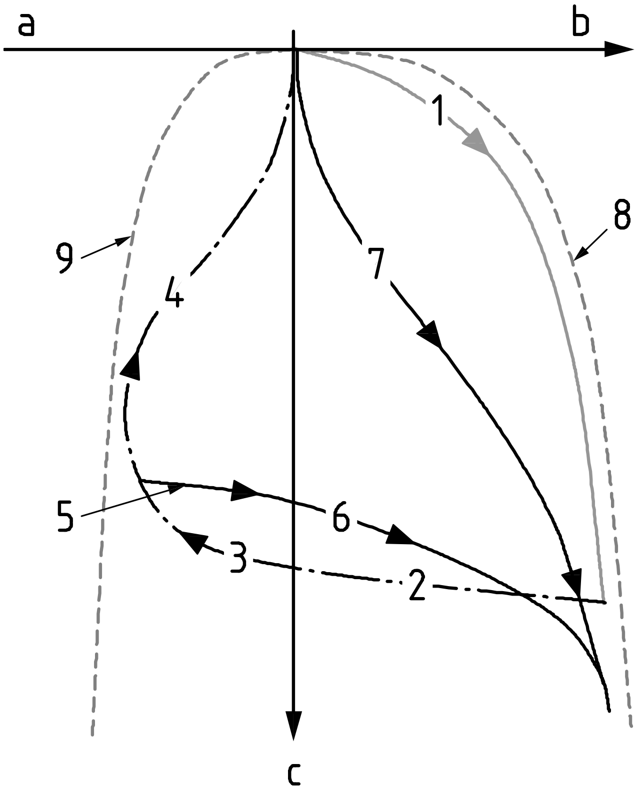

Key

1	Initial penetration	7	Re-penetration following lift-off
2	Uplift	8	Ultimate penetration resistance, Qu= NcsuD
3	Further uplift resisted by suction	9	Ultimate suction resistance, Qu-suc
4	Suction decays if uplift continues	a	Negative reaction (i.e. suction)
5	Suction releases with re-penetration	b	Normal seabed reaction force, Q
6	Further penetration	c	Penetration, z

Figure A.18 — Randolph & Quiggin soil model characteristics for different modes [294]

A.10.4.2 Design for ultimate limit state

No additional guidance offered.

A.10.4.3 Design for fatigue state

A.10.4.3.1 General

No additional guidance offered.

A.10.4.3.2 Design options

A.10.4.3.2.1 Elastic model

For initial conservative screening evaluations, an elastic stiffness can be used. Examples where an elastic stiffness model have been used are given in References [90] and [78]. If the SCR has a lazy wave configuration, the motions at the touchdown point will be reduced versus a standard SCR. The motions can be sufficiently small to minimize cyclic loading effects. Both model tests and analytical models suggest that the soil stiffness, $k = \Delta Q/\Delta z$, normalized by the maximum bearing pressure ($N_c s_u$) for pipe displacements, Δz, of 0,000 3D to 0,002D (where D is pipe diameter) ranges from about 200 to 300. A normalized stiffness $k/(N_c s_u)$ of 200 is therefore recommended. For such small displacements, it is also not likely that the pipe will significantly penetrate and form a trench. A bearing capacity factor (N_c) in the range 5 to 6 should be used to determine the vertical soil stiffness. Many deep-water offshore deposits are characterized by an upper crust with fairly uniform shear strengths (s_u) that can be up to 15 kPa in the upper 1 m to 1,5 m. There is often a reduction in shear strength below the crust followed by an increase following a normally consolidated trend. Due to uncertainties in the pipe penetration, the strength reduction below the crust should not be used to determine the vertical soil stiffness, but the shear strength through the crust should be used. Qualified geotechnical advice is recommended to determine the appropriate shear strength.

For a standard SCR without a lazy wave configuration, the expected motions will be greater and the soil will likely experience more inelastic deformations and reductions in stiffness from cyclic loading. Sectional model tests on a 0,51 m diameter pipe in Gulf of Mexico clay subjected to 1-year winter storm conditions have shown that even for a small number of cycles the average normalized elastic stiffness can be considerably less than the 200 to 300 range for the small displacements noted above [90]. The recommended normalized value for initial screening for a standard SCR is therefore reduced to 100. However, for this case, the pipe will likely penetrate further into the soil and form a trench, because of the inelastic displacements and the effects of cyclic loading. Therefore, a higher bearing capacity factor of 8 is recommended to determine the soil stiffness from the normalized value.

A.10.4.3.2.2 Non-linear models

Non-linear models are recommended if the SCR does not meet fatigue requirements with the elastic screening model described above.

Two types of non-linear are available. The first developed by Randolph and Quiggin [294] is depicted above in Figure A.18. This model has the advantage of directly inputting the shear strength profile rather than interpreting a single representative value. The various input parameters for this model are described in detail in Reference [294]. Although the model does not explicitly account for cyclic loading effects, the re-penetration of the pipe, especially for case where the pipe separates from the soil with lift-off, will provide much lower stiffness values than for case without lift-off. This non-linear model is available in the commercial software code Orcaflex™. Geotechnical expertise is advised in the selection of the input parameters.

The other non-linear model is based on sectional tests performed on Gulf of Mexico and Angolan soil [89]. These tests cyclically loaded an instrumented sectional riser with a prototype pipe diameter of 0,51 m and length of 100 m. The predicted versus measured fatigue profiles were then compared after 120 cycles of loading. The non-linear soil model was based on shorter (< 1 m long) segment tests that were cycled vertically. The tests were performed with a few hundred cycles of loading. Based on the segment data, a hyperbolic soil model was derived which showed very good agreement between the measured and predicted results for the sectional tests. The non-linear soil model was a hyperbolic model, which represents an assemblage of points after the soil has degraded for a few hundred cycles. The hyperbolic formulae for the Gulf of Mexico and Angola soils are the following:

$$Q_n = \frac{Z_n}{(A' + B'Z_n)} \tag{A.44}$$

$$A' = \frac{(1 - X)Z_{nu}}{Q_{nu}} \tag{A.45}$$

$$B' = \frac{X}{Q_{nu}} \tag{A.46}$$

where

Q_n is the normalized force per unit length of pipe $(Q/(N_c s_u D))$;

Z_n is the normalized displacement (z/D);

X is a curve fitting parameter (approximately 0,85 to 1,0);

Z_{nu} is the normalized displacement at Q_{nu} which is the normalized force at or near the peak action.

For Gulf of Mexico soil, the parameters X, Z_{nu}, and Q_{nu} that best fit the experimental results were 0,96, 0,10 and 0,35, respectively. For Angolan soil, the best fit parameters were 0,98, 0,10 and 0,125, respectively.

A.10.4.3.3 Trenching effects

The formation of a trench during the life of an SCR can have an impact on the SCR fatigue life. The trench can be modelled explicitly in the SCR fatigue analyses or correction factors applied depending on the location, direction of loading-vessel position and trench depth.

Details on modelling the trench shape are given in Reference [295]. Their analyses using a non-linear soil model for a trench with a maximum depth of 5 pipe diameters using three possible trench geometries is summarized in Table A.5 for Gulf of Mexico soil.

Table A.5 — Relative lengths of fatigue life for GoM soil and max. depth of 5D

Platform Motion Position	Average for 3 trench geometries	Range
Near	2,11	1,65 – 2,44
Far	1,03	0,77 – 1,19
Cross	1,05	0,97 – 1,10
NOTE Numbers represent ratio of fatigue life for an SCR with a 5D trench relative to a flat seabed, modelled using a non-linear seabed model (from Reference [295])		

Experimental results for a 3D trench indicate the ratio of fatigue life for the trench condition versus a flat seabed is 1,05 [89]. The boundary conditions for these tests (no moment at loading point) are best represented by the 'far' platform motion position, which compares favourably to the average Gulf of Mexico ratio (1,03) shown in Table A.5.

The trench depth is difficult to determine and, in addition to the vessel motion positions, will form as a result of mechanical pipe-soil interaction and potential erosional processes. If field observations can verify potential trench depths (3D to 5D maximum depth) based on similar vessels and SCRs, Table A.5 can be used to adjust fatigue calculations based on a flat seabed. For the 'near' platform motion, the lower bound value of the range is recommended. For the 'far' and 'cross' positions, the average is recommended. If the trench depth cannot be verified, no adjustments to the flat seabed results should be applied.

A.10.4.3.4 Cyclic and consolidation effects

The results regarding the combined effects of cyclic loading and consolidation are somewhat mixed. Cyclic loading for undrained conditions will result in significant reductions in the soil stiffness, especially for cases where the pipe separates from the soil [89]. Soil consolidation from the dissipation of pore pressures developed from cyclic loading will consolidate the soil and result in increases in stiffness over long time periods. The combined process is further complicated by the potential for water entrainment after a pause period with no cyclic loading followed by an event that can cause significant fatigue damage.

When evaluating the potential effects of cyclic loading the following information should be considered:

a) Load-controlled segment tests (see Reference [369]) in kaolin soil performed in a centrifuge on a 1 m diameter prototype pipe showed a decrease in stiffness for continuous loading for about 60 days (prototype time for consolidation). From 60 days to 1 800 days of continuous loading, the soil stiffness increased to levels 2 to 3 times the initial stiffness. The dimensionless time factor for 90 % consolidation for a pipe embedded half a pipe diameter is about 2 [160]. The dimensionless time factors for the 60-day and 1 800-day cases were 0,5 and 12, suggesting partially drained and fully drained conditions. API RP 2RD indicates that the loading at the touchdown point is displacement rather than load-controlled.

b) Displacement controlled segment tests (see Reference [33]) in Angolan soil on a 0,174 m diameter pipe subjected to 600 cycles with 18 day pause periods after 200 and 400 cycles indicate that after each pause period the soil secant stiffness increases. The tests were performed with displacements sufficient to cause separation of the pipe from the soil. For 50 to 100 cycles after each wait period, the soil stiffness returns to the same degradation trend observed before the wait period. The stiffness degradation appears to be continuing beyond 600 cycles. The dimensionless time factor, *T*, at the end of the testing was 5,65, suggesting full consolidation. The continuous degradation of the soil suggests that upon re-penetration of the pipe into the soil water entrainment occurred, negating consolidation effects, acknowledging that in these tests the pipe was locked in place during the pause periods and did not penetrate or reconsolidate the soil under self-weight or the forces that can occur in a typical SCR touchdown zone.

c) Displacement-controlled segment tests in Gulf of Mexico soil (see Reference [4]) soil on a 0,05 m pipe were performed with a 1 000 cycles of loading and pause periods every 100 cycles. The times for the first 7 pause periods were between 1 to 2 hours. The final two pause periods were 2,5 and 13 hours. In contrast to the displacement-controlled tests on the Angolan soil described in item b), the pipe was free to settle during the pause periods. After each pause period, the soil stiffness increased and then degraded with additional cyclic loading. For these tests, however, there was a long-term increase in stiffness of a factor of about 1,5 to 2 from the stiffness observed after 100 cycles to end of the first seven packets of loading. The final two packets of loading appear to suggest that the increase has levelled off. When the test was complete, the soil stiffness appears to be continuing to decrease. This tests likely represent an upper limit on pipe settlement. The field case will depend on the level of excess pore pressure developed by the cyclic loading, the pipe flexibility and the constraints of the pipe from the vessel and pipeline away from the touchdown zone. The dimensionless time factor, *T*, at the end of the 1 000 cycles was 29, suggesting full dissipation of pore pressures.

d) Sectional centrifuge test in Gulf of Mexico soil (see Reference [89]) on a 0,51 m diameter prototype pipe loaded for about 120 cycles indicated a continual increase in fatigue life, suggesting a decrease in soil stiffness. The displacements for the test corresponded to a 1-year winter event. The overall decrease from the first cycle of loading to 120 cycles suggests about a factor of 4 decrease in stiffness. The dimensionless time factor, *T*, after the 120 cycles of loading was about 0,07, suggesting mostly an undrained response. Subsequent loading events included 40 cycles of a 100-year event, 80 cycles of a 1-year event followed by a pause period of about 1,8 days prototype time for consolidation, another 40 cycles of a 1-year. event and another 40 cycles of a 100-year event. The dimensionless time factor, *T*, at the end of this testing sequence was 0,24, suggesting a partially drained condition. Although direct fatigue determinations were not made beyond the initial 120 cycles of loading, the measured moment data for the final 1-year event shows a further reduction in the maximum moment, suggesting that the cyclic degradation effects were more dominant than the consolidation effects.

e) Centrifuge displacement-controlled segment tests (see Reference [177]) on a 0,5 m diameter pipe were conducted in kaolin clay consolidated to provide an overlying crust (with OCR up to 20) transitioning to normally consolidated clay at depth. Cyclic tests included conventional displacement limited tests with ranges of ± 0,02D up to 0,2D, but also hybrid tests that were load-controlled during penetration, but displacement-controlled uplift to above the seafloor at each cycle. The latter type of tests showed similar cyclic evolution of unload stiffness to the displacement-controlled tests, in spite of the greater potential for water entrainment. The data illustrate the effects of over-consolidation ratio, with lower regain in stiffness (after initial remoulding) for the tests in soil with OCR = 5, compared to the tests in normally consolidated soil.

The information in items a) to e) should be used to help determine the combined effects of cyclic loading and consolidation. Additional testing should be considered, especially for soil conditions different from those typically found in deepwater (circa 1 m crust overlying normally consolidated clay) or for clay soils outside of those already investigated with model tests like those described in items a) to e). Additional model tests are also suggested if the potential reduction in soil stiffness beyond a few hundred cycles of loading is required to achieve the required fatigue life.

Either segment or sectional tests can be performed. Segment tests are on short pipe sections and can be performed either under 1-g conditions or in a centrifuge. Sectional tests are on 100 m plus long prototype sections of the SCR that extend through the touchdown zone [89]. These tests are most practically performed in a centrifuge. An advantage of these tests is that they can simulate interactions between the pipe and soil along the length of the section which will help determine the impact of the pipe settlement during pause periods.

For both segment and sectional tests displacement- or load-control can be considered. Expert advice is recommended on selection of the type of loading. There is still some debate which one or a combination of the two is most appropriate. However, API RP 2RD indicates the motions at the TDP are displacement controlled. Segment tests should include testing over a range of displacements including those sufficient to cause pipe-soil separation. Sectional tests should be performed mostly at displacement or loading levels that cause the most fatigue damage (1/2-year to 2-year events). Larger events can be considered to investigate their impact on cyclic degradation and consolidation. The overall testing should be performed for several thousand cycles and for time periods sufficient to investigate significant consolidation effects ($T > 2$), with the dimensionless time factor, T, determined following Reference [369].

A.10.5 Geotechnical design for top tension risers

A.10.5.1 General

This subclause provides additional information and guidance pertinent to geotechnical design of conductors for top tension risers.

A.10.5.2 Jetted conductors

A.10.5.2.1 General

The conductor is the well foundation and its main function is to resist the axial and lateral loading actions imposed at the wellhead. In stiff clays and sands conductors are generally grouted into pre-drilled oversized holes or driven in-place. However, a technique analogous to wash boring, called jetting, is a feasible alternative for installing conductors in soft clays that are often encountered in deep water. Having originated in the Gulf of Mexico, conductors are now jetted in most deep-water basins in the world [188]. In recent years, many jetted conductors have successfully been installed. Very little literature has been published regarding jetting design, practice and case histories of failures. References [188] and [2] present design approaches and examples of case histories.

The approach for estimating the short-term axial bearing capacity of a conductor is based on the principle of the weight on bit (WOB) available for jetting and reciprocation to penetrate a conductor [188]. This implies that the immediate capacity is not controlled by the soil conditions, but rather by the available weight on bit and the installation method. Physically, the last soil resistance measured during installation, which is given by the last WOB measured, is equal to the immediate capacity. Maximizing the WOB during jetting is therefore of prime importance. This last WOB should be maximized and should be equal to at least 80 % of the available WOB during jetting. The available WOB will typically be calculated by adding the self-weight of the surface conductor, the weight of the wellhead housing, the weight of the drill collars, and the drill ahead tool. Application of this method for estimating long-term axial bearing capacity of jetted conductors is demonstrated in Reference [376]. Common terms used in conductor jetting operation are:

- bottom hole assembly (BHA): the portion of the drill string inside the conductor from the landing or running tool to the drill bit;
- drill-ahead tool: a tool similar to a running tool, except that the drill pipe and BHA assembly can be released from the tool, leaving the tool on the well conductor, allowing continued drilling while the conductor remains in place;
- drilling assembly: composite of drill pipe and BHA;
- weight on bit (WOB): the portion of total weight of drilling assembly not supported by the drill rig; the weight of the drilling assembly supported by the soil.

A.10.5.2.2 Short-term axial bearing capacity

The relationship given in 10.5.2.2 for the change in average friction factor along the conductor, $\Delta\alpha_t$, was derived from installation data obtained in the deep water Gulf of Mexico [188]. Using the same approach outlined in Reference [188], $\Delta\alpha_t$ for conductor installations in deep-water Angola seabed was established as presented in Reference [129]. The same approach can be used to develop site-specific $\Delta\alpha_t$ relationship with appropriate calibration and validation against field installation data.

A.10.5.2.3 Long-term axial bearing capacity

The experiments conducted in Reference [376] simulated normally-consolidated to lightly over-consolidated (1,0 ≤ OCR < 2) deep-water Gulf of Mexico seabed conditions. A similar approach can be used to investigate long-term axial bearing capacity of jetted piles in other regions.

A.10.5.2.4 Soil-structure interaction for well integrity assessment

Response of a top tensioned riser (TTR) system near or below the BOP stack largely depends on the soil behaviour under a specific loading condition. Riser-well-soil interaction analysis is carried out to investigate the following two conditions as part of the TTR system design:

- strength: the reaction of the riser at the ultimate limit state when the vessel has moved a considerable distance from the mean position;
- fatigue: the fatigue that occurs within the system as a result of repeated cyclic motions with a range of amplitudes and frequencies.

The first loading scenario can occur when a vessel is drastically shifted from its original/normal operating position as a result of a drift-off or a drive-off event. The former has to do with loss of station keeping caused by an environmental loading (e.g. loop current) whereas the drive-off loading can be intentional (i.e. the vessel is moved to facilitate drilling operations). In either case, the loading can be considered as a slow monotonic condition that occurs within tens of minutes to hours. Because this problem is concerned with the limit state condition of the system, the soil response at both low and ultimate state conditions is important to the overall conductor design assessment.

Given the often large differences in the structural stiffness of various components in a TTR system above and below seafloor, it is often difficult to assess whether softer or stiffer estimates of soil response will yield conservative predictions for the design. Stiffer estimates would be more likely to suggest a critical bending moment will occur above seafloor, while softer estimates would suggest more critical moments below seafloor. The situation becomes more complicated for the system components that have a capacity sensitive to combination of axial and bending actions, for example the connection at the lower marine riser package (LMRP).

The fatigue problem is governed by the cyclic actions that occur throughout the life cycle of the riser. These actions can occur from the:

- environmental actions on vessel and top portion of the riser;
- vortex induced vibrations (VIV) on the riser.

Analyses have shown that the peak loading actions are not necessarily the major contributors to the fatigue damage. Rather smaller loading actions caused by more frequent loading events are responsible for most of the fatigue damage. Therefore, characterization of the soil response at small amplitude displacements is particularly important for the fatigue problem. The p–y curves developed for ultimate limit state design of pile foundations for steel jackets subjected to monotonic and cyclic storm or hurricane loading are applicable to the case of well strength analysis. However, they are not suitable for fatigue limit state (FLS) assessment of TTR well systems [376].

The approach for the development of p-y curves for FLS assessment of TTR well systems is based on the degraded soil secant stiffness (unload-reload stiffness) at the steady-state condition in sands and clays. Results from model tests have indicated that damping in clays can play a role in fatigue damage. As such, p-y models have been developed to cover a range of complexity from fatigue p-y curves only to fatigue p-y curves coupled with soil damping (modelled by dashpot). Fatigue p-y curves without soil damping are typically used for base case level studies (initial analysis) that are carried out first. If fatigue life does not pass the acceptance criterion, more refined analysis can be carried out, which includes hysteretic soil damping and/or obtaining more geotechnical information to increase accuracy of soil parameters. For complex situations and/or where site-specific soil samples are available, laboratory testing is recommended to develop fatigue *p-y* curves. An example of the apparatus and approach is given in Reference [376].

A.10.5.3 Geotechnical input to well strength assessment

No additional guidance is offered.

A.10.5.4 Geotechnical input to well fatigue assessment

A.10.5.4.1 General

Context on the development of the soil-structure interaction for well fatigue analysis, which form the basis of the guidance outlined in this subclause are provided in References [370], [373] and [374]. The approach has been validated through field monitoring programs. Reference [254] presents specifics of a field monitoring program of an instrumented well installed in the North Sea with the seabed comprising layered clays and sands. Reference [306] compares the stresses measured in the field during drilling operations to those obtained numerically from a full three-dimensional (3D) finite element (FE) analyses model of the blowout preventer (BOP), wellhead (WH), conductor, and surface casing versus the field measured data obtained. The numerical analyses used the backbone *p-y* response outlined in earlier editions of this document and API RP2GEO and the spring-only method presented in References [370], [373] and [374]. Sensitivity studies were also performed. They concluded that the spring-only method yields good prediction of the stresses measured in the field in the conductor and the surface casing.

Reference [196] presented field measurements made at the lower marine riser package (LMRP) location from monitoring a well installed in normally consolidated to lightly over-consolidated clays in deep-water Gulf of Mexico and evaluated performance of the spring-only method presented in References [370], [373] and [374] through 3D FE numerical modelling and fatigue analysis. The numerical model consisted of the well system below the LMRP to 50 m below the seafloor and simulated sea states observed during the drilling operation. The measured motions and fatigue damage obtained from the loggers were compared to those estimated from predictive methods using the spring-only method and it was concluded that the spring-only model performs satisfactorily in predicting the deformations (displacements and rotations) measured at the top of the LMRP; hence, providing a more accurate prediction of the system (LMRP, wellhead and casings) response and thereby, its fatigue damage.

Reference [148] presented a detailed well monitoring program with improvements made to the algorithm and measurement accuracy technique for the purpose of well fatigue assessment in layered sand and clay seabed. The sand layers ranged from loose to very dense and the clay strata consisted of soft to very stiff at depth. Reference [244] conducted fatigue analysis using the backbone *p-y* outline in earlier editions of this document and API RP2GEO and the spring-only method outlined in References [373] and [374]. They concluded that the predictions made with the spring-only method provided BOP response similar to those observed in the field. However, the use of the API model significantly overestimated 'measured' conductor fatigue life above the seafloor. Ultimately, the spring-only method was considered more suitable for wellhead fatigue assessment than the backbone *p-y* curve in earlier editions of this document and API RP2GEO.

The guidance given specifically states that the soil-structure interaction in the fatigue analysis model should not be done with simulating the vessel/rig in offset position. This is solely to avoid erroneous numerical results arising from user errors or limitations in the existing tools and software packages. The issue of vessel offset and soil response was investigated for a wide range of motions and initial offsets in the centrifuge tests presented in References [373] and [374]. The soil response was found to be independent of the initial offset positions (i.e. the soil degradation and resistance in both with and without offset were found to be the same). Shape and characteristics of fatigue *p-y* differ from those of monotonic *p-y*. The stresses needed for input to well fatigue analysis is typically obtained through numerical analysis with the model of the well and foundation soil (represented by *p-y* springs) combined. If the intention is to specifically evaluate fatigue damage from a situation where the vessel/rig is in offset, separate simulations will be required for each offset motion and fatigue motion phases with the appropriate *p-y* used to model the soil response for each loading condition (i.e. monotonic *p-y* for offset loading and fatigue *p-y* for fatigue loading).

A.10.5.4.2 Clays

A.10.5.4.2.1 Spring-only method

No additional guidance is offered

A.10.5.4.2.2 Spring-dashpot method

Soil–structure interaction analysis may include material damping (hysteretic) in the soils and structural materials as well as the foundation radiation damping. The energy dissipated during each load-unload loop is termed hysteretic damping. Radiation damping (also known as the geometric damping or geometric attenuation) differs from material damping in which elastic energy is dissipated by viscous, hysteretic or other mechanisms. Estimating each type of damping in a system is often difficult due to complex interplay of material damping and radiation damping in the dynamic solution. The effects can be approximated in a linear analysis by introducing equivalent viscous damping with energy dissipation equal to that dissipated by hysteresis, an example of which was demonstrated in Reference [374].

Simplified models of soil pressure-displacement (*p-y*) behaviour are generally applicable to conditions involving (1) monotonic loading associated with a well strength analysis or (2) repeated loading cycles associated with a fatigue analysis. In the former loading scenario, the backbone curve most appropriately characterizes soil resistance, while a fully degraded “steady state” *p-y* loop best describes soil resistance for a fatigue analysis. Transient loading, such as occurs in earthquake or impact loading, involves an intermediate case between these extremes where soil resistance degrades from the backbone curve to various levels of reduced stiffness that can approach the fully degraded steady state condition. Such cases can warrant a full nonlinear *p-y* model capable of tracking this evolution (see Figure A.19).

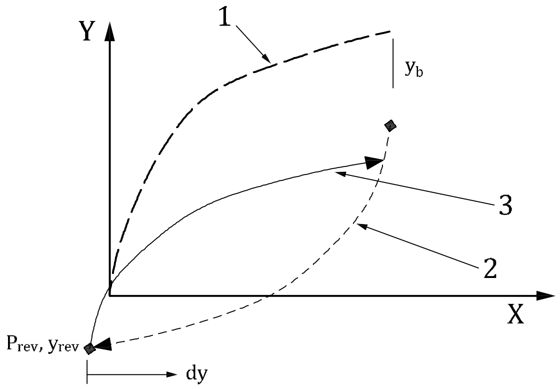

Figure A.19 a) Degrading p-y model

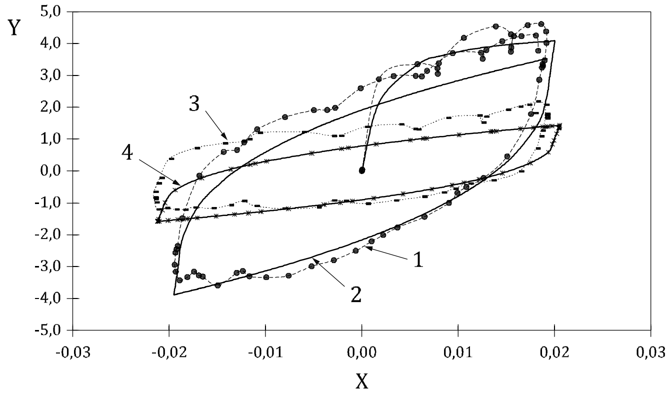

Figure A.19 b) Experimental data

Key

1 Initial excursion (backbone)

2 Unload cycle N

3 Reload cycle N + ½

X Lateral soil displacement, y

Y Lateral soil pressure, p

Key

1 First cycle measured

2 First cycle model

3 Last cycle measured

4 Last cycle model

X Normalized lateral displacement, y/D

Y Normalized lateral soil pressure, p/s_uD

Figure A.19 — Full degrading p-y model [18]

Back-analysis of centrifuge test data in normally consolidated clay (see Figure A.19 b)) shows that a complete description of the evolution of soil resistance under cyclic loading can be described by a model in Reference [183] comprising the following components:

— a hyperbolic model per Formula (A.47) for the backbone curve;

— a power law model per Formula (A.48)) for unload-reload cycles;

— a stiffness degradation model per Formula (A.49) describing the reduction in stiffness with increasing numbers of loading cycles N.

$$\frac{P}{s_u D} = \frac{K_{max}}{1 + f K_{max}(\Delta y/D)}(\Delta y/D) \tag{A.47}$$

$$\Delta P = R_f K_0 (\Delta y/D)^n s_u D \tag{A.48}$$

$$R_f(N + 1/2) = R_f(N)\left[1 + \left\{0{,}5R_f(N)\right\}^{1/t}\right]^{-t} \tag{A.49}$$

The stiffness reduction factor R_f equals 1 for N=1/2 and is updated after each half-cycle, i.e. after each load reversal. This permits analysis of varying amplitudes of cyclic displacement Δy_{cyc} during unloading versus reloading. Thus, the stiffness degradation component of the model can accommodate decaying motion and purely random motion. This approach to describing stiffness degradation under cyclic loading follows the approach presented in References [181] and [182] for describing elemental soil stiffness degradation during cyclic loading.

The model employs five input parameters: K_{max} and f to describe the initial stiffness and curvature of the backbone curve, K_0 and n to describe the unload-reload loop, and a stiffness degradation parameter t, which is a function of cyclic displacement magnitude $\Delta y_{cyc}/D$. The first four parameters are depth-dependent. Table A.6 shows parameters [183] derived from centrifuge test data on a 0,914-m diameter pile in a normally consolidated kaolin test bed subjected to 500 loading cycles having a displacement amplitude at the pile head equal to 0,05 D, where D is pile diameter. Applied loading in this case was symmetric, i.e. cyclic loading was applied with zero initial displacement offset. Reference [183] presents input parameters derived for other conditions of applied loading and initial offset.

Figure A.20 a) illustrates the procedure for evaluating the parameter t in Formula A.49 from stiffness degradation data for a given cyclic displacement magnitude Δy_{cyc}. Figure A.20 b) shows a compilation of fits to experimental data for various cyclic displacement magnitudes Δy_{cyc}. These data are derived from centrifuge tests in soft clay having applied pile head displacements of 0,025 D (M1) and 0,05 D (M2). For actual implementation into a numerical model, the t versus Δy_{cyc} shown in Table can be expressed in tabular form.

The parameters given in Table A.6 and Table A.7 have been derived from centrifuge testing simulating fatigue loading (≤0,05 D) on a 0,914-m diameter pile. While Formulae (A.47) to (A.49) can be applicable to larger cyclic motions, the model parameters require re-calibration.

Table A.6 — Degrading *p-y* model parameters for soft clay

Depth z/D	Backbone curve		Cyclic unload-reload	
	K_{max}	F	K_0	n
0	688	0,136 2	62,37	0,653 3
1,04	2 351	0,226 5	24,13	0,348 9
2,07	2 867	0,219 5	25,57	0,331 6
3,11	3 326	0,146 8	62,77	0,442 5
4,15	3 957	0,101 1	131,84	0,522 1
5,19	4 912	0,081 6	245,90	0,586 5
6,23	5 331	0,074 9	333,60	0,621 2
7,27	3 059	0,060 0	640,79	0,750 1
8,31			1 180,01	0,823 0
9,34			1 500,00	0,907 5

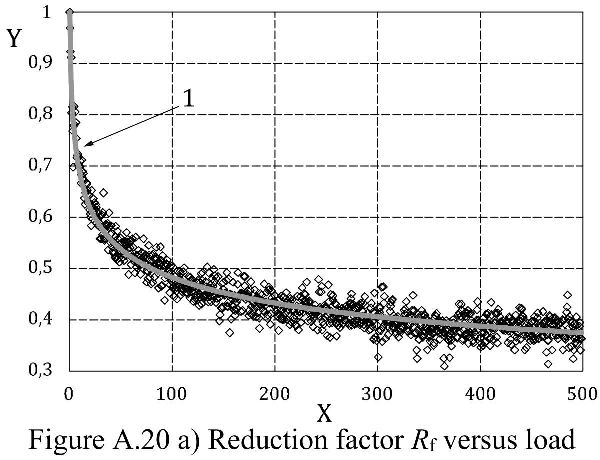

Figure A.20 a) Reduction factor R_f versus load cycle

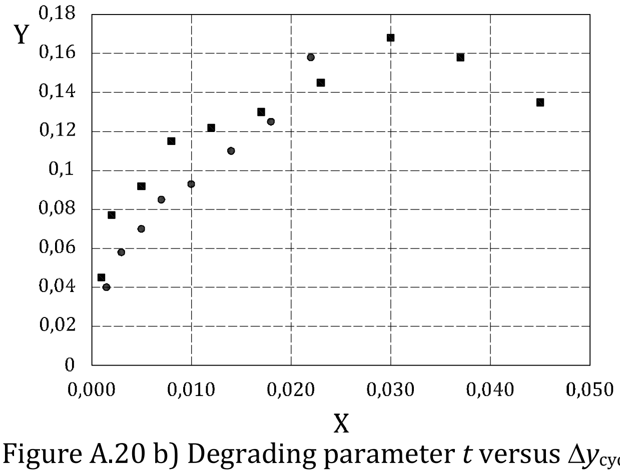

Figure A.20 b) Degrading parameter t versus Δy_{cyc}

Key

1 Model

X Load cycle N

Y Soil resistance reduction factor, R_f

Key

X Cyclic displacement Δy_{cyc}

Y Degradation factor t

Figure A.20 — Conceptual diagram of seabed stiffness

Table A.7 — Degradation parameter t versus cyclic displacement magnitude $\Delta y_{cyc}/D$

Dy_{cyc}/D	t
0	0
0,002	0,04
0,003	0,058
0,005	0,07
0,007	0,085
0,010	0,093
0,014	0,110
0,018	0,125
0,022	0,158
0,05	0,158

A.10.5.4.3 Sands

No additional guidance is offered.

A.10.5.5 Geotechnical considerations in conductor driving analysis

A.10.5.5.1 General

Adequately predicting and mitigating tip damaging and the propagation of tip indents/buckles of conductor pipes driven in very dense sands, cemented soils, weak rock or in presence of boulders is a critical design issue, as the wall thickness and tip annulus area of conductor pipes are generally smaller than for foundation piles, thus increasing this risk, and any damage at pile tip will render well drilling impossible. Recommendations in this respect are provided in subclause.

Driving closely spaced and relatively flexible conductor pipes can generate risks of interaction complicating the subsequent drilling operations. One option that can be considered is the installation of conductor pipes with inclined shoes so that some conductor pipes deviate away from the adjacent pipes. The installation of conductor pipes with inclined shoes is described in this subclause.

A.10.5.5.2 Conductor pipe installation

The process involving conductor pipe installation is similar to pile driving. Pile installation considerations are described in 8.7.12. Some additional guidance specific to conductors are provided in this subclause.

A.10.5.5.3 Minimum wall thickness

A.10.5.5.3.1 General

The minimum wall thickness requirements for piles can be insufficient to mitigate the risk of local over-stressing for conductors. For instance, wall thickness values as small as 14 mm (~0,55 in) to 16 mm (~0,63 in) are generally not acceptable for 0,762 m (30 in) to 0,914 m (36 in) diameter conductor pipes.

A.10.5.5.3.2 During driving

The following is recommended for implementation during conductor pipe driving:

a) The allowable maximum driving stresses as estimated from wave formula analyses should possibly be decreased to less than 80 % to 90 % of the yield strength in the following cases (often associated with larger uncertainties):

— use of steam or diesel hammers instead of hydraulic hammers;

- maximum driving stresses not predicted at or close to pipe head (e.g. above the driving shoe or close to the pile tip);
- presence of hard driveable layers (with noticeable tip reflection ratio, i.e. ratio between reflected and incident stress wave).

b) The wave formula analyses undertaken to predict the driving stresses should take into account soil variability, particularly to simulate the effect of local harder layers/pockets at pile tip.

c) For foundation piles, the total stress during driving should be estimated at any point along the conductor pipe and should include the driving stress, the weight of the hammer assembly and the bending stresses due to inclination of the conductor pipe/hammer as well as due to conductor pipe deviation.

A.10.5.5.4 Driving fatigue

Driving fatigue assessment for conductor pipes follows the same guiding rules as for driven piles, particularly if the sections are welded.

If the conductor pipe segments are connected by means of mechanical connectors, larger stress concentration factors (SCF) can possibly be applicable. The applicable SCF should be defined by the manufacturer.

A.10.5.5.5 Conductor tip damage and buckling

A.10.5.5.5.1 General

The potential to damage the tip of the conductor pipe as well as to propagate any potential damage during driving should be verified. The risk is considered highest in the following conditions:

- in presence of very dense sands, cemented soils, very weak rock or boulders;
- for the case of drive-drill-drive installation sequences, after drilling when driving is resumed (without soil support on the inside of the conductor pipe);
- at shallow depth or when the shaft resistance is small compared to the end bearing resistance.

Although the results of wave formula analyses give some insight into the potential of pile tip overstressing during driving, this type of analysis remains a 1D analysis that does not properly capture the potential for localized buckling.

A.10.5.5.5.2 Damage during driving

Lateral and near vertical point loading actions that can cause local damages, evaluated using upper bound theory for an assumed plastic hinge mechanism, are presented in Reference [3]. These formulae were verified by means of 3D elastoplastic finite element analyses.

The dynamic point loading actions acting locally on the conductor pipe tip during driving should be evaluated and compared to the loading actions that can cause damage. This requires some assumptions to be taken regarding the proportion of the conductor pipe annulus hitting a harder layer or an obstacle, such as a boulder, and the static resistance to be overcome (for a boulder, this will be the force required to either push the boulder into the surrounding soil or split the boulder, whichever is less). Wave equation analyses simulating the selected scenarios either in a 1D traditional wave equation model or a dynamic 3D FE model will then be performed. An example of wave equation model of a large diameter pile hitting a boulder is presented in Reference [175], which provides:

- A stiffness criterion based on the ratio conductor pipe diameter/wall thickness and the elastic moduli of soil and pile. This allows verifying whether the soil elastic response is stiffer than the one of the pile. Otherwise, any inwards pile deformations will spring back and recover elastically.

— A strength criterion as a function of the wall thickness and the soil strength. There should be enough pressure from the soil acting on the initial small damaged area of the pile tip to cause further yielding of the steel.

If the high-level evaluation indicates a potential for damage/imperfection propagation, a numerical model simulating pile extrusion, such as presented in Reference [128], may be implemented.

A.10.5.5.6 Installation with inclined shoes

To reduce the risk of interaction of closely-spaced conductor pipes, the peripheral conductor piles can be deviated away from the group. Installing an inclined (bent) driving shoe will allow creating a tendency for the pile to deviate in a particular direction. Predicting the path followed by the conductor pipe during driving is necessary so that the lateral deviation can be controlled.

As conventional beam-column theory will not be applicable in this case. Reference [336] describes a simple finite difference model to predict the path of a bent shoe during driving, extending the equations presented in Reference [274] for deviation of curved/bent piles. The parameters acting on the deviation of the pile are the axial tip and side resistance of the pile, the lateral soil resistance, and the length and inclination of the driving shoe, with the latter three parameters having most effect.

A.10.5.6 Geohazards for well installations

A.10.5.6.1 Mass transport complexes

Proper identification and geotechnical characterization of mass transport complexes (MTC) that will be penetrated by conductors is necessary to assess the performance of conductors with respect to installation and field service. MTCs can exhibit different strength characteristics than conformable deposits, which can affect installation and performance of the conductor.

A.10.5.6.2 Excess pore water pressure

Pore water pressure in the seabed soils is typically hydrostatic. In some geological settings, excess pore water pressures can exist. Reference [124] provides a brief review of these settings. The presence of unconsolidated sediments and *in situ* pore water pressures that exceed hydrostatic values constitutes a hazard to the well drilling equipment and operational crews. It is recommended for site characterization to include evaluation of excess pore water pressure for well installation purposes.

A.10.5.6.3 Earthquake ground motion

Ground motions caused by earthquakes will induce additional actions on the conductor. These actions can be evaluated during integrity analyses considering that the conductor BOP stack and other appurtenances respond as a single degree of freedom. *P-y* curves for soil-structure interaction should consider the cyclic nature of the loading action as well as its relatively larger magnitude compared to motions caused by other environmental actions, such as currents.

Because permanent wells and their conductors are unattended, the magnitude of the ground motions for integrity analyses does not have to follow the considerations in ISO 19901-2, which apply for fixed steel structures and fixed concrete gravity structures for which exposure incorporates first and foremost life safety, with secondary consideration for environmental exposures caused by system failures, and economic losses to the owners and operators. Subsea field architectures that only include subsea gathering and distribution systems and structures, present no direct exposure to human life. For this reason, the decision to incorporate earthquake actions are typically designed with consideration given to mitigation and prevention of hydrocarbon releases and tolerable levels of damage.

Tolerable levels of damage include consideration of costs associated with production down time and schedule, and costs for replacement and rehabilitation of damaged facilities. An example of an evaluation of tolerable levels for hydrocarbon releases used by industry in the Gulf of Mexico is provided in Reference [152].

A.10.6 Foundation design for riser towers – general

A.10.6.1 General

No further design guidance is offered.

A.10.6.2 Foundation options

No further design guidance is offered.

A.10.6.3 Loading actions and safety factor

No further design guidance is offered

A.10.6.3.1 Loading actions

No further design guidance is offered

A.10.6.3.2 Recommended safety factors

No further design guidance is offered

A.10.6.4 Soil design parameters

No further design guidance is offered

A.10.6.5 Design challenges

A.10.6.5.1 General principles

In the design of riser tower foundations in uplift, the following aspects should be considered:

a) penetration and retrieval;

b) holding capacity including long-term uplift capacity;

c) long-term displacement;

d) soil reactions to be used for the structural design

More information on these design aspects can be found in References [197], [13], [79], [88] and [109].

The capacity should be checked both for the permanent actions and for the sum of permanent and cyclic actions. If the cyclic actions are small compared to the permanent actions, the permanent actions condition can be critical because the strength can be smaller for this condition than for the condition where the cyclic actions are included.

The undrained shear strength for the permanent actions should be reduced to account for long term creep effects (see e.g. References [227], [219] and [335]). For sustained loading action due to loop currents that are expected to last several days up to two weeks, it is recommended to apply a strength reduction factor of 20 % on the undrained shear strength. The same 20 % reduction is recommended for long-term permanent actions.

The effect of pore pressure redistribution and swelling should also be considered, since this can lead to reduction in effective stresses and undrained shear strengths, and hence reduce the capacity under transient wave loading action [219]. In cases where the permanent action acts for many months or more, it can also be necessary to consider whether drained or partially-drained conditions can develop, and the extent to which full base suction can be maintained. References [88] and [94] show that the capacity of a typical suction caisson of depth to diameter ratio between 4 to 6 under a sustained loading action in normally to slightly over-consolidated clay can be only about 70 % of the capacity for a rapid loading action. This reduction, however, only considers the loss in reverse end bearing (base suction). An additional reduction in undrained shear strength of 20 %, should also be considered. Therefore, the reduction in base suction should include both the reduction in shear strength and the reduction from drainage for base suction. Numerical analyses with specific geometries and soil conditions will provide better estimates of the potential reductions from drainage long term creep effects.

Drainage and pore pressure redistribution can also influence the undrained shear strength under cyclic loading actions, but the shear strength for the sum of permanent and cyclic loading actions will be higher than for the permanent loading actions due to rate effects (see e.g. Reference [9]).

The potential of gapping for suction caissons along the wall above stiffeners or sections with increased wall thickness should be evaluated. In cases with ring stiffeners, it is necessary to evaluate the potential of trapped water between ring stiffeners (see e.g. Reference [13]). If gapping or trapped water is possible, the effect that such gaps will have on the drainage path and resistance due to lack of contact along the wall should be considered.

The capacity of suction caissons can depend on passive underpressure inside the caisson that contributes to reverse end bearing (REB). If REB is relied upon, proper sealing can be critical, especially for the part of the underpressure generated by long period environmental actions, such as loop currents. If the anchor top valve seals cannot be guaranteed, either a back-up cap behind the valves or a monitoring program should be considered to assure the desired integrity over the lifetime of the suction caissons. Seepage simulations through an unsealed valve can be conducted to evaluate the effect of a leak on bearing capacity. If proper sealing is not ensured, the suction caissons should be designed to resist sustained uplift action without taking REB into account, or with a reduced REB taken into account allowing for the effect of leakage. If REB is not taken into account, the capacity is calculated from the skin friction of the inner and outer walls with appropriate adhesion factors. The increase of capacity with time and the REB capacity with closed versus open top are described in A.11.5.2.2.4 and A.11.5.2.2.7.

Sustained permanent tension and creep fatigue for long periods of several years or more was further assessed in Reference [197], which showed the drainage effect in relation to phenomenon known as stress relaxation around the pile perimeter. The effect of drainage can result in increased soil strength and foundation capacity. The tests also showed that the magnitudes of time effects on soil strength increase with increasing water content and plasticity and presented governing relationships for creep behaviour.

A.10.6.5.2 Assessment of effect of sand layers on suction anchors

A simple seepage check on drawdown of a suction pile with the tip in sand layer is recommended. The calculated flow should ensure that the vertical displacement of the pile for the duration of the peak dynamic action remains small and within the elastic range of soil plug load-displacement response.

As illustrated in Figure A.21, the discharged water flow, Q, can be calculated by:

$$Q = \frac{2\pi kH}{Ln\left(\frac{r_1}{r_2}\right)}\frac{p}{\gamma_w} \qquad \text{(A.50)}$$

where

k	is the coefficient of permeability of sand layer;
H	is the sand layer thickness;
p	is the applied underpressure;
r_1	is the radius of the suction anchor;
r_2	is the radius of influence soil under suction, which is typically about 5 times the anchor radius;
γ_w	is the water unit weight.

Using Formula (A.50), the flow across the suction pile for the duration of the peak dynamic action can be calculated, from which the potential uplift of the suction plug can be calculated. This will determine if the vertical displacement is sufficiently small to ensure that suction anchor stability remains satisfied.

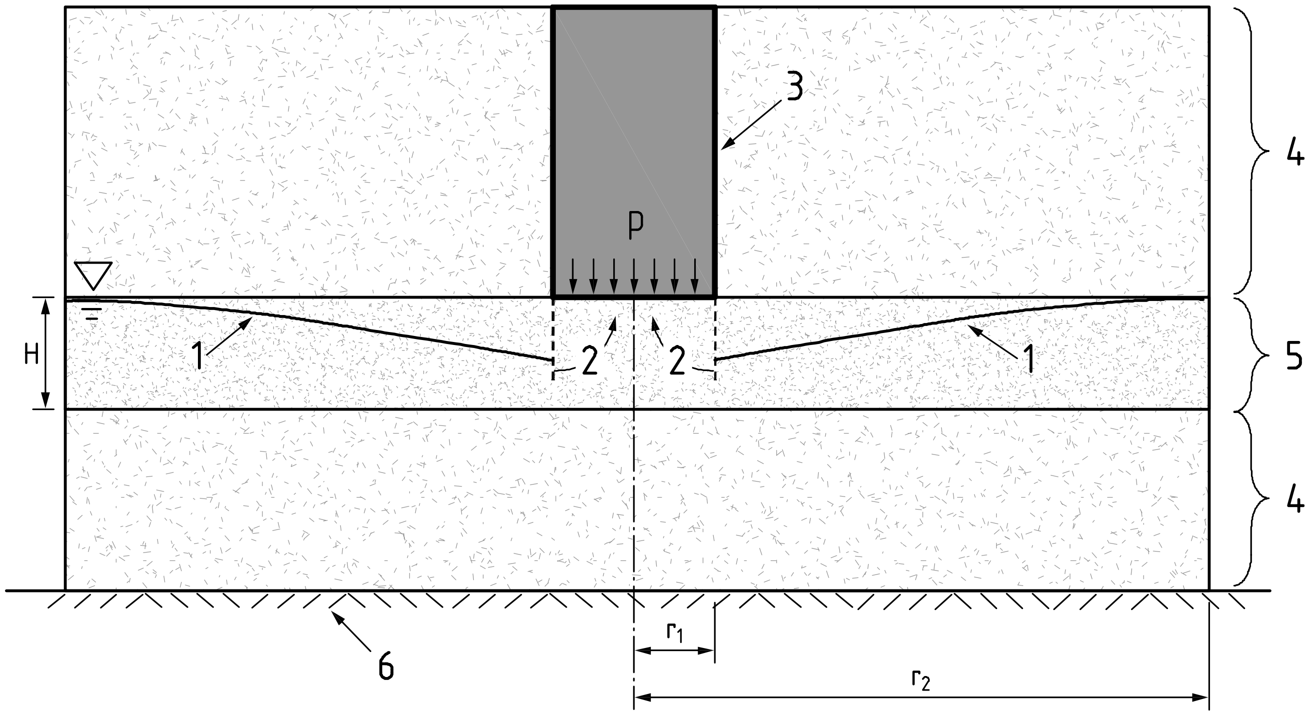

Key

1	Drawdown	H	sand layer thickness
2	Flow, Q	p	applied underpressure
3	Suction pile	r_1	radius of suction anchor
4	Clay layer	r_2	radius of influence soil under suction. Typically, about 5 times the anchor radius
5	Sand layer		
6	Top of impervious layer		

Figure A.21 — Illustration of water flow in sand layer below a suction pile under tension

A.10.6.6 Inspection and monitoring

An inspection program should be considered as integral part of the foundation design. The inspection program should include the use of instrumentation to monitor critical aspects of the foundation performance, during both installation and operation.

If at any time during the service life of the structure, the inspection program reveals conditions, or behaviour, which are detrimental to the integrity of the foundation or structure, maintenance or remedial action should be carried out, as necessary.

A.10.7 Geotechnical design for flowlines and pipelines

A.10.7.1 General

Pipeline design considers ultimate and fatigue limit states related to the stresses in the pipeline and the movements of the associated end connections, including sections that transition into a catenary riser or lift off the seabed into a termination assembly.

Geotechnical analysis leads to estimates of pipeline embedment and the force–displacement response in the axial and lateral directions. The simplest axial and lateral pipe–soil interaction (PSI) model comprises limiting friction factors for each direction of movement, while more complex models capture features, such as the accumulation of soil berms beside the pipe during cyclic motion.

In PSI calculations, the vertical pipe-seabed contact force during operation should be assumed equal to the submerged weight of the pipe and contents over the main length of a pipeline, remote from end or inline connections. It should be considered whether an alternative assumption or model is more appropriate in the following situations:

a) close to where pipelines terminate at a point of fixity;

b) along very short pipelines (e.g. spools); or

c) where pipelines are supported on crossings or by buckle management structures.

Examples are given in Reference [57].

The method of estimating PSI parameters can be refined over the project development depending on project drivers, as highlighted in Figure A.22. More detailed data and models generally lead to narrower design ranges of PSI parameters. The potential influence of PSI parameter uncertainty on design outcomes and project costs for different aspects of pipeline design is discussed in Reference [359].

Detailed advice on methods of geotechnical PSI analysis is provided in the SAFEBUCK Guideline and DNV F114 Recommended Practice (see References [307], and [111]and [377]).

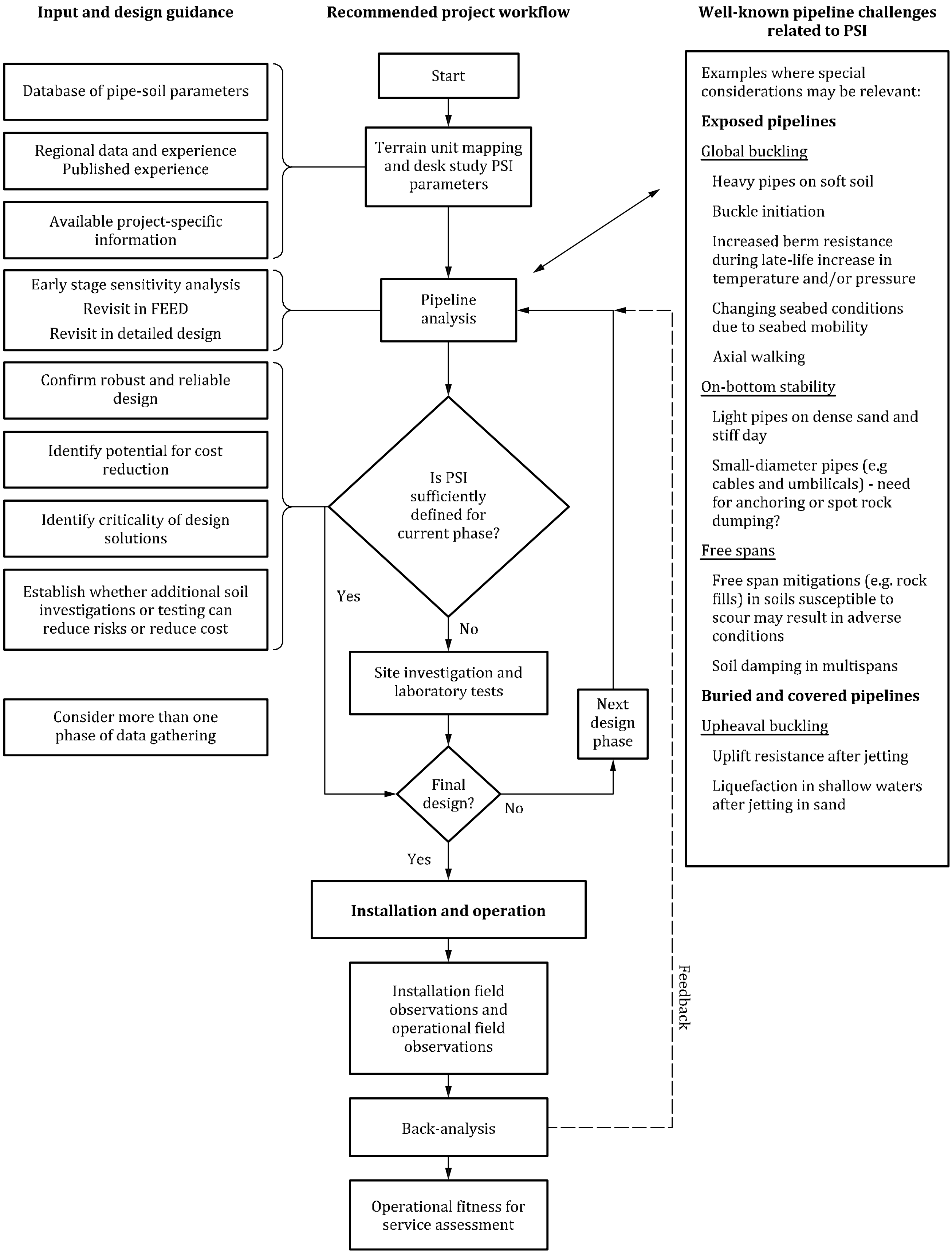

Figure A.22 — Example of pipe-soil interaction workflow during a project (based on Reference [111])

A.10.7.2 Actions on pipelines

The geotechnical PSI analysis should consider all applicable actions on the pipeline, because they affect the rate, duration and frequency of loading, and therefore the resulting soil response.

The actions and motions imposed during laying govern the pipeline embedment at the start of operation and initial in-service performance. The actions on a pipeline after laying include hydrodynamic or thermal loading, internal and external pressure and changes in self-weight from changes in contents, including rapid cycles of changing weight from slug flow. An element of pipeline can also be subjected to actions from adjacent sections of pipeline including a connected catenary riser, and from end connections.

Accumulation of axial movements (pipeline 'walking') can occur due to operating cycles of internal pressure and temperature, which can affect external connections. Where walking leads to increased compressive axial forces, a risk of lateral buckling of the pipeline arises. A pipeline can also be susceptible to external loading from debris flows and turbidity currents that arise from submarine slides and snag or impact loading from foreign objects.

A.10.7.3 Soil reaction forces

A.10.7.3.1 Pipeline–soil interaction models

The geotechnical PSI analysis should provide PSI parameters that fully define the PSI response for the type of pipeline analysis being undertaken. For example, for initial design, the pipe–soil response can be represented solely by limiting values of axial or lateral pipe–soil resistance, or by bi-linear elastic – perfectly plastic behaviour in the axial and lateral directions. The pipe-soil response can be incorporated into a structural model of the pipeline by attaching pipe–soil model elements at intervals along the pipeline. This approach is analogous to the *t*–*z* and *p*–*y* action transfer methods of analysing pile response.

The limiting pipe–soil resistance is typically expressed as an equivalent friction factor applied to the effective pipeline weight. However, axial and lateral friction factors are not intrinsic soil properties, but are affected by other parameters, such as the embedment and the drainage condition, with the latter depending on the duration (or rate) of loading or movement and cumulative consolidation of the seabed over the operational life.

To capture more complex effects of interaction, particularly the large displacement behaviour, additional aspects of the response can be modelled, including brittle break-out behaviour and cyclic berm growth during lateral movement, as shown in Reference [63].

A.10.7.3.2 Low, best and high estimates of soil and PSI parameters

The geotechnical PSI analysis should consider best estimates and also both low and high estimates of all soil parameter inputs, since the low and high estimate pipe-soil resistance forces do not necessarily result from the corresponding extreme inputs. Also, for different design aspects, either high or low pipe-soil resistance can be most onerous, as illustrated in Figure A.23 for lateral buckling and walking. The selection of soil parameter inputs should follow the guidance in 5.3.

Suitable test methods for determining soil strength parameters are described in ISO 19901-8. Additional advice on the determination of near-surface soil parameters for pipeline design is discussed in References [348] and [171]. PSI analysis has a particular requirement for pipe-soil interface strength properties, which are discussed in A.10.7.5.

To consider the full range of PSI parameters, the geotechnical PSI analysis can be performed deterministically (e.g. by combining 'best' or 'worst' combinations of parameters in individual calculations), or probabilistically (by considering the statistical distribution of input variables, e.g. via a Monte Carlo method as described in Reference [357]). Since deterministic approaches cannot correctly capture the likely range of PSI resistance (see e.g. Reference [357]), probabilistic approaches are more reliable.

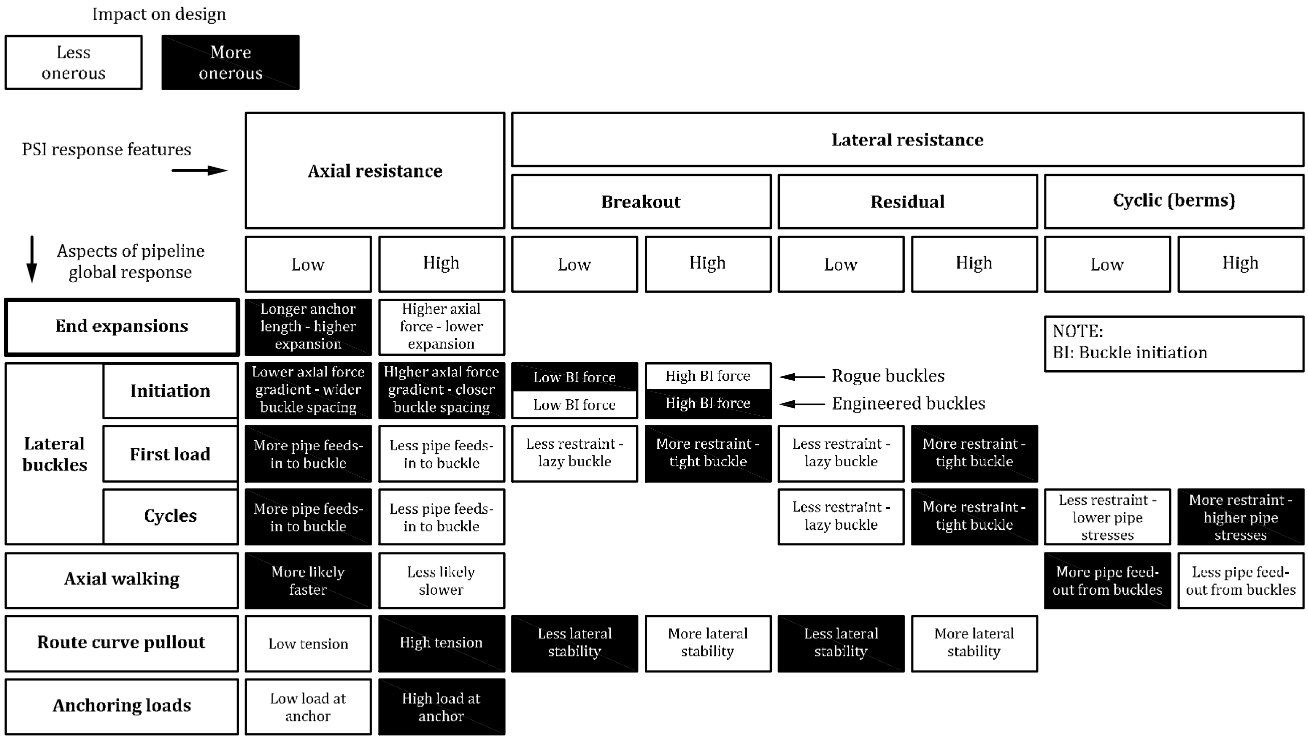

Figure A.23 — Design impact of low and high values of PSI resistance (based on Reference [111])

A.10.7.3.3 Drained and undrained behaviour during pipe-soil interaction

In fine-grained sediments, pipeline laying is usually an undrained process. Dissipation of the lay-induced excess pore pressures typically takes days or weeks. Lateral pipeline movements in response to hydrodynamic action or thermal expansion generally involve undrained deformation, although consolidation between events can cause disturbed soil to regain strength. Axial pipeline movements can be drained or undrained in fine-grained soil since the relevant drainage distances are shorter than for lateral movement.

In coarse-grained sediments, pipeline installation and operation will generally occur under fully drained conditions. In intermediate soils, such as silts, silty sands and silty clays, it can be necessary to consider both drained and undrained conditions.

In a design analysis, the anticipated durations of axial and lateral pipeline movement or loading should be compared with the relevant rates of consolidation to establish whether drained, undrained or partially-drained conditions will prevail. It can be necessary to perform analysis of both short and long duration pipe movements relative to the soil consolidation to bracket the expected range of PSI parameters.

Approximate durations are provided in Reference [160] for consolidation under vertical or lateral pipeline loading, and in References [297] and [367] for axial pipeline movement. Key values of dimensionless time, T_{50}, for 50% dissipation of pore pressure are provided in Table A.8. The dimensional time, t_{50}, is calculated from T_{50} using the coefficient of consolidation, c_v, and pipe diameter, D. This time can be compared to the duration of a loading or movement event, t_{event} to estimate the relevant drainage condition(s). Since the transition between undrained and drained conditions spans approximately a factor 100 in time, if $t_{event} > 10t_{50}$, then drained conditions can be assumed, and if $t_{event} < t_{50}/10$, then undrained conditions can be assumed [160], [367]. For the intermediate range, both undrained and drained conditions can be considered, or a more detailed analysis can be performed to justify a narrower range of conditions.

Table A.8 — Consolidation periods during pipe-soil interactions (based on References [160], [297] and [367])

Dimensionless time, $T_{50} = c_v t_{50}/D$	T_{50}
Vertical loading	0,1
Lateral loading	0,02
Axial loading	0,005

A.10.7.4 As-laid pipeline embedment

A.10.7.4.1 Introduction

In strong but mobile soils, such as sands, the as-laid embedment will initially be a small fraction of the diameter, but can be subject to change during the operational life if sediment transport occurs (see A.10.7.7). For softer seabed conditions, such as lightly over-consolidated clays, carbonate muds and silts, the as-laid embedment is usually stable with time.

On a hard or rocky seabed, the embedment of a pipeline is negligible. Instead, the available pipe-soil resistance is controlled by the friction coefficient of the pipe coating – hard soil / rock interface, and for lateral pipe movement the local slope, or ruggedness, of the hard soil / rock surface has a strong influence (see Reference [165]).

A.10.7.4.2 Static penetration resistance

In undrained conditions, the vertical resistance, V, of a pipeline penetrating into undrained soil should be calculated as the sum of two resistance terms, one related to the shear strength at invert level $s_{u,invert}$ and one representing the buoyancy force due to the submerged unit weight, γ', of the displaced soil:

$$\frac{V}{D} = a s_{u,invert} \left(\frac{w}{D}\right)^{b} + f_b \left(\frac{\gamma' A'}{D}\right) \quad \text{(A.51)}$$

where

D is the pipeline diameter;

w is the pipe invert penetration;

A' is the embedded cross-sectional area of the pipe (see Figure A.24).

The constants a and b vary with the shear strength profile and the pipe-soil roughness, and a cut-off function improves accuracy at shallow depths (for $w/D < 0{,}1$), as discussed in References [289], [290], [246] and [34]. The buoyancy factor, f_b, represents enhancement of the buoyancy force due to soil heave around the pipe.

Values of $a \sim 6$, $b \sim 0{,}25$, and $f_b = 1{,}5$ can be used, in the absence of site-specific or more advanced analysis.

For drained conditions, estimation of pipeline embedment is more uncertain due to the influence of soil density and dilatancy as well as the friction angle. Experimental observations show an approximately linear relationship between penetration resistance divided by pipe diameter and embedment, when a pipe is pushed vertically into the seabed (see e.g. Reference [381]).

The drained penetration resistance can be estimated directly from the CPT profile (see e.g. Reference [352]) or bearing capacity calculations can be used by analogy with a strip foundation (see e.g. Reference [111]).

The long-term embedment of a pipeline laid on coarse-grained soils is often controlled by sediment transport, particularly in shallow waters, where seabed currents and wave action are significant (see A.10.7.7).

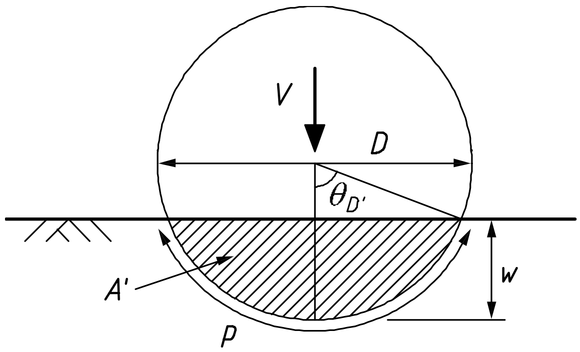

Figure A.24 — Pipeline embedment notation

A.10.7.4.3 Static lay effect: force concentration at touchdown point

The static force concentration at the touchdown point should be estimated using the following approach, in the absence of site-specific or more detailed analysis.

For a pipeline of submerged weight (per unit length) W', the maximum vertical action V_{max} within the touchdown zone is a function of the pipeline bending stiffness EI, the horizontal component of near-seabed lay tension T_0, and the seabed stiffness k (defined as the ratio of penetration resistance to embedment, V/w, in units of modulus or kN/m/m). V_{max}/W' should be estimated as described in Reference [289]:

$$\frac{V_{max}}{W'} \approx 0{,}6 + 0{,}4\left(\frac{EIk}{T_0^2}\right)^{0{,}25} \tag{A.52}$$

This relationship is accurate in the range $T_0^{1{,}5}$ / $((EI)^{0{,}5}\, W') > 1$, with progressively greater over estimation of V_{max} for lower values.

A.10.7.4.4 Dynamic lay effects

Metocean conditions, vessel motion, changes in pipeline tension and hydrodynamic loading of the hanging pipe will induce a combination of vertical and horizontal motion of the pipeline at the seafloor during laying. Even small lateral or vertical movements can cause disturbance, local softening and erosion of the seafloor in the touchdown zone, increasing the pipeline embedment.

The duration that an element of pipe is exposed to these motions at the seafloor depends on the lay rate and the length of the touchdown zone. Interruptions in laying, or poor metocean conditions, can lead to deeper local embedment of the pipe, while rapid lay, such as during the final lay-down of the suspended catenary, will lead to reduced embedment, as shown in References [352] and [350].

The geotechnical PSI analysis should use the fully remoulded strength profile as input into Formula (42) to allow for dynamic lay effects in estimating the as-laid pipeline embedment in undrained conditions. Formulae (42) and (43) are then solved simultaneously, iterating where necessary.

This use of the fully remoulded strength has been validated from many field observations to be accurate, on average, as described in Reference [359]. In general, this experience is based on the remoulded strength being determined from the last cycle of a cyclic T-bar penetrometer test carried out consistent with the recommendations in ISO 19901-8, which indicates that the test should involve ten cycles unless no further degradation is evident over three or more cycles.

The use of this strength value can underestimate the embedment during periods of high swell or downtime during lay, while overestimating it during benign conditions or during final lay-down of the pipeline catenary (see e.g. References [351] and [352]) or for soils that do achieve repeatable T-bar resistance within ten cycles. Therefore, the geotechnical PSI analysis should also consider the potential impact that a wider range of undrained strength will have on the as-laid embedment and the subsequent pipeline response.

Field observations of pipeline embedment after laying are valuable to validate designs and to allow pipeline response predictions to be updated, as shown in References [324] and [209].

For projects where the embedment can have a critical influence on one or more pipeline limit states, centrifuge model tests with detailed simulation of the lay process can be used to reduce the as-laid embedment uncertainty, as described in Reference [353] and [145].

A.10.7.5 Axial soil resistance

The geotechnical PSI analysis should assess the axial pipe-soil resistance using a method based on the framework shown in Figure A.25, reflecting recent research and practice (see References [356], [320], and [172], and the summary provided in Reference [359]). The method is outlined as follows.

Axial pipeline movement involves shear failure at or close to the pipe-soil interface. The submerged pipe weight, W', controls the normal stresses at the pipeline–soil interface. The normal force, N, from the integrated normal contact stresses around the pipeline periphery exceeds the vertical contact force due to the curved shape of the pipe surface. The resulting wedging factor, $\zeta = N/V$ defines the resulting enhancement of the normal force by this wedging effect, and varies with embedment as described in Reference [354]:

$$\zeta = \frac{N}{V} = \frac{2\sin\theta_{D'}}{\theta_{D'} + \left(\sin\theta_{D'}\cos\theta_{D'}\right)} \quad \text{for} \quad \frac{z}{D} \leq 0{,}5, \quad \zeta = 1{,}27 \quad \text{for} \quad \frac{z}{D} > 0{,}5 \tag{A.53}$$

with the pipe-soil contact half-angle $\theta_{D'}$ (in radians) given by:

$$\theta_{D'} = \cos^{-1}\left(1 - \frac{2z}{D}\right) \tag{A.54}$$

In drained conditions, the steady (‘residual’) axial resistance (or traction) T_{res} is controlled by the large-displacement interface friction angle, δ_{res}, enhanced by the wedging effect. Laboratory tests show that δ_{res} varies with stress level and interface roughness (see References [256], [51] and [348]). The drained residual axial resistance, $T_{res,d}$, expressed as a friction factor, $T_{res,d}/W'$, is:

$$\frac{T_{res,d}}{W'} = \zeta \tan\delta_{res} \tag{A.55}$$

In undrained conditions on soft normally-consolidated (or lightly over-consolidated) clay that has fully remoulded during pipe lay, it can be assumed that the pre-consolidation pressure of the surficial soil contacting the pipe is controlled by the pipe weight, if this weight has been applied to the seabed for sufficient time for the soil to consolidate. Using this assumption, a SHANSEP or Cam clay-type model can be used to assess the undrained residual axial friction factor, $T_{res,u}/W'$ as described in Reference [12]:

$$\frac{T_{res,u}}{W'} = \zeta R_{nc} OCR^{m} = \zeta \left(\frac{s_{u-int-res}}{\sigma'_{v0}}\right)_{nc} \left(\frac{W'_{max}}{W'}\right)^{m} \tag{A.56}$$

The parameter $R_{nc} = (s_{u\text{-int-res}}/\sigma'_{vo})_{nc}$ is the normally-consolidated interface undrained strength ratio, at large displacements. The index parameter, m, is equivalent to the plastic volumetric strain ratio in Cam clay or the SHANSEP over-consolidation index. The apparent overconsolidation ratio, OCR, is the ratio between the previous maximum pipe weight (e.g. when flooded for hydrotesting), W'_{max} and the current pipe weight, W'. This reflects the level of over-consolidation and therefore enhanced strength created by any previous elevated pipe weight, and is applicable if that elevated weight was sustained for sufficient time for full consolidation. If partial dissipation has occurred, a fraction of this change in strength can be relied on. The parameter, m, is typically in the range 0,5 to 1. The interface strength parameters, δ, R_{nc} and m, depend on the soil and interface type.

The interface model parameters should be measured in low stress interface shear box tests, as described in References [356] and [51], or via shallow penetrometer devices (see References [366] and [310]). The drained parameter, δ, can alternatively be measured via tilt table tests (see Reference [256]). As an alternative to site-specific testing, databases of other relevant testing can be used to estimate these parameters, such as Reference [348], but the uncertainty is likely to be greater.

Values of key interface strength parameters for soft clays from the database of Reference [348] are shown in Table A.9. These can be applicable for initial design estimates in the absence of site-specific data, but should be confirmed during the design process via site-specific testing.

Table A.9 — Database values of pipe-soil interface properties (from Reference [348])

	Normally-consolidated residual interface undrained shear strength ratio $\left({s_{u,int,res}}/{\sigma'_{no}}\right)_{nc}$	**Drained interface strength ratio** $\tan(\delta_{res})$
Low estimate (P10) value	0,22	0,34
Best estimate: median (P50) value	0,33	0,50
High estimate (P90) value	0,46	0,89

As described in A.10.7.3.3, the relevant interface drainage condition should be considered. This depends on the duration of the pipe movement and any history of previous movement. In clay, it is common that the primary consolidation period exceeds the duration of any startup or shutdown event, so movements are undrained. However, full consolidation occurs during the intervening operational period. In sands, it is common that consolidation occurs more rapidly than the mobilization of axial resistance, so fully drained conditions apply throughout. If consolidation occurs concurrently with continuous pipe movement, it leads to a transition in axial resistance from undrained to drained values that can be quantified by the period required for 50 % of this transition, t_{50} (see Figure A.25 as well as A.10.7.3.3).

For soft clays, consolidation between movements leads to contraction and an increase in undrained strength. This process of 'consolidation hardening' causes the axial resistance to rise towards the drained value over several cycles, as observed in model tests (see Reference [320]), and *in situ* SMARTPIPE tests at the seafloor (see Reference [38]), as well as being replicated in coupled numerical analysis (see Reference [367]). Field observations of pipeline walking and expansion behaviour appear to confirm a build-up in axial resistance over the operating life of pipelines laid on soft clays and silts, as reported in References [171] and [142].

The geotechnical PSI analysis should consider the potential for consolidation hardening and adopt design values of axial friction that encompass any range of axial friction created by consolidation hardening over the design life. If consolidation hardening is expected to occur, the design undrained axial friction can be defined on a cycle-by-cycle basis, converging towards the drained value with increasing cycles (such methods are provided in References [355] and [111]). Alternatively, a simpler approach, but which will lead to a wider range of pipeline responses, is to consider design cases that span the full range of axial friction for the entire life, i.e. ensure the design is acceptable if the initial undrained resistance applies for the full design life, and also for the drained value to apply for the full design life.

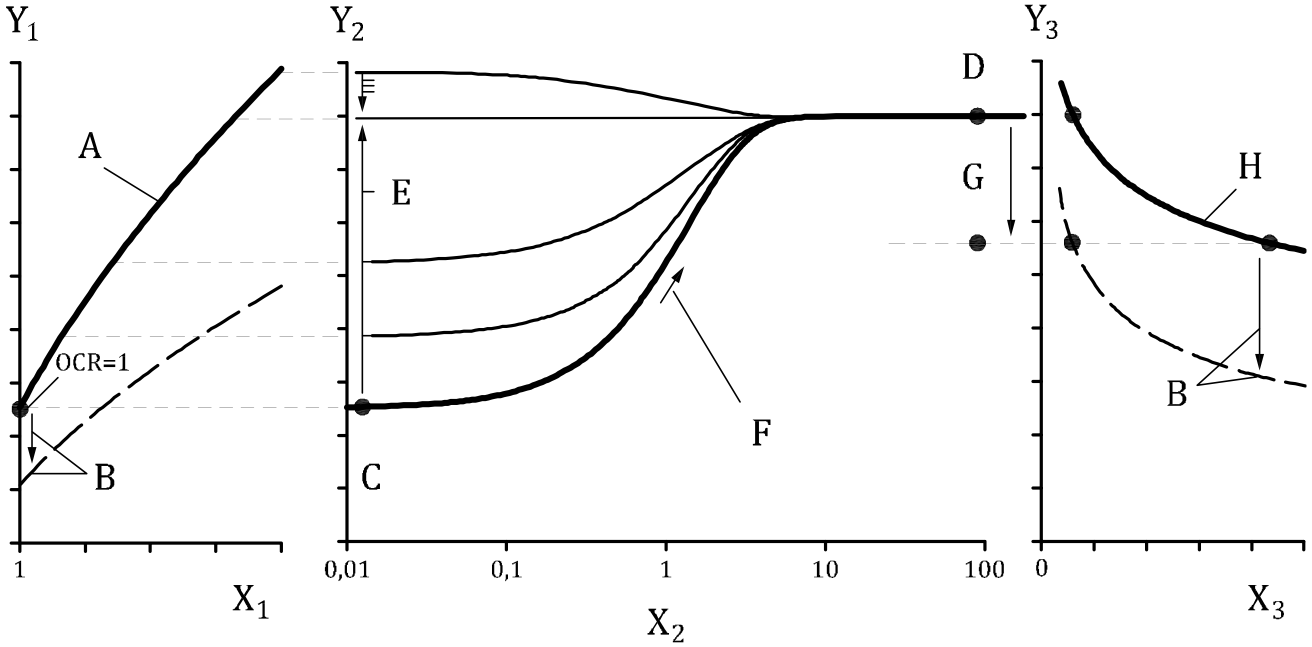

Key

X1	Pipe-induced over-consolidation ratio, OCR = W'_{max}/W'	A	Effect of OCR on $s_{u,int,res}$
Y1	Undrained limit, $T_{res,u}/W'$	B	Lower pipe roughness
X2	Consolidation time, t/t_{50} (or elapsed time to pipe movement)	C	Undrained limit, $T_{res,u}/W'$
		D	Drained limit
Y2	Residual axial friction, T_{res}/W'	E	Transition to critical state (i.e. condition at which $T_{res,d}$ = $T_{res,u}$) due to cycles of sliding and consolidation
X3	Average normal pipe-soil stress, $\zeta W'/p$	F	Transition to drained conditions due to consolidation during axial movement
Y3	Drained limit, $T_{res,d}/W'$	G	Higher stress or lower roughness
		H	Effect of stress level on δ_{res}

Figure A.25 — General model for residual axial pipe-soil resistance (from Reference [359])

A.10.7.6 Lateral pipe-soil resistance

A.10.7.6.1 General

Lateral pipe–soil resistance during break-out and large amplitude cyclic movement is influenced by the embedment of the pipeline, the vertical loading acting on the pipeline, the soil properties and the history of previous movements.

In undrained conditions, two characteristic types of large amplitude lateral response can occur depending on the pipe weight, characterised by the ratio W'/s_uD for undrained conditions. For 'light' pipes (with values of W'/s_uD below about two), the pipeline tends to rise after breaking out from its initial position. The lateral resistance reaches an initial breakout value (H_{brk} in Figure A.26 a)) before reducing to a residual resistance (H_{res}) where the pipeline sweeps horizontally with a berm of soil being pushed ahead of the pipe.

Subsequent cycles of lateral movement lead to a steady increase in the restraint provided by the increasing size soil berms deposited at the end of previous cycles and any further embedment into the seabed (see Figure A.26 b)), which can be important for accurate modelling of pipeline fatigue (see Reference [63]).

For values of W'/s_uD greater than about two ('heavy' pipes), the pipeline typically embeds further after the initial break-out resistance is mobilised. This increasing embedment, coupled with the growth of a soil berm adjacent to the pipe, leads to a steady increase in the lateral resistance (see Figure A.26 b)).

In drained conditions the 'light' pipe type of response is observed.

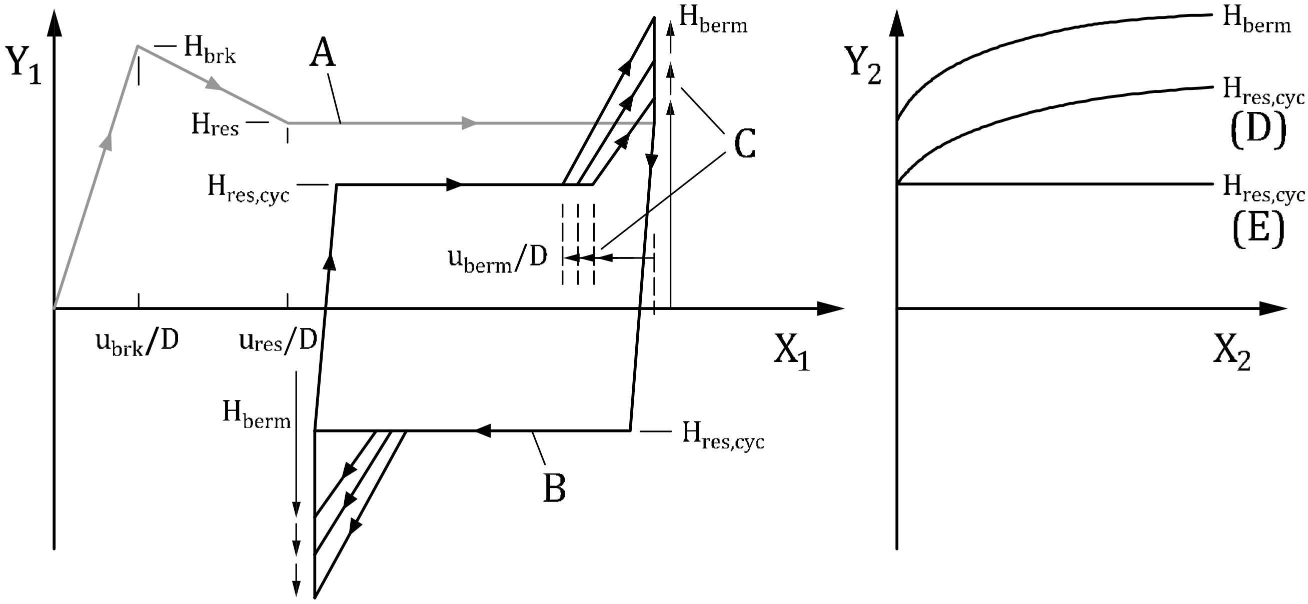

(a) Typical load-displacement response

(b) Typical cyclic evolution of resistance components

Key

X_1	Lateral displacement, u/D	A	First load response
Y_1	Equivalent lateral friction, H/W'	B	Cyclic response
X_2	Cycles of lateral displacement, N	C	Berm resistance and extent increase with cycles
Y_2	Equivalent lateral friction, H/W'	D	'Heavy' pipe
		E	'Light' pipe

Figure A.26 — Large amplitude cyclic lateral pipe-soil responses (from Reference [359])

A.10.7.6.2 Monotonic lateral resistance parameters

The lateral PSI parameters, H_{brk}, and H_{res}, can be estimated using theoretical yield envelopes or empirical expressions.

Yield envelopes for predicting H_{brk} define limiting combinations of vertical and horizontal pipe-soil resistance. The approach is similar to the methodology given in A.7.7.1 for shallow foundations. For undrained conditions, yield envelopes for shallowly-embedded pipelines are given in References [290], [245], [246] and [232]. For drained conditions, yield envelopes for shallowly-embedded pipelines are given in References [381] and [338]. For more complex soil strength profiles, project-specific numerical analyses can be performed using finite element software or similar.

Empirical expressions for lateral PSI parameters have been developed from model testing in drained conditions (see e.g. Reference [345]) and undrained conditions (see e.g. Reference [359]). These methods generally express H_{brk} and H_{res} as the sum of components that vary with pipe weight ('friction') and soil strength ('passive'). Since the expressions evolved from distinct sets of model tests, they can be reliable only for the conditions for which the model tests were performed.

Empirical expressions for lateral PSI parameters are subject to significant uncertainty and their relevance should be established for a particular design situation. Since the expressions evolved from distinct sets of model tests, they can give erroneous results outside the conditions for which the model tests were performed. It is therefore necessary to confirm, on a case-by-case basis, whether the design inputs (pipeline and soil parameters) are within the range of the data that underlies any empirical expression for lateral PSI parameters.

High calculated values of H_{brk}, i.e. significantly above unity, can be ignored if it is demonstrated that they are not relevant because a buckle will not initiate from loading in the horizontal direction. In the situation of $H_{\text{brk}} > 1$, the flowline can buckle upwards initially. In this case, the resistance to motion is the pipe submerged weight, which is equivalent to a friction factor of 1,0. A cap of 1,0 may be applied on H_{brk} if it is shown that the likely pipeline buckling mode is upwards rather than lateral, such that an upwards buckle offers lower resistance than a lateral buckle. The as-laid out-of-straightness in the vertical and horizontal direction influences the likely buckling mode, as well as the soil resistance to movement in each direction.

A.10.7.6.3 Advanced aspects of lateral PSI response

The geotechnical lateral PSI analysis should consider whether standard calculation models for pipeline embedment and axial or lateral resistance (see e.g. References [111] and [307]) are able to adequately capture the pipe-soil interaction behaviour in non-standard conditions. Such conditions can include:

- unusual site-specific soil strength profiles or layering;
- partial drainage;
- cyclic lateral movement and the build-up of additional resistance in soil berms;
- pipeline responses close to structures or within spools;
- a high variation in embedment over short distance of pipeline (e.g. free spans);
- regions of pipeline that are affected by sediment transport or scour (see A.10.7.7).

Potential analysis methods to adopt in these conditions are discussed in References [57], [359] and [349].

A.10.7.7 Sediment transport and scour

If the geotechnical PSI analysis identifies that seabed mobility can occur, the design process should assess the potential impact on pipeline limit states.

If the seabed is mobile, scour beneath a pipeline can form a free span. The suspended sections of the pipeline can sag into the scour hole, or sufficient length of the pipeline can be undermined to cause the remaining span shoulders to fail in bearing due to the pipe weight, resulting in lowering of the pipeline relative to the seafloor. Sediment can also be deposited around the pipe. A consequence of these processes is that the pipeline embedment can evolve with time and free spans can form and remain stable or can evolve, migrate or be eliminated (see References [104], [330] and [210]).

Spans can be subjected to vortex-induced vibration leading to fatigue, greater exposure to submarine slides and a change in the hydrodynamic stability (see e.g. References [210] and [211]). Scour and sediment transport can also affect the pipeline behaviour at engineered buckles due to the evolving embedment and resulting changes in lateral resistance.

Scheduled monitoring of scour and sediment transport can form part of a design strategy for limit states that evolve gradually over time such that intervention is possible if required (e.g. fatigue and pipeline walking). Observations of existing nearby pipelines can be useful to quantify the likely behaviour of new pipelines.

Laboratory techniques to quantify the erosion properties of natural seabed sediment samples are described in References [60] and [248]. Methods for assessing the likelihood of scour and sediment transport and the subsequent changes in embedment are described in References [330], [122] and [123]. Techniques for assessing the condition of pipeline free spans are outlined in Reference [113]. Mitigation methods, such as rock dumping and other stabilisation methods, can be used to rectify unacceptable free spans.

A.10.7.8 Damping from pipeline-seabed interaction in free span analysis

Pipeline free spans or slugging-related issues for a pipeline bridging over a sleeper require assessment for fatigue potential. The stiffness and damping provided by the soil supports can have a significant influence on the fatigue rate. Reference [113] provides practical advice on the assessment of free span behaviour. Recommendations of soil damping ratio in Reference [113] are provided based on soil classification (clay – for three consistencies from very soft to hard; sand – loose, medium or dense) and free span length. Damping ratios from 0,5 % to 3 % are specified, increasing with soil stiffness and reducing with span length.

In contrast to these recommended levels of damping, recent work discussed in Reference [334] has shown significantly higher damping levels for a partially embedded pipe on the seafloor in very soft clay. Their results were obtained by modelling a 0,3 m (1 ft.) diameter pipe embedded 0,25D, varying the amplitudes and frequencies of motion to determine both hysteretic and radiation damping ratios. The analyses considered both types of damping and a combination rule proposed to determine the sum of both components (see Figure A.27).

The results indicated very significant and greater levels of damping versus what is usually considered in design, including the advice in Reference [113]. For example, for loading periods from 0,1 s to 1 s (1 Hz to 10 Hz), the damping ratio from radiation damping alone was about 0,2. For very long loading periods (100 s), where radiation damping is negligible, the damping ratio ranged from about 0,22 to 0,38 for displacements ± 0,006D to ± 0,04D.

Preliminary sensitivity analyses have been performed to assess the potential impact of these high damping ratios on the fatigue of a pipeline span. The pipe diameter considered was 0,46 m (18 in) while the span length was about 50 m. The results show significantly reduced displacements at the shoulders and mid-point of the span for higher damping levels. In addition, about a 15 % to 25 % reduction in the stress range at the mid-span was observed for damping ratios greater than 20 %. This level of stress reduction will increase fatigue life or allow longer acceptable span lengths.

Analyses similar to those performed by Reference [334] can be used to define appropriate damping ratios for other conditions.

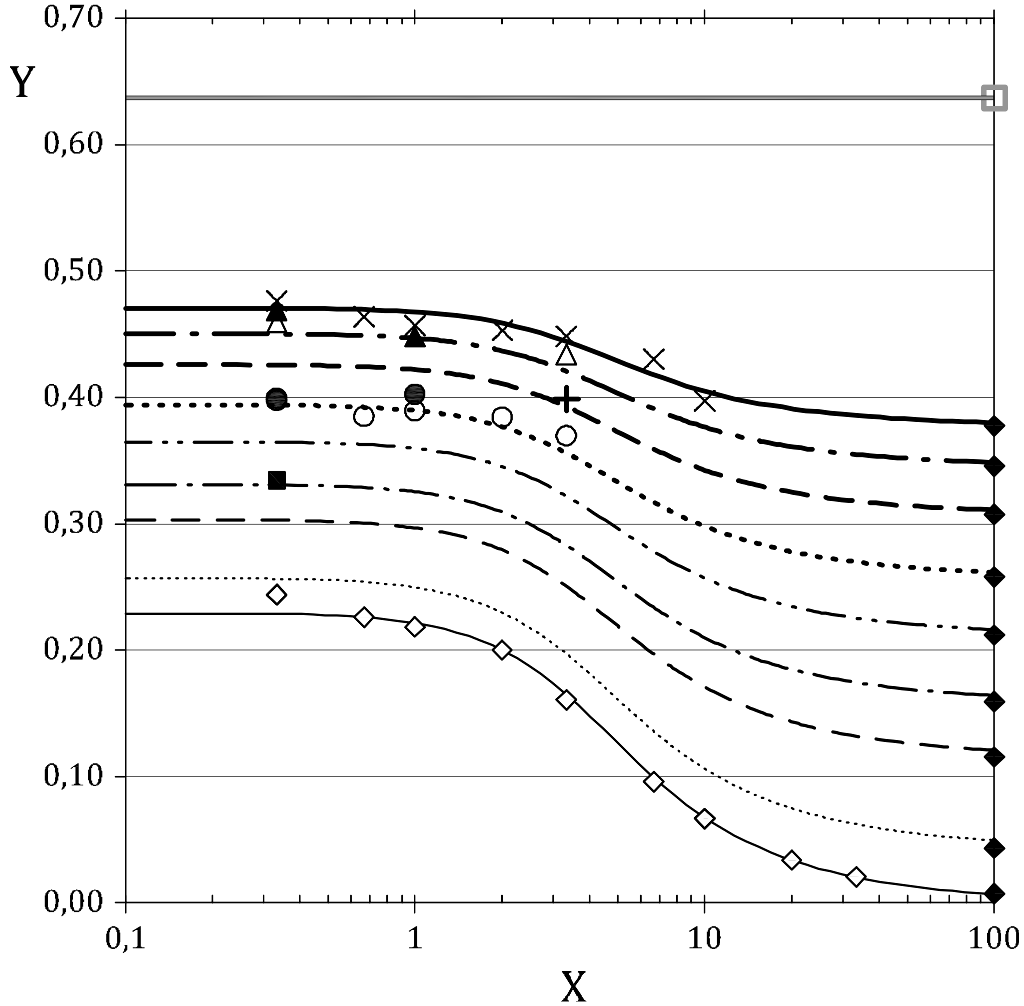

Key

X	Normalized period, T/T*	✚	FEA (exp), 0,02
Y	Damping ratio (combined), D	○	FEA (exp), 0,01
□	Theoretical maximum material hysteric damping	●	FEA (std), 0,01
═══	Maximum combined damping	■	FEA (std), 0,004
───	Comb. Damp. Rule, SA displ./dia.=0,04	◆	FEA (std), material hysteric damping only
— · —	0,03	D	$D_{hyst} + a \times D_{rad}$
— — —	0,02	D_{hyst}	Material hysteretic damping ratio
·······	0,01	a	Fraction of energy not dissipated by material hysteresis
— · · —	0,006	D_{rad}	Radiation damping
— · —	0,004	Displ./dia	Displacement / pipe diameter
— — —	0,003	FEA	Finite element analysis
·······	0,002	EXP	Explicit solution
───	0,000 2 or less (radiation damping only)	SA	Single amplitude
◇	FEA (exp) radiation damping only	STD	Standard (implicit) solution
✕	FEA (exp), single amplitude displacement/pipe diameter =0,04	T	Period
△	FEA (exp), 0,03	T*	100 * pipe diameter / shear wave velocity
▲	FEA (std), 0,03		

Figure A.27 — Damping ratios for 0,3 m diameter pipe resting on seafloor (from Reference [334])

A.10.7.9 Submarine slides and density flows: simulation and pipeline impact analysis

A.10.7.9.1 General

This subclause sets out a recommended procedure for the simulation of submarine slides and density flows (both referred to as 'flows' here) and the resulting pipeline impact analysis following the steps listed in 10.7.2.

A.10.7.9.2 Rheology characterization

Characterization of flow materials is typically carried out using a rheometer. Flow characteristics of soils can be described using non-Newtonian rheological models, such as the Herschel-Bulkley model, which can be expressed using either fluid mechanics (Formula (A.57) or geotechnical notation (Formula (A.58), as:

$$\tau = \tau_y + K\dot{\gamma}^n \tag{A.57}$$

$$s_{u,op} = s_{u0}\left[1 + \eta\left(\frac{\dot{\gamma}}{\dot{\gamma}_{ref}}\right)^{\beta}\right] \tag{A.58}$$

where

τ_y (or s_{u0}) is the yield stress or strength at very low or zero strain rate γ,

K is a (dimensional) 'consistency' parameter,

η is a dimensionless viscosity parameter, while n (=β) express the dependency of strength on strain rate.

τ and $s_{u,op}$ both represent the mobilized or apparent shear stress (strength). The alternative forms of Formulae (A.57) and (A.58) are fully interchangeable and achieve the same objective of a rate dependent mobilized 'strength' of the flow material (see e.g. References [52], [225], [226] and [99]). Selecting the reference strain rate $\dot{\gamma}_{ref}$ to match the strain rate in conventional geotechnical element tests allows data from different tests to be combined.

The parameters in Formulae (A.57) and (A.58) should be estimated through laboratory testing that covers the relevant range of strength, shear strain rate and moisture content. Using a vane-in-cup rheometer in accordance to ASTM D2196 [31] is recommended for high strain rate testing. It is recommended to conduct the rheology tests at soil temperatures representing the site conditions for a range of moisture contents.

A.10.7.9.3 Flow simulation

Simulation of the run-out process of a submarine slide or flow can be performed numerically using techniques of varying complexity. It is common for depth-averaged Eulerian models to be used, with the slide running out over a 3D bathymetry (see References [344], [323], [260], [230] and [184]). More complex analyses, using computational fluid dynamics or a large deformation finite element method, can also be used to simulate slide behaviour, as shown in References [146] and [120].

Analyses of submarine slide and flow behaviour are often calibrated on a site-by-site basis, using relic slides that are identified from the bathymetry, geophysical data and sample dating (see e.g. References [73], [146] and [230]).

A.10.7.9.4 Mobilized shear strength of slide / flow material

In assessing the impact force on a pipeline, the relevant flow velocity v is the *relative* velocity between the moving density flow (or soil) and the pipeline. This is important for conditions where a flow might engulf a pipeline and carry it forward until such point where equilibrium is achieved between the forces exerted on the pipeline by the decelerating flow and the structural forces induced in the deformed pipeline. Appropriate values of operational shear strength need to be assessed, taking account of the strain rate dependency of soil stiffness and shear strength. The nominal shear strain rate in the soil flowing around the pipeline, $\dot{\gamma}$, is expressed as:

$$\dot{\gamma} = f\frac{v}{D} \tag{A.59}$$

Use f = 1 when calculating $\dot{\gamma}$ to find τ and Re_{nN} to use in the fluids-based approach (Formula (A.61)). Use f = 0,9 when calculating $s_{\mathrm{u\text{-}op}}$ and Re_{nN} to use in the geotechnical-fluid hybrid approach (Formula (A.64)). This difference in definitions of nominal shear strain rate originates from the calibration of each approach.

A.10.7.9.5 Impact forces on pipelines

The forces arising from pipeline-flow interaction, including situations at the onset of a slide, can be estimated analytically using the estimated properties of the flow material. When a flow impacts a pipeline, the force that is applied to the pipeline depends on (i) the inertia (mass density) of the material, which is deflected around the pipe, and (ii) the strength (or mobilized shear stress) within the material, which is deformed as it flows around the pipe. The relative influence of the material inertia and strength depends on a non-Newtonian Reynolds number:

$$Re_{nN} = \frac{\rho v^2}{\tau}\ or \frac{\rho v^2}{s_{u-op}} \tag{A.60}$$

Approaches to estimate impact forces have initially developed from fluid dynamics-based principles where the force is assumed to be generated by fluid drag, with velocity dependent drag coefficients. For values of Re_{nN} greater than 2, drag forces dominate and models based on fluid mechanics alone, with velocity dependent drag coefficients, can be used (see Reference [371]). Subsequently, a combined geotechnical-fluid approach (see References [358], [292], [308] and [222]) was developed using the data presented in Reference [371], which is also suitable at low Re_{nN} where the strength of the debris can dominate the impact force. Both methods are outlined in this subclause. Impact forces can be calculated using both methods, which should yield similar results. In case of a discrepancy, reference should be made to the experimental and numerical dataset given in Reference [371] that underpins the two approaches, and other relevant data, in order to compare the suitability of each calculation method.

The force also depends on the angle of attack of the flow relative to the alignment of the pipeline, θ, where θ = 90° for flow perpendicular to the pipe axis, and θ = 0° for flow parallel to the pipeline.

One of the following expressions for impact forces should be used. Both can be evaluated for comparison, and if there is an unacceptable discrepancy between the methods, then reference should be made to the underlying data to evaluate which approach is most suitable.

a) Fluids-based approach

For the two extremes of attack angle, the pipeline force per unit length, F, is:

$$F_{\theta=90} = \left[C_{D,90}\left(\frac{1}{2}\rho v^2\right)\right]\mathrm{D} \qquad \text{and} \qquad F_{\theta=0} = C_{D,0}\left(\frac{1}{2}\rho v^2\right)D \tag{A.61}$$

where v is the depth-averaged flow velocity over the height of the pipe. For fully-engulfed flow around a pipe, the velocity-dependent drag factors are given by [371]:

$$C_{D,90} = 1{,}4 + 17{,}5\ Re_{nN}^{-1.25} \qquad \text{and} \qquad C_{D,0} = 0{,}08 + \ 9{,}2\ Re_{nN}^{-1.1} \tag{A.62}$$

For a laid-on-seafloor pipeline [371]:

$$C_{D,90} = 1{,}25 + 11{,}0\ Re_{nN}^{-1.15} \tag{A.63}$$

b) Geotechnical-fluid hybrid approach

In the geotechnical-fluid hybrid approach, the impact force for perpendicular attack comprises two terms. The first term relates to inertial loading, with a drag factor, $C_{\mathrm{D\text{-}90}}$, and the second relates to strength loading, with a bearing factor, $N_{p\text{-}90}$. The axial impact force includes an adhesion factor, f_a:

$$F_{\theta=90} = \left[C_{D,90}\left(\frac{1}{2}\rho v^2\right) + N_{p-90}s_{\mathrm{u,op}}\right]\mathrm{D} \qquad \text{and} \qquad F_{\theta=0} = f_{a,0}s_{\mathrm{u,op}}\pi D \tag{A.64}$$

For fully engulfed flow around a pipe, $C_{D,90}$ = 0,6, $N_{p\text{-}90}$ = 11,9 and $f_{a,0}$ = 1,4. Lower values may be used for a smaller depth of soil above the pipe, or if the flow only passes over the exposed upper part of the pipe (see References [232] and [386]).

For general impact angles (0° < θ < 90°), the solutions from Formula (A.61) and Formula (A.64) for an engulfed pipe can be used to derive parallel and perpendicular components of force per unit pipe length [371]:

$$\text{Perpendicular force, } F_{\theta,perp} = F_{\theta=90}\sin\theta \qquad \text{and} \qquad \text{Parallel force, } F_{\theta=0}\cos\theta \tag{A.65}$$

Alternatively, a yield envelope approach can be used to evaluate the normal and lateral force coefficients for a given direction of flow, θ. The envelope can be represented by extending the geotechnical approach above to an envelope of the following form [292]:

$$\left(\frac{N_p}{N_{p-90}}\right)^p + \left(\frac{f_a}{f_{a,0}}\right)^q = 1 \text{ with } N_p = N_{p-90}(sin\theta)^r \tag{A.66}$$

Using Formula (A.66), values of N_p and f_a can be found for general values of θ. Separate loading components in the parallel and perpendicular directions are then calculated by substituting these factors in place of $N_{p\text{-}90}$ and $f_{a\text{-}0}$ in Formula (A.65), and taking v as the normal component, v sin θ. The drag coefficient, $C_{D\text{-}90}$ is replaced for inclined attack to be $C_D = C_{D,90}$ / sin θ (see Reference [292]).

Numerical studies provide guidance on the selection of parameters p, q and r for inclined attack (see References [292] and [222]).

A.10.7.9.6 Additional considerations

Formulae (A.60) to (A.66) are for horizontal drag forces in the flow direction. Vertical forces in the form of gravitational and vortex induced vibrations (VIVs) were also observed in the flume experiments and numerical analyses. VIV can cause fatigue stresses on pipelines. Reference [377] presents the calculated Strouhal number versus the Re_{nN} from the experiments and numerical analyses.

Glide blocks and out-runner blocks are intact pieces of cohesive sediments that depart from the parent flow often due to hydroplaning and stretching. The framework outlined in A.10.7.9.2 and A.10.7.9.3 can also be applied to determine the flow characteristics of such material for simulation while geotechnical approaches are more suitable for estimating the impact forces. Reference [375] provides an example of the determination of flow characteristics and impact forces.

A.11 Geotechnical design of anchors for floating structures

A.11.1 General

This clause provides recommendations for the geotechnical design of anchoring systems for floating offshore structures and mobile offshore units. It is applicable to stationkeeping systems with catenary, semi-taut-line or taut-line moorings. Since there is no ISO document available with respect to vertical tethering (TLP structures), reference is made to API RP 2T [24]. The torpedo anchor of Figure A.33 is another example of a vertically tethered anchor with different design recommendations and safety factors than for a TLP.

The options that are available for anchoring floating structures include:

— drag embedment anchors;

— anchor piles, comprising driven, suction, vibro-driven, jetted, or drilled and grouted piles;

— plate anchors, including drag-embedded, or direct-embedded plate anchors;

— other anchor types, such as gravity anchors and gravity-embedded anchors (free-falling ‘torpedoes’).

Recommended design criteria and ultimate limit state (ULS) design safety factors for anchoring systems are given in ISO 19901-7. In selecting anchor options, soil conditions, required system performance and reliability, installation and the test loading (where relevant) should be considered. The structural strength of anchors and mooring lines should be demonstrated to be adequate with respect to the required anchoring capacities.

The design of the anchoring system should ensure that allowable limits of stress, displacement and fatigue in the anchor, and cyclic degradation in the surrounding soil are not exceeded during and after installation. The anchoring system above the seafloor should include provisions for inspection and maintenance.

A number of design and installation issues for driven piles, suction piles, plate anchors, and gravity-embedded anchors, all of which are capable of resisting vertical forces, are addressed in A.11.5 through A.11.7. These issues include anchor ultimate holding capacity (UHC) evaluation, installation, and pull testing.

Some of the technological aspects of the design of suction piles, plate anchors and gravity-embedded anchors are still under development. Specific and detailed recommendations are given in this clause to the extent possible. General statements are also used to indicate that some particular aspects should be considered, and references are given for further guidance.

A.11.2 Soil investigation

Seafloor and soil conditions should be investigated for the intended site to provide data for the anchoring system design. Details about equipment and procedures for marine soil investigations are provided in ISO 19901-8.

It is recommended to perform a high quality, high-resolution geophysical survey over the entire areal extent of the foundation system. The survey should use geophysical equipment and practices appropriate to the water depth of interest and provide high-resolution imaging of the seafloor as well as detailed stratigraphic information to a reasonable penetration below the zone of influence of the foundation system. The survey should include the mapping and description of all seafloor and sub-bottom features that can affect the foundation system. This survey should be subjected to a realistic geological interpretation so that it can then serve as a guide to develop a scope of work for the vertical and horizontal extent of the geotechnical investigation (i.e. number, depth, and location of soil borings and/or *in situ* tests, such as cone penetrometer tests and CPTU) and to aid in the interpretation of the acquired geotechnical data. Further information on geophysical marine survey is provided in 19901-10.

The stratigraphic data thus obtained should be integrated with geotechnical data collected subsequently, or with existing geotechnical data (if any), to assess constraints imposed on the design by geological features, and to allow for soil data interpolation and/or extrapolation in the event the anchor locations are shifted due to changes in mooring line lengths and/or headings, field layout, platform properties, and mooring leg properties. Guidance about the integration of geophysical and geotechnical data is provided in ISO 19901-10

The sampling and *in situ* testing scope and intervals should ensure that each significant stratigraphic layer is properly characterized. The minimum vertical extent of the site investigation should be related to the expected zone of influence of the actions imposed by the base of the foundation and should exceed the anticipated design penetration by at least the anchor diameter or anchor fluke width. If reverse end bearing (REB) at the suction anchor pile tip is taken into account in the vertical capacity analysis, soil characterization up to three diameters for suction piles or three fluke widths for plate anchors below the design penetration depth is more appropriate. It is critical to ensure that no high-permeability layers are present within the zone influenced by the mobilization of REB, particularly if the anchor is expected to resist long-duration forces, such as those imposed by loop currents.

The content and scope of a deep-water soil investigation should always be tailored to the project-specific conditions. If no previous experience is available for the site, the minimum scope should consist of one boring with alternating sampling and CPTU testing at each anchor cluster. Increasing the number of soil investigation points should be considered, if these boreholes show great vertical and/or lateral variability across the mooring pattern. If high quality geotechnical data already exist in the general vicinity of the anchor pattern and little variation of soil properties is inferred over the areal extent of the foundation, or if extensive experience with the chosen foundation concept in the area can be drawn upon, the above recommendations can be modified as appropriate.

A.11.3 Anchor types

A.11.3.1 Drag embedment anchors

Traditional drag embedment anchors (Figure A.28) were initially used for mobile (temporary) mooring operations. Drag anchor technology has advanced considerably in recent years. Engineering and testing indicate that the new generation of fixed fluke drag anchors develops high holding power even in soft soil conditions. A high efficiency drag anchor is generally considered to be an attractive option for mooring applications because of its easy installation and proven performance. The anchor section of a mooring line can be preinstalled and test loaded prior to floating structure installation.

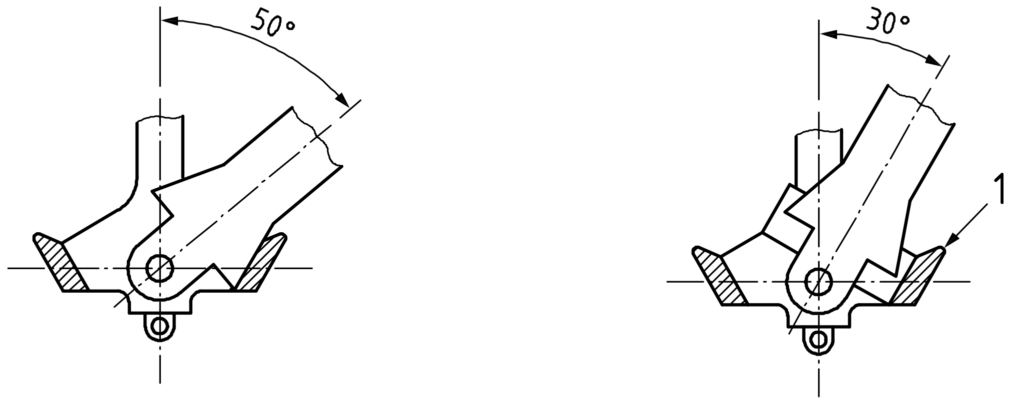

a) Detail view - 50° soft clay seabed **b) Detail view - 30° sand seabed**

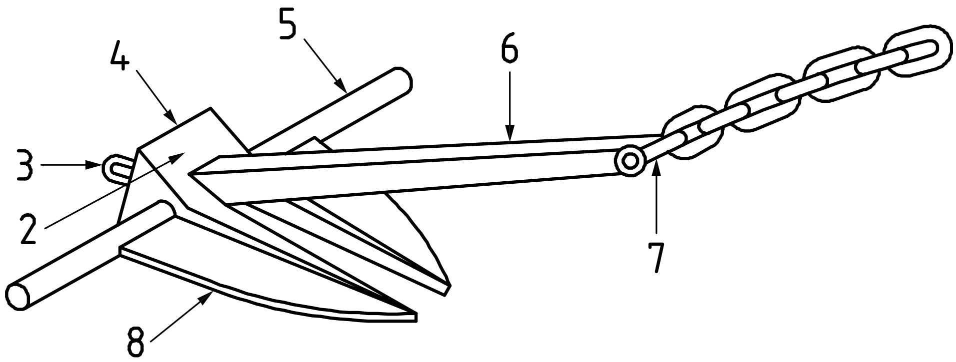

c) General view

Key

1	adapter block	5	stock
2	tripping palm	6	shank
3	crown padeye	7	shackle
4	crown	8	fluke

Figure A.28 — Traditional drag embedment anchor

A.11.3.2 Driven anchor piles

The resistance of a driven anchor pile to uplift and lateral loading is primarily a function of pile dimensions, the manner in which the pile is installed and loaded, and the type, stiffness, and strength of the soil adjacent to the pile. Horizontal capacity can be increased considerably by adding special elements, such as skirts or wings to the pile top. Driven anchor piles can be designed to develop high lateral and vertical resistances, and be very stable over time.

Vibro-driving (see Reference [194]), jetting (see Reference [188]) or drilling and grouting techniques can be considered for other types of anchor piles. Disturbance of soil during vibro-driving, jetting or drilling operations should be evaluated.

A.11.3.3 Suction anchor piles

Suction anchor piles can be used for large deep-water mooring systems and can be designed for very high mooring line tensions. They are typically tall steel cylindrical structures with or without internal stiffener systems. The cylinder unit is open at the bottom and closed at the top (see Figure A.29). A suction anchor pile is installed by first lowering it into the soil to self-penetration depth (i.e. penetration due to the submerged pile weight). The remainder of the required penetration is achieved by pumping the trapped water from the inside of the pile. The differential pressure thus created (generally called 'under-pressure' or 'suction') results in an additional driving force on the anchor top, which drives the pile into the soil. As the penetration increases, the driving force needed normally increases, requiring a gradually increasing differential pressure.

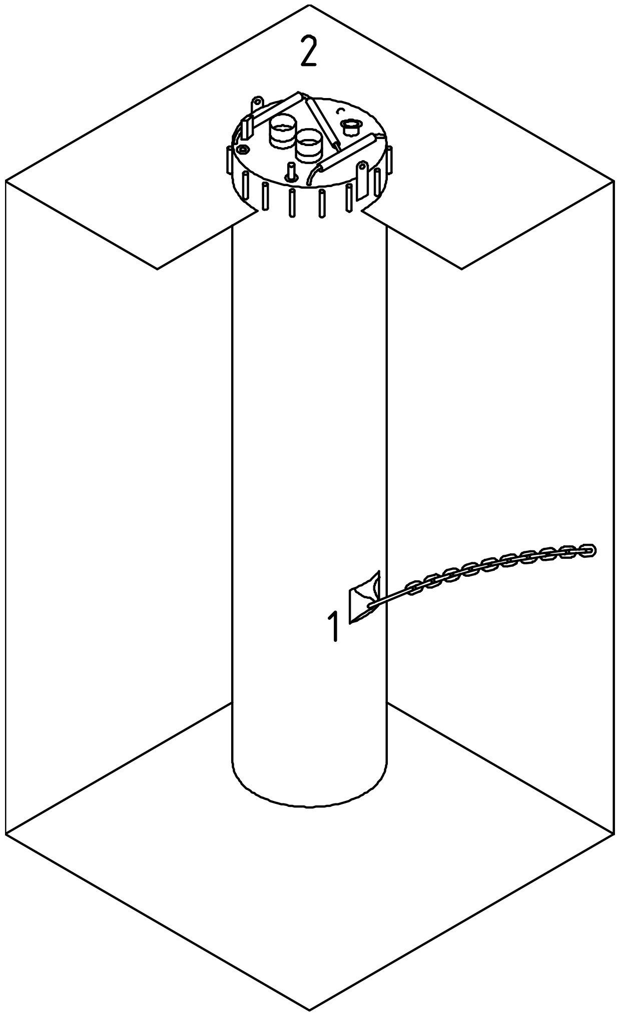

Key

1 padeye

2 anchor top cover with installation aids, venting hatches and anodes

Figure A.29 — Suction anchor pile

After reaching design penetration, the water outlet is closed, allowing the suction anchor pile to achieve substantial capacity to resist horizontal forces, vertical uplift forces, moments and combinations of these.

For suction anchor piles embedded in clay and with a closed outlet, the capacity to resist mooring line tensions is governed by the undrained shear strength of the soil around and beneath the anchor. The capacity depends on depth of penetration, anchor diameter, shear strength of the clay, shear strength at the clay–anchor wall interface, mooring line inclination, and the location of the attachment point. In the case where the top part is left open or retrieved, or for long-term uplift components, pull-out of the anchor can also be a possible failure mechanism.

The holding capacity is generally greater if the anchor pile is prevented from tilting. To avoid tilting, the line attachment point can be lowered from the top of the anchor to a point on the anchor wall at an optimal depth below the seafloor. The location of the optimal line attachment point depends on the shear strength profile, the shear strength at the clay–anchor wall interface, the mooring line inclination, the submerged anchor weight, and the depth-to-diameter ratio of the anchor. The optimal location is typically two-thirds to three-quarters of the length of the anchor pile downwards from the seafloor.

As suction anchors are shallow structures compared with driven piles, deep soil borings are not required, but more detailed soil data are needed at shallow depths than for driven piles. Suction anchors have mainly been applied in cohesive clay type soils. Suction embedment penetration through sand or granular layers is feasible, provided the suction anchor design takes this into account [337]. Penetration into non-cohesive granular type soils requires special considerations which are described in A.11.5.2.2.1.

Suction anchor length-to-diameter ratios can vary from 2:1 for stiff clay soils to as much as 7:1 for very soft clay soils. Suction anchors are often designed with large depth-to-diameter ratios in soft clays since the upper part of soft clay deposits provides limited bearing capacity and skin friction.

A suction caisson is a suction anchor that is relatively shallow in height and is designed for relatively small penetration. The submerged weight of the suction caisson can make up a large part of the anchor's vertical holding capacity. A multi-cell concrete structure with a large footprint and a shallow skirt penetration is an example of suction caisson (see Figure A.30 and Reference [329]). The vertical capacity is derived mainly from its self-weight plus possibly some skin friction and internal suction. Horizontal resistance is generated by skirt penetration and friction between the soil layers subject to shear.

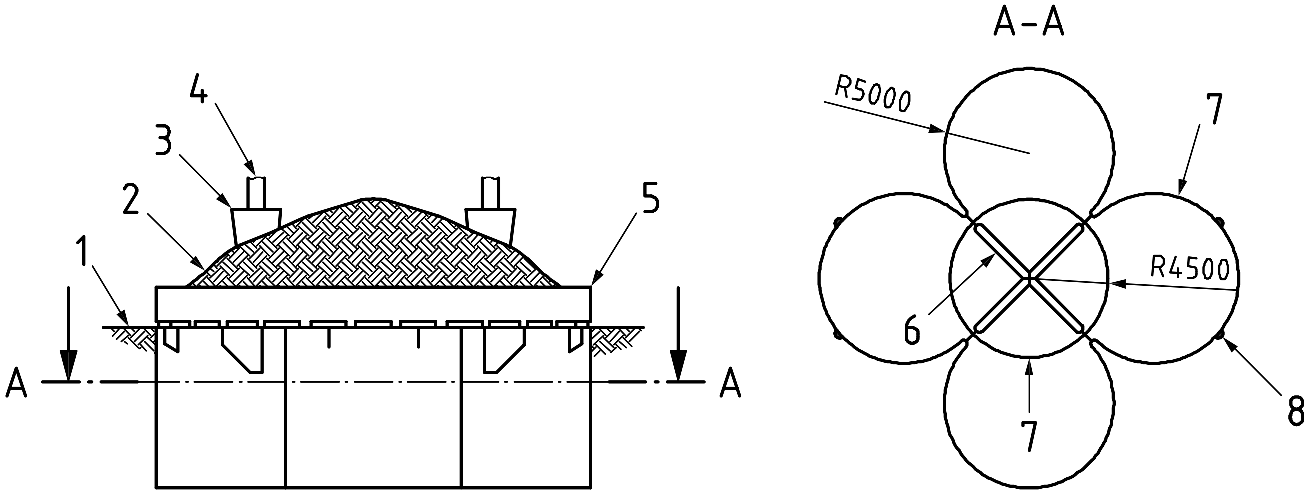

Key

1	seafloor	5	parapet wall
2	iron ore	6	stiffeners (beam)
3	tendon receptacle	7	anchor skirt
4	tendon	8	towing padeye

Figure A.30 — Suction caisson anchor

A.11.3.4 Plate anchors

A.11.3.4.1 General

Plate anchors were initially used by the US Navy for the anchoring of fleet mooring buoys. They are installed at deep penetration beneath the seafloor where the generally higher soil strength allows the use of relatively small plate anchors for high mooring actions. Plate anchors typically have significant vertical holding capacity. This allows the use of taut-leg mooring systems where the anchor line can intersect the seafloor at significant inclinations. Plate anchors can be placed in two broad categories: drag-embedded and direct-embedded.

A.11.3.4.2 Drag-embedded plate anchors

Drag-embedded plate anchors are embedded to deep penetration in a manner similar to drag anchors. During installation, the anchor is first placed on the seafloor, and as the anchor is pulled along the seafloor, it penetrates the soil. Initially, the anchor dives more or less parallel to the fluke, progressively rotating until the target depth is achieved. Following embedment, the anchor fluke is oriented such that it becomes nearly perpendicular to the mooring line and applied loading (a process called ‘keying’ or ‘triggering’), providing high horizontal and/or vertical holding capacity depending on the orientation of the line.

These drag-embedded plate anchors are often referred to as vertically loaded anchors (VLA). Two VLAs are commonly used by the offshore industry: Stevmanta (see Reference [305]) and DENNLA (drag-embedded near normally loaded anchor) (see Reference [141]). The Stevmanta anchor uses a bridle system to convert from its installation configuration to its plate anchor operational orientation whereas the DENNLA anchor uses an articulated shank (Figure A.31).

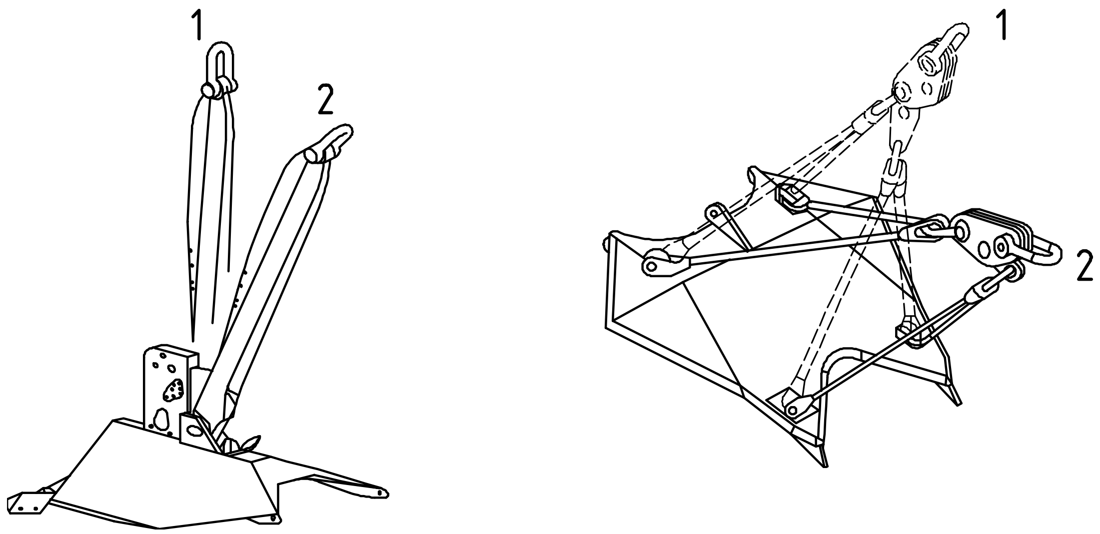

a) Dennla Mk4 **b) Stevmanta**

Key

1 normal (or near normal) loading mode

2 installation mode

NOTE These anchors are examples of suitable products available commercially. This information is given for the convenience of users of this document and does not constitute an endorsement by ISO of these products.

Figure A.31 — Drag-embedded plate anchors (VLA)

A.11.3.4.3 Direct-embedded plate anchors

Direct embedment of plate anchors can be achieved by suction, impact or vibratory hammer, propellant, or hydraulic ram.

Suction-embedded plate anchors have been used for major offshore mooring operations. As an example, the suction-embedded plate anchor (SEPLA) uses a so-called 'suction follower' which is essentially a reusable suction anchor with its tip slotted for insertion of a plate anchor. The suction follower is retracted by reversing the pumping action once the plate anchor achieves its design depth, and can be used to install additional plate anchors (Figure A.32). In the SEPLA concept, the fluke of the plate anchor is embedded in vertical position, and adequate fluke rotation is achieved during a keying process by pulling on the mooring line [362].

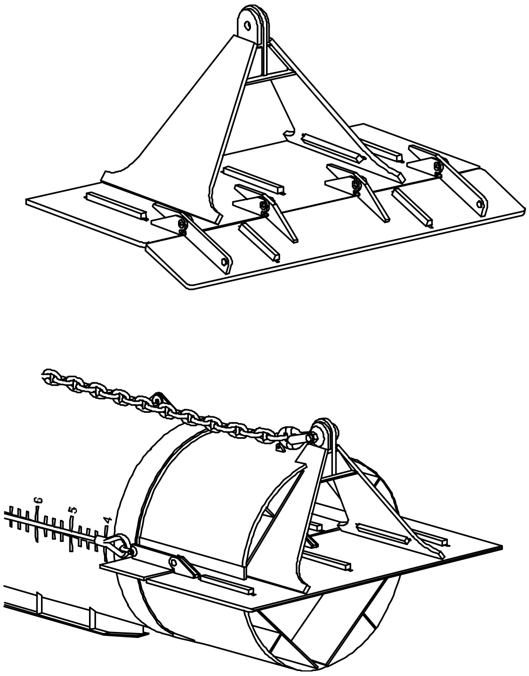

a) Plate anchor

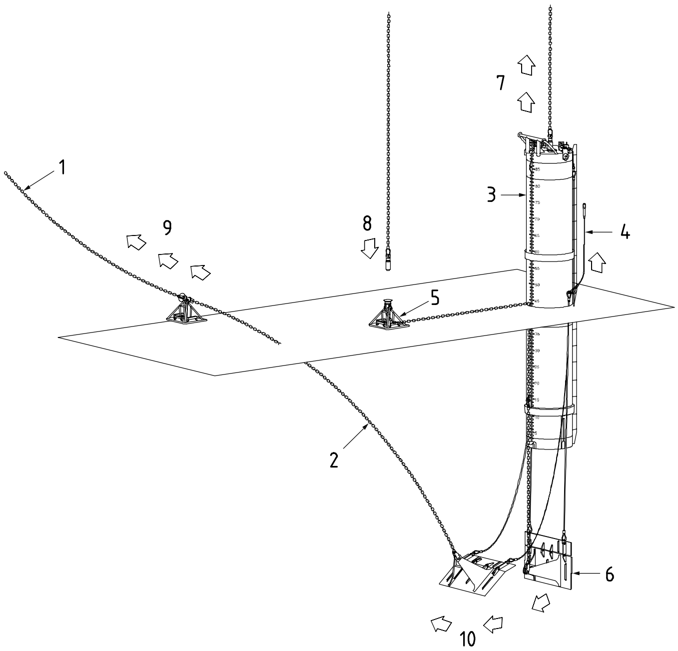

b) Installation

Key

1	mooring line	6	SEPLA anchor
2	forerunner chain	7	recovery of suction follower
3	suction follower	8	docking subsea connector
4	retainer/recovery lines	9	tensioning mooring line
5	subsea connector mudmat	10	keying plate anchor

NOTE This anchor is an example of suitable product available commercially. This information is given for the convenience of users of this document and does not constitute an endorsement by ISO of this product.

Figure A.32 — Suction-embedded plate anchor (SEPLA)

A.11.3.5 Gravity anchors

Gravity anchors are deadweight anchors which commonly consist of concrete or steel blocks, scrap metal or other materials of high density. Their uplift capacity is primarily derived from their own submerged weight. Their horizontal capacity is a function of the friction between the anchor and the soil and of the shear strength of the soil beneath the anchor. Gravity anchors typically require relatively hard seabed conditions to provide sufficient bearing capacity.

Gravity anchors are typically more suitable for small mooring systems in relatively shallow water, where holding capacity requirements are limited and/or where ballast can be added relatively easily to the gravity anchor. Gravity anchors are generally not used for large deep-water mooring systems.

Gravity anchors can be designed with skirts for enhanced horizontal capacity, to improve the bearing capacity (if needed), to mitigate piping below the edges of the structure base induced by rocking motions and to ensure that scour does not undermine the base.

A.11.3.6 Gravity-embedded (free-falling) anchors

Gravity-embedded anchors are commonly shaped as ‘torpedo’ steel structures which penetrate the seabed by free-falling and are used as anchoring solution in soft clayey soils. The anchors are lowered by means of an installation line to a designated free-fall drop height above seafloor and penetrate to the target depth below seafloor by kinetic energy obtained during the free-fall (see Figure A.33 and References [53], [220] and [383]).

Gravity-embedded anchors obtain significant horizontal and inclined holding capacity by lateral soil resistance against the wings and friction along the soil–steel interface.

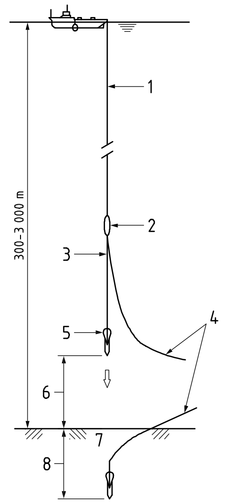

a) Installation principle

b) ‘Torpedo’ pile [53]

c) OMNI-Max anchor [387]

d) Deep penetrating anchor [164]

Key

1	installation line	5	anchor
2	release unit	6	drop height
3	lead line chain	7	seafloor
4	permanent mooring line	8	penetration depth

NOTE These anchors are examples of suitable products available commercially. This information is given for the convenience of users of this document and does not constitute an endorsement by ISO of these products.

Figure A.33 — Gravity-embedded free-falling anchors

A.11.4 Geotechnical design of drag anchors

A.11.4.1 General

Recommended safety factors for holding capacity of drag anchors are given in ISO 19901-7:2013, Table 6.

When used for mobile moorings, the design safety factors for drag anchors are substantially lower than those for mooring line tensions. The rationale is to allow the anchor to move instead of the mooring line breaking in the event of mooring over-loading. Anchor movements of the most heavily loaded lines would normally cause favourable redistribution of the mooring line tensions. This is expected to help the mooring system survive environmental actions exceeding those from the ULS design situation.

Evaluation of the holding capacity of drag anchors is addressed in this subclause and in Reference [116].

The holding capacity of a drag anchor in a particular soil condition represents the maximum horizontal steady pull that can be resisted by the anchor at continuous drag. This includes the resistance of the chain or wire line into the soil for an embedded anchor, but excludes the friction of the chain or wire on the seafloor.

Drag anchor holding capacity is a function of several factors, including:

— Anchor type: fluke area, fluke angle, fluke shape, anchor weight, tripping palms, stabilizer bars, etc. Figure A.34 shows drag anchors commonly used by the offshore industry.

— Anchor behaviour during deployment: opening of the flukes, penetration of the flukes, depth of burial of the anchor, stability of the anchor during dragging, soil behaviour over the flukes, etc.

Furthermore, a long drag distance can be required for an anchor to reach full penetration and develop the ultimate holding capacity. This can be acceptable for anchoring a drill rig in an open water location, but is likely to be unacceptable for a production location where the seafloor is congested with subsea installations.

Due to the wide variation of these factors, predicting the holding capacity of a drag anchor is difficult. A verification of the holding capacity can be determined after the anchor is deployed and test loaded. If drag anchor holding capacity does not meet design capacity, contingency measures should be taken into account.

Anchor performance data for the specific anchor type and soil condition should be obtained if possible. In the absence of credible anchor performance data, Figure A.35 and Figure A.36 can be used to estimate the holding power of drag anchors commonly used to moor floating vessels, acknowledging that the holding capacity curves in Figure A.36 and Figure A.37 do not include a design safety factor and are based on the assumption that the anchor reaches full penetration.

Figure A.36 and Figure A.37 are reproduced from Reference [23], except that the holding capacity curves for the Moorfast (or Offdrill II) and Stevpris anchors were upgraded, based on model and field test data and field experience. The design curves presented in Figure A.35 and Figure A.36 represent, in general, the lower bounds of the test data. The tests used to develop the curves were performed at a limited number of sites. As a result, the curves are for use in generic soil types such as soft clay (i.e. normally consolidated clay with undrained shear strength increasing monotonically with depth) and sand.

Recent studies indicate, however, that several parameters, such as soil strength profile, lead-line type (wire rope versus chain), cyclic actions and anchor soaking, can significantly influence anchor performance in soft clay. Also, some high efficiency anchors have demonstrated substantial resistance to vertical actions in soft clay. Furthermore, there are new versions of high efficiency anchors that are not covered by Figure A.35 and Figure A.36.

As Figure A.35 and Figure A.36 only provide anchor holding capacity estimates, more detailed analyses are needed, if uncontrolled anchor drag cannot be tolerated in congested subsea locations where it can cause damage to existing subsea installations. If it is impractical to apply an installation tension required to completely avoid future anchor drag, it can be necessary to demonstrate that the extent of anchor drag that can occur will not encroach on the existing subsea installations in the area.

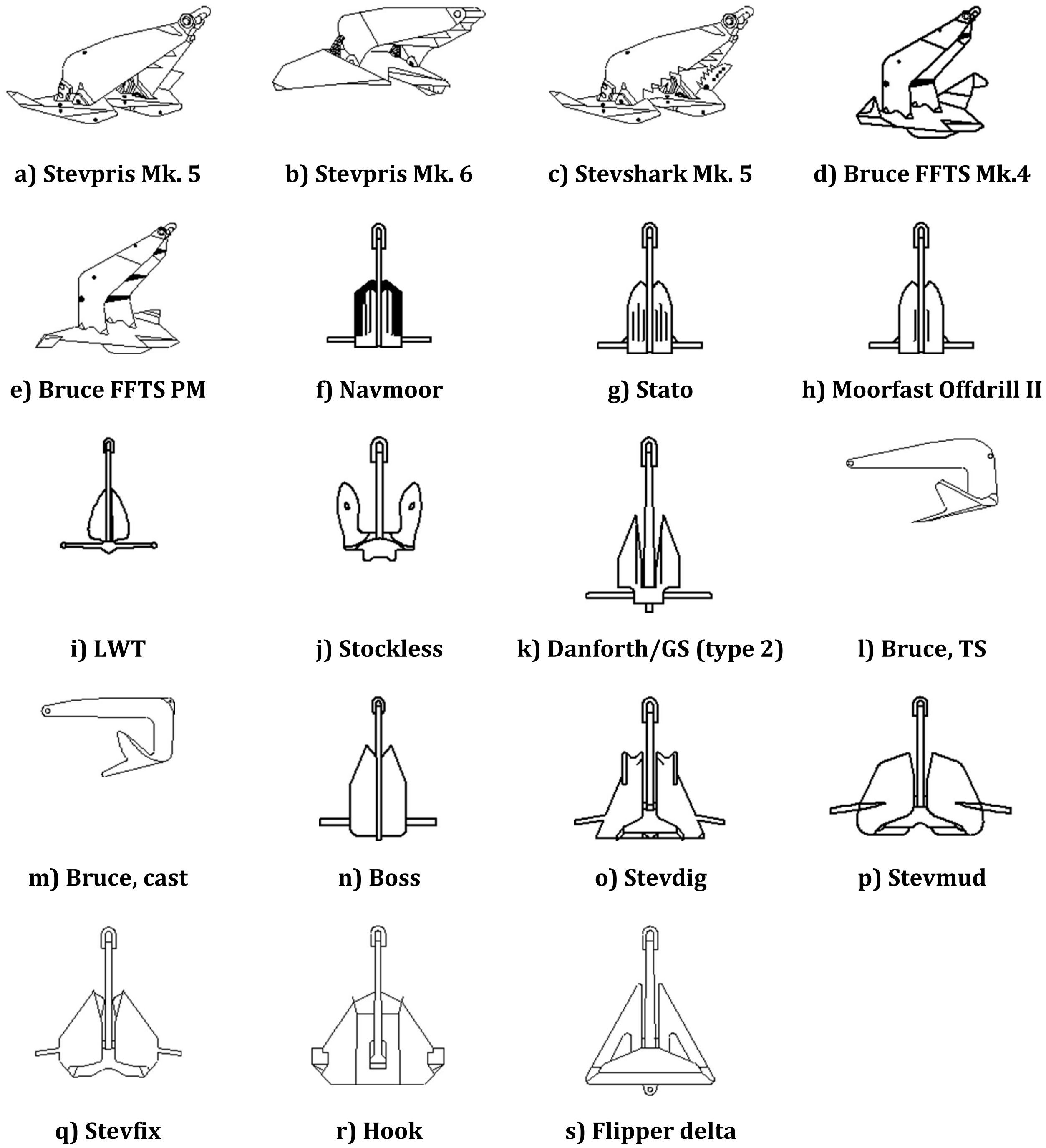

NOTE These anchors are examples of suitable products available commercially. This information is given for the convenience of users of this document and does not constitute an endorsement by ISO of these products.

Figure A.34 — Drag embedment anchors

A.11.4.2 Effect of shear strength gradient in clay

Centrifuge test data, as well as results from analytical studies using a calibrated drag embedment anchor prediction tool, indicate that a more or less linear relationship exists between the anchor holding capacity and the shear strength gradient of the clay [125]. Significant deviations from this linear relationship are observed when the shear strength seafloor intercept and/or the sensitivity of the clay are varied in addition to the shear strength gradient. In general, the effect of the various parameters on the anchor holding capacity in clay accentuates with increasing degree of mobilisation of the anchor capacity. This relationship also varies with the anchor type and anchor size.

Due to the complexity of the problem, a reliable, calibrated prediction tool that can take all influencing parameters into account should be used to establish a basis for design of drag embedment anchors [101].

A.11.4.3 Effect of lead-line type in clay

Field tests and analytical studies indicate that in soft clay, when the lead-line is steel wire line, an anchor can penetrate deeper and give significantly higher holding capacity than when a chain lead-line is used. For the limited cases studied, an anchor connected to steel wire line provided 15 % to 40 % higher holding capacity than the same anchor connected to chain. This is in good agreement with the results from a full-scale test programme. The studies were limited to high efficiency anchors in soft clay with a fairly constant shear strength gradient. A side effect is that the required anchor installation tension is reached with less drag, if a wire lead-line is used instead of a chain lead-line.

A.11.4.4 Effect of cyclic loading in clay

Cyclic loading affects the static undrained shear strength, s_u, in two ways.

a) During a storm, the rise time from mean to peak loading can be about 3 s to 5 s (1/4th of a wave frequency tension cycle), as compared to 0,5 h to 2 h in a static consolidated undrained triaxial test. This higher loading rate leads to an increase in the undrained shear strength and, consequently, in the anchor holding capacity.

b) As a result of repeated cyclic loading during a storm, the undrained shear strength decreases. The degradation effect increases with increasing over-consolidation ratio of the clay.

The cyclic shear strength values used in geotechnical design are generally based on cyclic laboratory tests with periods of typically 1 s to 10 s and therefore account for both these effects.

More information about the prediction of cyclic loading effects are provided in References [116], [117], [16] and [10]. More general considerations about the effects of cyclic loading in clay are described in A.8.3.2.3.

A.11.4.5 Effect of anchor soaking in clay

Soil set-up due to thixotropy can lead to a significant increase in anchor holding capacity in a few hours or days after installation (see for example results from temporary stoppage during instrumented field tests reported in Reference [103]). Over the subsequent weeks, soil set-up due to thixotropy effects gradually increases in combination with soil consolidation (dissipation of excess pore water pressure).

Generally speaking, drag embedment anchors should therefore be installed without stoppage. A temporary interruption before reaching the prescribed installation tension can prevent further anchor penetration, if the increased tension required to restart the anchor after stoppage is higher than the pull available from the installation equipment. The consequence is that the long-term anchor capacity is no higher than that given by the installation tension of the initial step plus the increase due to post-installation effects (thixotropy/consolidation and cyclic loading effects). On the other hand, once the anchor starts to drag after a set-up period, this effect disappears completely.

In a design situation, in which the anchor installation tension is intended to ensure stationkeeping of a floating structure without anchor drag, a safety factor should be applied to the predicted post-installation effects (set-up and cyclic loading), and an adequate overall safety margin should be considered to determine the installation tension meeting such design requirements. In this case, the set-up effect can represent a significant contribution to the total holding capacity, which should be reduced for anchor penetration depths less than 2,5 fluke widths and should be set to zero, if the fluke penetration depth is very shallow (see further discussion in Reference [116]).

A.11.4.6 Capacity in clay under inclined line loading

For deeply embedded drag embedment anchors (>2 to 2,5 fluke widths) the allowable uplift angle at the seafloor for ULS intact condition or redundancy checks can be as high as 20°, if proper anchor installation analyses have shown that the uplift angle at the seafloor is significantly less than the uplift angle at the anchor padeye.

It is not advisable to apply a high uplift angle at the seafloor during the initial shallow penetration of the anchor; otherwise, full penetration depth of the anchor can possibly not be achieved. After reaching a penetration depth greater than 2 to 2,5 fluke widths, the mooring line uplift angle at the seafloor can be gradually increased. This issue is discussed in some detail in Reference [116].

Significant evidence supports the use of a non-zero uplift angle at the seafloor on drag embedment anchors that penetrate sufficiently deep into soft clay. The following additional guidelines are proposed in this respect:

a) Uplift angles at the seafloor should not be accepted for certain operations with mobile moorings where the soil conditions have not been thoroughly investigated or the anchor installation tension is insufficient to ensure deep anchor penetration.

b) The maximum uplift angle at the seafloor should be assessed in accordance with the principles outlined herein under the design situations for the ULS intact and redundancy checks.

c) A zero uplift angle should be maintained until the recommended minimum anchor penetration depth has been reached.

d) The anchor holding capacity should be reduced by a factor *R*, which is a function of the seafloor uplift angle, and accounts for the reduced friction due to shorter embedded line length. The *R* values in Table A.10 are applicable for Bruce FFTS Mk. IV and Stevpris Mk. V anchors.

Table A.10 — *R* values for Bruce FFTS Mk. IV and Stevpris Mk. V anchors

Seafloor angle (°)	0	5	10	15	20
R	1,0	0,98	0,95	0,89	0,81

In areas that are susceptible to seabed trenching, the effect of possible trenching in combination with uplift should be evaluated to ensure sufficient anchor capacity.

For taut-leg mooring systems, where mooring lines with seafloor angle greater than 20° impose significant vertical forces on the anchor at all times, a typical solution is to use anchor piles or plate anchors for which design guidelines are provided in A.11.5 and A.11.6.

A.11.4.7 Drag distance and penetration depth in soft clay

Many factors affect the drag–penetration depth relationship, including site-specific soil data (e.g. soil stratigraphy, seafloor shear strength, average shear strength gradient, soil sensitivity), and the size and type of anchor. For screening-level analysis, drag distance and penetration depth estimates from Reference [257] are presented in Figure A.35 and Table A.11, respectively. This information is valid for chain lead-lines and shear strength gradients of 1,4 kPa/m to 2,0 kPa/m. Deviation from this range can affect these values, especially the penetration depth estimates.

If the anchor design relies on further penetration to reach holding capacity, the additional drag to resist the design intact actions should not over-load neighbouring lines.

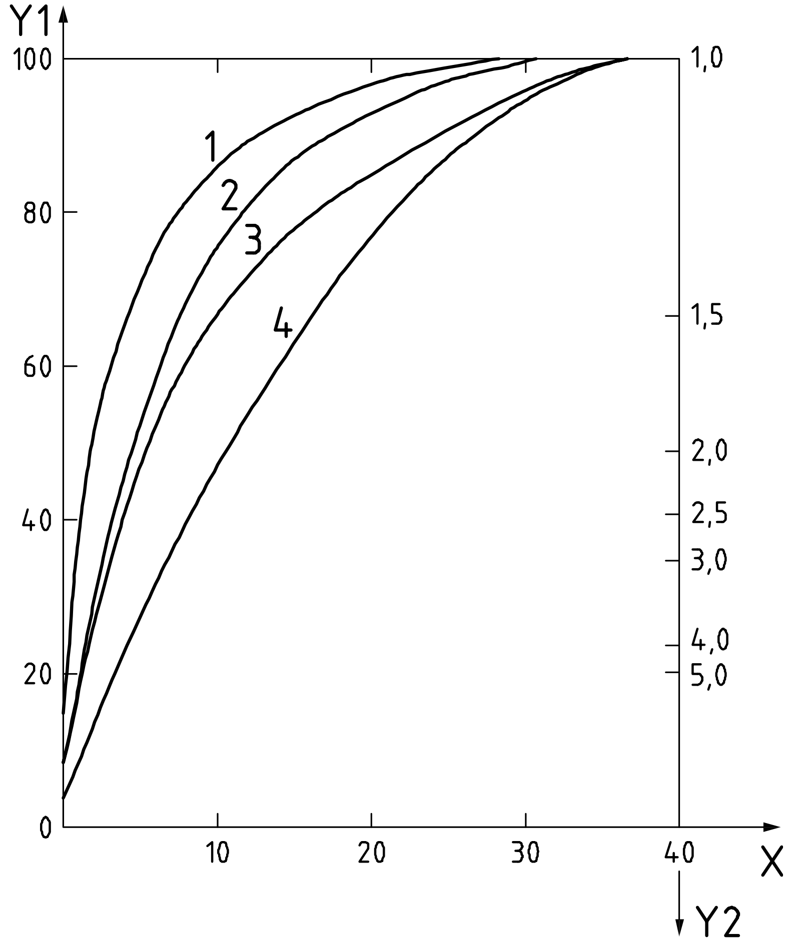

Key

1 stockless anchor (fixed)

2 Hook anchor

3 anchor types Bruce, FFTS Mk. III / Bruce TS / Danforth / GS (type 2)[a] / LWT[a] / Moorfast / Navmoor / Offdrill II[a] / Stato / Stevmud / Stevpris Mk. III

4 anchor types Boss[a] / Flipper Delta[a] / Stevdig[a] / Stevin[a]

X drag distance/ fluke length

Y1 percent of maximum capacity

Y2 corresponding safety factor

[a] Assumed based on geometric similarities.

Figure A.35 — Holding capacity versus drag distance in soft clays [257]

Table A.1 — Estimated maximum fluke tip penetration [257]

Anchor type	Normalized fluke tip penetration (fluke lengths)	
	Sands/Stiff clays	**Mud (e.g. soft silts and clays)**
Stockless (fixed fluke)	1	3
Moorfast Offdrill II	1	4
Boss Danforth Flipper Delta GS (type 2) LWT Stato Stevfix	1	4,5
Stevpris Mk. III Bruce FFTS Mk. III Bruce TS Hook Stevmud	1	5

A.11.4.8 New anchor designs

New anchor designs and improvements to existing anchors continue to be developed. However, well controlled instrumented tests and field performance data are insufficient for predicting the performance of many of these innovative high efficiency anchors, although results from such tests can still be used to calibrate anchor prediction tools (see A.11.4.9). Just as important as the ultimate holding capacity is the ability to predict drag–penetration–tension relationships for mobilized loadings, which are much less than the ultimate holding capacity. In the absence of better information, the holding capacities of these new anchors can be conservatively estimated from:

$$H_{\mathrm{n}} = H_{\mathrm{s}} (A_{\mathrm{n}} / A_{\mathrm{s}})^{n} \tag{A.67}$$

where

- H_{n} is the holding capacity of new design;
- H_{s} is the holding capacity of reference design (e.g. Bruce FFTS Mk. III or Stevpris Mk. III in Figure A.36 and Figure A.37) of the same weight;
- A_{n} is the fluke area of new design;
- A_{s} is the fluke area of reference design of same weight;
- n is the 1,4 factor commonly used for high efficiency drag anchors.

The fluke area ratio $A_{\mathrm{n}}/A_{\mathrm{s}}$ can be obtained from anchor manufacturers.

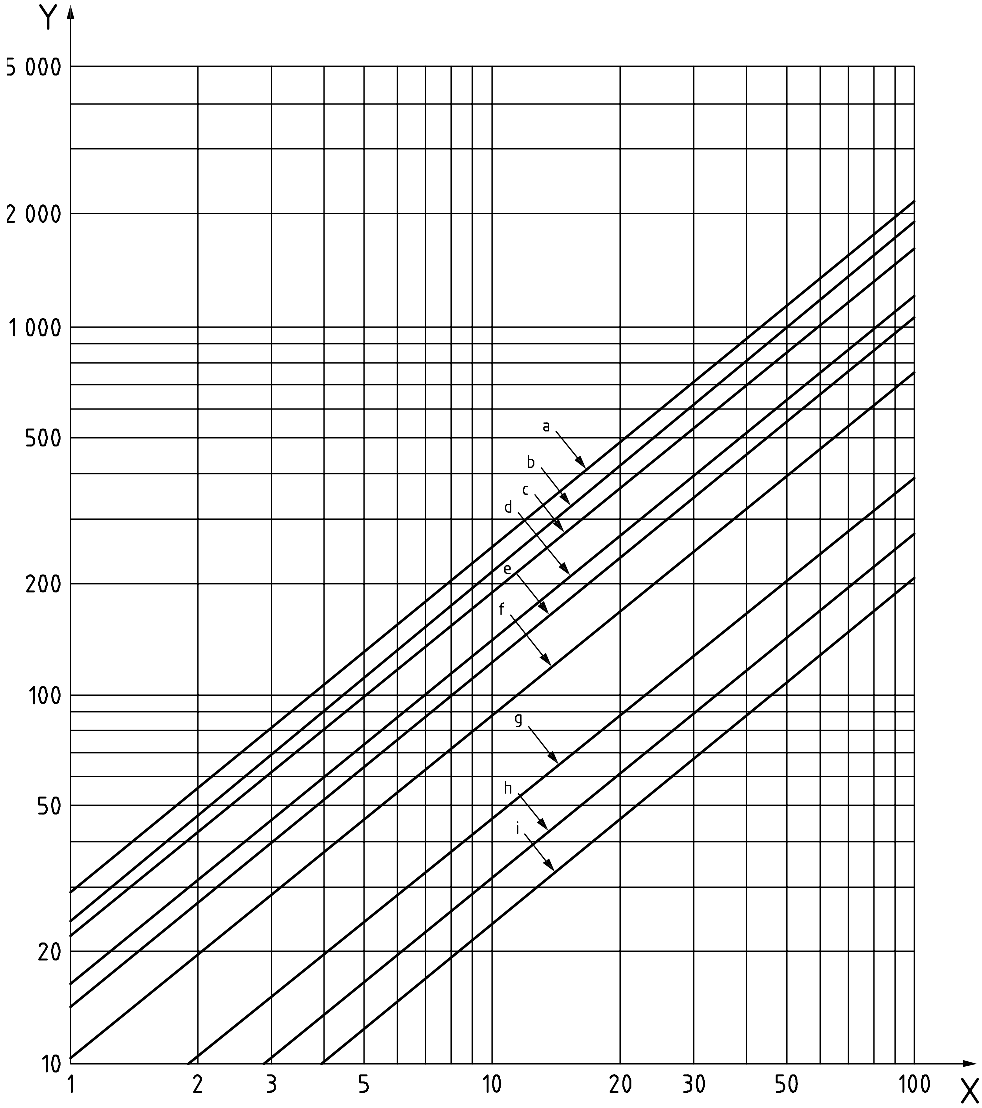

Key

X anchor weight (kips)

Y anchor holding capacity (kips)

a Bruce FFTS Mk. III, Stevpris Mk. III

b Navmoor, Stato, Boss

c Bruce TS, Hook, Stevfix

d Flipper Delta, Stevin, Stevdig

e Moorfast, Offdrill II

f Danforth, GS, LWT

g Stockless, fixed fluke

h Bruce, cast

i Stockless, movable fluke

NOTE 1 Fluke angles set for soft clay seafloor condition as per manufacturer's specification

NOTE 2 1 kip = 4,448 kN.

NOTE 3 This figure was reproduced from Reference [257], except that the holding capacity curves for the Moorfast (or Offdrill II) and the Stevpris anchors were upgraded. The design curves reflect data valid for anchor designs as of 1987. New anchor designs have since been developed, but the curves for these new designs were not included. The design curves in this figure do not include a design safety factor and assume that the anchor reaches full penetration (see A.11.4.1).

NOTE 4 These anchors are examples of suitable products available commercially. This information is given for the convenience of users of this document and does not constitute an endorsement by ISO of these products.

Figure A.36 — Anchor system holding capacity in soft clay

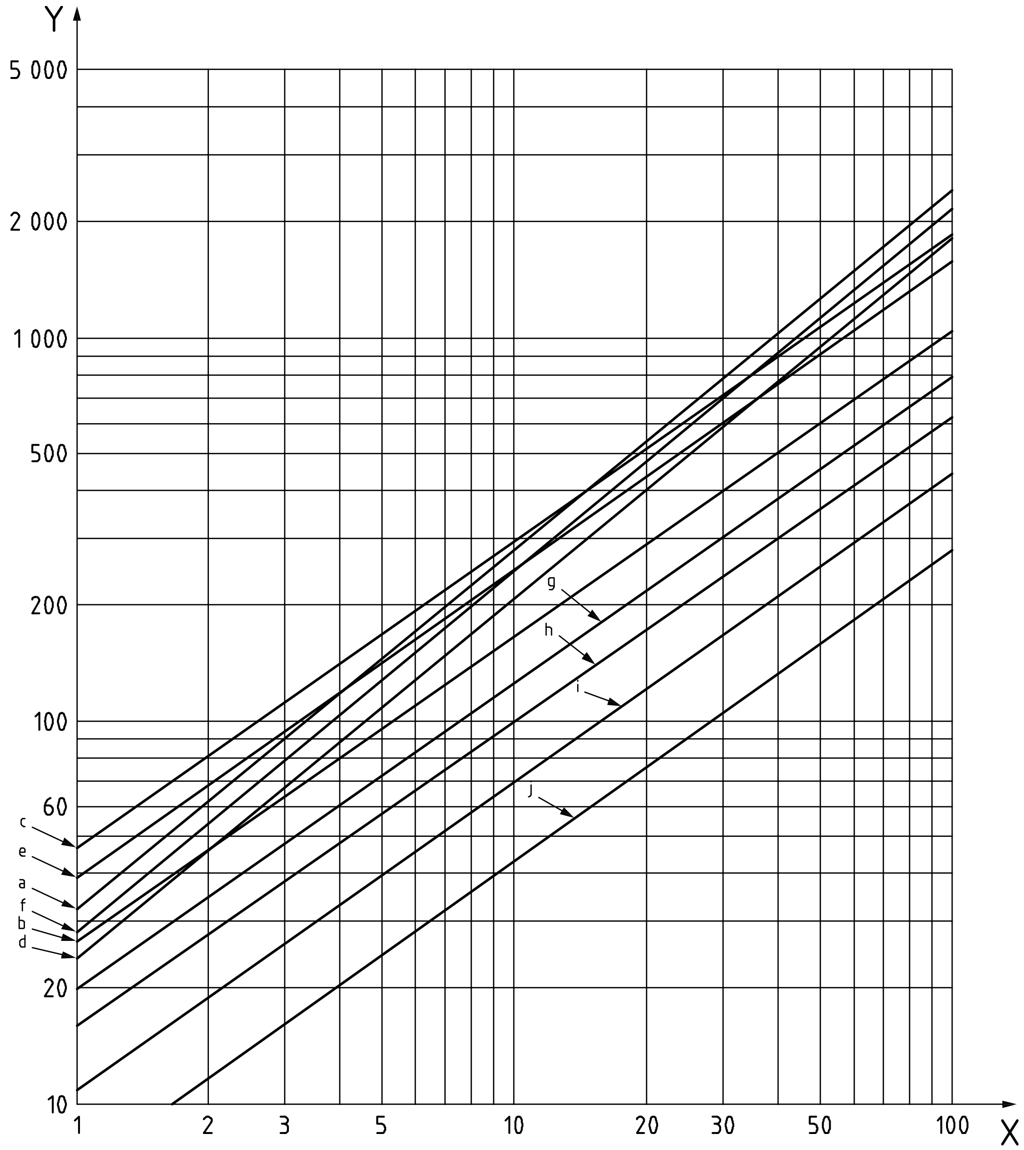

Key

X anchor weight (kips)

Y anchor holding capacity (kips)

Fluke angles set for sand seafloor condition as per manufacturer's specification.

a Navmoor, Boss

b Stevin

c Stevfix, Stevdig

d Stevpris, straight shank, Bruce TS

e Bruce, cast

f Stato, 30° pulse angle

g Danforth GS, LWT

h Moorfast, Offdrill II, 20° fluke angle, Hook

i Stockless, 35° fluke angle

j Stockless, 48° fluke angle

NOTE 1 1 kip = 4,448 kN

NOTE 2 This figure was reproduced from Reference [257]. The design curves reflect data valid for anchor designs as of 1987. New anchor designs have since been developed, but the design curves for these new designs were not included. The design curves in this figure do not include a design safety factor and assume that the anchor reaches full penetration (see A.11.4.1).

NOTE 3 These anchors are examples of suitable products available commercially. This information is given for the convenience of users of this document and does not constitute an endorsement by ISO of these products.

Figure A.37 — Anchor system holding capacity in sand

A.11.4.9 Analytical tools for anchor performance evaluation

Analytical tools based on limit equilibrium principles for anchor embedment and capacity calculation in soft clay are available. These tools allow modelling of different anchor designs and provide detailed anchor performance information, such as anchor movement trajectory, anchor rotation, mooring line profile below the seafloor and ultimate anchor capacity. Recommendations for these tools to yield reliable predictions include the following:

a) The analytical tool should be calibrated against results from high quality instrumented tests by field testing or centrifuge testing performed on the type of anchor of interest.

b) The soil properties should be well known, which is not necessarily the case when designing and installing drag embedment anchors. Where the soil properties are uncertain, suitable upper and lower bound soil parameters should be established, and the anchor design should be based on the more conservative prediction.

c) Users should be aware of the tool's limitations and should be familiar with mooring operations. For example, some tools typically show that the anchor penetration increases continuously, leading to higher and higher anchor holding capacity. In such cases, the user should consider limiting the drag distance for calculating the anchor holding capacity to a distance that does not result in unacceptable vessel excursions.

d) Empirical formulae or field experience, if available, should be used to support analytical predictions;

e) The analytical tool should be able to handle layered soil profiles. Some tools can handle layered clay profiles with sand layers of limited thickness while other tools cannot model layered soil profiles.

A.11.4.10 Anchor holding capacity in sand

No significant study on the behaviour of drag embedment anchors in sand has been carried out since the US Navy's study [257]. Anchors do not achieve deep penetration in sand and no uplift resistance can be relied upon from shallow penetration anchors in any soil conditions, i.e. the line uplift angle at the seafloor should be zero. Moreover, scour effects on anchor embedment should be taken into account when drag anchors installed in sand are still visible at the seafloor.

Contrary to anchors in soft clay, anchors in sand do not gain any additional capacity from post-installation effects due to thixotropy, consolidation or cyclic loading effects. In this case, the initial anchor installation tension should be set high enough to provide the required safety factor for the anchors and the mooring system accounting for the uncertainty in the loading calculation [116].

The limited capacity of mobile offshore drilling units (MODU) winches can result in shallow anchor penetration during installation in dense sand. In some cases anchors are visible at the seafloor after installation. In the cases of shallow penetration, it is not recommended to assume that the anchors continue to penetrate upon overloading. Anchor penetration during installation should be estimated and the anchor capacity at estimated penetration depth should be evaluated using the analytical method presented in Reference [259].

A.11.4.11 Anchor holding capacity in soils other than soft clay and sand

Predicting anchor holding capacity in hard clay, calcareous sand, coral or rock seafloor and layered soil profiles is complex and is dependent upon the detailed soil/rock data for the location of each anchor cluster. In these soils/rocks, the anchor penetration is often very shallow, which means that the same precautions as recommended for anchors in sand (see A.11.4.10) should be followed.

Figure A.35 and Figure A.36 should not be used for carbonate and calcareous materials. Anchor performance in similar seabed conditions or limit equilibrium methods should be used for design as described in Reference [80]. In carbonate or calcareous materials, the effect of the imposed loading regime (e.g. impact of short-term, sustained loading and cyclic/dynamic loading on soil strength) should be taken into account (potential cyclic degradation) as described in A.6.3.

A.11.4.12 Holding capacity generated by friction along the mooring line

The holding capacity generated by friction of chain and steel wire line on the seafloor can be estimated by:

$$P_{cw} = f\, L_{cw}\, W'_{cw} \tag{A.68}$$

where

P_{cw} is the chain or wire line holding capacity;

f is the coefficient of friction between chain or wire line and the seafloor;

L_{cw} is the length of chain or wire line in contact with the seafloor;

W'_{cw} is the submerged unit weight of chain or wire line.

The coefficient of friction depends upon the nature of the seafloor and on the type of mooring line. Static (starting) friction coefficients are normally used to compute the holding power of the line and sliding coefficients are normally used to compute the friction forces on the line during mooring deployment.

If more specific data are not available for chain and wire line, the generalized coefficients given in Table A.12 can be used for various seafloor conditions, such as soft mud, sand and clay. Guidance for calculation of the seabed friction is also provided in Reference [116]. However, industry experience indicates that coefficients of friction can vary significantly for different soil conditions, and higher values for the sliding coefficient of friction have been encountered. In calcareous and carbonate materials, lower values are possible (see Reference [325]), coupled with low chain embedment in dense or cemented materials.

NOTE Considerations about capacity generated by friction along the mooring line apply to all types of anchors with deeply embedded anchor line attachment padeye, not to drag anchors only.

Table A.12 — Mooring line friction coefficients

Anchor type	**Coefficient of friction** f	
	Static	**Sliding**
Chain	1,0	0,7
Wire line	0,6	0,25

A.11.4.13 Installation of drag anchors

Drag anchor installation tolerances should be established and should be considered in the anchor's geotechnical, structural, and installation design. Typical tolerances to be considered are:

— allowable deviation from target heading of the mooring line attachment to limit padeye side loadings and rotational moments on the anchor padeye;

— minimum penetration required before test loading to achieve the required holding capacity.

For drag anchors used in permanent moorings, the anchor design should incorporate adequate installation information to ensure that the anchor has reached the target penetration depth, thereby meeting the safety requirements of the mooring system for the actual soil and design situations. Typical information to be monitored and recorded includes:

a) drag anchor installation line tension versus time;

b) catenary shape of installation line based on line tension and line length to verify that uplift at the seafloor during embedment is within allowable ranges and to verify anchor position;

c) direction of anchor embedment;

d) drag distance;

e) final anchor penetration depth.

Acceptance criteria for drag anchors used in mobile (i.e. temporary) moorings should be established on a case-by-case basis.

A.11.4.14 Out-of-plane loading of anchors

In areas prone to revolving storms, MODUs experiencing a one or multiple line failure can exert forces on the anchor that are out-of-plane to the installation direction. This can cause a reduction in the holding capacity of the drag anchor and potentially anchor dragging [151]. On the other hand, drag anchors are also capable of generating significant holding capacity in the out-of-plane direction.

For MODU moorings where the possible consequences of out-of-plane loading are seen as a risk, possibly due to nearby infrastructure, this should be taken into account in the design of the anchoring system. Selection of the appropriate drag anchor in combination with sufficient installation tension to fully embed the anchor, can increase the out-of-plane resistance of the drag anchor. Out-of-plane loading can also cause additional drag distance to reach ultimate holding capacity and should be considered in the design of the anchor pattern. The structural capacity of the drag anchor should also be evaluated for out-of-plane loading.

A.11.5 Geotechnical design of anchor piles

A.11.5.1 Driven anchor piles

A.11.5.1.1 Basic considerations

Driven anchor piles can be designed to provide adequate capacity for both catenary and taut-leg mooring systems. The design of driven anchor piles builds on the strong industry background in the evaluation of geotechnical properties and the axial and lateral capacity prediction for driven piles, as developed and documented in this document. The recommended design criteria from ISO 19902 and from this document should be applied for the design of driven anchor piles, but with some modifications to reflect the differences between mooring anchor piles and fixed platform piles.

The design of a driven anchor pile should consider four potential failure modes:

a) pull-out due to axial forces;

b) overstress of the pile and mooring line attachment padeye due to lateral bending;

c) lateral rotation and/or translation;

d) fatigue due to environmental and installation actions.

In most anchor pile designs, the mooring line is attached to a padeye located on the pile below the seafloor to enhance the lateral capacity. As a result, the design should consider the mooring line angle at padeye connection resulting from the inverse catenary through the upper soil layers. Calculation of the soil resistance above the padeye location should also consider remoulding effects due to this trenching of the mooring line through the upper soil layers.

Driven anchor piles in soft clay typically have aspect ratios (penetration-to-diameter) of 25 to 30. Piles having such aspect ratios behave as if horizontally fixed in position at the pile tip, and consequently deflect laterally and fail in bending before translating laterally as a rigid body.

As argued in Reference [238], static p–y curves can be considered for the calculation of lateral soil resistance. Cyclic p–y curves can be more appropriate for fatigue calculations. A modification to the current p–y curves (as described in 8.5 and A.8.5) has been proposed in Reference [326] to ensure that lateral displacements are not over-predicted. Degrading the p–y curves for lateral displacements by more than 10 % of the pile diameter should be considered. In addition, when lateral displacements associated with cyclic actions at or near the seafloor are relatively large (e.g. exceeding y_c as defined in 8.5 for soft clay), reducing or neglecting the soil-pile skin friction through this zone should be considered.

The design of driven anchor piles should consider typical installation tolerances, which can affect the calculated soil resistance and the pile structure. Pile verticality affects the angle of the mooring line at the padeye, which changes the components of horizontal and vertical mooring line forces that the pile is expected to resist. Underdrive affects the axial pile capacity and can result in higher bending stresses in the pile. Padeye orientation (azimuth) can affect the local stresses in the padeye and connecting shackle. Horizontal positioning can affect the mooring scope and/or angle at the vessel fairlead and should be considered when balancing mooring line pretensions.

A.11.5.1.2 Safety factors for driven anchor piles

Factors of safety for holding capacity of driven anchor piles are given in ISO 19901-7:2013, Table 7. Information on coupling between vertical and horizontal capacities can be found in A.11.5.2.2.5. Axial safety factors consider that the pile is primarily loaded in tension, and are therefore higher than for piles loaded in compression. As with other piled foundation systems, the calculated ultimate axial soil resistance should be reduced if soil set-up, which is a function of time after installation, is not complete before significant forces are imposed on the anchor pile.

As the lateral failure mode for piles is considered to be less catastrophic than the vertical mode, lower factors of safety are recommended for lateral pile capacity. Use of separate safety factors for vertical and lateral pile capacities can be straightforward for simple beam-column analysis [see A.11.5.2.2.3 item c)], but more complex methodologies do not differentiate between vertical and lateral pile resistance. The safety factor should be in accordance with the ISO 19901-7 criteria and the guidelines of A.11.5.2.2.5.

A.11.5.1.3 Basic considerations for structural strength design

The structural strength design for driven anchor piles should be based on the guidance provided in ISO 19902 and ISO 19901-7. Pile stresses should be limited by the provisions of ISO 19902 under ULS intact condition.

Anchor piles should be checked for fatigue caused by in-place mooring line forces. Fatigue damage due to pile driving stresses should also be calculated and combined with in-place fatigue damage. For typical mooring systems, fatigue damage due to pile driving is much higher than that caused by in-place mooring line forces.

Further guidance on fatigue damage design for driven piles can be found in References [114], [179] and [65].

A.11.5.1.4 Installation of driven anchor piles

Refer to 9.2.3.

A.11.5.2 Design of suction anchor piles

A.11.5.2.1 Basic considerations

A suction anchor can take many forms, ranging from a gravity base with skirts to a no-ballast suction anchor that resists all applied actions by soil friction, lateral resistance and reverse end bearing (REB). Typically, the suction anchor will have a closed top, but if that is not the case the reverse end bearing can still be mobilized by the sum of inside skirt wall friction. It should be checked that the contribution from inside skirt wall friction do not exceed the reverse end bearing which can be the limiting factor after significant set up has occurred for a slender anchor.

Generally, a suction anchor is technically feasible for soft to medium hard soils. For very soft soils, a suction anchor extends deep into the soil in order to reach competent bearing material. For very hard soils, it is sometimes not possible for the suction anchors to penetrate deep enough to provide adequate in-place strength. Some useful information for the design of suction anchors is provided in References [18], [118] and [174].

The design of suction anchors for floating systems includes the following aspects:

— penetration and removal;

— holding capacity;

— overstress of the pile and mooring line attachment padeye due to lateral bending;

— soil reactions or soil-structure interaction analyses for structural design.

In areas such as the Gulf of Mexico, where action effects of tropical cyclonic storms can exceed the capacity of the mobile mooring or mobile anchoring system, the design of suction piles should consider an anchor failure mode that reduces the chance of anchor pull-out. For site conditions where the presence of hard soil layers can limit suction anchor penetration, other anchor types should be considered instead.

The calculation of the representative holding capacity of the anchor should be based on the design value of the soil properties. Anchor adequacy with respect to installation should be checked against high estimate soil strength properties. If faced with larger-than-usual scatter in soil data, the designer should consider increasing the safety factors given in ISO 19901-7.

If the REB at the anchor tip is to be relied upon, it can possibly not be correct to add the representative value of the end bearing to the representative value of the skin friction to obtain the representative value of the axial capacity of the suction pile as the mobilization of REB can require large pile pullout displacements [94], [281].

The impact of the mooring line geometry in the soil on anchor forces should be considered since the geometry can affect the relationship between the horizontal and vertical anchor forces. The inverse catenary of the mooring line in the soil can make the mooring line angle steeper at the anchor padeye than at the seafloor. This steeper angle can result in a reduced horizontal force, but an increased vertical force at the anchor padeye. Both an upper and lower bound inverse catenary should be checked to ensure the worst-case anchor loading is established.

A.11.5.2.2 Analysis methods

A.11.5.2.2.1 Penetration analysis

A typical penetration analysis includes the calculation of three quantities for all penetration depths, which are

— the penetration resistance exerted on the anchor by the soil;

— the required under-pressure to allow anchor embedment;

— the critical pressure that can cause the soil plug to fail.

The under-pressure (‘suction’) required for the pile to achieve design penetration should be properly estimated. Minimum under-pressures are vital input parameters to the structural design of the anchor. Furthermore, the pumps used during installation should be capable of generating adequate under-pressure.

a) Penetration resistance in clay

The penetration resistance can be calculated as the sum of the side shear and end bearing on the side wall and any other protuberances. Protuberances include mooring and lifting padeyes, longitudinal or ring stiffeners, changes in wall thickness, mooring chain, launching skids, and others. For an anchor in clay without protuberances and with a flat tip, the installation resistance at a given tip penetration depth, z, can be calculated by:

$$Q_{\text{tot}} = Q_{\text{side}} + Q_{\text{tip}} \tag{A.69}$$

$$Q_{\text{side}} = A_{\text{wall}} \, (\alpha_{\text{ins}} \, s_{\text{uDSS}})_{\text{AVE}} \tag{A.70}$$

$$Q_{\text{tip}} = (N_{\text{c}} \, s_{\text{utip AVE}} + \gamma' z) \, A_{\text{tip}} \tag{A.71}$$

where

Q_{tot}	is the total penetration resistance;
Q_{side}	is the resistance along the sides of the pile;
Q_{tip}	is the resistance at the pile tip;
A_{wall}	is the sum of inside and outside wall areas embedded in the soil;
A_{tip}	is the pile tip cross-sectional area (excluding contained soil);
α_{ins}	is the friction factor during installation [see item a)];
$\alpha_{ins}\ s_{uDSS}$	is the side friction;
$(\alpha_{ins}\ s_{uDSS})_{AVE}$	is the average side friction from seafloor to depth z;
N_c	is the bearing capacity factor [see item b)];
$s_{utip\ AVE}$	is the average of triaxial compression, triaxial extension, and DSS undrained shear strength at anchor tip level;
γ ‘	is the effective unit weight of soil;
Z	is the tip penetration depth.

1) Friction factor during installation, α_{ins}

The friction factor during installation, α_{ins}, is usually defined as the ratio of remoulded shear strength over undisturbed shear strength, which is as the inverse of the soil sensitivity. The friction factor can be determined by various methods for which fall cone, UU triaxial and miniature vane (minivane) are the most common. The typical range of α_{ins} for soft clays is 0,2 to 0,5.

There can be uncertainty in the soil sensitivity since it is influenced by the quality of the intact strength that it is related to. Alternatively, the side friction, $\alpha_{ins}s_{uDSS}$, can be equated to the direct measurement of remoulded shear strength through fall cone, UU triaxial or minivane tests. The remoulded strength used in design should reflect both the directly measured value and the value derived from the intact strength divided by the sensitivity.

Some installation records have shown that the interface shear strength mobilized during installation can, at a given depth, be less than $\alpha_{ins}s_{uDSS}$. In cases where the full interface shear strength, $\alpha_{ins}s_{uDSS}$, cannot be mobilized along the anchor wall, such as when the anchor is painted or subjected to unusual surface treatment, a correction factor should be applied to α_{ins} to properly predict the penetration resistance [18], [67], [109]. Ring shear tests, with the actual wall surface modelled in the tests, can also be used to measure the actual interface shear strength.

2) Bearing capacity factor, N_c

The value of the bearing capacity factor, N_c, to be used to calculate the penetration resistance of the anchor tip or of a given protuberance depends on the shape of the protuberance and the ratio of the width of the protuberance over the embedment depth of the protuberance. Values of N_c ranging from 5,1 to 9,0 for strip and circular footings are recommended in Reference [318].

Because the anchor wall thickness is usually small compared to the anchor diameter and the embedment depth, the pile tip is usually considered to be a deeply embedded strip footing with an associated bearing capacity factor, N_c, equal to 7,5. The values of N_c to be used in Formula (A.71) are summarized in Table A.13.

A detailed example of the calculation of N_c is given in Reference [127]. Values of N_c different from those of Table A.13 are acceptable provided that they can be documented by appropriate modelling and test results.

Table A.13 — Recommended N_c factor

Purpose	Shape or area	N_c

Calculation of pile tip penetration resistance	Strip	7,5
Calculation of critical under-pressure causing soil plug failure [see A.11.5.2.2.1 item c)]	Circular	6,2 to 9,0 depending on embedment ratio [318]
Calculation of penetration resistance of protuberances [see A.11.5.2.2.1 item 3)]	Varies	5,0 to 13,5 [257]

3) Changes in penetration resistance due to protuberances

Formulae (A.69) to (A.71) should be modified if protuberances are present. The change in penetration resistance due to the presence of mooring and lifting padeyes, longitudinal or ring stiffeners, mooring chain, launching skids, pile tip other than flat (i.e. bevelled) or any other internal or external protuberance should be addressed to assess the changes in friction and end bearing resistance caused by the protuberances. Most protuberances cause an increase in penetration resistance, except for internal ring stiffeners which can cause a decrease in internal side friction if they are closely spaced [18], [67].

b) Required under-pressure

The required under-pressure, ΔU_{req}, to embed the anchor can be calculated as follows:

$$\Delta U_{req} = (Q_{tot} - W') / A_{in} \tag{A.72}$$

where

Q_{tot} is the total penetration resistance;

W' is the submerged weight of the anchor during installation;

A_{in} is the plan view inside area where under-pressure is applied.

c) Critical and allowable under-pressures

The critical under-pressure at a given depth, ΔU_{crit}, defined as the under-pressure that causes a general reverse end bearing failure at the anchor tip and large soil heave within the anchor, can be calculated at a given depth as follows:

$$\Delta U_{crit} = N_c\, s_{utip\,AVE} + [A_{inside}\, (\alpha_{ins}\, s_{uDSS})_{AVE}] / A_{in} \tag{A.73}$$

where

A_{inside} is the inside lateral area of anchor wall.

In shallow water, the critical under-pressure should not exceed the water cavitation pressure.

The recommended allowable under-pressure, ΔU_{allow}, defined as the maximum under-pressure to be applied to the anchor, can be calculated as the critical under-pressure divided by an appropriate safety factor. The minimum value of the safety factor is typically 1,5. Lower values can be acceptable provided that the soil plug behaviour is monitored during installation and it is confirmed that no plug failure occurred, and provided that the calculated allowable under-pressure is acceptable for the pile steel structure (i.e. no risk of buckling).

d) Soil plug heave inside anchor

The soil heave inside the anchor during installation can be estimated by assuming that a percentage of the soil volume displaced by the cross-sectional area of the anchor goes inside the anchor. This percentage depends on anchor tip geometry and mode of penetration (i.e. self-weight penetration versus penetration by under-pressure). It is commonly assumed that 50 % of the soil displaced by the cross-sectional area of the anchor tip goes inside the anchor during self-weight penetration if the anchor tip is flat.

The final elevation of the internal plug surface depends on the wall thickness variations, internal soil plug stability, and spacing and type of any internal stiffeners [8].

Soil heave should be accounted for in calculating the required pile stick-up and total length.

e) Penetration in sand

Procedures for calculating skirt penetration resistance of skirted foundations in sand can be found in References [15], [178] and [314].

The skirt penetration resistance in sand consists of the two components, skirt wall friction and tip resistance, as for clay. The bearing capacity and skirt wall friction have typically been calculated by two different models:

1) Bearing capacity approach

In the bearing capacity model, the penetration resistance is calculated as;

$$P_f = Q_{tip} + Q_{side} = q_{tip} A_{tip} + f_{s,av}\, A_{wall} \quad \text{(A.74)}$$

where

q_{tip} is $0{,}5\gamma' t N_{\gamma\_} + qNq$;

$fs_{,\text{av}}$ is $0{,}5\ \gamma' z K \tan\delta$ (average friction over skirt length);

A_{tip} is πDt;

A_{wall} is $2Dz$ (sum of inside and outside);

Nq is $e^{\pi tan\varphi}.\ \tan^2(45+\varphi/2).N_{\gamma\_}=1{,}5(Nq-1)\tan\varphi$;

Q is the effective overburden pressure outside skirt at skirt tip level;

γ' is the effective unit weight of sand;

φ is the peak drained friction angle of sand (angle based on a reference vertical effective consolidation stress of σ'_{vc}=200 kPa);

r is the roughness factor between skirt wall and sand (r=0,9 is suggested used);

δ is the friction angle between sand and skirt wall $\delta = r\varphi$;

K is the ratio between horizontal and initial vertical effective stresses at skirt wall (K=0,8 is suggested used);

T is the skirt wall thickness (assumed to be small compared to the diameter);

D is the diameter of foundation or anchor (external D can be used since t is small);

Z is the depth below sand surface.

Formula (A.74) for skirt wall friction assumes homogeneous sand conditions. For a horizontally layered soil profile the wall friction can be calculated as the sum of the contributions from the different soil units. For foundations or anchors with long skirt walls, the skirt wall friction can give an important additional vertical stress outside the skirt wall. This increase can cause an increased skirt tip resistance. With reference to Reference [15], this contribution can be added to the *in situ* effective overburden;

$$q = \gamma' z + \alpha_f f_{s,tip} = \gamma' z\left(1 + \alpha_f K tan\delta\right) \quad \text{(A.75)}$$

where

α_{f} is the ratio between vertical normal stress increase and skirt wall friction at skirt tip level (α_{f}=1 suggested);

$f_{\text{s,tip}}$ is the skirt wall friction at skirt tip level.

2) Empirical CPT resistance approach

In the CPT resistance approach, the penetration resistance is linked to the measured cone tip resistance as follows:

Pf is $Q_{\text{tip}} + Q_{\text{side}} = k_{\text{tip}} qc A_{\text{tip}} + A\text{wall} \int k_{\text{side}} q_c(z)\_dz$;

q_c is the cone tip resistance measured in CPT tests;

k_{tip} is the empirical skirt tip constant related to q_c;

k_{side} is the empirical skirt wall friction constant related to q_c

As presented in Reference [15], the empirical constants derived from back calculations of skirts penetrated by self-weight only may give a large range as illustrated below:

k_{tip} = 0,01 – 0,55 when k_{side} = 0,0015 and

k_{tip} = 0,03 – 0,60 when k_{side} = 0,0010.

Empirical constants can also be found in Reference [115]. These are also factors suggested for skirt penetration without the use of under-pressure.

A CPT based method for installation of suction caissons in sand is suggested in Reference [314].

f) Penetration in sand- effect of under-pressure

By applying under-pressure in a sand without silt or clay layers, the under-pressure will cause seepage flow of water from the outside to the inside skirt compartment. This flow will change the effective stresses in the sand with an increase along the outside skirt wall while beneath the skirt tip and along the inside skirts the effective stresses will decrease. In total, this will result in a significantly reduced penetration resistance where approximately all the tip resistance and the skirt wall friction along the inside skirt wall approach zero. The maximum achievable penetration depth in a clean sand can simplified be assumed equal to the anchor diameter (z/D=1) [178]. This assumes a typical submerged weight of the anchor whilst a very high submerged weight can increase the possible penetration depth. More details on critical and allowable under-pressure can be found in References [15] and [178]. With respect to potential soil heave inside anchors penetrated by under-pressure, a simplified rule of thumb suggests a soil heave equal to 5 % of the penetration depth as a general guidance.

g) Penetration in layered soils

If there are continuous clay layers in the sand, the water flow will be prevented and the potential reduction in the overall penetration resistance when installed by under-pressure will be significantly reduced. The under-pressure that can be achieved is significantly higher than the under-pressure that will give critical gradients in a pure sand. The maximum achievable penetration depth can also increase significantly from what is possible in pure sand. The pressure gradient where the vertical effective stresses are getting close to zero is denoted "critical gradient". The main reasons why the under-pressure required to give critical gradients in the underlaying sand in this case is higher is because the under-pressure will have to produce an uplift force that exceeds the sum of skirt wall friction in the layers above the sand layer and the submerged weight of the soil plug above the sand layer being penetrated. In addition to these components, the remaining part of the under-pressure should be able to initiate a flow in the underlaying sand layer and into the anchor. This flow will in turn make both skirt tip resistance and inside skirt wall friction more or less vanish, i.e. a situation which is similar to the situation when penetrating a pure sand layer with the exception that the flow pattern will be different representing a lateral flow coming from the surrounding part of the sand layer rather than from outside seabed and around the skirt. Skirt penetration in layered soils have been performed with success (see Reference [270]), but a general advice is to make sure to have enough pump capacity and monitor that the anchor actually is penetrating at all times. If the anchor is not continuously penetrating, the inside soil plug can possibly be lifted rather than creating further penetration. A penetration model for installation in layered soils is provided in Reference [201].

For situations with a dense sand layer within a clay matrix, penetration resistance of internal protuberances like longitudinal plate stiffeners should be considered, because these can experience significant tip resistance. In some projects, a water injection system has been implemented at the tip of such internal plates to reduce the tip resistance [1].

h) Cyclic penetration as mitigation measure

If the soil resistance is much higher than expected or the maximum allowable suction pressure is limited, cyclic penetration of the suction anchor can be performed. Cyclic penetration as a mitigation measure for installation has been demonstrated in Reference [322], as also illustrated in Figure A.38. The sequences for the mitigation measure are as follows:

1) Penetrate the anchor using self-weight with top ventilation hatch opened. The hatch is closed after self-weight penetration has ceased and before pumping can be started.

2) Penetrate the anchor deeper by evacuating entrapped water and creating under-pressure.

3) If under-pressure reaches the allowable limit, reverse the pumping directing and create overpressure. The anchor should be jacked up (suggested upward movement per cycle as a starting point can be 0,5 m).

4) Penetrate the anchor again by creating under-pressure.

5) Apply the cyclic penetration until target penetration is achieved.

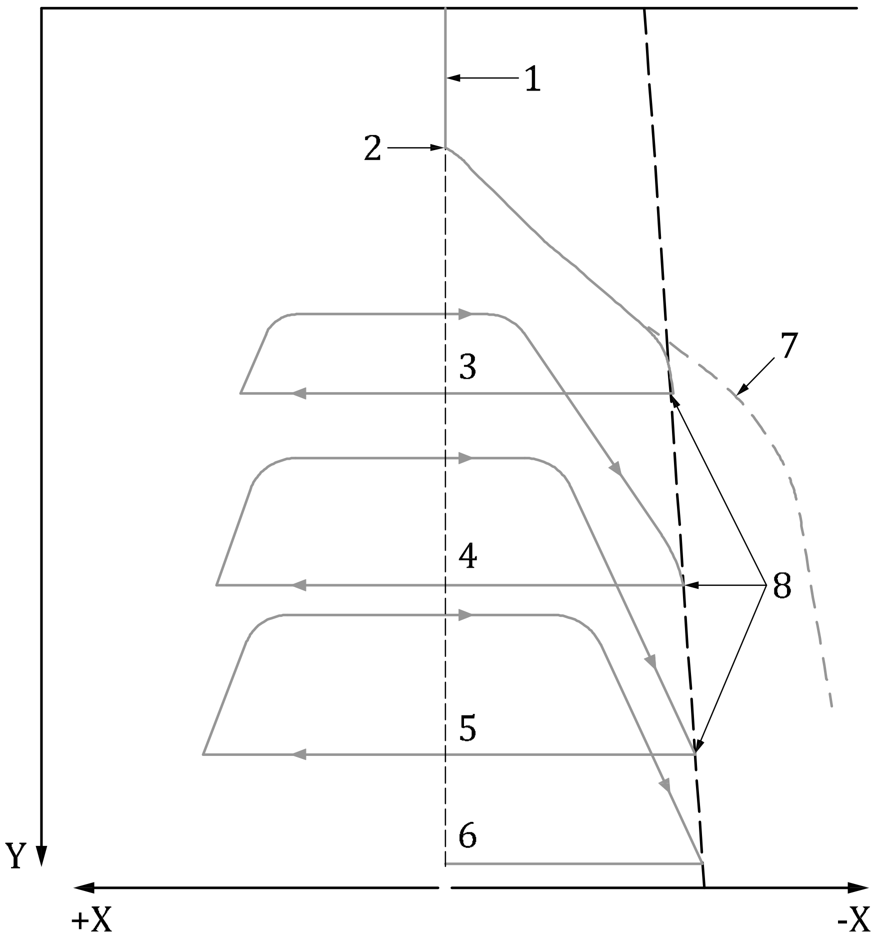

Key

+-X Positive and negative differential pressure
Y Penetration depth
1 Weight penetration
2 Start pumping water out of bucket
3 1st cycle
4 2nd cycle
5 3rd cycle
6 Stop pumping at target depth
7 Required negative differential pressure (suction) without cycling
8 Lower bound pressure limit (pump cavitation)

Figure A.38 — Example sequences of cyclic penetration in stiff clay [322].

A.11.5.2.2.2 Removal analysis

The geotechnical analysis should also consider anchor retrieval for the following cases:

a) Mobile (temporary) moorings where anchor removal is needed for reuse of the anchoring system or to clear the seafloor. The suction pile retrieval procedure and analysis should account for the estimated maximum set-up time.

b) Permanent moorings where local regulations require removal of the anchors after the structure has reached the end of its service life. The suction pile retrieval procedure and analysis should be based on full soil set-up.

c) Mobile or permanent moorings where installation tolerances are exceeded, a mooring line is damaged during installation, or for other contingencies.

The extraction pressure required to retrieve the anchor, $(\Delta U_{\mathrm{req}})_{\mathrm{retr}}$, can be calculated by:

$$(\Delta U_{\mathrm{req}})_{\mathrm{retr}} = (Q_{\mathrm{tot}}\,(t = t_{\mathrm{r}}) + W') / A_{\mathrm{in}} \tag{A.76}$$

where

$Q_{\mathrm{tot}}\,(t = t_{\mathrm{r}})$ is the total soil resistance at time of retrieval, t_{r}, in which time $t = 0$ is defined as the time at the end of penetration;

W' is the submerged weight of the anchor during retrieval;

A_{in} is the plan view inside area where extraction pressure is applied.

When calculating the total soil resistance during retrieval, $Q_{\mathrm{tot}}\,(t = t_{\mathrm{r}})$, Formula (A.69) can be used with some modifications. The interface shear strength can be higher than its value during installation due to soil set-up. Guidance on assessing the increase in friction factor with time is given in A.11.5.2.2.4.

The designer should also consider possible differences between end bearing resistance in tension and compression for protuberances. In addition, the maximum extraction pressure used should not be higher than the pressure causing soil plug failure.

The vessel removing the anchor is often capable of applying a lifting force on the anchor with the recovery line. This assistance can significantly reduce the required extraction pressure and should be included in the removal analysis. Therefore, any loading taken by the lifting line during retrieval can be subtracted from the numerator in Formula (A.76).

The effect of the maximum extraction pressure on the steel structure of the suction pile should also be considered (see A.11.5.2.3).

A.11.5.2.2.3 Holding capacity

Analysis and design tools to determine the capacity of suction anchors can be classified as one of three general methods [18], [67]. These are, in order of decreasing detail:

— the finite element method (FEM) or other advanced numerical analysis;

— limit equilibrium or plastic limit analysis methods (models involving soil failure mechanisms);

— semi-empirical methods (highly simplified models of soil resistance including beam-column models).

For the analysis and design of suction anchors for anchoring deep-water floaters, the central focus is the ultimate capacity of the suction anchor and not the loading–displacement behaviour.

It is recommended that suction pile designs for permanent moorings use FEM, limit equilibrium techniques or plastic limit analysis. For mobile moorings with mainly horizontal actions, semi-empirical methods, such as beam-column analysis using lateral loading or axial shear transfer–displacement curves (i.e. p–y, t–z, Q–z curves described in 8.4 and 8.5), are also considered adequate, if suitably modified. A method to modify p–y curves to account for the larger diameter of suction piles and to ensure lateral displacement is not overestimated can be found in Reference [326]. The merits and shortcomings of each method are discussed in the following.

a) Finite element method (FEM)

As discussed in References [18] and [67], the FEM is the most rigorous general method of analysis available for complex structural systems (including soil continua and soil-structure interaction). The FEM identifies the critical failure mechanism without prior user assumptions, provided an appropriate constitutive model is used. The FEM also has many advantages including the ability to include complex geometries, spatially varying soil properties, and nonlinear constitutive behaviour with failure criterion. Major disadvantages include the required specialist knowledge of advanced numerical analysis and the large time investment to set up a model.

In ductile systems (foundations in soft clays are usually in this category), the ultimate capacity of the system is independent of the sub-failure properties (e.g. Young's modulus, Poisson's ratio, see Reference [77]). It has been shown that carefully formulated and executed analyses give system capacities that compare favourably with the few exact, analytical solutions available [286].

FEM software programs are widely available and have been used to advantage for assessing specific suction pile configurations, matching the few experimental results available and providing calibration of simpler models. Such analyses require special expertise and a significant investment in time and are therefore not yet well suited to parametric studies or conventional design iteration, such as are required for finding the optimum anchor line attachment point.

However, FEM analysis can be warranted for complex loading and/or soil conditions where little experience is available, or to gain insight on specific behavioural aspects of the foundation (i.e. assessment of pore pressure changes and effective stress path at any point within the soil mass).

b) Limit equilibrium or plastic limit analysis methods

As discussed in References [18] and [67], these models are more approximate than FEM models, but are generally much easier to use than general FEM programs. The methods involve estimating the ultimate capacity of plastic systems using assumed failure mechanisms. These mechanisms are typically based on a combination of experimental observation, more rigorous numerical or analytical studies, and engineering judgment. These methods can also include the ability to incorporate complex geometry and soil strength variability and do not require characterizing sub-failure behaviour.

Disadvantages of these methods are the approximate nature of the analysis and the difficulty of generalizing results, i.e. the need to calibrate the models to experiment or more rigorous analysis for specific structural configurations and soil profiles. For example, changes in soil strength profile, anchor geometry, mooring line loading inclination, anchor padeye attachment point, or loading type (e.g. duration, frequency, ratio of cyclic-to-mean loading component) can require a change in the basic geometry of the assumed failure mechanism.

In general, there are two approaches that can be taken using assumed mechanisms: the limit equilibrium method and the plastic limit analysis method. In the limit equilibrium method, a failure mechanism is assumed, usually described in terms of one or more geometric parameters [12]. The body force distribution, stress boundary conditions, and the stress or force distribution on failure surfaces are estimated, and a search is conducted to find the geometry that is closest to the equilibrium conditions. The plastic limit analysis method also uses an assumed failure mechanism with the added requirement that the mechanism satisfies kinematic constraints (e.g. incompressibility for a purely cohesive material, displacement continuity) [287], [252].

A possible failure mechanism is shown in Figure A.39. Other proposed mechanisms can be found in References [252], [321]and [283]. Depending on the failure mechanism, the anchor is shown to resist vertical uplift actions by self-weight, skin friction, REB and/or shear and/or rotational failure at the pile tip, passive and active earth pressure, and soil flow around the pile.

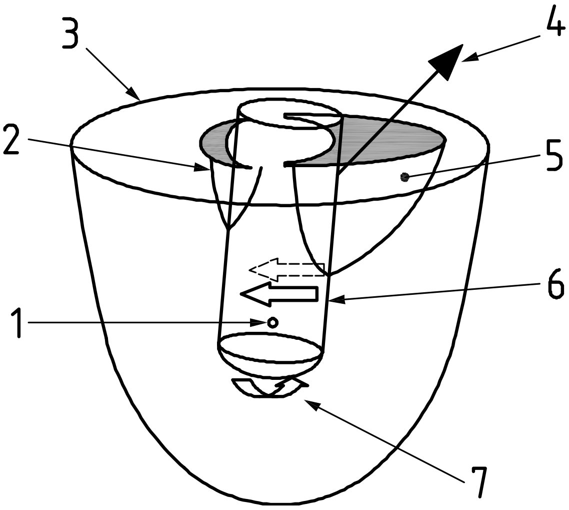

Key

1 centre of rotation
2 active wedge failure zone
3 boundary of soil volume shown
4 applied action
5 passive wedge failure zone
6 flow around zone
7 tip rotational resistance

Figure A.39 — Three-dimensional view of a possible failure mechanism

In some limit equilibrium methods, the circular area is transformed to a rectangle of the same area with the width equal to the diameter, and 3D effects are accounted for by side shear factors [12].

In general, both limit equilibrium and limit analysis methods give upper bound estimates of ultimate capacity such that minimizing the ultimate capacity with respect to the geometric parameters give the ‘best’ answer for the particular mechanism. However, the ‘best’ answer is not always close to the ‘true’ answer depending on the assumed mechanism. In the limit equilibrium method, the result is not a true upper bound if the mechanism does not satisfy kinematic constraints. A discussion of these methods is provided in Reference [77].

A number of existing computer programs implement these methods, but there is no single general, industry accepted program or procedure. Selected models have been shown to compare favourably with more rigorous FEM results for soft clay profiles and various anchor geometry and mooring line attachment points [17], [71].

Automated solutions using these approaches generally require much less input description and are much easier to use than general FEM programs. As a result, they are well suited for conducting parametric studies and design iterations. These solutions do not necessarily converge to correct capacity estimates even with great care and analyst skill, and results from different formulations can give significantly different answers. Thus, obtaining accurate results is greatly dependent on the analyst’s engineering judgment.

c) Semi-empirical methods – beam-column analysis

As discussed in References [18] and [67], these models are the most approximate, but generally are the easiest to use if computer programs with FEM, limit equilibrium or plastic limit analysis methods are not available. They are labelled semi-empirical to suggest that they incorporate the basic mechanics of a suction pile loaded to failure, but depend on a set of empirical rules to represent the soil resistance. These rules are typically less general than for the methods discussed in items a) and b). For example, they do not explicitly incorporate soil failure mechanisms, but instead represent the soil resistance as a loading distribution varying along the boundary of the soil-pile interface. It is difficult to generalize such a loading distribution for a wide range of soil profiles so a particular solution can apply, for instance only to a normally consolidated strength profile. Rules for constructing these distributions are typically based on a combination of experimental and analytical results. In the so-called beam-column model, the soil is represented by uncoupled, nonlinear soil springs along the pile boundary. The beam-column method can provide estimates of the loading–displacement history up to and including the full capacity of the soil-pile system.

In the beam-column model, the soil resistance is represented by uncoupled, nonlinear soil springs (*p*–*y* curves), which describe the sub-failure behaviour of the local soil resistance as well as the peak capacity [243], [237]. In the *p*–*y* formulations for piles (see 8.5), the curves exhibit softening behaviour (i.e. reduced resistance with continued displacement) to account for the effects of cyclic loading [238]. It has been argued in Reference [166], that ultimate capacity estimates for piles, and thus for suction piles as well, should be based on non-softening (static) *p*–*y* curves. In this model, the governing equations of a beam on a (nonlinear) elastic foundation are solved iteratively until an equilibrium solution is found for a given value of the applied force. The user can gradually increase the force in subsequent steps until the solution no longer converges, a point which is interpreted as failure.

The beam-column model has been used by geotechnical engineers for almost 50 years for the analysis of laterally loaded piles. Hence, it has the decided advantage of being a familiar tool. There are many beam-column programs in use, including general purpose programs where forces as well as nonlinear springs can be prescribed at virtually any point on the pile, as well as special versions where nonlinear spring construction is automated based on minimal soil property input. Thus, there can be an understandable tendency for engineers to select these programs for suction pile analysis. The user should be aware that these programs have significant limitations. As detailed in References [18] and [67], the limitations of conventional beam-column models include, but are not limited to:

- Ignoring the fact that the resistance elements depend on the deformation mode and ignore the coupling between the resistance elements, which can lead to large errors, particularly for relatively short piles.
- Not including independent side shear resistance components on active and passive sides to model different relative shear displacements between the soil and the pile on the two sides.
- Not including the coupling between the horizontal and vertical soil resistance components along the pile sides and thus not showing the effect of inclined anchor forces. It is possible in principle to couple these elements (*p*–*y* and *t*–*z* curves), but this has only been done in special cases (see Reference [164]).
- Requiring input that is not essential to the capacity assessment, such as pile bending stiffness and sub-failure soil response, and producing output that is of little interest for the analysis, such as moment and shear profiles and resistance–deformation response that are probably not very accurate. Because most piles are stiffened shells, the beam equations are of doubtful validity and are largely irrelevant with regard to stresses in the pile. A better pile model in these circumstances is actually a rigid body that can be approximated by setting the pile flexural rigidity (EI) to an arbitrary large value (see ISO 19902 and ISO 19901-7 for recommendations on structural design).
- Requiring user intervention to determine the pile capacity. In most beam-column programs, the ultimate capacity is determined by trial and error, gradually increasing or decreasing applied forces until the minimum force that produces numerical instability (interpreted to be the 'failure limit') is found.
- Requiring special elements for rotational, vertical and horizontal tip resistance.
- Not explicitly including effects such as soil-pile interface roughness and loss of soil contact on the back side of the pile.

It is possible to formulate and implement a beam-column program that overcomes most of the above limitations. There seems to be little incentive to do so however, as other methods are available that are simpler to implement and can be especially tailored for suction pile analysis.

A.11.5.2.2.4 Increase of side friction with time

As described in A.11.5.2.2.1 item a), the side friction at a given depth can be calculated as $\alpha_{ins}.s_{uDSS}$. With the passage of time after installation, the side friction increases through soil thixotropic effects and pore pressure redistribution at the soil-pile interface, i.e. set-up. Set-up effects are often addressed by estimating the change in the friction factor, α_{ins}, with time. Set-up mainly influences the vertical capacity, and to a lesser extent the horizontal capacity of suction piles [14].

The set-up process can be different for that part of the anchor penetrated by weight and that part penetrated by under-pressure. For suction piles in highly plastic clays, the set-up time can be long and there can be a permanent loss of shear strength, whereby the ultimate side friction after full set-up is less than the original undisturbed shear strength (i.e. the friction factor, α_{ins}, is less than 1,0 after full set-up), both for that part of the anchor penetrated by weight and that part penetrated by under-pressure.

Some researchers [14] have reported that the part of the anchor penetrated by under-pressure is expected to typically have a shorter set-up time and a lower ultimate side friction after full set-up than the part penetrated by weight. Figure A.40 shows a typical soil set-up prediction graph for a large diameter suction anchor in typical Gulf of Mexico soils (a), and for a driven pile (b). The methods in References [14] and [47] are shown to illustrate the potential differences in set-up time and ultimate friction for different parts along the side of the anchor. The set-up along the part of the anchor penetrated by under-pressure can occur much faster, but the permanent reduction can be larger. The method in Reference [47] was developed for driven piles with a ratio of diameter-to-wall thickness of less than 40. The method in Reference [14] was proposed for penetration by under-pressure. Both methods should be applied with caution outside the range of data used in their development. Other methods developed for driven piles include the one described in Reference [361]. There is no single industry-wide accepted set-up curve. Based on suction anchors installed and later retrieved in soft Gulf of Mexico clay the set-up characteristics can be found in Reference [190].

As with other piled foundation systems, the calculated anchor ultimate capacity should be reduced if soil set-up is not expected to be completed before significant forces are imposed on the anchor pile.

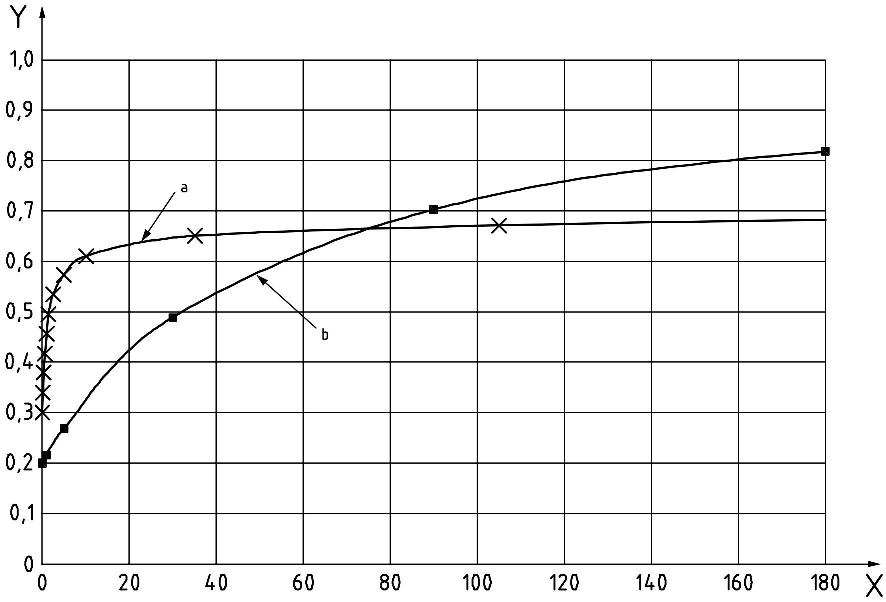

Key

X time after installation (days)

Y friction factor α = (side friction at time t) / (undisturbed soil shear strength)

a Reference [14] – α_{ins} during installation = 0,3 ; α at 90 % set-up = 0,65.

b Reference [47] – Pile diameter = 1,83 m (6 ft) ; wall thickness = 46 mm (1,8 in) ; average curve.

Figure A.40 — Example of increase in friction factor with time

Set-up can be addressed in various ways during design. The designer can ensure adequate anchor capacity if:

— the suction pile is designed with partial soil set-up;

— the suction pile is installed well in advance of the floating structure hook-up to ensure adequate soil set-up when the mooring system experiences design actions;

— for a limited amount of time between installation of the mooring system and the part of production, reduced extreme action criteria can be assumed, based on suitable risk analysis.

A.11.5.2.2.5 Coupling between horizontal and vertical capacity

When a suction anchor resists design actions, the vertical and horizontal components of the anchor capacity are not mobilized independently. Coupling vertical and horizontal capacities can be important in some cases. Studies have shown that for mooring line angles at the padeye between 15° and 45° (as measured from horizontal), it can be non-conservative to neglect this coupling [12], [287].

This subclause is for illustration only and is not intended to be used for design. The example failure interaction diagram shown in Figure A.41 is typical of suction piles with a length-to-diameter ratio of 5, in soil with a linear increasing shear strength profile and low shear strength at the seafloor. The mooring padeye is located on the pile shell, about two thirds of the way down from the seafloor. In this example, the diagram shows that if the force is primarily vertical, with mooring padeye angles from 40° or 45° to 90°, the failure mode is controlled by vertical pull-out and 100 % of the vertical capacity is available. In a similar manner, if the force is primarily horizontal, with mooring line padeye angles from zero to 15°, the failure mode is controlled by horizontal pull-out and 100 % of the horizontal pile capacity is available. In this case, the maximum horizontal capacity is equal to 1,8 times the vertical capacity. If, however, the mooring line padeye angle is between 15° and 40°, less than maximum vertical and horizontal capacities are available. In the example shown, only 90 % of the vertical capacity is available, and the available horizontal capacity is reduced from an original 180 % to 150 % of the vertical capacity.

Examples of failure interaction diagrams can be found in References [86] and [32].

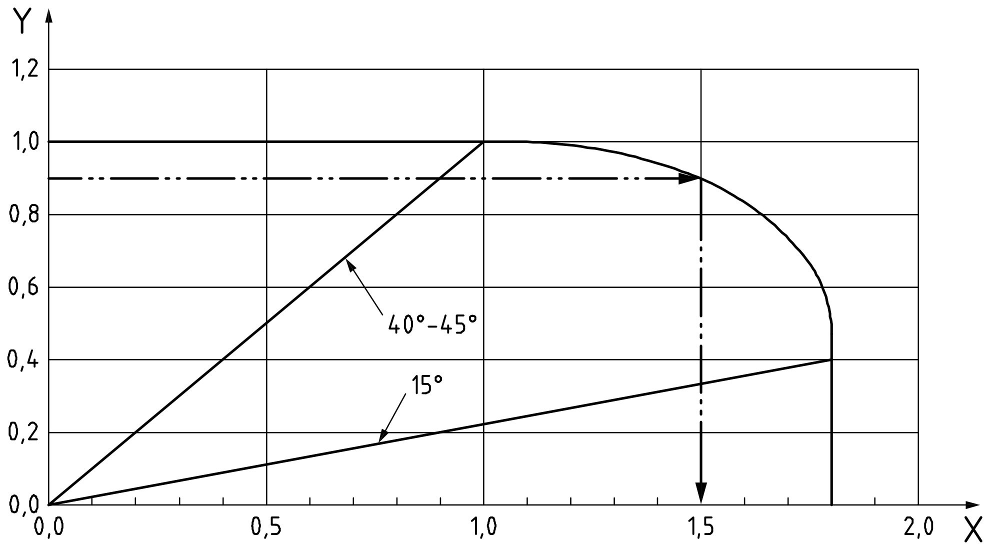

Key

X	H/ Vmax	H	horizontal loading component
Y	V/ Vmax	Vmax	vertical ultimate capacity of the anchor, for purely vertical actions
V	vertical loading component		

NOTE 1 This interaction diagram is for illustration only and is not intended to be used for design.
NOTE 2 Loading angles at mooring padeye are measured from the horizontal.

Figure A.41 — Example of failure interaction diagram

A.11.5.2.2.6 Safety factors and allowable actions for suction anchor piles

Safety factors for holding capacity, defined as the calculated capacity divided by the maximum anchor action from dynamic analysis, are provided in ISO 19901-7:2013, Table 7 for axial and lateral actions. Axial safety factors consider that the pile is primarily loaded in tension, and are therefore higher than for piles loaded in compression. As the lateral failure mode for piles is considered to be less catastrophic than the vertical one, lower safety factors have been recommended for lateral capacity. Guidance on coupling between vertical and horizontal capacities is given in A.11.5.2.2.5.

The safety factor used in design should be based on the failure mechanism controlling the capacity and not only on the mooring line padeye angle. Although mooring line padeye angle and failure mechanisms are related, other parameters, such as soil profile, anchor geometry and mooring line attachment point, are also important in determining failure mechanisms. The minimum factors of safety should be as per ISO 19901-7:2013, Table 7. It is recommended to establish ultimate capacity envelopes for the selected padeye location. The allowable action envelope can then be found by dividing the lateral and vertical action components along the ultimate capacity envelope by their respective design safety factors (these factors are different for vertical and lateral actions). Once an envelope of allowable action is derived, the design actions can be transposed onto this envelope to ensure minimum safety factors are met. This approach is similar to that used for shallow foundations.

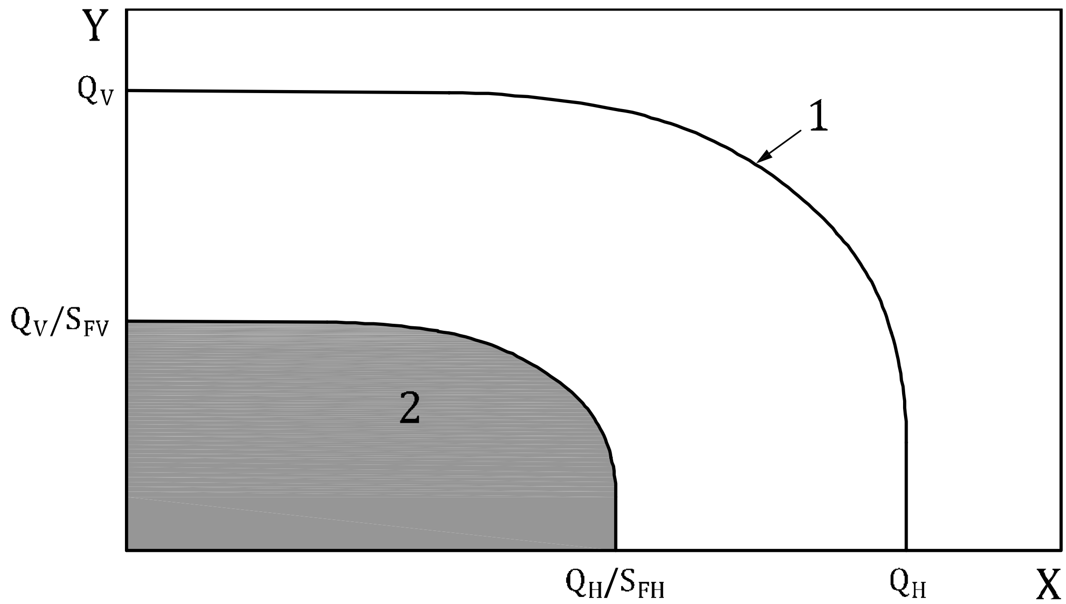

Key

X Horizontal action

Y Vertical action

Q_V Vertical ultimate capacity

Q_H Horizontal ultimate capacity

S_{FV} Axial safety factor

S_{FH} Laterall safety factor

1 Envelope of design resistance

2 Envelope of allowable design action

Figure A.42 — Illustration of envelopes with factors of safety for ULS design

A.11.5.2.2.7 Other special considerations

The following aspects with respect to analysis methods should be considered:

a) Closed vs. open top

The top of the anchor should remain sealed throughout the life of the field, if the REB at the anchor tip is to be relied upon in design, unless the sum of inside friction is equal or larger than the REB. With increased soil set-up and side friction, the need for REB decreases and, thus, the requirement to maintain a sealed top cap also decreases. For anchors with essentially horizontal loading, a sealed top is not essential for ensuring capacity, and the top part can be removed after installation [93].

b) Strength anisotropy

Anchor holding capacity calculations should be performed with anistropic shear strength, including the effects of combined static and cyclic loading history.

c) Internal ring stiffeners

For large long-term actions and for suction piles that are not sealed at the top, the skin friction along the inside skirt wall is an important contribution to the capacity. The inside wall friction can be significantly lower than the original shear strength due to the disturbance during installation, especially if the anchor has internal stiffeners. In piles with ring stiffeners, clay from the upper part of the profile, possibly mixed with seafloor water, can be trapped between the stiffeners and give low capacity at larger depth. In such cases, the compartment between the ring stiffeners can also act as a drainage channel [18], [67], [108].

d) Gapping

A gap can form on the outside at the active side (i.e. 'back' side) of the anchor. There are uncertainties on how to predict gap formation, unless the clay is soft and with essentially zero strength intercept at the seafloor or if the loading duration is lower than needed for significant suction dissipation to take place at the back of the pile, in which cases a gap is not expected to form. If gapping is possible and anchor capacity is not sufficient in this case, conservatively placing the anchor padeye attachment point at the depth required for the suction anchor top to move 'backwards' (i.e. away from the direction of the mooring line) should be considered during loading to prevent gap formation. Such precaution will avoid the possibility of free water to dissipate down through a gap all the way to skirt tip level and thereby potentially compromise the utilization of full reverse end bearing if relied upon for anchor capacity. Several experts have investigated the optimized padeye location by taking into account that free gapping has occurred (see References [282] and [110]).

e) Installation tolerances

The allowable installation tolerances (e.g. tilt and orientation) should be included in the holding capacity calculations, as tilt and out-of-plane loading can reduce the holding capacity of the anchor.

f) Change in outer diameter

Variations in outer diameter with depth can reduce the outside interface strength. In general, designs with variations in outside anchor diameter should be avoided.

g) Sand layers

Sand layers, if present, can have a significant effect on holding capacity. It should be ensured that the sand layers do not cause excessive drainage and pore pressure redistribution that can negatively affect the REB, particularly if the anchor is to resist long-duration loadings (see A.11.5.2.2.1, item e)).

h) Distance between installation locations

In the event that an anchor needs to be retrieved and re-installed, the determination of the minimum distance between the first location and the subsequent location should ensure that the soil disturbed during the first installation is not mobilized when the anchor resists the design action at the subsequent location. Industry practise has typically been to suggest a distance of 3 diameters centre to centre in the direction of the loading, while 2 diameters are often suggested perpendicular to the side of the loading.

i) Sustained actions

The duration of sustained actions (e.g. creep under loop current action) and the period of cyclic loading should be considered, and the anchor capacity should be adjusted to account for these effects. Examples of capacity reduction as a function of action hold time for vertically loaded anchors in Gulf of Mexico clays can be found in References [87].

j) Seabed trenching from large amplitude movements of ground chain

Large amplitude movements of the ground chain can cause significant trenching of the seabed sediments in front of anchors. When site specific conditions make the mooring more susceptible to trenching, such as turret-type mooring systems or buoy moorings in the long swell of West Africa (see References [44] and [96]), such trenching can extend to the suction anchor chain padeye depth and can compromise the anchor capacity.

NOTE All types of anchors embedded in soft clays can be subject to trenching in case of semi-taut to taut deep-water mooring systems subject to large amplitude chain motions. The occurrence of large trenches in front of suction anchors in the Gulf of Guinea is well documented, but more site observations are needed to cover other types of anchors (i.e. drag anchors, driven anchor piles, plate anchors and gravity-embedded anchors) in other geographical areas (e.g. offshore Brazil and the Gulf of Mexico).

This is a particular risk with taut and semi taut-leg moorings where both small amplitude wave cycles and large amplitude motions imposed by the sea surface floater applied to the mooring line and transmitted to the ground chain can lead to the trench formation. While all soil types can be damaged by this process, soft and sensitive soils are most prone to substantial degradation, which can ultimately lead to the soil being uplifted into suspension and transported away, resulting in trench formation. There are no published methods available today that can predict the final trench shape but one interesting phenomenon that has been observed in the field is tunnelling in the soil towards the chain padeye [347] occurring as an effect of the chain movement between high and low-tension chain configuration in relation to the surface vessel motions. The assessment of whether or not chain trenching is a risk in any particular case should first consider the mooring line, the change in inverse catenary configuration and the loading (or surface vessel motions) applied [265] with close cooperation between mooring and geotechnical specialists. Chain trenching in front of the anchor can also occur with catenary moorings, unless chain motion can be controlled by design such that trenching will not propagate back from the touchdown point towards the anchor sufficiently to compromise its holding capacity. It is expected that locations where long amplitude swell leads to regular and repeated large amplitude chain motions (e.g. as experienced at some West African locations) are more likely to lead to significant trench formation than locations where small amplitude wave loading dominates, with only occasional large amplitude motions during significant storm events.

If potential chain trenching is identified as a risk, then some of the following mitigations can be considered for incorporating the impact of trenching or decreasing the amplitude of mooring line and ground chain motions:

1) design the anchor assuming an appropriate size trench;

2) increase the number of mooring lines in the most-heavily loaded clusters;

3) increase the mooring radius for changing the mooring configuration from a taut/semi-taut setting to a more catenary setting (where seafloor infrastructure configuration and floater offset limit can allow for such increase in mooring radius). if chain motion can be controlled to limit trenching propagation to an adequate setback distance from the anchor;

4) Consider spread-mooring systems which are less susceptible to transmit the surface floater motions to the ground chain than turret-type moorings;

5) Consider different padeye depths to determine the optimal configuration with respect to anchor capacity while minimizing the impact of the trench.

Where a risk of chain trenching is identified and accounted for in design, it is recommended that the development and propagation of trenching should be regularly monitored by subsea inspections [30] in order to ensure that the trench design assumptions and the anchor capacity remain applicable. 3D finite element analysis [5], [136], [75], [347] or other appropriate tools (e.g. centrifuge testing as described in Reference [75]) that can incorporate the actual trench geometry should be used to assess the in-place holding capacity of an anchor including a chain trench. Where the reduction in anchor capacity because of the trench is found critical, removing the anchor and relocating it laterally in virgin soil away from the trench should be considered (possible option for suction anchors, drag-embedded or gravity-embedded anchors when driven anchor piles that cannot be retrieved will need to be replaced).

k) Combination of skirt wall friction and reverse end bearing to calculate ultimate pull out capacity

Peak skirt wall friction is generally mobilized faster (less vertical displacement) than the reverse end bearing for suction anchors when the anchor is pulled out. Caution should therefore be made when calculating the ultimate axial holding capacity. Combining reverse end bearing based on a bearing capacity factor of N_c=9 works nicely with use of the peak skirt wall friction factor along the outside skirt wall [193].

A combination of these considerations can be used to arrive at a suitable suction pile design. Due to the complexity of analysing the capacities of large suction piles for permanent mooring systems, a geotechnical specialist should be consulted.

A.11.5.2.3 Basic considerations for structural strength design

Guidance and design criteria for structural design of suction anchor piles are given in ISO 19901-7. The purpose of this subclause is to provide basic considerations to be taken into account by the structural designer in collaboration with the geotechnical designer.

The suction pile structure and its installation appurtenances should be designed for the maximum actions induced by suction anchor handling, transportation, lifting, upending, lowering, recovery, embedment, and extraction (where relevant).

For anchor embedment, the estimated upper bound suction under-pressure required to embed the anchor to its design penetration should be used for the design of anchor wall and anchor cap structure. However, the maximum suction under-pressure used need not be higher than the suction at which internal soil plug uplift occurs.

The estimated maximum internal pressure required to extract the anchor (where relevant) should be used for the design of anchor wall and anchor cap structure.

In all cases (i.e. embedment or extraction), the maximum under-pressure available during installation (or maximum internal pressure for extraction) will be the minimum value between the required installation under-pressure (or extraction pressure) and the pressure that the anchor is structurally designed to resist without damage. Guidance about the buckling strength of suction piles is given in Reference [92].

A.11.5.2.4 Installation of suction anchors

In order to verify that the suction pile installation is successful and in agreement with design assumptions, for both permanent and mobile (temporary) moorings, the following data should be monitored and recorded during installation:

a) structure and pile identification, water depth and reference elevation of readings of anchor penetration markings;

b) distance from intended seafloor location (with mention of installation tolerance);

c) penetration of the pile under its own weight;

d) installation under-pressure (suction), corrected for hydraulic pressure losses in the pumping system;

e) final penetration depth (with mention of design target penetration);

f) pumping flow-rate and pile penetration rate;

g) date and time of starts and stops in penetration, including set-up time;

h) verticality (with mention of installation tolerance);

i) orientation (with mention of installation tolerance);

j) any unusual behaviour during installation.

For permanent mooring systems, other parameters usually monitored include plug soil stability at all depths and soil plug elevation (and heave) at final penetration.

A.11.6 Geotechnical design of plate anchors

A.11.6.1 Basic considerations

For plate anchors, the ultimate holding capacity is often defined as the ultimate pull-out capacity (UPC), which is the force in the mooring line at which the soil around the anchor fails. At UPC, the plate anchor starts moving through the soil in the general direction of the mooring line with no further increase in resistance or with a gradual reduction in resistance. However, for some designs, the plate anchor starts diving deeper upon over-loading (i.e. the mooring line force at the anchor is greater than the original UPC), until it reaches a more competent soil layer where the over-load can be resisted.

The plate anchor UPC is a function of:

— soil undrained shear strength at the anchor fluke;

— projected area of the fluke;

— fluke shape;

— bearing capacity factor;

— depth of penetration.

When determining the anchor UPC, the disturbance of the soil due to the soil failure mode should be considered. This disturbance is generally accounted for in the form of an empirical reduction factor. This factor should be based on reliable test data and relevant studies. Typically, in order to generate a deep failure mode, the plate anchor's penetration depth in clay should be about 4,5 times the equivalent width (i.e. minimum dimension) of the fluke. If the final depth does not generate a deep failure mode, the bearing capacity factor should be reduced accordingly (see e.g. Reference [117]).

Plate anchors get their high holding capacity from their embedment into more competent soil. Therefore, it is important that the anchor's penetration depth is established during the installation process.

A design method applicable to all types of plate anchors in clay is described in Reference [117]. The various anchor types differ in terms of installation method, but they all end up as a plate anchor after rotation/keying/triggering.

For all types of plate anchor, it is important to verify by measurement the installation depth, i.e. the depth equals the target installation depth of the anchor. During subsequent rotation/keying there is generally a loss in penetration depth which should be taken into account when setting the target installation depth.

A plate anchor achieves its UPC by having its fluke oriented nearly perpendicular to the direction of the applied loading. To ensure that the fluke rotates to achieve a maximum projected bearing area, the plate anchor design and installation procedure should:

a) As part of the installation, facilitate rotation of the fluke to a position that ensures that, when the anchor is subjected to a higher tension during a design event, the fluke continues to rotate to a position perpendicular to the direction of the applied tension.

b) Ensure no significant loss of penetration occurs during anchor rotation, which can move the fluke into weaker soil. The pull-out capacity of plate anchors partly penetrated into a stiffer layer underlying a soft layer should consider the influence of the overlying soft layer on the long-term capacity. Loss of penetration during anchor rotation/keying/triggering in such situations should be given special attention.

c) Have the structural integrity to sustain fluke rotation about both horizontal and vertical axes, depending on the type of plate anchor and its installation orientation.

Factors of safety for holding capacity of plate anchors are provided in ISO 19901-7:2013, Table 8.

A.11.6.2 Prediction method for drag-embedded plate anchors

A.11.6.2.1 General

The following aspects of drag-embedded plate anchor performance should be determined:

a) anchor line mechanics;

b) installation performance;

c) holding capacity performance.

All three aspects are closely linked and influence one another, as described in A.11.6.2.2 to A.11.6.2.4.

A.11.6.2.2 Anchor line mechanics

As discussed in References [117] and [253], anchor line mechanics strongly influences the drag-embedded plate anchor's final orientation and depth below the seafloor, which in turn governs the holding capacity of the anchor.

Figure A.43 is a schematic of an anchor line configuration showing the inverse catenary of the line as it cuts through the soil. As the line tension increases, the anchor continues to penetrate and the inverse catenary of the embedded line increases the line angle at the anchor attachment point. The deeper the anchor penetrates, the larger the angle at the attachment point becomes, which ultimately sets the limit for penetration leading to continuous drag of the anchor without forerunner increase in tension.

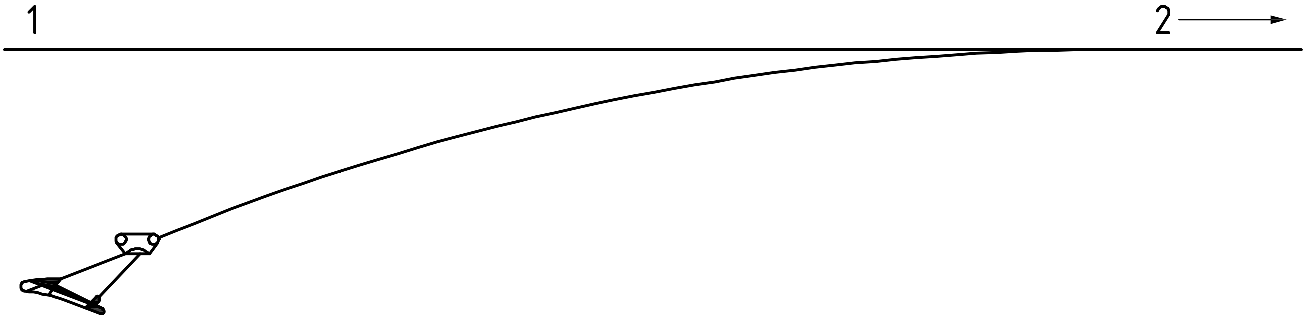

Key

1 seafloor

2 seafloor mooring force

Figure A.43 — Schematic of anchor line configuration during embedment

In general, this problem is approached in the same manner as that for predicting the displaced shape of a catenary, fixed at both ends, and deformed by its own weight plus bearing pressures exerted from the soil normal to the line and the shear resistance tangential to the line. The governing differential equations for this system of forces are nonlinear and require an iterative numerical solution.

A.11.6.2.3 Installation performance

As discussed in References [117] and [253], the capacity of a drag-embedded plate anchor depends strongly on its final orientation and depth below the seafloor, hence prediction of the anchor trajectory during installation is a critical issue. Figure A.44 is a schematic diagram showing a typical anchor trajectory and sequence of anchor orientations as the anchor line is dragged along the seafloor.

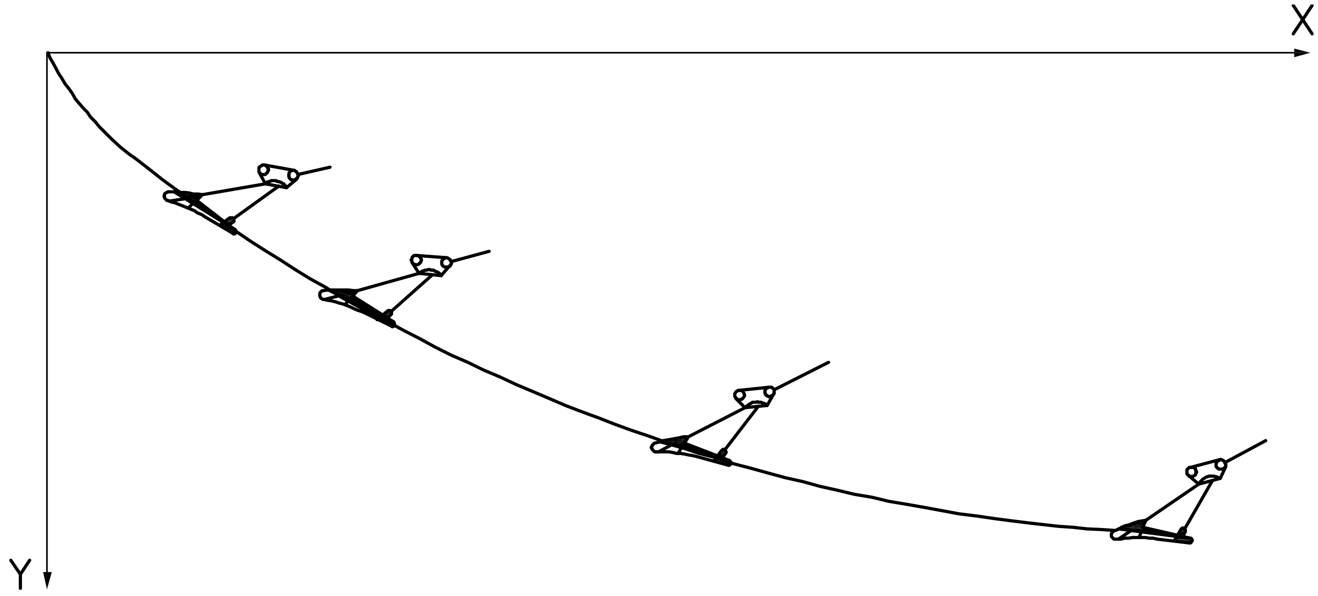

Key

X drag distance

Y anchor embedment depth

Figure A.44 — Anchor trajectory and fluke orientation during embedment

Methods for predicting this trajectory generally fall into four groups.

1) Empirical methods: these are typically based on correlations with observed anchor performance and dependent on anchor characteristics (i.e. weight) and an approximate measure of the soil resistance. However, many of these field studies are not available in the public domain.

2) Limit equilibrium methods: these take into account a more detailed description of soil and anchor geometry/weight. The methods are based on an estimated soil reaction distribution on the anchor at failure. Site specific soil and anchor information can be incorporated in detail. This approach is most commonly used, and commercial software based on this approach is available (see Reference [102]).

3) Plastic limit analysis: this is similar to the limit equilibrium methods. Virtual work principles are used to minimize the calculated failure capacities with respect to the geometric parameters defining the failure mechanism at any anchor depth, anchor orientation, and anchor line conditions.

4) Advanced numerical methods, including FEM: these have the potential for obtaining a rigorous solution for all aspects of anchor behaviour. In practice, however, they have considerable limitations. A complete solution would require a FEM defining nonlinear material behaviour, nonlinear boundary conditions, and large strain and large deformation theory. Therefore, even a simple anchor trajectory prediction requires substantial effort to formulate, set up, and solve. However, FEM can be used to check calculations or enhance other prediction methods.

A.11.6.2.4 Holding capacity performance

As discussed in References [117] and [253], anchor holding capacity is only a special case of the installation sequence and, hence, the methods underlying installation prediction described in A.11.6.2.3 are directly applicable.

Provided that the penetration depth of the plate anchor is known and the clay is homogeneous (i.e. non-layered), the holding capacity can be expressed on the basis of conventional bearing capacity theory in conjunction with the anchor line solution, i.e.:

$$F_{\max} = N_c \, A_{\text{eff}} \, \eta \, s_{u,\text{AVE}} \tag{A.77}$$

where

F_{max} is the ultimate holding capacity (UHC);

A_{eff} is the effective area of the anchor accounting for shape and projected area;

N_c is the bearing capacity factor determined, for example, from the method of characteristics or FEM solutions;

η is the empirical reduction factor accounting for progressive failure (i.e. strain softening) when loaded towards failure (see discussion of this factor in Reference [117]);

$s_{u,AVE}$ is the measure of the local average undrained shear strength within the failure zone at the design penetration depth, corrected for effects of cyclic loading (see Reference [117]).

For layered clay, the ultimate holding capacity will be dependent on the position of the anchor relative to the layer boundary (see Reference [117] for guidance).

Overall, considerable judgment and experience is required to evaluate the input parameters for any of the predictive methods. Examples of anchor analysis can be found in References [304] and [103].

A.11.6.3 Factors of safety for drag-embedded plate anchors

Factors of safety for drag-embedded plate anchors are higher than those for drag anchors because overloading of plate anchors normally results in pull-out, while drag anchors, deeply penetrated in soft to stiff clay, either drag horizontally or dig deeper, thereby developing constant or higher holding capacities.

For plate anchors that exhibit similar over-loading behaviour to drag anchors, using drag anchor factors of safety can be considered, assuming the behaviour can be verified by appropriate field tests and experience.

A.11.6.4 Prediction method for direct-embedded plate anchors

Anchor capacity determination for direct-embedded plate anchors is identical to that shown for drag-embedded anchors, with the following exceptions:

— final anchor penetration depth is accurately known;

— nominal penetration loss during keying should be included (usually taken as 0,25 to 1,0 times the fluke's vertical dimension, or B in Figure A.45, depending on shank and keying flap configuration);

— calculation of effective fluke area should use an appropriate shape factor and projected area of fluke with keying flap in its set position.

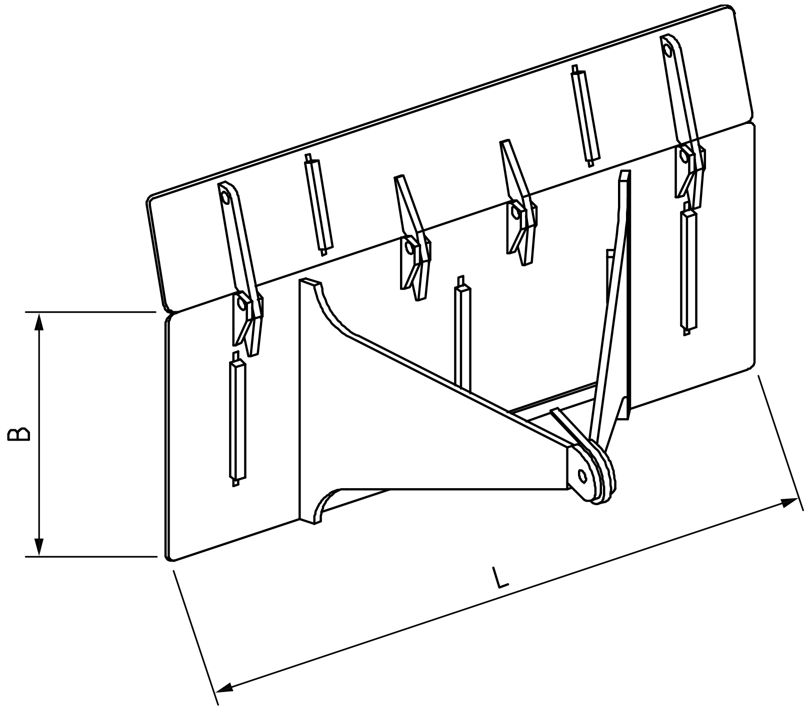

Key

B width

L length

Figure A.45 — Definition of anchor fluke dimensions for a direct-embedded plate anchor

A.11.6.5 Installation of plate anchors

A.11.6.5.1 Installation tolerances

Plate anchor installation tolerances should be established and should be considered in the anchor's geotechnical, structural, and installation design. Typical tolerances to be considered are:

— allowable deviation from target heading of the mooring line attachment to limit padeye side loadings and rotational moments on the anchor padeye;

— minimum penetration required before test loading to achieve the required holding capacity (with allowable loss of anchor penetration during anchor keying/test loading for direct-embedded plate anchors).

A.11.6.5.2 Drag-embedded plate anchors

For drag-embedded plate anchors used in permanent moorings, the anchor design should incorporate adequate installation information to ensure that the anchor reaches the target penetration depth, thereby meeting the safety requirements of the mooring system for the actual soil and design situations. Typical information to be monitored and verified is:

— drag distance;

— drag anchor installation line tension versus time and drag distance;

— catenary shape of installation line based on line tension and line length to verify that uplift at the seafloor during embedment is within allowable ranges and to verify anchor position;

— direction of anchor embedment;

— final anchor penetration depth (not dictated by failure of a shear pin).

Reference [117] provides further guidance on drag-embedded plate anchors.

A.11.6.5.3 Direct-embedded plate anchors

Direct embedment of plate anchors can be achieved by suction, impact or vibratory hammer, propellant, hydraulic ram, or gravity. Installation procedures should be developed and installation analyses should be performed for direct-embedded plate anchors to verify that the anchors can be embedded to the design depth. The installation analysis should also consider plate anchor retrieval, if applicable.

For the embedment analysis for a suction-embedded plate anchor, the risk of causing uplift of the soil plug inside the suction embedment tool should be considered. The allowable under-pressure to avoid soil plug uplift should exceed the required embedment under-pressure by a factor of at least 1,5 [see A.11.5.2.2.1 item c)]. In order to verify that the plate anchor installation is successful and in agreement with the design assumptions, the parameters listed in A.11.5.2.4 should be recorded.

A.11.6.6 Out-of-plane loading of plate anchors

In areas prone to revolving storms, MODUs experiencing one or multiple line failures can exert forces on the anchor that are out-of-plane to the installation direction. This can cause a reduction in the holding capacity of the plate anchor and potentially anchor dragging [151]. On the other hand, plate anchors are also capable of generating significant holding capacity in the out-of-plane direction.

The design of the anchoring system for MODU moorings should take into account the possible consequences of out-of-plane loading, possibly due to nearby infrastructure, . Selection of the appropriate plate anchor in combination with sufficient installation tension to fully embed the anchor can increase the out-of-plane resistance of the plate anchor. The structural capacity of the plate anchor should also be evaluated for out-of-plane loading.

A.11.7 Geotechnical design of other types of anchors

A.11.7.1 Gravity anchors

A.11.7.1.1 General considerations

The gravity anchor structures should satisfy the design requirements for all failure modes including sliding, bearing capacity, overturning and uplift, for both installation and service ULS or ALS conditions.

The recommendations and methodologies presented in 7.3 and 7.4 for the design of shallow foundations are generally applicable for the design of gravity anchor structures.

Except specified otherwise in A.11.7.1.2 to A.11.7.14, the ULS design safety factors for holding capacity of gravity anchors as defined in ISO 19901-7 are applicable.

A.11.7.1.2 Sliding resistance

The sliding resistance of gravity anchors should take into account the following:

a) For the design verification under sustained or longer duration loading (including loading due to currents, tide, squall events), the safety factor should be increased to at least 2,0.

b) In addition to the recommendations in 7.4.2, the shearing resistance between the gravity structure and the underlying soil should consider the drainage conditions (particularly for longer duration loading) of the degradation due to cyclic loading and/or sustained loading, and of the potentially reduced contact area between the gravity base and the soil.

c) If the gravity anchor is equipped with skirts, no contribution from the soil resistance above the skirt tip level should be accounted for, unless the absence of any scour or material loss due to piping is demonstrated by a dedicated study. In addition, appropriate internal stiffeners should be incorporated in the structural design to avoid undesired soil failure within the skirt compartments.

A.11.7.1.3 Uplift resistance

For gravity anchors without skirts, the uplift resistance should not be higher than the submerged weight of the structures.

For gravity anchors with skirts:

- the contribution from friction along the skirts can be included, if the absence of any scour or material loss due to piping has been demonstrated by a dedicated study;
- for the case of short duration (cyclic) uplift loading, cyclic tensile stresses (relative to ambient water pressure) may be demonstrated as acceptable in design, if the recommendations presented in 7.4.5 are followed.

A.11.7.1.4 Serviceability

No additional guidance.

A.11.7.2 Gravity-embedded anchors

A.11.7.2.1 Basic considerations

Examples of applications of gravity-embedded anchors are given in References [53], [220] and [387].

The hydrodynamic design of gravity-embedded anchors should ensure that the anchor maximizes its free-fall velocity prior to impact with the seafloor and achieves directional stability during free-fall in order to obtain the maximum penetration within the seabed sediments.

The hydrodynamic characteristics of the anchor should be such that the anchor maintains its verticality during the free-fall phase of installation through the water column. In addition, any initial inclination of the anchor should be self-corrected during free-fall to ensure anchor verticality upon impact with the seafloor. Specifically, this should be achieved by:

a) ensuring that the centre of gravity of the anchor is as low as possible;

b) maximizing the distance between the centre of gravity and centre of buoyancy;

c) maximizing the distance between the centre of gravity and area centroid of the anchor;

d) establishing a drop height above the seafloor which gives the anchor sufficient time to correct any initial inclination;

e) limiting the drop height to ensure that the anchor trajectory cannot be adversely affected by lateral currents.

The embedment and capacity of gravity-embedded anchors should take into account relevant field experience and scale test results. Assessment of these anchors will require additional scale testing and/or large displacement numerical modelling where:

- relevant field experience is limited;
- variable soil conditions exist, potentially hindering anchor embedment;
- soils exhibit unconventional behaviour (e.g. carbonate materials with high susceptibility to cyclic degradation);
- complex loading conditions prevail.

For gravity-embedded anchors with an asymmetric shape, such as the OMNI-Max anchor with a lateral arm on the anchor body (see Figure A.33 c)), the following additional considerations apply:

a) the intersection of the body centre line and the resultant hydrodynamic force due to asymmetric parts, such as the anchor arm, should be slightly above the centre of gravity in order to compensate the rotation induced by horizontal velocity;

b) the design of the anchor arm (e.g. size, angle) should be optimized to reduce anchor inclination during free-falling by means of computational fluid dynamics (CFD) or experiment;

c) the free-falling height should be restricted based on the actual directional stability obtained from CFD or experiment;

d) synthetic rope can be recommended to service as the anchor line in order to compensate inclination [315].

A.11.7.2.2 Impact velocity prediction

The velocity of the anchor at the point of impact with the seafloor influences the penetration depth and therefore holding capacity of the anchor. The impact velocity is a function of the drop height above the seafloor, the drag characteristics of the anchor and trailing line (rope or chain), and the anchor properties such as the projected area and submerged weight.

The impact velocity can be predicted by considering the forces acting on the anchor during free-fall:

$$m.a = W_s - F_{drag} \quad \text{(A.78)}$$

where

m is the penetrator (anchor) mass;

a is the anchor acceleration

W_s is the submerged weight of the anchor and attached line;

F_{drag} is the hydrodynamic drag acting on the anchor/line.

Assuming the soil acts as a dense viscous fluid, the hydrodynamic drag force acting on the anchor and the line can be calculated in accordance with:

$$F_{drag} = ½\, C_D\, \rho\, A_p\, v^2 \quad \text{(A.79)}$$

where

C_D is the drag coefficient;

ρ is the fluid density;

A_p is the projected area of the anchor and attached line;

v is the anchor/line velocity.

The drag on the anchor and line depends largely on the drag coefficient. The drag coefficient should be determined experimentally or through the use of computational fluid dynamics (CFD).

A.11.7.2.3 Geotechnical design and analysis

Given the interdependency of the anchor ultimate pull-out capacity (UPC) and penetration depth on the soil strength, the geotechnical design of gravity-embedded anchors should consider both the anchor penetration and holding capacity, using the same set of soil parameters. Calculations of the holding capacity and penetration depth should be performed with each of the lower bound, best estimate and upper bound soil properties, and the combination which provides the lowest holding capacity adopted in the design.

The general criteria for calculating the axial capacity of piles in cohesive soils given in 8.1.3 can be applied for the design of gravity-embedded anchors, with the following modifications to account for the inherent differences in geometry, installation methodology and loading conditions:

a) In determining the frictional resistance, the contributions of both the anchor shaft and fins should be considered, with the same value of skin friction factor, α, applicable for both anchor components;

b) In determining the bearing resistance, the contributions of both the anchor shaft and fins can be considered, although the contribution from the anchor fins will typically be minor. For a deeply embedded anchor, bearing capacity factors of $N_c = 9$ and $N_c = 7{,}5$ should be adopted for the anchor shaft and fins, respectively (based on bearing capacity factors for deeply embedded circular and strip footings (see References [318] and [262]). However, if the anchor is shallowly embedded, then the bearing capacity factors for the anchor shaft and fins should be adjusted accordingly.

The axial capacity determined using this methodology represents the anchor capacity following the complete dissipation of any excess pore pressures generated during installation. The capacity immediately after installation will generally be lower and this should be accounted for if consolidation analyses indicate that the design action will be applied prior to the completion of consolidation.

The lateral capacity of a gravity-embedded anchor can be determined using the *p*–*y* approach detailed in 8.5.3, assuming that the anchor (including the fins) can be represented as a cylindrical pile of varying diameter, with the following possible modifications and verifications:

— The lateral resistance–displacement *p*–*y* curves for smooth cylindrical piles are defined in 8.5.2. However, gravity-embedded anchors are not cylindrical but rather present a rectangular cross-sectional area to any applied lateral action. This results in additional shear resistance from the soil between the anchor fins, which is not considered when using 8.5.2 and 8.5.3. Hence, it can be possible to argue that a higher lateral bearing capacity factor can be adopted for gravity-embedded anchors. This should be verified using experimental results or finite element modelling.

— For a gravity-installed anchor which is completely embedded below the seafloor, the additional lateral resistance provided by the shearing between the top of the anchor and the soil may also be included when determining the lateral capacity.

— There are inherent differences between a slender cylindrical pile loaded at the seafloor and a gravity-embedded anchor situated at some depth below the seafloor.

When determining the capacity of gravity-embedded anchors, the allowable installation tolerances (i.e. orientation and rotation) should be included in the capacity calculations, as tilt and out-of-plane loading can affect the holding capacity of the anchor.

The finite element method (FEM) can be used to evaluate the ultimate anchor pull-out capacity as well as the increase in anchor capacity with time following installation. The results of any FEM analyses should be verified against laboratory and field test results as well as calculations using alternative methods.

As for driven anchor piles (see A.11.5.1) and suction piles (see A.11.5.2), the impact of the mooring line inverse catenary in the soil on anchor forces should be considered, since the mooring line geometry can affect the relationship between the horizontal and vertical anchor capacity.

A.11.7.2.4 Installation penetration

A number of factors should be considered when determining the penetration of gravity-embedded anchors, i.e. drop height, end bearing resistance of shaft and fins, wall friction, fluid drag forces and buoyancy, not only of the anchor but also of the attached mooring line. The equilibrium of forces on an advancing anchor can be formulated as:

$$m.a = W_s - F_b - F_f - F_{drag} \tag{A.80}$$

where

W_s is the submerged weight of the anchor and attached line;

m is the mass of the penetrator (anchor) in water;

a is the anchor acceleration;

F_b is the bearing resistance;

F_f is the frictional resistance;

F_{drag} is the inertial/drag resistance [from Formula (A.79)].

The effective mass of the penetrator is equal to the mass of the penetrator (i.e. anchor) plus the added mass of the fluid and soil that is decelerated with the penetrator. This is calculated as twice the volume of the anchor multiplied by the density of the soil. It was found that the added mass of slender, cylindrical bodies moving along their long axis was negligible (see Reference [43]); thus, for a typical torpedo pile, the mass, m, is only the mass of the anchor. For more complicated shapes, including the added mass in calculating m should be considered.

Soil resistance is a function of strain rate and should therefore be accounted for by applying a dynamic strain rate factor to the bearing and frictional resistance forces. Several methods have been proposed (see e.g. References [342] and [262]), which are essentially empirical based, i.e. determined through laboratory and field testing. The strain rate factor typically varies between approximately 1 and 2, depending on the anchor velocity.

The bearing resistance, F_b, and frictional resistance, F_f, of a penetrating anchor can be given by:

$$F_b = S_e\,(s_u\,N_c\,A_p) \tag{A.81}$$

where

S_e is the soil strength strain rate factor.

The bearing capacity factor, N_c, of the anchor shaft and fins should be based on those for circular and strip foundations, respectively, taking into account the effect of the penetration depth to width ratio of the structural element:

$$F_f = S_e\,[(\alpha_{ins}\,s_u\,A_s)\,/\,S_t] \tag{A.82}$$

where

α_{ins} is the anchor skin friction factor ($\alpha_{ins} \leq 1$);

S_t is the soil sensitivity.

The skin friction factor, α_{ins}, should account for the reduced wall friction from possible separation or reduced contact pressure between the anchor and the soil during anchor penetration through the seabed sediments. The frictional resistance is rate dependent and can be difficult to assess accurately. A value of skin friction factor $\alpha_{ins} = 1$, representing the case of no separation, can be adopted as a conservative design assumption.

A.11.7.2.5 Cyclic actions

Cyclic actions can have two potentially counteractive effects on the static axial capacity of a gravity-embedded anchor. Repetitive actions can result in the generation of excess pore pressures in the soil surrounding the anchor, thereby reducing the effective stresses in the soil and ultimately resulting in a reduction in the anchor capacity. On the other hand, rapidly applied actions can result in an increase in the anchor capacity due to strain rate effects. The resultant influence of cyclic loading on the axial capacity will be a function of the combined effects of the magnitudes, cycles and rates of change of the applied actions, the structural characteristics of the anchor and the type of soil in which it is installed.

Lateral cyclic actions can cause a deterioration of the lateral bearing capacity of the soil below that provided under static loading. This should be considered when assessing the lateral capacity of a gravity-embedded anchor.

A.11.7.2.6 Out-of-plane loading

Gravity-embedded anchors with the mooring line padeye situated at the top of the anchor can generally be loaded in any direction. However, unless the exact orientation of the applied action to the anchor can be verified following installation, the lateral capacity should be calculated assuming that the action is oriented such that the minimum anchor projected area is considered. This will therefore provide the minimum lateral anchor capacity.

The exact anchor orientation to be considered will be dependent on the fin plan geometry but, for example, for an anchor with four fins, the minimum capacity is calculated when the action is applied at an orientation of 45° to the fins (see Figure A.46).

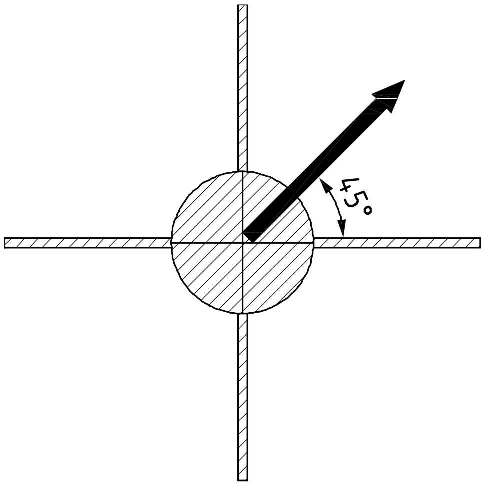

Figure A.46 — Anchor plan view showing applied loading direction

A.11.7.2.7 Safety factors for gravity-embedded anchors

Similar factors of safety than those for driven anchor piles, provided in ISO 19901-7:2013, Table 7 for axial tension forces and lateral forces, can be applied to gravity-embedded anchors.

The failure mechanism mobilized depends not only on the mooring line padeye angle, but also on the soil profile, anchor geometry and mooring line attachment point. Therefore, the selection of appropriate safety factors to adopt in design requires consideration of the governing failure mode.

A.11.7.2.8 Installation of gravity-embedded anchors

In order to verify that the anchor installation occurs in accordance with the design assumptions, the following data should be monitored and recorded during the installation of gravity embedded anchors:

a) anchor identification and water depth;

b) distance from intended seafloor location (with mention of installation tolerance);

c) penetration depth (with mention of design target penetration);

d) orientation (with mention of installation tolerance);

e) any unusual behaviour during installation.

During installation of a gravity-embedded anchor, high excess pore pressures are generated in the soil in the immediate vicinity of the anchor. These high excess pore pressures reduce the effective stress in the soil along the anchor shaft, resulting in a lower short-term capacity. Following installation, the friction on the sides of the anchor increases with time due to thixotropic effects and the dissipation of the excess pore pressures generated during installation, i.e. set-up. The rate of excess pore pressure dissipation is a function of the coefficient of consolidation of the soil, the anchor geometry, and the presence of any soil layering. Although set-up influences both the vertical and horizontal capacity, the increase in vertical capacity is more significant.

The set-up time allowed prior to application of the design mooring action should be sufficient to ensure that the soil surrounding the anchor has consolidated adequately in order for the soil to provide sufficient resistance.

A.11.8 Pre-tensioning of mooring lines and test loading of anchors

A.11.8.1 General

All moorings should be subject to test loading prior to initial use and again after any substantive change to the mooring configuration, whether by intent or by some natural or accidental event. Test loading can have multiple purposes, including:

— to ensure adequate holding capacity of the anchoring system;

— to eliminate slack in the embedded portion of the mooring lines;

— to allow detection of any significant installation-induced damage to mooring components, with various levels of tensioning required in each case.

The requirements for test loading of anchors, to be defined by the designer of the mooring system, are given in ISO 19901-7:2013, 10.4.6, with additional guidance in A.11.8.2 to A.11.8.6.

A.11.8.2 Permanent moorings

The primary function of an anchor in a permanent offshore mooring system is to hold the lower end of a mooring line in place under all design situations. If anchor drag cannot be tolerated and the extreme line tension causes the anchor to drag, then the anchor has failed to fulfil its intended function. However, limited drag of an anchor does not necessarily lead to the complete failure of a mooring system, although for permanent moorings the performance of the anchor when subjected to over-loading should be assessed.

The specification of the anchor installation tension is most critical in soil conditions where the anchors do not penetrate deeply. In these cases, no post-installation effects (i.e. consolidation and cyclic effects) can be relied upon resulting in higher installation tension than if anchors were embedded deeply in soft clay. For permanent moorings, pre-set anchors (e.g. anchor piles) should be considered if the specified installation tension cannot be achieved by use of winches on the floating structure.

The following applies in accordance with ISO 19901-7:2013, 10.4.6.2:

a) For mooring lines with drag anchors, in soft clay where deep anchor penetration can be achieved, test loading magnitude equal to at least 80 % of the force induced by the environmental design situation as determined by a dynamic analysis of the intact condition. In hard, sandy or layered soils where anchor penetration can be limited to less than or no more than one fluke length, test loading level equal to 100 % or more of the force induced by the environmental design situation of the intact condition.

b) For mooring lines with fixed anchors (e.g. anchor piles), the minimum acceptable level of test loading should ensure that the mooring line's inverse catenary is sufficiently formed to prevent unacceptable mooring line slacking due to additional inverse catenary cut-in and change in shape of the embedded part of the line during storm conditions.

c) Duration of the installation test loading tension of at least 15 min.

In defining the test loading magnitude, the designer should consider the uncertainties in the calculated force and the consequences of potential platform displacement resulting from anchor movement. The test loading tension should also be set high enough such that the additional drag to resist the design intact actions does not over-load neighbouring lines. The installation tension should be measured using a reliable calibrated system and documented.

A.11.8.3 Mobile (temporary) moorings

For mooring lines with drag anchors, the installation test loading magnitude should be determined by consideration of a number of factors, including type of anchor, soil conditions, winch pull limit and anchor retrieval. The following applies in accordance with ISO 19901-7:2013, 10.4.6.3:

a) installation test loading tension at a winch should not be less than the larger of the extreme line tensions for an intact mooring under the design situation or serviceability limit state (SLS);

b) installation test loading tension at the anchor shank should not be less than three times the anchor weight;

c) for moorings in proximity to other installations, the installation test loading tension at a winch should not be less than the mean line tension for an intact mooring under the design situation for ULS;

d) duration of the installation test loading tension should be at least 15 min.

A.11.8.4 Test loading for drag anchors

Reference [116] gives guidance in planning and executing installation of drag-embedded anchors. It also provides alternative guidance on how to determine the anchor installation tension.

A.11.8.5 Test loading for anchor piles and plate anchors

For anchor piles (i.e. driven piles or suction piles) and plate anchors, the installation records should demonstrate that the anchor penetration is within the range of upper and lower bound penetration predictions developed during the anchor geotechnical design. In addition, the installation records should confirm the expected installation behaviour, i.e. self-weight penetration, embedment behaviour (i.e. driving behaviour for driven piles, embedment under-pressure for suction piles, or drag embedment force for drag-embedded plate anchors), and that the anchor orientation is consistent with the anchor design. Under these conditions, test loading of the anchor to the loading conditions defined in ISO 19901-7:2013, 10.4.6 should not be required.

Plate anchors should be subjected to adequate keying/triggering loading to ensure that sufficient anchor fluke rotation takes place and that the associated loss of penetration depth is within that expected and accounted for in the specification of the target penetration depth. The keying tension required and amount of estimated fluke rotation should be based on reliable geotechnical analysis and should be verified by prototype or model-scale testing. The keying analysis used to establish the keying tension should also include analysis of the anchor's rotation when subjected to the ULS intact and redundancy check tensions. If the calculated anchor rotation during keying differs from the anchor rotation during redundancy check conditions, the anchor's structure should be designed for any resulting out-of-line loading to ensure that the structural integrity of the plate anchor is not compromised.

Drag-embedded plate anchors should be test loaded to the loading conditions defined in ISO 19901-7:2013, 10.4.6, unless at least one of the following conditions is satisfied:

a) the anchor installation tension (drag-in tension) is equal or greater than the anchor required test tension, and the anchor is not keyed in the opposite direction;

b) soil properties at the anchor location have been established accurately (see A.11.2), and the depth of the anchor after keying is known with reasonable accuracy and is equal to or greater than the minimum depth used for the anchor design.

Reference [117] provides further guidance regarding installation effects on the penetration depth of plate anchors, anchor keying and rotation, and methods for verification of the as-installed penetration depth.

In cases where the installation records show significant deviation from the predicted values and these deviations indicate that the anchor holding capacity is compromised, test loading of the anchor to the test conditions defined in ISO 19901-7:2013, 10.4.6 can be required. This can be an acceptable option to prove holding capacity for temporary moorings. However, testing anchors to the tension used for the ULS intact check does not necessarily prove that required anchor holding safety factors are met, which is of special concern for permanent mooring systems. Consequently, if the installation records show that the anchor holding capacity is significantly smaller than calculated and safety factors are not met, the following measures to ensure adequate factors of safety should be considered:

a) additional soil investigation to establish and/or confirm soil properties at the actual anchor location;

b) retrieval of the anchor, and re-installation at a new undisturbed location;

c) retrieval of the anchor, and re-design and reconstruction of the anchor to meet design requirements and re-installation at an undisturbed location;

d) delay of vessel hook-up to provide additional soil consolidation.

A.11.8.6 Test loading for gravity-embedded anchors

As for anchor piles, test loading of gravity-embedded anchors to the loading conditions defined in ISO 19901-7:2013, 10.4.6 should not be required as long as the installation records confirm that the minimum required embedment used to calculate the anchor holding capacity is achieved.

Bibliography

[1] AAS P.M., SAUE M., AARSNES J., *Design predictions and measurements during installation of suction anchors with and without water-flow system to help installation through layered soil profiles*. Proc. Offshore Technology Conf., paper OTC 20294, Houston, Texas, May 2009

[2] AKER, T.J., *Jetting of Structural Casing in Deepwater Environments: Job Design and Operational Practices*. SPE Drilling & Completion, 2008. 23(1): p. 15.

[3] ALDRIDGE, T., CARRINGTON, T., AND KEE, N., *Propagation of pile tip damage during installation*, Proc. 1st, Intl. Sym.on Frontiers in Offshore Geotechnics, ISFOG 2005. 2005, Francis: Perth, Australia. p. 823-828.

[4] AL-JANABI, H. A., AUBEBY, C.P., CHEN, J., AND LUO, M., *Experimental measurement of touchdown zone stiffness for SCR in Gulf of Mexico Clay*. Proc. Offshore Technology Conference (OTC), Houston,2019, May, Paper OTC-29504-MS.

[5] ALDERLIESTE, E.A., ROMP, R.H., KAY, S. & LOFTEROD, A, (2016), *Assessment of Seafloor Trench for Suction Pile Moorings; a Field Case*, Proc. Offshore Technology Conference, OTC-27035-MS.

[6] ALM T., HAMRE L., *Soil model for pile driveability predictions based on CPT interpretations*. Proc. Intl. Conf. on Soil Mechanics and Geotechnical Engineering, ICSMGE, Istanbul, Turkey, June 2001

[7] AL-SHAFEI, KHAIL, *Engineering for Calcareous Sediments.* Proceedings of the Second International Conference on Engineering for Calcareous Sediments, Bahrain, 21-24 February 1999, Volume 2.

[8] ANDERSEN K., ANDRESEN L., JOSTAD H.P., CLUKEY E., *Effect of skirt geometry on set-up outside suction anchors in soft clays*. Intl. Conf. on Offshore Mechanics and Arctic Engineering, OMAE, paper OMAE2004-51564, Vancouver, 2004

[9] ANDERSEN K.H., *Bearing capacity under cyclic loading – Offshore, along the coast and on land*. The 21st Bjerrum Lecture, Oslo, 23 Nov. 2007. Canadian Geotechnical J., 2009, 46, pp. 513–535

[10] ANDERSEN, K.H., *Cyclic soil parameters for offshore foundation design*. The 3rd ISSMGE McClelland Lecture. Frontiers in Offshore Geotechnics III, ISFOG'2015, Meyer (Ed). Taylor & Francis Group, London, ISBN: 978-1-138-02848-7. Proc., 5-82. Revised version in: http://www.issmge.org/committees/technical-committees/applications/offshore and click on “Additional Information”, (2015).

[11] ANDERSEN K.H., *Cyclic clay data for foundation design of structures subjected to wave loading*. Proc. Intl. Conf. on Cyclic Behaviour of Soils and Liquefaction Phenomena, Bochum, Germany, 2004, pp. 381–387

[12] ANDERSEN K.H., JOSTAD H.P., *Foundation design of skirted foundations and anchors in clay*. Proc. Offshore Technology Conf., paper OTC 10824, Houston, Texas, May 1999

[13] ANDERSEN K.H., JOSTAD H.P., *Shear strength along inside of suction anchor skirt wall in clay*. Proc. Offshore Technology Conf., paper OTC 16844, Houston, Texas, May 2004

[14] ANDERSEN K.H., JOSTAD H.P., *Shear strength along outside wall of suction anchors in clay after installation*. Proc. Intl. Seminar on Offshore and Polar Engineering, ISOPE, Kyushu, Japan, 2002

[15] ANDERSEN K., JOSTAD H.P., DYVIK R., *Penetration of offshore skirted foundations and anchors in dense sand*. ASCE Journal of Geotechnical Engineering, 2008, 134 (1), pp. 106–116.

[16] ANDERSEN K.H., LAURITZSEN R., *Bearing capacity for foundation with cyclic loads*. ASCE Journal of Geotechnical Engineering, 1988, 114 (GT5), pp. 540–555

[17] ANDERSEN K.H., MURFF J.D., RANDOLPH M., *Deepwater anchor design practice – Vol. II-2 Suction caisson anchors – 3D finite element analyses and comparison with simplified capacity prediction methods*. Phase II Report submitted to API/Deepstar, 2004

[18] ANDERSEN K.H., MURFF J.D., RANDOLPH M.F., CLUKEY E., ERBRICH C., JOSTAD H.P. ET AL., *Suction anchors for deepwater applications*. Proc. Intl. Symposium on Frontiers in Offshore Geotechnics, ISFOG, Perth, Australia, September 2005

[19] ANDERSEN, K.H. (2004). *Cyclic clay data for foundation design of structures subjected to wave loading*. Invited Keynote Lecture: International Conf. on Cyclic Behaviour of Soils and Liquefaction Phenomena, CBS04, Bochum, Germany. 2004. Proc. p. 371 – 387, A.A.Balkema Publishers, Ed Th. Triantafyllidis.

[20] ANDREWS, D.C., JEWELL, R.J., *Engineering for Calcareous Sediments.* Proceedings of the International Conference on Calcareous Sediments/Perth/15-18 March 1988 Hardcover – 1 Jan. 1988

[21] ANG, A & TANG, W., *Probability Concepts in Engineering: Emphasis on Applications to Civil and Environmental Engineering*, 2nd Edition, 2006.

[22] API RP 2GEO, *Geotechnical and foundation design considerations*

[23] API RP 2SK, *Recommended practice for design and analysis of stationkeeping systems for floating structures*

[24] API RP 2T, *Recommended practice for planning, designing and constructing tension leg platforms*

[25] API RP2SK. *Design and Analysis of Stationkeeping Systems for Floating Stryctures*.

[26] API RP2T. *Planning, Designing and Constructing Tension Leg Platforms*.

[27] API Std 2RD. *Dynamic risers for floating production systems*.

[28] API RP 2RD, *Design of Risers for Floating Production Systems (FPSs) and Tension-Leg Platforms (TLPs)*.

[29] API RP 16Q, *Design, Selection, Operation, and Maintenance of Marine Drilling Riser Systems*

[30] ARSLAN H., PETERMAN B.R., WONG P.C., BHATTACHARJEE S., *Remaining capacity of the suction pile due to seabed trenching*. Proc. Intl. Seminar on Offshore and Polar Engineering, ISOPE, Hawaii, June 2015

[31] ASTM D2196, *Standard Test Methods for Rheological Properties of Non-Newtonian Materials by Rotational Viscometer*

[32] AUBENY C., HAN S., MURFF J.D., *Refined model for inclined load capacity of suction caissons*. Proc. 22nd Intl. Conf. on Offshore Mechanics and Arctic Eng., OMAE, Cancun, Mexico, 2003

[33] AUBENY, C. P., WHITE, T. A., LANGFORD, T., MEYER, V., AND CLUKEY, E.C. *Seabed Stiffness Model for Steel Catenary Risers*, Proc. Intl. Sym. on Frontiers in Offshore Geotechnics (ISFOF), 2105Oslo, June

[34] AUBENY, C.P., SHI, H. AND MURFF, J.D. (2005). *Collapse loads for a cylinder embedded in trench in cohesive soil*, International Journal of Geomechanics, ASCE, 5(4):320-325.

[35] AUBENY, C.P. AND BISCONTIN, G., *Seafloor-riser interaction model*. Int. Journal of Geomechanics, 2009, ASCE, 9(3), 133-141.

[36] AXELSSON G., *Long term set up of driven piles in sand*. PhD thesis, Royal Institute of Technology, Stockholm, Sweden

[37] BAECHER G.B., CHRISTIAN J.T., Reliability and statistics in geotechnical engineering. John Wiley & Sons, 2003

[38] BALLARD, J.-C., VAN DEN ABEELE, F. & DE BRIER, C., (2013). *Influence of axial response on pipeline end expansion and walking*. 6th International Pipeline Technology Conference, Ostend, Belgium. Paper S30-01.

[39] BARTHELEMY H.C., MARTIN R., LE TIRANT P.M., NAUROY J.F., *Grouted driven piles: An economic and safe alternate for pile foundations*. Proc. 19th Offshore Technology Conf., Houston, Texas, paper OTC 5409, May 1987

[40] BEA R.G., *Dynamic response of marine foundations*. Proc. Intl. Symposium Ocean Structural Dynamics '84, Corvallis Oregon, Oregon State University, 11-13 September 1984

[41] BEA R.G., LITTON R.W., NOUR-OMID S., CHANG J.Y., VAISH A.K., *A specialized design and research tool for the modelling of near-field pile-soil interactions*. Proc. 16th Offshore Technology Conf., paper OTC 4806, Houston, Texas, May 1984

[42] BEA R.G., VAHDANI S., GUTTMAN S.I., MEITH R.M., PAULSON S.F., *Analysis of the performance of piles in silica sands and carbonate formations*. Proc. 18th Offshore Technology Conf., paper OTC 5145, Houston, Texas, May 1986

[43] BEARD R.M., *Expendable doppler penetrometer for deep ocean sediment measurements*. In: Strength Testing of Marine Sediments: Laboratory and In-Situ Measurements, ASTM Special Technical Publication 883, Philadelphia, 1985, pp. 101–124

[44] BHATTACHARJEE S., MAJHI S., SMITH D., GARRITY R., *Serpentina FPSO mooring integrity issues and system replacement: Unique fast track approach*. Proc. Offshore Technology Conf., paper OTC 25449-MS, Houston, Texas, May 2014

[45] BHATTACHARYA S., CARRINGTON T.M., ALDRIDGE T.R., *Design of FPSO piles against storm loading*. Proc. Offshore Technology Conf., paper OTC 17861, Houston, Texas, May 2006

[46] BITTAR, E., LEHANE, B., LIU, Z., NADIM, F., LACASSE, S., *Assessment of the Unified CPT Design Method for Axial Capacity of Driven Piles in layered Deposits*

[47] BOGARD D., *Effective stress and axial pile capacity: Lessons learned from Empire*. Proc. Offshore Technology Conf., paper OTC 13059, Houston, Texas, May 2001

[48] BOGARD J.D., MATLOCK H., *Applications of model pile tests to axial pile design*. Proc. 22nd Offshore Technology Conf., Houston, Texas, paper OTC 6376, May 1990

[49] BOGARD J.D., MATLOCK H., AUDIBERT J.M.E., BAMFORD S.R., *Three years' experience with model pile segment tool tests*. Proc. 17th Offshore Technology Conf., paper OTC 4848, Houston, Texas, 1985

[50] BOND A.J., JARDINE R.J., *Shaft capacity of displacement piles in a high OCR clay*. Géotechnique, 1995, March, 45 (1), pp. 3–23

[51] BOUKPETI N. & WHITE D.J. (2017). *Interface shear box tests for assessing axial pipe-soil resistance*. Géotechnique 67(1):1-13

[52] BOUKPETI, N., WHITE, D. J. & RANDOLPH, M. (2012). *Strength of fine-grained soils at the solid–fluid transition*. Geotechnique, 62(3):213 -226.

[53] BRANDAO F.E.N., HENRIQUES C.C.D., DE ARAUJO J.B., FERREIRA O.C.G., DOS SANTOS AMARAL C., *Albacora Leste field development – FPSO P-50 mooring system concept and installation*. Proc. Offshore Technology Conf., paper OTC 18243, Houston, Texas, May 2006

[54] BRANSBY M., RANDOLPH M.F., *Combined loading of skirted foundations*. Géotechnique, 1998, 48 (5), pp. 637–655

[55] BRANSBY M., RANDOLPH M.F. ,*The effect of embedment depth on the undrained response of skirted foundations to combined loading*, Soils and Foundations, JGS, 1999, 39 (4), pp. 19–33

[56] BRANSBY M.F., YUN G., *The undrained capacity of skirted strip foundations under combined loading*. Géotechnique, 2009, 59 (2), pp. 115–125

[57] BRANSBY M.F., ZHOU H., LOW H.E., RAMM M. & WHITE D.J. 2017. *Pipe-Soil Structure Interaction: Best Practices for Spools, Buckle Initiators, End Connections and Sand Waves*. Proc. Offshore Technology Conference, Houston, USA, Paper OTC27689.

[58] BRIAUD J.-L., FELIO G., TUCKER L., *Influence of cyclic loading on axially loaded piles in clay*. Research Report API PRAC 83-42, Phase 2, Pile Response to Static and Dynamic Loads, Dec. 1984

[59] BRIAUD J.-L., GARLAND E., *Influence of loading rate on axially loaded piles in clay*, Research Report API PRAC 83-42, Phase 1, Pile Response to Static and Dynamic Loads, March 1984

[60] BRIAUD, J. L., TING, F. C. K., CHEN, H. C., CAO, Y., HAN, S. W. AND KWAK, K.W., (2001). *Erosion function apparatus for scour rate predictions*. Journal of Geotechnical and GeoEnvironmental Engineering, 127(2), pp. 479–481.

[61] BRIDGE C.D., HOWELLS H.A., *Observations and modeling of steel catenary riser trenches*. Proc. 17th Intl. Seminar on Offshore and Polar Engineering, ISOPE, Lisbon, Portugal, paper ISOPE-2007-468, July 2007

[62] BRINCH-HANSEN J., *A revised and extended formula for bearing capacity*. The Danish Geotechnical Institute, Bulletin No. 2, Copenhagen, 1970

[63] BRUTON D., CARR M., WHITE D.J., *The influence of pipe-soil interaction on lateral buckling and walking of pipelines: The SAFEBUCK JIP*. Proc. Intl. Conf. on Offshore Site Investigation and Geotechnics, SUT OSIG, London, U.K., September 2007, pp. 133–150

[64] BUCKLEY, R.M., JARDINE, R.J., KONTOE, S. BARBOSA, P, SCHROEDER, F.C., *Full-scale observations of dynamic and static axial responses of offshore piles driven in chalk and tills*, Géotechnique [https://doi.org/10.1680/jgeot.19.TI.001], 2019.

[65] BUITRAGO J., WONG P.C., *Fatigue design of driven piles for deepwater applications*. Proc. 13th Intl. Seminar on Offshore and Polar Engineering, ISOPE, Honolulu, Hawaii, May 2003

[66] BURD, H.J., ABADIE, C.N., BYRNE, B.W., HOULSBY, G.T., MARTIN, C.M., MCADAM, R.A., JARDINE, R.J., PEDRO, A.M.G., POTTS, D.M., TABORDA, D.M.G., ZDRAVKOVIC, L. AND PACHECO ANDRADE, M. 2020b. *Application of the PISA design model to monopiles embedded in layered soils*. Géotechnique, under review.

[67] BURD, H.J., TABORDA, D.M.G., ZDRAVKOVIC, L., ABADIE, C.N., BYRNE, B.W., HOULSBY, G.T., GAVIN, K.G., IGOE, D.J.P., JARDINE, R.J., MARTIN, C.M., MCADAM, R.A., PEDRO, A.M.G. AND POTTS, D.M. 2020a. *PISA design model for monopiles for offshore wind turbines: application to a marine sand*. Géotechnique, https://doi.org/10.1680/jgeot.18.P.277.

[68] BUTTERFIELD R., GOTTARDI G., *A complete three dimensional failure envelope for shallow footings on sand*. Géotechnique, 1994, 44 (1), pp. 181–184

[69] BYRNE B.W., HOULSBY G.T., *Observation of footing behaviour on loose carbonate sand*. Géotechnique, 2001, 51 (5), pp. 463–466

[70] BYRNE, B.W., BURD, H.J., ZDRAVKOVIC, L., ABADIE, C.N., HOULSBY, G.T., JARDINE, R.J., MARTIN, C.M., MCADAM, R.A., PACHECO ANDRADE, M., PEDRO, A.M.G., POTTS, D.M. AND TABORDA, D.M.G. 2019. *PISA design methods for offshore wind turbine monopiles*. Offshore Technology Conference, Houston, Texas. Paper number 293373

[71] BYRNE, B.W., HOULSBY, G.T., BURD, H.J., GAVIN, K.G., IGOE, D.J.P., JARDINE, R.J., MARTIN, C.M., MCADAM, R.A., POTTS, D.M., TABORDA, D.M.G. AND ZDRAVKOVIC, L. 2020. *PISA design model for monopiles for offshore wind turbines: Application to a stiff glacial clay till*. Géotechnique, https://doi.org/10.1680/jgeot.18.P.255.

[72] BYRNE, B.W., MCADAM, R.A., BURD, H.J., HOULSBY, G.T., MARTIN, C.M., BEUCKELAERS, W.J.A.P., ZDRAVKOVIC, L., TABORDA, D.M.G., POTTS, D.M., JARDINE, R.J., USHEV, E., LIU, T., ABADIAS, D., GAVIN, K., IGOE, D., DOHERTY, P., SKOV GRETLUND, J., PACHECO ANDRADE, M., MUIR WOOD, A., SCHROEDER, F.C., TURNER, S. AND PLUMMER, M.A.L. 2017. *PISA: new design methods for offshore wind turbine monopiles*. Proceedings of the 8th International Conference on Offshore Site Investigation and Geotechnics, London: Society for Underwater Technology, Vol 1, pp. 142-161.

[73] CARLTON, B., VANNESTE, M., FORSBERG, C.F., KNUDSEN, S., LØVHOLT, F., KVALSTAD, T., HOLM, S., KJENNBAKKEN, H., MAZHAR, M.A., DEGAGO, S. AND HAFLIDASON, H., 2019. *Geohazard assessment related to submarine instabilities in Bjørnafjorden, Norway*. Geological Society, London, Special Publications, 477(1), pp.549-566.

[74] CASSIDY M.J., CHEONG J., *The behaviour of circular footings on sand subjected to combined vertical-torsion loading*, Intl. Journal of Physical Modelling in Geotechnics, 2005, 5 (4), pp. 1–14

[75] CATHIE D., SASSI K., BLANC M., THOREL L. AND WALLERAND R. (2020), *Holding capacity of suction anchors with trench - Centrifuge test results and interpretation*. ISFOG 2020

[76] CHEN J-Y., MATAREK B.A., CARPENTER J.F., YOUNG A., GILBERT R.B., PUSKAR F., VERRET S., *Analysis of potential conservatism in foundation design for offshore platform assessment*. Offshore Technology Research Centre Report to the MMS and API, OTRC Library Number 8/09B198, September 2009

[77] CHEN W.F., *Limit Analysis and Soil Plasticity*. Elsevier Publishing Comp., Amsterdam, 1975

[78] CHEN ET AL. (2019) *Practice of Riser-Soil Interactions at Touch Down Zones for Steel Catenary Risers*, OTC Paper No. 29553, Proceedings of the Offshore Technology Conference, Houston, Texas, May 2019.

[79] CHEN, W. AND RANDOLPH, M.F., *Uplift Capacity of Suction Caissons under Sustained and Cyclic Loading in Soft Clay*, Journal of Geotechnical and Geoenvironmental Eng., ASCE, 133 (11), 2007b, p. 1352–1363

[80] CHOW F.C., BANIMAHD M., TYLER S., RATHMELL A., OSTOJIC M., HOLLAND B., *Investigating Drag Anchor Behaviour in Calcareous Materials on the North West Shelf of Australia*. OSIG 2017 London pp 1206-1213

[81] CHOW F.C., JARDINE R.J., NAUROY J.-F., BRUCY F., *Time-related increases in the shaft capacities of driven piles in sand*. Géotechnique, 47 (2), 1997, pp. 353–361

[82] CIRIA, 2012, *The rock manual: The use of rock in hydraulic engineering (2nd edition)*, CIRIA Report C683

[83] CLARK A.R., WALKER B.F., *A proposed scheme for the classification and nomenclature for use in the engineering description of middle eastern sedimentary rocks*. Géotechnique, 1977, 27 (1), pp. 93–99

[84] CLARKE J. (ed.). *Large-Scale Pile Tests in Clay*. Thomas Telford Publ., London, U.K., 1993

[85] CLAUSEN C.J.F., AAS P.M., KARLSRUD K., *Bearing capacity of driven piles in sand, the NGI approach*. Proc. 1st Intl. Symposium on Frontiers in Offshore Geotechnics, ISFOG, Perth, Australia, September 2005, pp. 677–682

[86] CLUKEY E., AUBENY C., MURFF J.D., *Comparison of analytical and centrifuge model tests for suction caissons subjected to combined loads*. Proc. 22nd Intl. Conf. on Offshore Mechanics and Arctic Engineering, OMAE, OMAE2003-37503, Cancun, Mexico, 2003

[87] CLUKEY E.C., TEMPLETON J.S., RANDOLPH M.F., PHILLIPS R., *Suction caisson response under sustained loop current loads*. Proc. Offshore Technology Conf., paper OTC 16843, Houston, Texas, May 2004

[88] CLUKEY, E. C., TEMPLETON, J. S., RANDOLPH, M. F, AND PHILLIPS, R., *Suction Caisson Response Under Sustained Loop Current Loads,*. Proc., 36th Offshore Technology Conference, OTC 16843, 2004, Houston, May.

[89] CLUKEY, E.C. AND ZAKKRI, A., *Recent Advances in Nonlinear Soil Models for Fatigue Evaluation of Steel Catenary Risers (SRCs)*, Proc. Offshore Technology Conference (OTC), Houston, Texas, May 1-4, 2017, Paper OTC-27627-MS.

[90] CLUKEY, E.C., TOGNARELLI, M.A., LI, G. G., GHOSH, R., PHILIPPS, R., ZAKERI, A., ELLIOT, B.J., BHATTACHATYYA, A. AND SUN, Q., *Simulation of SCR behaviour at touchdown zone - Part II: testing of a sectional SCR model in a geotechnical centrifuge*. Proc 1st Offshore Technology Conf. Brazil, Rio de Janeiro, Brazil, 2011, Paper BrOTC 22569.

[91] COCJIN, M., GOURVENEC, S., WHITE, D.J., RANDOLPH, M.F. 2017. *Theoretical framework for predicting the response of tolerably mobile subsea installations*. Geotechnique. 67(7),608-620. DOI: 10.1680/jgeot.16.P.137

[92] COLLIARD D., WALLERAND R., *Design and installation of suction piles in West Africa deepwaters*. Proc. 2nd BGA Intl. Conf. on Foundations, ICOF, British Geotechnical Association, Univ. of Dundee, Scotland, U.K., 2008

[93] COLLIAT J.-L., BOISARD P., ANDERSEN K.H., SCHROEDER K,. *Caisson foundations as alternative anchors for permanent mooring of a process barge offshore Congo*. Proc. Offshore Technology Conf., paper OTC 7797, Houston, Texas, May 1995

[94] COLLIAT J.-L., DENDANI H., JOSTAD H.P., ANDERSEN K.H., THOREL L., GARNIER J. ET AL. *Centrifuge testing of suction piles in deepwater Nigeria clay – Effect of stiffeners and set-up time*. Proc. Intl. Symposium on Frontiers in Offshore Geotechnics, ISFOG II, Perth, Australia, November 2010

[95] COLLIAT, J-L, GOURVENEC, S., MORGAN, N., CLUKEY, E., SCHROEDER, K., RUINEN, R., LACASSE, S. & LITTLE, R. (2017) *The new standard ISO 19901-4 for geotechnical and foundation design considerations*, Proc. 8th Int. Conf. on Offshore Site Investigation and Geotechnics (OSIG), London, UK. 2:787-796.

[96] COLLIAT JL., SAFINUS S, BOYLAN N, SCHROEDER K. (2018), *Formation and Development of Seabed Trenching from Subsea Inspection Data of Deepwater Gulf of Guinea Moorings*, Proc. Offshore Technology Conference, OTC-29034-MS

[97] COLLIAT J.L., VERGOBBI P., PUECH A., *Friction degradation and set-up in hard clays offshore Congo and Angola*. Proc. Offshore Technology Conf., Houston, Texas, OTC paper 7192, Houston, Texas, May 1993

[98] CORTI, R., GOURVENEC., S., DIAMBRA, A. & RANDOLPH, M.F. (2017), *Application of a memory surface model to predict whole-life settlements of a sliding foundation*, Computers in Geotechnics, 88:152–163 https://doi.org/10.1016/j.compgeo.2017.03.014

[99] COUSSOT, P. (1997). *Mudflow Rheology and Dynamics*, Rotterdam, Balkema.

[100] COYLE H.M., REESE L.C., *Load transfer for axially loaded piles in clay*. ASCE Journal of Soil Mechanics and Foundation Div., 1966, March, 92 (SM2), pp. 1–26

[101] DAHLBERG R., RESSEGUIER S., *Improved predictions of MODU fluke anchors increases the confidence in mooring system design*. Proc. Offshore Technology Conf., paper OTC 20085, Houston, Texas, May 2009

[102] DAHLBERG R., RONOLD K.O., STROM P.J., MATHIESEN J., *New calibrated design code for plate anchors in clay*. Proc. Offshore Technology Conf., paper OTC 16109, Houston, May 2009

[103] DAHLBERG R., STROM P.J., *Unique onshore tests of deepwater drag-in plate anchors*. Proc. Offshore Technology Conf., paper OTC 10989, Houston, Texas, May 1999

[104] DAMGAARD, J.S. AND PALMER, A.C. (2001), *Pipeline stability on a mobile and liquefied seabed: a discussion of magnitudes and engineering implications*. Proceedings, 20th International Conference on Offshore Mechanics and Arctic Engineering, Rio de Janeiro.

[105] DAVIS E.H., BOOKER J.R,. *The effect of increasing strength with depth on the bearing capacity of clays.* Géotechnique, 1973, 23 (4), pp. 551–563

[106] DEAN, E.T.R. (2009), *Offshore Geotechnical Engineering: Principles and Practice*, ICE Publishing, ISBN: 978-0727736413. pp.552.

[107] DEEKS, A., ZHOU, H., KRISDANI, H., BRANSBY, F. & WATSON, P. (2014). *Design of direct on-seabed sliding foundation*. In Proceedings of the 33rd international conference on ocean, offshore and arctic engineering, San Francisco, USA, paper V003T10A024, http://dx.doi.org/10.1115/OMAE2014-24393. New York, NY, USA: ASME.

[108] DENDANI H., *Suction anchors: Some critical aspects for their design and installation in clayey soils*. Proc. Offshore Technology Conf., paper OTC 15376, Houston, Texas, May 2003

[109] DENDANI H., COLLIAT J.-L., *Girassol: Design analysis and installation of the suction anchors*. Proc. Offshore Technology Conf., paper OTC 14209, Houston, Texas, May 2002

[110] DENGFENG FU, YOUHU ZHANG, YUE YAN, HANS PETTER JOSTAD, *Effects of tension gap on the holding capacity of suction anchors*, Marine Structures, Volume 69, 2020, 102679, ISSN 0951-8339, https://doi.org/10.1016/j.marstruc.2019.102679.

[111] DNV-RP-F114, *Pipe-soil interaction for submarine pipelines*.

[112] DNV -RP-F204, *Riser Fatigue*.

[113] DNVGL -RP-F105, *Free spanning pipelines*.

[114] DNV-RP-C203, *Fatigue Design of Offshore Steel Structures*.

[115] DNVGL-RP-C212, *Offshore soil mechanics and geotechnical engineering*.

[116] DNV-RP-E301, *Design and Installation of Fluke Anchors in Clay*

[117] DNV-RP-E302, *Design and Installation of Plate Anchors in Clay*

[118] DNV-RP-E303, *Geotechnical Design and Installation of Suction Anchors in Clay*

[119] DOHERTY J.P., DEEKS A.J., *Elastic response of circular footings embedded in a non-homogeneous half-space*. Géotechnique, 2003, 53 (8), pp. 703–714

[120] DONG, Y., WANG, D., & CUI, L. (2019). *Assessment of depth-averaged method in analysing runout of submarine landslide*. Landslides, 17, 543 - 555.

[121] DOYLE E.H., *Pile installation performance for four TLP's in the Gulf of Mexico*. Proc. Offshore Technology Conf., OTC paper 10826, Houston, Texas, May 1999

[122] DRAPER S., GRIFFITHS T., CHENG L., WHITE D.J. & AN. H. 2018*. Modelling changes to submarine pipeline embedment and stability due to pipeline scour*. Proc. Conf. on Ocean, Offshore & Arctic Engineering, Madrid, Spain. Paper OMAE2018-77985

[123] DRAPER, S., AN, H., CHENG, L., WHITE D.J. & GRIFFITHS, T.G. 2015. *Stability of subsea pipelines during large storms*. Invited paper to Special Issue 'Advances in Fluid Mechanics for Offshore Engineering' of the Philosophical Transactions of the Royal Society, Part A. Phil. Trans. R. Soc. A: DOI: 10.1098/rsta.2014.0106.

[124] DUGAN, B., ET AL., *Offshore sediment overpressures: Overview of mechanisms, measurement and modeling*, in Frontiers in Offshore Geotechnics II, S. Gourvenec and D. White, Editors. 2010, CRC Press: Perth, Australia. p. pp. 271-276.

[125] DUNNAVANT T.W., KWAN C.T., *Centrifuge modelling and parametric analyses of drag anchor behaviour*. Proc. Offshore Technology Conf., paper OTC 7202, Houston, Texas, May 1993

[126] DUTT R.N., DOYLE E.H., COLLINS J.T., GANGULY P., *A simple model to predict soil resistance to driving for long piles in deepwater normally consolidated clays*. Proc. Offshore Technology Conf., paper OTC 7668, Houston, Texas, May 1995

[127] ERBRICH C., HEFER P., *Installation of the Laminaria suction piles – A case history*. Proc. Offshore Technology Conf., paper OTC 14240, Houston, Texas, May 2002

[128] ERBRICH, C.T., BARBOSA-CRUZ, E. AND BARBOUR, R., *Soil-Pile Interaction during Extrusion of an Initially Deformed Pile*, Proc. 2nd Intl. Sym. on Frontiers in Offshore Geotechnics, ISFOG 2010, S. Gourvenec and D. White, Editors. 2010: Perth, Australia. p. pp. 489–494.

[129] EVANS T.G., FEYEREISEN S., RHEAUME G., *Axial capacities of jetted well conductors in Angola*. Proc. Intl. Conf. on Offshore Site Investigation and Geotechnics, SUT OSIG, London, U.K., Nov. 2002

[130] EVANS T.G., FINNIE E., LITTLE R., JARDINE R., ALDRIDGE T.R., *BP Clair phase 1 – Geotechnical assurance of driven piled foundations in extremely hard till*. Proc. 2nd Intl. Symposium on Frontiers in Offshore Geotechnics, ISFOG II, Perth, Australia, November 2010

[131] FENG X., GOURVENEC S., *Optimal shear key interval for offshore shallow foundations*. Proc 32nd Intl. Conference on Ocean and Arctic Engineering, OMAE, Nantes, 2013

[132] FENG X., RANDOLPH M.F., GOURVENEC S., WALLERAND R., *Design approach for rectangular mudmats under fully three dimensional loading*. Géotechnique, 2014, 64 (1), pp. 51–63. DOI:10.1680/geot.13.P.051

[133] FENG, X. & GOURVENEC, S. (2015), *Consolidated undrained load-carrying capacity of mudmats under combined loading in six degrees-of-freedom*. Géotechnique, 65(7): 563-575. http://dx.doi.org/10.1680/geot./14-P-090

[134] FENG, X., GOURVENEC, G., RANDOLPH, M.F., WALLERAND, R. AND DIMMOCK, P. (2015), *Effect of a surficial crust on mudmat capacity under fully three-dimensional loading*. Geotechnique 65 (7), 590-603. DOI: 10.1680=geot.14.P.167

[135] FENG, X., GOURVENEC, S. & RANDOLPH, M. F. (2014a), *Optimal skirt spacing for subsea mudmats under loading in six degrees of freedom*. Appl. Ocean Res. 48, 10–20.

[136] FENG, X., GOURVENEC, S. & WHITE, D.J. (2019), *Load Capacity of Caisson Anchors Exposed to Seabed Trenching*, Proc. Ocean Engineering, 171, 181-192, https:/doi.org/10.1016/j.oceaneng.2018.09.027.

[137] FENG, X., RANDOLPH, M.F AND GOURVENEC, S. (2016), *An analytical solution for the undrained horizontal–torsional resistance of mudmats*. Geotechnique 67 (4), 325-337. DOI: 10.1680/jgeot.16.P.026

[138] FINNIE I.M.S., MORGAN N., *Torsional loading of subsea structures*. Proc. 14th Intl. Offshore and Polar Engineering Conf., ISOPE, Toulon, France, 2004

[139] FOCHT J.A., KOCH K.H., *Rational analysis of the lateral performance of offshore pile groups. Proc. 5th Offshore Technology Conf., Houston, Texas, paper OTC 1896, May 1973*

[140] FOCHT J.A., KRAFT L.M., *Axial performance and capacity of piles. In: Planning and Design of Fixed Offshore Platforms*, McClelland B., Reifel M.D. (eds.), Van Nostrand Reinhold Comp, New York, 1986, pp. 763–800

[141] FOXTON P., *Latest developments for vertically loaded anchors*. Proc.2nd IBC Intl. Conf. on Mooring & Anchoring, Aberdeen, U.K., June 1997

[142] FRANKENMOLEN S., ANG S-Y, PEEK R., CARR M., MACRAE I., WHITE D.J. & RIMMER J. (2017), *Pipe-clamping mattress to stop flowline walking*. Proc. Offshore Technology Conference, Houston, USA. Paper OTC 27815.

[143] FUGRO. *Axial pile capacity design method for offshore driven piles in sand*. Fugro Engineers BV Report No. P1003 to API, Issue 3, 5 August 2004

[144] GALLAGHER K.A., ST. JOHN H.D., *Field scale model studies of piles as anchorages for buoyant platforms*. Proc. European Offshore Petroleum Conf., paper EUR 135, London, U.K., 1980

[145] GAUDIN C. & WHITE D.J. (2012), *Centrifuge modelling to support the design of subsea pipelines*. Proc. GeoCongress 2012, San Francisco, ASCE STP225 2402-2411.

[146] GAUER, P., KVALSTAD, T. J., FORSBERG, C. F., BRYN, P., AND BERG, K. (2005), *The last phase of the Storregga slide: simulation of retrogressive slide dynamics and comparison with slide-scar morphology*. Marine Petroleum Geology, 22, 171-178.

[147] GAVIN K., JARDINE R., KARLSRUD K., LEHANE B., *The effects of pile ageing on the shaft capacity of offshore piles in sand*. Proc. Intl. Symposium on Frontiers in Offshore Geotechnics, ISFOG III, September 2015, Olso, Norway

[148] GE, M., B. KEBADZE, J. HENDERSON, A. ZAKERI, B. MERCAN, AND S. KILLBOURN, *Recent Improvements in Subsea Wellhead Fatigue Monitoring Algorithm and Accuracy Using Verification and Calibration Techniques*, Proc. Offshore Technology Conference (OTC). 2017: Houston, Texas, USA.

[149] GEORGIADIS M., *Development of p-y curves for layered soils*. Proc. Intl. Conf. on Geotechnical Practice in Offshore Engineering, ASCE, Austin, Texas, 1983, pp. 536–545

[150] GILBERT R.B., CHEN J.Y., MATEREK B., PUSKAR F., VERRET S., CARPENTER J., YOUNG A., MURFF J.D., *Comparison of observed and predicted performance for jacket pile foundations in hurricanes*. Proc. Offshore Technology Conference, Houston, Texas, paper OTC 20861, May 2010

[151] GILBERT, R. G., ET AL. (2009). *Analytical and experimental modeling of out-of-plane loading of plate anchors*. Offshore Technology Conf., Houston.

[152] GILBERT, R.B., WARD E. G., AND WOLFORD, A. J., *A Comparative Risk Analysis of FPSO's with Other Deepwater Production Systems in the Gulf of Mexico*, Proc. Offshore Technology Conference. 2001, Offshore Technology Conference: Houston, Texas. p. 16.

[153] GOURVENEC S., *Effect of embedment on the undrained capacity of shallow foundations under general loading*. Géotechnique, 2008, 58 (3), pp. 177–185

[154] GOURVENEC S., *Failure envelopes for offshore shallow foundation under general loading*. Géotechnique, 2007, 57 (9), pp. 715–727

[155] GOURVENEC S., *Shape effects on capacity of rectangular footings under combined load*. Géotechnique, 2007, 57 (8), pp. 637–646

[156] GOURVENEC S., RANDOLPH M.F., *Consolidation beneath skirted foundations due to sustained loading*. Intl. Journal of Geomechanics, January/February, 2010, 10 (1), pp. 22–29

[157] GOURVENEC S., RANDOLPH M.F., *Effect of foundation embedment and soil properties on consolidation response*. Proc. Intl. Conf. on Soil Mechanics and Geotechnical Engineering, ICSMGE, Alexandria, Egypt, 2009, pp. 638–641

[158] GOURVENEC S., RANDOLPH M.F., *Effect of strength non-homogeneity on the shape and failure envelopes for combined loading of strip and circular foundations on clay*. Géotechnique, 2003, 53 (6), pp. 575–586

[159] GOURVENEC S., STEINEPREIS M., *Undrained limit states of shallow foundations acting in consort*. Intl. Journal of Geomechanics, 2007, 7 (3), pp. 194–205

[160] GOURVENEC S.M. & WHITE D.J. 2010. *Elastic solutions for consolidation around seabed pipelines*. Proc. Offshore Technology Conference, Houston. Paper 20554

[161] GOVONI, L., GOURVENEC, S. & GOTTARDI, G. (2011), *A centrifuge study on the effect of embedment on the drained response of shallow foundations under combined loading. Géotechnique*, 61(12): 1055-1068. http://dx.doi.org/10.1680/geot.7.00109

[162] GRAJALES-SAAVEDRA, F., AUBENY C.P., DREW, D., JEANJEAN, P., AND ZAKERI, A. (2017b). *Upper Bound Plastic Limit Analysis of Laterally Loaded Piles in Stratified Soils*. Proceedings, Society for Underwater Technology, 8th International Conference on Offshore Site Investigation and Geotechnics, London, September

[163] GRAJALES-SAAVEDRA, F., AUBENY C.P., JEANJEAN, P., AND DREW, D. (2017a). *Plastic Limit Analysis of Laterally Loaded Piles and Wells Conductors in Soil Profiles with Crust*. Proceedings, Offshore Technology Conference, Houston, TX, Paper 27785.

[164] GRANDE L., *Samvirke Mellom Pel og Jord*. Lic. Techn. Thesis, NTH, Institute for Soil Mechanics and Foundation Engineering, Trondheim, Norway, 1976

[165] GRIFFITHS T.G., WHITE D.J., DRAPER S.D., CHENG L.C., LEIGHTON A. & FOGLIANI A. 2019. *Lateral resistance of 'rigid' pipelines and cables on rocky seabeds*. Canadian Geotechnical Journal. 56(6):823-839

[166] HAMILTON J.M., MURFF J.D., *Ultimate lateral capacity of piles in clay*. Proc. Offshore Technology Conf., paper OTC 7667, Houston, Texas, May 1995

[167] HAN, F., GANJU, E., PREZZI, M, ZAHEER, M., *Axial resistance of open-ended pipe pile driven in gravelly sand*, Géotechnique 70(2):1-40, DOI: 10.1680/jgeot.18.p.117, 2019

[168] HEEREMA E.P., *Relationship between wall friction, displacement and horizontal stress in clay and sand for pile drivability analysis*. Ground Engineering, (12) 1, January 1979

[169] HELFRICH S.C., YOUNG A.G., EHLERS C.J., *Temporary seafloor support of jacket structures*. Proc. 12th Offshore Technology Conf., Houston, Texas, paper OTC 3750, May 1980

[170] HIGHTER W.H., ANDERS J.C., *Dimensioning footings subjected to eccentric loads.* ASCE Journal of Geotechnical Engineering, 1985, 111 (GT5), pp. 659–665

[171] HILL A. & WHITE D.J. (2015). *Pipe-soil interaction: Recent and future improvements in practice*. Proc. Int. Symp. on Frontiers in Offshore Geotechnics (ISFOG).387-392

[172] HILL A., WHITE D.J., BRUTON D.A.S., LANGFORD T., MEYER V., JEWELL R. & BALLARD J-C. (2012). *A new framework for axial pipe-soil interaction illustrated by a range of marine clay datasets*. Proc. Int. Conf. on Offshore Site Investigation and Geotechnics. SUT, London. 367-377

[173] HO, T., JARDINE, R. J. & ANH-MINH, N. (2011), *Large-displacement interface shear between steel and granular media*. Géotechnique 61(3):221.

[174] HOGERVORST J.R., *Field trials with large diameter suction piles*. Proc. Offshore Technology Conf., paper OTC 3817, Houston, Texas, May 1980

[175] HOLEYMAN, A., PERALTA, P. AND CHARUE, N., *Boulder-soil-pile dynamic interaction*, Proc. 3rd Intl. Sym. on Frontiers in Offshore Geotechnics, ISFOG 2015, V. Meyer, Editor. 2015, Taylor & Francis Group: Oslo, Norway. p. pp. 563-568.

[176] HOLTZ R.D., *Stress Distribution and Settlement of Shallow Foundations*, In: Foundation Engineering Handbook. Fang H.Y. (ed.), Kluwer Academic Publishers Group, 2nd Edition, 1991

[177] HOU, Z., SAHDI, F., GAUDIN, C. AND RANDOLPH, M.F., *Centrifuge modelling of pipe-soil interaction in clay with crust layer*. Submitted for publication, 2020

[178] HOULSBY G.T., BYRNE B.W., *Design procedures for installation of suction caissons in sand*. Proc. of the institution of Civil Engineers. Geotechnical Engineering 158, July 2005, issue GE3, pages 135-144.

[179] HUNT R.J., CHAN J.H.-C., DOYLE E.H., *Driving fatigue estimation for Ursa TLP 96in OD piles*. Proc. 9th Intl. Seminar on Offshore and Polar Engineering, ISOPE, Brest, France, May 1999

[180] IEC 61400-3, *Wind turbines — Part 3: Design requirements for offshore wind turbines*

[181] IDRISS, I.M., ET AL., *Behavior of Soft Clays under Earthquake Loading Conditions*, Proc. Offshore Technology Conference (OTC). 1976: Houston, Texas, USA.

[182] IDRISS, I.M., ET AL., *Nonlinear Behavior of soft clays during cyclic loading*. Journal of the Geotechnical Engineering Division of the American Society of Civil Engineers (ASCE), 1978. 104(GT12): p. 1429-1445.

[183] ILUPEJU, O.,AUBENY, C., *P-y Analysis of Laterally Loaded Offshore Piles and Well Conductors and Piles Installed in Normally Consolidated to Lightly Over-Consolidated Clays*. in review, 2018

[184] INGARFIELD, S., SFOUNI-GRIGORIADOU, M., DE BRIER, C., & SPINEWINE, B. (2016). *The Importance of Soil Characterisation in Modelling Sediment Density Flows and Implications in Assessing Infrastructure Interaction*. Offshore Technology Conference. doi:10.4043/27237-MS

[185] ISO 2394, *General principles on reliability for structures*

[186] JARDINE R., CHOW F., OVERY R., STANDING J., *ICP design methods for driven piles in sands and clays*. Imperial College, Thomas Telford Publ., London, 2005

[187] JARDINE R.J., ANDERSEN K., PUECH A., *Cyclic loading of offshore piles: Potential effects and practical design*. Proc. SUT Conf. on Offshore Site Investigations and Geotechnics, SUT OSIG, London, September 2012

[188] JEANJEAN P., *Innovative design method for deepwater surface casings*. Proc. Society of Petroleum Engineers Technical Conf., paper SPE 77357, San Antonio, Texas, October 2002

[189] JEANJEAN P., *Re-assessment of p-y curves for soft clays from centrifuge testing and finite element modelling*. Proc. Offshore Technology Conf., paper OTC 20158, Houston, Texas, 2009

[190] JEANJEAN P., *Setup characteristics of suction anchors for soft Gulf of Mexico clays: Experience from field installation and retrieval*. Offshore technology Conf., paper OTC 18005, Houston, Texas May 2006.

[191] JEANJEAN P., WATSON P.G., KOLK H.J., LACASSE S., *RP2GEO: The new API recommended practice for geotechnical engineering*. Proc. Offshore Technology Conf., Houston, Texas, paper OTC 20631, May 2010

[192] JEANJEAN, P., MILLER, D., BROOKS, H., YOGENDRAKUMAR, M., *Lessons learned from pile driving and monitoring in gravels on the Northstar Artificial Island*, ISFOG Conference, ISBN: 978-1-138-02848-7, 2015

[193] JEANJEAN, P., ZNIDARCIC, D., PHILLIPS, R., KO, H.Y., PFISTER, S. AND SCHROEDER, K. (2006). *Centrifuge testing on suction anchors: Doublewall, stiff clays, and layered soil profile*. Proc. Offsh. Techn. Conf., OTC 18007, Houston, May.

[194] JONKER G., MIDDENDORP P., *Subsea installations using vibratory piling hammers*. Proc. Offshore Technology Conf., paper OTC 5776, Houston, Texas, May 1988

[195] JOSTAD H.P., ANDERSEN K.H., *Potential benefits of using skirted foundations for jack-up platforms*. Proc. Offshore Technology Conf., Houston, Texas, paper OTC 18016, May 2006

[196] KANNALA, J., A. ZAKERI, M.L. GE, AND B.E. KEBADZE, *Performance Evaluation of Recently Developed Soil Models in Well Conductor Fatigue Analysis using Field Measurements*. Proc. Offshore Technology Conference (OTC). 2016: Houston, Texas.

[197] KARLSRUD K., JENSEN T.G., WENSAAS LIED E.K., NOWACKI F., SIMONSEN A.S., *Significant ageing effects for axially loaded piles in sand and clay verified by new field load tests*. Proc. Offshore Technology Conference, Houston, Texas, May 2014, paper OTC-25197-MS

[198] KARLSRUD K., NADIM F., HAUGEN T., *Piles in clay under cyclic axial loading - Field tests and computational modelling*. Proc. 3rd Intl. Conf. on Numerical Methods in Offshore Piling, Nantes, France, 1986, Editions Technip, pp. 165–190

[199] KAY. S., GOURVENEC, S., PALIX, E., ALDERLIESTE, E. (2021), *Intermediate Offshore Foundations*, ISBN 9781138353534

[200] KERCIKU A.A, BHATTACHARYA S, BURD H.J AND LUBKOWSKI Z.A (2008), *Fixity of pile foundations in seismically liquefied soils for buckling calculations – An Eigenvalue analyses*, The 14th World Conference on Earthquake Engineering October 12-17, 2008, Beijing, China

[201] KLINKVORT, R.T., H.STURM AND K.ANDERSEN. 2019. *Penetration model for installation of skirted foundations in layered soils*. J. Geotech. Geoenviron. Eng. 145 (10): 04019085-1. https://doi.org/10.1061/(ASCE)GT.1943-5606.0002106

[202] KOLK H.J., BAAIJENS A.E., SENDERS M., *Design criteria for pipe piles in silica sands*. Proc. 1st Intl. Symposium on Frontiers in Offshore Geotechnics, ISFOG, Perth, September 2005, pp. 711–716

[203] KRAFT L.M., FOCHT J.A., AMARASINGHE S.F., *Friction capacity of piles driven into clay*. ASCE Journqal of Geotechnical Engineering Div., 1981 November, 107 (GT11), pp. 1521–1541

[204] KRAFT L.M., LYONS C.G., *State of the art: Ultimate axial capacity of grouted piles*. Proc. 6th Offshore Technology Conf., Houston, Texas, paper OTC 2081, May 1974

[205] LACASSE, S., NADIM, F., ANDERSEN, K.H., KNUDSEN, S., EIDSVIG, U.K., YETGINER, G., GUTTORMSEN, T., EIDE, A. (2013a). *Reliability of API, NGI, ICP and Fugro Axial Pile Capacity Calculation Methods*, In Proceedings of Offshore Technology Conference 2013 (OTC 2013). Houston, Texas, USA. (OTC 24063-MS). Richardson: Offshore Technology Conference

[206] LACASSE, S., NADIM, F., BOYLAN, N., LIU, Z. & CHOI, Y.J. (2019). *Risk Assessment and Management for Geotechnical Design of Offshore Installations*. In Proc. Offshore Technology Conference 2019 (OTC 2019). Houston, Texas, USA. (OTC 29398-MS). Richardson: Offshore Technology Conference.

[207] LADD C.C., FOOTT R., *New design procedure for stability of soft clays*. ASCE Journal of Geotechnical Engineering Div., 1974 July, 100 (7), pp. 763–786

[208] LADD C.C., FOOTT R., ISHIHARA K., SCHLOSSER F., POULOS H.G., *Stress deformation and strength characteristics, State-of-the-art report*. Proc. IX Intl. Conf. on Soil Mechanics and Foundation Engineering, ICSMFE, Tokyo, Japan, 2, 1977, pp. 421–494

[209] LECKIE S., DRAPER S., WHITE D.J., CHENG L., GRIFFITHS T. & FOGLIANI A. (2018). *Observed changes to the stability of a seabed pipeline caused by seabed mobility*. Ocean Engineering 169:159-176.

[210] LECKIE S., MOHR H., DRAPER S., MCLEAN D., WHITE D.J. & CHENG L. (2016). *Sedimentation-induced burial of subsea pipelines: observations from field data and laboratory experiments*. Coastal Engineering 114:137-158

[211] LECKIE, S., DRAPER, S., WHITE, D.J., CHENG, L. & FOGLIANI N. (2015). *Lifelong embedment and spanning of a pipeline on a mobile seabed*. Coastal Engineering. 95:130-146.

[212] LEHANE B.M. AND GUO F. (2017). *Lateral response of piles in cemented soil and weak rock*. Geotechnique, dx.doi.org/10.1680/jgeot.16.P.132.

[213] LEHANE B.M., JARDINE R.J., *Displacement pile behaviour in glacial clay*. Canadian Geotechnical Journal, 1994, 31 (1), pp. 79–90

[214] LEHANE B.M., LI LICHEN AND BITTAR E., (2020), *CPT-based load-transfer formulations for driven piles in sand*, GLETT-D-20-00096, DOI: 10.1680/jgele.20.00096, Geotechnique Letters

[215] LEHANE B.M., SCHNEIDER J.A., XU X., *The UWA-05 method for prediction of axial capacity of driven piles in sand*. Proc. 1st Intl. Symposium on Frontiers in Offshore Geotechnics, ISFOG, Perth, Australia, September 2005, pp. 683–689

[216] LEHANE ET. AL., *CPT-Based Axial Pile Capacity Design Method for Driven Piles in Clay*

[217] LEHANE, B.M., LIM, J.K., CAROTENUTO, P., NADIM, F., LACASSE, S., JARDINE, R.J. AND VAN DIJK, B.F.J. 2017. *Characteristics of Unified Databases for Driven piles*. Proc. 8th International Conf. Offshore Investigation and Geotechnics: Smarter solutions for offshore developments, Society for Underwater Technology, 1, 162-194.

[218] LEHANE, B.M., LIU, Z.Q., BITTAR, E., NADIM, F., LACASSE, S., JARDINE, R.J., CAROTENUTO, P., RATTLEY, M., JEANJEAN, P., GAVIN, K., GILBERT, R., HAAVIK, J.B., MORGAN, N. (2020). *A new 'Unified' CPT-based axial pile capacity design method for driven piles in sand*. In Frontiers in Offshore Geotechnics IV, Austin, TX.

[219] LIEDTKE, E., ANDERSEN, K.H., ZHANG Y., AND JEANJEAN, P. (2019), *Monotonic and cyclic soil properties of Gulf of Mexico clays*. Submitted for publication at OTC 2019 conference.

[220] LIENG J.T., TJELTA T.I., SKAUGSET K., *Installation of two prototype deep penetrating anchors at the Gjoa field in the North Sea*. Proc. Offshore Technology Conf., paper OTC 20758, Houston, Texas, May 2010

[221] LITTON, R.W., STRINGER, M.E., CLUKEY, E.C., CHEN, J-Y., KUTTER, B., WILSON, D.W., ZHENG, B-L., AND ZHOU, Y-G. (2014), *Centrifuge study of Offshore platform response to earthquake excitations*, Proceedings, Offshore Technoogy Conference, Houston, Texas, Paper 25206.

[222] LIU, J., TIAN, J. AND YI, P. (2015), *Impact forces of submarine landslides on offshore pipelines*. Ocean Engineering 95:116-127.

[223] LIU, T.F., QUINTEROS, V. S., JARDINE R.J., CARRARO, A.H., ROBINSON, J., *A unified database of ring shear steel-interface tests on sandy-silty soils*, ECSMGE Conference, doi: 10.32075/17ECSMGE-2019-0268, 2019.

[224] LIU, Z., ELKHATIB, S., NADIM, F., & LACASSE, S. (2020). *Reliability of Five Axial Pile Capacity Design Methods – A Case Study*. In Z. Westgate (Ed.), 4th International Symposium on Frontiers in Offshore Geotechnics, Austin, Texas. Nov. 8-11, 2021. Hawthorne: Deep Foundations Institute

[225] LOCAT, J. AND DEMERS, D. (1988), *Viscosity, yield stress, remoulded strength, and Liquidity Index relationships for sensitive clays*. Canadian Geotechnical Journal, 25(4):799-806.

[226] LOCAT, J. (1997), *Normalized rheological behaviour of fine muds and their flow properties in a pseudoplastic regime*. Debris-Flow Hazards Mitigation: Mechanics, Predication and Assessment, Water Resources Engineering Division, American Soc. Civil Engineers (ASCE).

[227] LUNNE T., ANDERSEN K.H., *Soft clay shear strength parameters for deepwater geotechnical design*. Proc. Intl. Conf. on Offshore Site Investigation and Geotechnics, SUT OSIG, London, U.K., September 2007

[228] LUNNE T., ROBERTSON P.K., POWELL J.J.M., *Cone Penetration Testing in Geotechnical Practice*. Blackie Academic & Professional, 1997

[229] LYSMER J., *Analytical procedures in soil dynamics*. Report No. UCB/EERC-79/29 presented at the ASCE Geotechnical Engineering Div. Specialty Conf. on Earthquake Engineering and Soil Dynamics, Pasadena, California, December 1978

[230] MALGESINI, G., TERRILE, E., ZUCCARINO, L., PARKER, E., & FRIEDMANN, Y. (2018). *Evaluation of Debris Flow Impact on Submarine Pipelines: A Methodology*. Offshore Technology Conference. doi:10.4043/28847-MS

[231] MANA. D.S.K; GOURVENEC, S. MARTIN, C. (2013). *Critical Skirt Spacing for Shallow Foundations under General Loading*. ASCE Journal of Geotechnical and Geoenvironmental Engineering, Vol. 139, Issue 9.

[232] MARTIN C.M. & WHITE D.J. (2012). *Limit analysis of the undrained capacity of offshore pipelines*. Géotechnique, 62(9):847-863

[233] MARTIN C.M., *New software for rigorous bearing capacity calculations*. Proc. Intl. Conf. on Foundations, Dundee, UK, 2003, pp. 581–592

[234] MARTIN, C.M. (2005). *Exact bearing capacity calculations using the method of characteristics*. Proc. 11th Int. Conf. of IACMAG, Turin, Vol. 4, pp 441-450.

[235] MARTIN, C.M. AND RANDPLPH, M. F., *Upper bound analysis of lateral pile capacity in cohesive soil*, *Geotechnique*, 2006, 56, No 2

[236] MARTIN, C.M. AND WHITE, D. J., *Limit analysis of the undrained bearing capacity of offshore pipelines*, Geotechnique, 2012, 62, No 9

[237] MATLOCK H., *Applications of numerical methods to some structural problems in offshore operations*. Journal of Petroleum Technology, 1963, pp. 1040–1046

[238] MATLOCK H., *Correlations for design of laterally loaded piles in soft clay*. Proc. 2nd Offshore Technology Conf., paper OTC 1204, Houston, Texas, April 1970

[239] MATLOCK H., FOO S.H.C., *Axial analysis of piles using a hysteretic and degrading soil model*. Proc. Intl. Conf. on Numerical Methods in Offshore Piling, Institution of Civil Engineers, ICE, London, UK, 1980, pp. 127–133

[240] MATSUMOTO, T., TAKEI, M., *Effects of Soil Plug on Behaviour of Driven Pipe Piles, Soils & Foundations*, June 1991

[241] MCANOY R.P.L., CASHMAN A.C., PURVIS O., *Cyclic tensile testing of a pile in glacial till*. Proc. 2nd Intl. Conf. on Numerical Methods in Offshore Piling, Austin, Texas, 1982, pp. 257–291

[242] MCCLELLAND B., EHLERS C.J., *Offshore geotechnical site investigations - Planning and design of fixed offshore platforms*. McClelland B., Reifel M.D. (eds.), Van Nostrand Reinhold Comp., New York, 1986, pp. 224–265

[243] MCCLELLAND B., FOCHT J.A., *Soil Modulus for Laterally Loaded Piles*. Trans. American Society of Civil Enginers, ASCE, 1958, 123 (1049)

[244] MERCAN, B., Y. CHANDRA, M. CAMPBELL, AND M.L. GE, *Soil Model Assessment for Subsea Wellhead Fatigue using Monitoring Data*, Proc. Offshore Technology Conference (OTC). 2017: Houston, Texas, USA.

[245] MERIFIELD R.S., WHITE D.J., RANDOLPH M.F., *Analysis of the undrained breakout resistance of partially embedded pipelines*. Géotechnique, 2008, 58 (6), pp. 461–470

[246] MERIFIELD, R.S., WHITE, D.J. AND RANDOLPH, M.F., *The effect of surface heave on the response of partially-embedded pipelines on clay*. ASCE J. Geotechnical & Geoenvironmental Engineering, 2009, 135(6):819-829

[247] MILLER T.W., MURFF J.D., KRAFT L.M., *Critical state soil mechanics model of soil consolidation stresses around a driven pile*. Proc. 10th Offshore Technology Conf., Houston, Texas, paper OTC 3307, May 1978

[248] MOHR H., DRAPER S., WHITE D.J. & CHENG L.C. (2018). *The influence of permeability on the erosion rate of fine-grained marine sediments*. Coastal Engineering. 140, pp. 124-135

[249] MONTRASIO L., NOVA R., *Settlements of shallow foundations on sand; Geometrical effects*. Géotechnique, 1997, 47 (1), pp. 49–60

[250] MULDER, T. AND ALEXANDER, J. (2001), *The physical character of subaqueous sedimentary density flows and their deposits*. Sedimentology, 48(2):269-299.

[251] MURFF J.D., *Pile capacity in a softening soil*. Intl. Journal of Numerical Analysis Methods in Geomechanics, 1980 April-June, 4 (2), pp. 185–189

[252] MURFF J.D., HAMILTON J.M., *P-ultimate for undrained analysis of laterally loaded piles*. ASCE Journal of Geotechnical Engineering, 1993, 119 (1), pp. 91–107

[253] MURFF J.D., RANDOLPH M.F., ELKHATIB S., KOLK H.J., RUINEN R., STROM P.J. ET AL. *Vertically loaded plate anchors for deepwater applications*. Proc. Intl. Symposium on Frontiers in Offshore Geotechnics, ISFOG, Perth, Australia, September 2005

[254] MYHRE, E., EILERTSEN, L.E., RUSSO, M., JOHANSEN, F, HART, C. & TORE J-K., *Successful Real Time Instrumentation Of The Conductor And Surface Casing Of An Exploration Subsea Well In The North Sea To Measure The Actual Loads Experienced During Drilling Operations*. Proc. Offshore Technology Conference (OTC). 2015, OTC Paper 25770: Houston, Texas, USA.

[255] NADIM, F, LACASSE, S., LIU, Z.Q., LEHANE, B.M. (2020), *Improving the reliability of the calculated axial capacity of piles in sand*, In Frontiers in Offshore Geotechnics IV, Austin, TX.

[256] NAJJAR, SS., GILBERT, R.B., LIEDTKE, E.A., MCCARRON, B. & YOUNG, A.G. (2007). *Residual shear strength for interfaces between pipelines and clays at low effective normal stresses*. ASCE Journal of Geotechnical and Geoenvironmental Engineering. 133(6): 695-706.

[257] NCEL, *Drag Embedment Anchors for Navy Moorings*. Technical Data Sheet 83-08R, Naval Civil Engineering Laboratory, June 1987

[258] NEN 6743 *Calculation method for bearing capacity of pile foundation, compression piles*.

[259] NEUBECKER S.N., RANDOLPH M.F., *The static equilibrium of drag anchors in sand*. Canadian Geotechnical Journal, 1996, 33, pp. 574–583

[260] NIEDORODA, A.W., REED, C.W., HATCHETT, L., YOUNG, A., LANIER, D., KASCH, V., JEANJEAN, P., ORANGE, D., AND BRYANT, W.,(2003). *Analysis of past and future debris flows and turbidity currents generated by slope failures along the Sigsbee Escarpment in the deep Gulf of Mexico*. Offshore Technology Conference, Houston, Paper OTC 15162.

[261] NOVAK M., SHARNOUBY B.E., *Stiffness constants of single piles*. ASCE Journal of Geotechnical Engineering Div., July 1983, 109 (7), pp. 961–974

[262] O'LOUGHLIN C.D., RANDOLPH M.F., RICHARDSON M., *Experimental and theoretical studies of deep penetrating anchors*. Proc. Offshore Technology Conf., paper OTC 16841, Houston, Texas, May 2004

[263] O'NEILL M.W., *Group action in offshore piles*. Proc. Intl. Conf. on Geotechnical Practice in Offshore Engineering, ASCE, Austin, Texas, 1983, pp. 25–64

[264] O'NEILL M.W., DUNNAVANT T.W., *An evaluation of the behaviour and analysis of laterally loaded pile groups*. Research Report No. UHCE 85-11, API, PRAC 84-52, University of Houston, Texas, Department of Civil Engineering, University Park, 1985

[265] O'NEILL. M., ERBRICH, C. & MCNAMARA, A. (2018), *Prediction of Seabed Trench Formation Induced by Anchor Chain Motions*, Proc. Offshore Technology Conference, OTC-29068-MS

[266] O'NEILL M.W., HASSAN K.M., *Drilled shafts: Effects of construction on performance and design criteria*. Proc. Intl. Conf. on Design and Construction of Deep Foundations, U.S. Federal Highway Administration, FHWA, 1, 1994, pp. 137–187

[267] O'NEILL M.W., HAWKINS R.A., AUDIBERT J.M.E., *Installation of pile group in overconsolidated clay*. ASCE Journal of Geotechnical Engineering Div., 1982, Nov., 108 (GT11), pp. 1369–1386

[268] O'NEILL M.W., MURCHISON J.M., *An evaluation of p-y relationships in sands*. Research Report No. GT-DF02-83, API PRAC 82-41-1, University of Houston, Texas, March 1983

[269] Ove ARUP & Partners. *Research on the behaviour of piles as anchors for buoyant structures – Summary Report*. Offshore Technology Report OTH 86 215, Dept. of Energy, London, U.K., 1986

[270] PANAYIDES, S., T. A. POWELL, AND K. SCHRØDER. 2017. *Penetration resistance of suction caissons in layered soils: A case study*. In Proc., Offshore Site Investigation and Geotechnics, OSIG 2017, 562–569. London: Society for Underwater Technology

[271] PELLETIER J.H., DOYLE E.H., *Tension capacity in silty clays – Beta pile test*. Proc. 2nd Intl. Conf. on Numerical Methods in Offshore Piling, Austin, Texas, 1982, pp. 163–181

[272] PELLETIER J.H., SGOUROS G.E., *Shear transfer behaviour of a 30-inch pile in silty clay*. Proc. 19th Offshore Technology Conf., paper OTC 5407, Houston, Texas, April 1987

[273] PEUCHEN J., DE RUIJTER M., GOEDEMOED S., *Commercial characterisation of calcareous soils*. Proc. 2nd Intl. Conf. on Engineering for Calcareous Sediments, Bahrain, February 1999, Al Shafei K.A. (ed.), A.A. Balkema, Rotterdam, 2000

[274] POSKITT, T.J., *The deflection of piles during driving*. Géotechnique, 1996. 46(2): p. 235-243.

[275] POULOS H.G., *Cyclic axial pile response - Alternative analyses*. Proc. Intl. Conf. on Geotechnical Practice in Offshore Engineering, Austin, Texas, ASCE, 1983, pp. 403–421

[276] POULOS H.G., DAVIS E.H., *Elastic Solutions for Soil and Rock Mechanics*. John Wiley & Sons, 1974

[277] POULOS H.G., RANDOLPH M.F., *Pile group analysis: A study of two methods*. ASCE Journal of Geotechnical Engineering Div., 1983, 109 (3), pp. 335–372

[278] PRANDTL L., *Eindringungsfestigkeit und festigkeit von schneiden*. Angew Math. U. Mech, 1 (15), 1920

[279] PUECH A., POULET D., BOISARD P., *A procedure to evaluate pile drivability analysis in the difficult soil conditions of the southern part of the Gulf of Guinea*. Proc. Offshore Technology Conf., paper OTC 8237, Houston, Texas, May 1990

[280] QUIROS G.W., YOUNG A.G., PELLETIER J.H., CHAN J. H.-C., *Shear strength interpretation for Gulf of Mexico clays*. Proc. of the Conference on Geotechnical Practice in Offshore Engineering, Austin, Texas, 1983

[281] RAINES R.D., UGAZ O., GARNIER J., *Centrifuge modelling of suction piles in clay*. Proc. Intl. Symposium on Frontiers in Offshore Geotechnics, ISFOG, Perth, Australia, September 2005

[282] RANDOLPH, M.F. & GOURVENEC, S. (2011), *Offshore Geotechnical Engineering*. Spon Press/ Taylor & Francis. ISBN: 978-0-415-47744-4. pp 528.

[283] RANDOLPH M., O'NEILL M.P., STEWART D.P., *Performance of suction anchors in fine-grained calcareous soils*. Proc. Offshore Technology Conf., paper OTC 8831, Houston, Texas, May 1998

[284] RANDOLPH M.F., *Analysis of stress-wave data from pile tests at Pentre and Tilbrook*. Proc. Intl. Conf. on Large-Scale Pile Tests in Clay, June 1992, Clarke J. (ed.), Thomas Telford, London, U.K., pp. 436–453

[285] RANDOLPH M.F., *Design considerations for offshore piles*. Proc. Intl. Conf. on Geotechnical Practice in Offshore Engineering, Austin, Texas, ASCE, April 27-29, 1983, pp. 422–439

[286] RANDOLPH M.F., HOULSBY G.T., *The limiting pressure on a circular pile loaded laterally in cohesive soil*. Géotechnique, 34 (4), 1984, pp. 613–623

[287] RANDOLPH M.F., HOUSE A.R., *Analysis of suction caisson capacity in clay*. Proc. Offshore Technology Conf., paper OTC 14236, Houston, Texas, May 2002

[288] RANDOLPH M.F., MURPHY B.S., *Shaft capacity of driven piles in clay*. Proc. 17th Offshore Technology Conf., Houston, Texas, paper OTC 4883, May 1985

[289] RANDOLPH M.F., WHITE D.J., *Pipeline embedment in deep water: Processes and quantitative assessment*. Proc. Offshore Technology Conf., paper OTC 19128, Houston, Texas, May 2008

[290] RANDOLPH M.F., WHITE D.J., *Upper bound yield envelopes for pipelines at shallow embedment in clay*. Géotechnique, 2008b, 58 (4), pp. 297–301

[291] RANDOLPH M.F., WROTH C.P., *An analytical solution for the consolidation around a driven pile*. Intl. Journal of Numerical Analysis Methods in Geomech., 1979, July-September, 3 (3), pp. 217–230

[292] RANDOLPH, M. F. AND WHITE, D. J. (2012), Inter*action forces between pipelines and submarine slides — a geotechnical viewpoint*. Ocean Engineering, 48:32-37.

[293] RANDOLPH, M.F. (2012), *Cyclic Interface Shearing in Sand and Cemented Soils and Application to Axial Response of Piles, Mechanical Behaviour of Soils Under Environmentally Induced Cyclic Loads*, CISM Courses and Lectures, C. di Prisco et al. (Eds.)Volume 534, 2012, pp. 481-528

[294] RANDOLPH, M.F. AND QUUIGGIN, P., N*on-linear hysteretic seabed model for catenary pipeline contact*, Proc. 28th Int. Conf. on Offshore Mech. and Arctic Eng., OMAE 2009, Honolulu, USA, Paper OMAE2009-79259.

[295] RANDOLPH, M.F., BHAT, S., JAIN, S. AND MEKHA, B.B., *Modeling the touchdown zone trench and its impact on SCR fatigue life*. Proc. Offshore Technology Conf., Houston, 2013, Paper OTC 23975.

[296] RANDOLPH, M.F., LEONG, E.C., HOULSBY, G.T., *One-dimensional analysis of soil plugs in pipe piles*, Geotechnique 41, No 4, 1991.

[297] RANDOLPH, M.F., WHITE, D.J. & YAN, Y. 2012. *Modelling the axial soil resistance on deepwater pipelines*. Géotechnique, 62(9):837-846

[298] REESE L.C., COX W.R., *Field testing and analysis of laterally loaded piles in stiff clay*. Proc. 5th Offshore Technology Conf., paper OTC 2312, Houston, Texas, April 1975

[299] REESE L.C., O'NEILL M., *Criteria for design of axially loaded drilled shafts*. Centre for Highway Research Report, University of Texas, August 1971

[300] REESE L.C., WRIGHT S.G., AURORA R.P., *Analysis of a pile group under lateral loading, in Laterally Loaded Deep Foundations: Analysis and Performance*. ASTM Special Technical Publication 835, 1984, pp. 56–71

[301] ROBERTSON, P. K. (2009). *Interpretation of cone penetration tests - A unified approach*. Canadian Geotechnical Journal, 46(11), 1337-1355

[302] ROESSET J.M., ANGELIDES C., *Dynamic stiffness of piles*. Proc. Intl. Conf. on Numerical Methods in Offshore Piling, Institution of Civil Engineers, ICE, London, U.K., 1980, pp. 75–81

[303] ROUSSEL H.J., *Pile Driving Analysis of Large Diameter High Capacity Offshore Pipe Piles*. Ph.D. Thesis, Tulane University, March 1979

[304] RUINEN R., *Penetration analysis of drag embedment anchors in soft clays*. Proc. Intl. Seminar on Offshore and Polar Engineering, ISOPE, Toulon, France, 2004

[305] RUINEN R., DEGENKAMP G., *Anchor selection and installation for shallow and deepwater mooring systems*. Proc. 11th Intl. Seminar on Offshore and Polar Engineering, ISOPE, Stavanger, Norway, June 2001

[306] RUSSO, M., S. KUZMICHEV, G. GRYTØYR, E.B. KEBADZE, A. ZAKERI, AND E.C. CLUKEY, *Measured wellhead loads during drilling operations. Benchmarking of wellhead FE model vs field data considering different soil models*. Journal of Offshore Mechanics and Arctic Engineering, American Society of Mechanical Engineers (ASME), 2016. 138.

[307] SAFEBUCK (2015), *Safe Design of Pipelines with Lateral Buckling. Design Guideline*. SAFEBUCK III. Document 5087471/01/C 15 January 2015. Atkins.

[308] SAHDI, F., GAUDIN, C., WHITE, D. J., BOYLAN, N., AND RANDOLPH, M. F. (2014), *Centrifuge modelling of active slide–pipeline loading in soft clay*. Geotechnique, 64(1):16-27.

[309] SALENÇON J., MATAR M., *Capacité portante des fondations superficielles circulaires*. Journal de Mécanique Théorique et Appliquée, 1982, 1 (2), pp. 237–267

[310] SCHNEIDER M., STANIER S., WHITE D.J. & RANDOLPH M.F. (2020). *Shallow penetrometer tests: theoretical and experimental modelling of the rotation stage*. Canadian Geotechnical Journal https://doi.org/10-1139/cgj-2018-0657, 57(4): 568–579

[311] SCHOFIELD A. N., *Interlocking and peak and design strengths*. Géotechnique, 56 (5), 2006, pp. 357–358; Discussions and response in Géotechnique, 58 (6), 2008, pp. 527–532

[312] SEMPLE R.M., RIGDEN W.J., *Shaft capacity of driven pipe piles in clay*. Proc. Intl. Symposium on Analysis and Design of Pile Foundations, San Francisco, ASCE, October 1984, pp. 59-79

[313] SENDERS M., RANDOLPH M.R., *CPT-based method for the installation of suction caissons in sand*. ASCE Journal of Geotechnical and. Geoenviron. Engineering, January 2009

[314] SENDERS, M., M. RANDOLPH, AND C. GAUDIN. 2007. *Theory for the installation of suction caissons in sand overlaid by clay*. In Proc., 6th Offshore Site Investigation and Geotechnicics Conf.: Confronting New Challenges and Sharing Knowledge, 429–438. Houston: Offshore Technology Conference.

[315] SHELTON J.T., NIE C., SCHULER D., *Installation penetration of gravity installed plate anchors – Laboratory study results and field history data*. Proc. Offshore Technology Conf., paper OTC 22502-PP, Rio de Janeiro, Brazil, October 2011

[316] SHEN, Z., FENG, X. & GOURVENEC, S. (2016), *Undrained capacity of surface foundations with zero-tension interface under planar V-H-M loading*, Computers in Geotechnics, 73: 47-57 http://dx.doi.org/10.1016/j.compgeo.2015.11.024

[317] SHEN, Z. FENG, X, GOURVENEC, S. (2017). *Effect of interface condition on the undrained capacity of subsea mudmats under six-degree-of-freedom loading*. Geotechnique 67 (4), 338-349. DOI: 10.1680/jgeot.16.P.097

[318] SKEMPTON A.W., *The bearing capacity of clays*. Proc. Building Research Congress, London, U.K., 1951

[319] SMITH E.A.L., *Pile driving analysis by the wave equation*. ASCE Journal of Soil Mechanics and Foundation Design, 86, August 1960

[320] SMITH, V.B. & WHITE D.J. (2014). *Volumetric hardening in pipe-soil interaction*. Proc. Offshore Technology Conference, Asia. Kuala Lumpur. Paper OTC-24856-MS

[321] SPARREVIK P., *Suction anchor – A versatile foundation concept finding its place in the offshore market*. Proc. 17th Intl. Conf. on Offshore Mechanics and Arctic Engineering, OMAE, paper 98-3096, Lisbon, Portugal, July 1998

[322] SPARREVIK, PER & STROUT, JAMES. (2015). *Novel monitoring solutions solving geotechnical problems and offshore installation challenges*. 10.1201/b18442-30.

[323] SPINEWINE, B., RENSONNET, D., CLARE, M., CAPART, H., DE THIER, T., & DAN-UNTERSEH GABRIELA. (2013). *Numerical Modelling of Runout and Velocity for Slide-Induced Submarine Density Flows: A Building Block of an Integrated Geohazards Assessment for Deepwater Developments*. Offshore Technology Conference. OTC-24180-MS doi:10.4043/24180-MS

[324] SRIKANDARAJAH, T., ROBERTS, G., TANSCHEIT, P., SOLANO, R.F., HANSEN, A. & ANTUNES, A.R. (2015), *Forward predictions for life-of-field assessments based on the observed lateral buckling behavior of operating deepwater pipelines*. Proc. Offshore Technology Conference, Houston. Paper OTC25961

[325] STANIER S.A., WHITE D.J., CHATTERJEE S., BRUNNING P., RANDOLPH M.F. (2015), *A Tool for ROV-based Seabed Friction Measurement*. Applied Ocean Research, 50 pp 155-162

[326] STEVENS J.B., AUDIBERT J.M., *Re-examination of p-y curve formulations*. Proc. Offshore Technology Conf., paper OTC 3402, Houston, Texas, May 1979

[327] STEVENS R.F., WILTSIE E.A., MIDDLEBROOKS B.S., *Controlled hard driving*. Proc. 2nd Intl. Conf. on Application of Stress-Wave Theory on Piles, Stockholm, Sweden, May 1984

[328] STEVENS R.F., WILTSIE E.A., TURTON T.H., *Evaluating pile drivability for hard clay, very dense sand and rock*. Proc. 15th Offshore Technology Conf., paper OTC 4205, Houston, Texas, May 1982

[329] STOVE O.J., BYSVEEN S., CHRISTOPHERSEN H.P., *New foundation systems for the Snorre development*. Proc. Offshore Technology Conf., paper OTC 6882, Houston, Texas, May 1992

[330] SUMER, B.M., FREDSØE, J. (2002). *The Mechanics of Scour in the Marine Environment*. World Scientific Publishing, Singapore.

[331] TABORDA, D.M.G., ZDRAVKOVIĆ, L., POTTS, D.M., BURD, H.J. BYRNE, B.W., GAVIN, K.G., HOULSBY, G.T., JARDINE, R.J., LIU, T., MARTIN, C.M. AND MCADAM, R.A., 2019. *Finite element modelling of laterally loaded piles in a dense marine sand at Dunkirk*. Géotechnique, https://doi.org/10.1680/jgeot.18.PISA.006.

[332] TAIEBAT H.A., CARTER J.P., NUMERICAL STUDIES OF THE BEARING CAPACITY OF SHALLOW FOUNDATIONS ON COHESIVE SOIL SUBJECTED TO COMBINED LOADING. GÉOTECHNIQUE, 2000, 50 (4), PP. 409-418

[333] TAPPER, L. MARTIN, C. BRYNE, B. LEHANE, B.M. (2015). *Undrained vertical bearing capacity of perforated shallow foundations*. Proceedings, International Symposium in Frontiers in Offshore Geotechnics. Oslo, Norway, 813- 818.

[334] TEMPLETON, J.S. III, BARRETT, M.J., AND CLUKEY, E.C. (2015). *Finite element analysis of soil damping for pipeline spanning*. Proc. 3rd International Synposium for Frontiers in Offshore Geotechnics (ISFOG), Oslo

[335] TEMPLETON, J.S., MURFF, J.D., GOODWIN, R.H. AND KLEJBUK, L.W., *Evaluating Soils and Hazards in the Mississippi Canyon*. Proc. Offshore Technology Conf., OTC 4964, 1985, Houston, May

[336] TERZAGHI K., *Theoretical Soil Mechanics*. Wiley, New York, 1943

[337] TJELTA T.I., *Geotechnical experience from the installation of the Europipe jacket with bucket foundations*. Proc. Offshore Technology Conf., paper OTC 7795, Houston, Texas, May 1995

[338] TOM J. & WHITE D.J. (2019). *Drained bearing capacity of shallowly-embedded pipelines*. ASCE J. Geotechnical and Geoenvironmental Engineering. 145(11) 04019097

[339] TOMLINSON M.J., *Pile Design and Construction Practice*. E. and F.N. Spon (efs.), 4th Edition, 1994

[340] TOMLINSON, M.J. (1996). *Recent advances in driven pile design*, Ground Engineering, 29, No. 10, 31-33.

[341] TOOLAN F.E., FOX D.A., *Geotechnical planning of piled foundations for offshore platforms*. Proc. Institution of Civil Engineers, ICE, Part 1, London, U.K., 1977, pp. 221–224.

[342] TRUE D.G., *Penetration of projectiles into seafloor soils*. Technical Report R-822, Civil Engineering Laboratory, Naval Construction Battalion Center, Port Hueneme, California, 93043, May 1975

[343] UKRITCHON B., WHITTLE A.J., SLOAN S.W., *Undrained limit analysis for combined loading of strip footings on clay*. ASCE Journal of Geotechnical and Geoenvironmental Engineering 1998, 124 (3), pp. 265–276

[344] VANNESTE, M., LØVHOLT, F., ISSLER, D., LIU, Z., BOYLAN, N.P. & KIM, J. 2019. *A Novel Quasi-3D Landslide Dynamics Model: From Theory to Applications and Risk Assessment*. Offshore Technology Conference, Houston, Paper OTC-29363-MS

[345] VERLEY R., SOTBERG T., *A soil resistance model for pipelines placed on sandy soils*. Proc. Intl. Conf. on Offshore Mechanics and Arctic Engineering, OMAE, Calgary, 1992, 5-A, pp. 123–131

[346] VERLEY, R. AND SOTBERG, T. (1992). *A soil resistance model for pipelines placed on sandy soils*. Proc. Intl. Conf. on Offshore Mechanics and Arctic Engineering, OMAE, Calgary, 5-A:123–131

[347] VERSTEELE, H., KUO, M.Y-H., CATHIE, D.N., SASSI, K. & ZEHZOUH, S. (2017), *Anchor Chain Trenching – Numerical Simulation of Progressive Erosion*, Proc. 8th International Conference – Offshore Site Investigation & Geotechnics, London,Vol. 1, pp. 971-977.

[348] WESTGATE Z.J., WHITE D.J. & SAVAZZI M. (2018). *Experience with interface shear box testing for axial pipe-soil interaction assessment on soft clay*. Proc. Offshore Technology Conference, Paper OTC-28671-MS

[349] WESTGATE Z.W., HANEBERG, W. & WHITE D.J. (2016). *Modelling the spatial variability in as-laid embedment for HPHT pipeline design*. Canadian Geotechnical Journal. 53(11): 1853-1865.

[350] WESTGATE Z.W., WHITE D.J., RANDOLPH M.F. & BRUNNING P. 2010. *Pipeline laying and embedment in soft fine-grained soils: Field observations and numerical simulations*. Proc. Offshore Technology Conf., Houston. Paper 20407

[351] WESTGATE, Z.J., RANDOLPH, M.F., WHITE D.J. AND LI, S. (2010). *The influence of seastate on as-laid pipeline embedment: a case study*. Applied Ocean Research. 32(3):321-331.

[352] WESTGATE, Z.J., WHITE, D.J. AND RANDOLPH, M.F. (2012). *Field observations of as-laid pipeline embedment in carbonate sediments*. Géotechnique 62 (9), 787-798.

[353] WESTGATE, Z.J., WHITE, D.J. AND RANDOLPH, M.F. (2013). *Modelling the embedment process during offshore pipe laying on fine-grained soils*. Canadian Geotechnical Journal, 1, 15-27.

[354] WHITE D.J. & RANDOLPH M.F. (2007). *Seabed characterisation and models for pipeline-soil interaction*. Int. Journal of Offshore & Polar Engng. 17(3):193-204. CD 11pp

[355] WHITE D.J., WESTGATE Z., BALLARD J-C, DE BRIER C. & BRANSBY M.F. 2015. *Best practice geotechnical characterisation and pipe-soil interaction analysis for HPHT flowline design*. Proc. Offshore Technology Conference. Houston. OTC26026-MS

[356] WHITE D.J., CAMPBELL M.E., BOYLAN N.P. & BRANSBY M.F. (2012). *A new framework for axial pipe-soil interaction illustrated by shear box tests on carbonate soils*. Proc. Int. Conf. on Offshore Site Investigation and Geotechnics. SUT, London. 379-387

[357] WHITE D.J., CATHIE D.N., *Geotechnics for subsea pipelines*. Proc. Intl. Symposium on Frontiers in Offshore Geotechnics, ISFOG II, Perth, Australia, November 2010

[358] WHITE D.J., RANDOLPH M.F., GAUDIN C., BOYLAN N.P., WANG D., BOUKPETI N., ZHU H. & SAHDI F. 2016. *The Impact of Submarine Slides on Pipelines: Outcomes from the COFS-MERIWA JIP*. Proc. Offshore Technology Conference, Houston OTC27034

[359] WHITE, DJ, CLUKEY EC, RANDOLPH MF, BOYLAN NP, BRANSBY MF, ZAKERI A, HILL AJ, JAECK C. 2017. *The state of knowledge of pipe-soil interaction for on-bottom pipeline design*. OTC 27623, Proc. Offshore Technology Conference, Houston.

[360] WHITEHOUSE R., *Scour at Marine Structures*. Thomas Telford Publ., London, U.K., 1998

[361] WHITTLE A.J., SUTABUTR T., *Prediction of pile set-up in clay*. Transportation Research Record, 1663, 1999, pp. 33–41

[362] WILDE B., TREU H., FULTON T., *Field testing of suction embedded plate anchors*. Proc. 11th Intl. Seminar on Offshore and Polar Engineering, ISOPE, Stavanger, Norway, June 2001

[363] WILTSIE E.A., STEVENS R.F., VINES W.R., *Pile installation acceptance in strong soils*. Proc. 2nd Intl. Conf. on Application of Stress-Wave Theory on Piles, Stockholm, Sweden, May 1984

[364] WOOD D.M. In: *Laboratory Investigations of the Behaviour of Soils under Cyclic Loading: A Review, Soil Mechanics - Transient and Cyclic Loads*. Pande G.N., Zienkiewicz O.C. (eds.), John Wiley & Sons, New York, Chapter 20, 1982

[365] WU, FU, CHEN, CHING-HSIANG, LITTON, RICHARD W. (2020). *Effect of Best-Estimate Clay P-Y Curves on Performance of Offshore Structures*, Paper 30889, Proc. Offshore Tech,. Conference, Houston, TX

[366] YAN Y., WHITE D.J. & RANDOLPH M.F. (2016). *Elastoplastic consolidation solutions for scaling from shallow penetrometers to pipelines*. Canadian Geotechnical Journal, 54:881–895 10.1139/cgj-2016-0286.

[367] YAN, Y., WHITE D.J. & RANDOLPH M.F. 2014. *Cyclic consolidation and axial friction on seabed pipelines*. Géotechnique Letters 4:165–169

[368] YANG Z.X., JARDINE R., GUO W.B., CHOW F., *A new and openly accessible database of tests on piles driven in sands*. Géotechnique Letters, 2015, 5, pp. 12–20, doi:10.1680/geolett.14.00075

[369] YUAN, F., WHITE, D. J. AND O'LOUGHLIN, D. O., *The evolution of seabed stiffness during cyclic movement in a riser touchdown zone on soft clay*. Geotechnique , 2016, July 10.1680/jgeot.15.P.161

[370] ZAKERI A., CLUKEY E., KEBADZE B., JEANJEAN P., WALKER D., PIERCEY G., J. TEMPLETON, L. CONNELLY, AND C. AUBENY. *Recent advances in soil response modeling for well conductor fatigue analysis and development of new approaches*. Proc. Offshore Technology Conf., paper OTC 25795-MS, Houston, Texas, May 2015

[371] ZAKERI, A. (2009). *Submarine debris flow impact on suspended (free-span) pipelines: Normal and longitudinal drag forces*. Ocean Engineering, 36:489-499.

[372] ZAKERI, A., STURM, H., DYVIK, R. AND JEANJEAN, P., *Development of a Novel Apparatus to Obtain Soil Resistance-Displacement Relationship for Well Conductor Fatigue Analysis*. Canadian Geotechnical Journal, 2017

[373] ZAKERI, A., CLUKEY, E.C., KEBADZE, B.E. AND JEANJEAN P., *Fatigue analysis of offshore well conductors: Part I – Study overview and evaluation of Series 1 centrifuge tests in normally consolidated to lightly over-consolidated kaolin clay*. Applied Ocean Research, 2016. 57: p. 78-95

[374] ZAKERI, A., CLUKEY, E.C., KEBADZE, B.E., AND JEANJEAN, P., *Fatigue Analysis of Offshore Well Conductors: Part II - Development New Approaches for Conductor Fatigue Analysis in Clays and Sands*. Applied Ocean Research, 2016. 57: p. 96-113.

[375] ZAKERI, A. AND B. HAWLADER, *Drag forces caused by submarine glide block or out-runner block impact on suspended (free-span) pipelines—Numerical analysis*. Ocean Engineering, 2013. 67: p. 89-99.

[376] ZAKERI, A., LIEDTKE, E. CLUKEY, E.C. AND JEANJEAN, P., *Long-term Axial Capacity of Deepwater Jetted Piles*. Geotechnique, 2014. 64(12): p. 966 –980.

[377] ZAKERI, A., HOEG, K. AND NADIM, F. (2008). *Submarine debris flow impact on pipelines: Drag forces, mitigation and control*. Offshore Technology Conference (OTC). Houston, Texas, Paper OTC19173.

[378] ZAKERI, A., H. STURM, AND P. JEANJEAN, *Validation and Extension of Soil Response Framework for Fatigue Analysis of Offshore Wells and Piles*, in Offshore Technology Conference. 2019, Offshore Technology Conference: Houston, Texas. p. 26.

[379] ZANDWIJK C.J., VOETEN J.A.J., HEEREMA E.P., *An improved pile drivability theory for Gulf of Mexico soils*. Proc. 16th Offshore Technology Conf., paper OTC 4503, Houston, Texas, May 1983

[380] ZDRAVKOVIĆ, L., JARDINE, R.J., TABORDA D.M.G., ABADIAS, D., BURD, H.J., BYRNE, B.W., GAVIN, K.G., HOULSBY, G.T., IGOE, D.J.P., LIU, T, MARTIN, C.M., MCADAM, R.A., MUIR WOOD, A., POTTS, D.M., SKOV GRETLUND, J. AND USHEV, E. 2019. *Ground characterisation for PISA pile testing and analysis*. Géotechnique, https://doi.org/10.1680/jgeot.18.PISA.001.

[381] ZHANG, J., STEWART, D.P. & RANDOLPH, M.F. (2002). *Modeling of shallowly embedded offshore pipelines in calcareous sand*. J. Geotechnical and Geoenvironmental Engineering, ASCE, 128(5): 363–371

[382] ZHANG, Y., ANDERSEN, K.H. (2017). *Scaling of lateral pile p-y curves response in clay from laboratory stress-strain curves*. Marine Structures 53 (2017) page 124-135

[383] ZHANG, Y., ANDERSEN, K.H., JEANJEAN, P. (2019), *Cyclic p-y curves in clays for offshore structures*. Proc Offshore Technolgoy Conference, Houston, OTC-29346-MS https://doi.org/10.4043/29346-MS

[384] ZHANG, Y., ANDERSEN, K.H., JEANJEAN, P., MIRDAMADI, A., GUNDERSEN, A.S., AND JOSTAD, H.P. (2017). *A framework for cyclic p-y curves in clay and application to pile design in GoM*. Proceedings, Society for Underwater Technology, 8th International Conference on Offshore Site Investigation and Geotechnics, London, September

[385] ZHOU, H., DEEKS, A.D., KAYNIA, A.M., MACONOCHIE, A., OP DEN VELDE, W. (2020). *Strength properties of subsea rockfills at low stress level*. In Z. Westgate (eds) 4th Int. Symp. on Frontiers in Offshore Geotechnics. USA.

[386] ZHU, H. AND RANDOLPH, M.F. (2011). *Numerical analysis of a cylinder moving through rate-dependent soils*. Ocean Engineering, 38(7), 943–953.

[387] ZIMMERMAN E.H., SMITH M.W., SHELTON J.T., *Efficient gravity installed anchor for deepwater mooring*. Proc. Offshore Technology Conf., paper OTC 20117, Houston, Texas, May 2009

[388] ZIOGOS, A., BROWN, M.J., IVANOVIC, A., & MORGAN, N. (2015), *Investigation of rock-steel interface testing for gravity foundations for marine energy generators*. In V. Meyer (eds) 3rd Int. Symp. on Frontiers in Offshore Geotechnics. Oslo, Norway. 10 -12 June 2015. Taylor & Francis Group, London. pp. 1245-1250. ISBN: 978-1-138-02848-7.

[389] ZIOGOS, A., BROWN, M.J., IVANOVIC, A., & MORGAN, N. (2021), *Understanding Rock-Steel interface properties for use in offshore applications*. Proc. Inst. of Civil Engineers: Geotechnical Engineering Journal, ISSN 1353-2618. Submitted 09/09/20, final reference to be updated.